Single and binary component adsorption of 1-alcohols from an alkane using various activated alumina adsorbents

by

Catharine Elizabeth Bosman

Thesis presented in partial fulfilment
of the requirements for the Degree

of

MASTER OF ENGINEERING
(CHEMICAL ENGINEERING)

in the Faculty of Engineering
at Stellenbosch University

Supervisor
Prof. Cara E. Schwarz

December 2019

DECLARATION

By submitting this thesis electronically, I declare that the entirety of the work contained therein is my own, original work, that I am the sole author thereof (save to the extent explicitly otherwise stated), that reproduction and publication thereof by Stellenbosch University will not infringe any third party rights and that I have not previously in its entirety or in part submitted it for obtaining any qualification.

Date: December 2019

PLAGIARISM DECLARATION

1. Plagiarism is the use of ideas, material and other intellectual property of another's work and to present is as my own.

2. I agree that plagiarism is a punishable offence because it constitutes theft.

3. I also understand that direct translations are plagiarism.

4. Accordingly all quotations and contributions from any source whatsoever (including the internet) have been cited fully. I understand that the reproduction of text without quotation marks (even when the source is cited) is plagiarism.

5. I declare that the work contained in this assignment, except where otherwise stated, is my original work and that I have not previously (in its entirety or in part) submitted it for grading in this module/assignment or another module/assignment.

Student number:

Initials and surname: C.E. Bosman

Signature: ……..

Date: December 2019

ABSTRACT

During surfactant production, an alcohol-alkane stream is produced which requires separation. Adsorption has been shown to be a technically viable process for the removal of single 1-alcohol contaminants from an alkane stream; however, little knowledge exists on the binary 1-alcohol adsorption.

The aim of this study was to gain knowledge on the single and binary component adsorption of 1-alcohol contaminants from a n-alkane solvent using activated alumina adsorbents. The objectives of the study included: (i) the measurement and investigation of single and binary component adsorption data; (ii) the modelling of the equilibrium adsorption isotherms; and, (iii) the modelling of the adsorption kinetics of these systems. Investigation of the experimental data included comparing the adsorption abilities of three activated alumina adsorbents (Activated Alumina F220, Selexsorb CDx® and Selexsorb CD®); investigating the effect of temperature, initial adsorbate concentration and alcohol carbon chain length on the adsorption of 1-alcohols (1-hexanol, 1-octanol and 1-decanol) from n-decane; a comparison of single and binary 1-alcohol adsorption; and, an investigation of interaction in the binary 1-alcohol systems.

Adsorption data was measured using a bench-scale batch adsorption system. The experimental procedure entailed immersing beakers containing alcohol-alkane solutions (1-alcohol concentration < 3.3 mass%) and adsorbent in a water bath, maintained at a specified temperature (25°C or 45°C), and measuring the alcohol concentration over time.

When comparing the adsorbents, Selexsorb CDx® and Selexsorb CD® were found to exhibit slightly greater adsorbent loadings than Activated Alumina F220 for most systems, with overall equilibrium adsorbent loadings of approximately 110 to 130 mg/g for the single component systems and slightly more, 128 to 150 mg/g, for the binary component systems.

Overall, increased temperature exhibited a corresponding increase in adsorbent loading. Adsorbent loading was found to increase with increasing initial alcohol concentration up to a concentration of approximately 1 to 1.2 mass% after which the equilibrium adsorbent loadings remained relatively constant. The alcohol carbon chain length had minimal effect on adsorption, with some cases exhibiting an increased rate of adsorption for the shorter chain alcohols.

When comparing the adsorption of a 1-alcohol in a single and binary component system (with the specific 1-alcohol having an equal initial concentration in both systems), the adsorbent loading of the 1-alcohol in the binary component system was notably poorer than in the corresponding single component system.

Consequently, antagonistic/competitive behaviour was found to be predominant in the initial adsorbate concentration range of 1 to 1.5 mass%.

For the single and binary component systems, the Redlich-Peterson (R^2 > 0.96) and Extended Freundlich models (R^2 > 0.85 for most systems) were found to provide the best correlation of the equilibrium data, respectively. The binary component isotherm models, however, provided poor correlation of the data. The single and binary component adsorption kinetics were found to be very similar with the pseudo-second-order model providing a good correlation of the kinetic data (R^2 > 0.96 for most systems). The Intra-particle diffusion model was almost equally well suited to the data.

Ultimately, the adsorption of single and binary 1-alcohols from n-decane using activated alumina adsorbents was found to be a technically viable process, with adsorption proposed to be dominated by weak chemisorption, and competitive adsorption slightly favouring shorter carbon chain alcohols.

OPSOMMING

Tydens surfaktantproduksie word 'n alkohol-alkaanstroom geproduseer wat skeiding benodig. Adsorpsie is gewys om 'n tegniese uitvoerbare proses te wees vir die verwydering van enkel 1-alkohol kontaminante uit 'n alkaanstroom, maar daar bestaan min kennis oor die adsorpsie van binêre 1-alkohole.

Die doel van hierdie studie was om kennis te verkry oor die enkel- en binêre komponent adsorpsie van 1-alkohol kontaminante uit 'n n-alkaan oplosmiddel deur geaktiveerde alumina adsorbeermiddels te gebruik. Die doelwitte van die studie het ingesluit: (i) die opmeting en ondersoek van enkel- en binêre komponent adsorpsiedata; (ii) die modellering van die ekwilibrium adsorpsie isoterme; en, (iii) die modellering van die adsorpsiekinetika van hierdie sisteme. Ondersoek van die eksperimentele data het vergelyking van drie geaktiveerde alumina adsorbeermiddels (Geaktiveerde Alumina F220, Selexsorb CDx® en Selexsorb CD®) ingesluit; die ondersoek van die effek van temperatuur, aanvanklike adsorbeermiddelkonsentrasie en alkoholkoolstofkettinglengtes op die adsorpsie van 1-alkohole (1-heksanol, 1-oktanol en 1-dekanol) van n-dekaan; 'n vergelyking van enkel- en binêre 1-alkohol adsorpsie; en, 'n ondersoek van interaksie in die binêre 1-alkoholsisteme.

Adsorpsiedata is gemeet met 'n banktoetsskaal lotadsorpsiesisteem. Die eksperimentele prosedure behels bekers wat alkohol-alkaanoplossings (1-alkoholkonsentrasie < 3.3 massa%) en adsorbeermiddel bevat, in 'n waterbad te dompel en die verandering in alkoholkonsentrasie oor tyd te meet. Die waterbad word gehandhaaf by spesifieke temperature (25 °C en 45 °C).

Wanneer die adsorbeermiddels vergelyk word, vertoon Selexsorb CDx® en Selexsorb CD® groter adsorbeerladings as Geaktiveerde Alumina F220 vir meeste sisteme, met algehele ekwilibrium adsorbeerladings van ongeveer 110 tot 130 mg/g vir die enkelkomponentsisteme en effens meer, 128 tot 150 mg/g vir die binêre komponentsisteme.

Oor die geheel het verhoogde temperatuur 'n korresponderende verhoging in adsorbeerlading vertoon. Adsorbeerlading is gevind om toe te neem met toenemende aanvanklike alkoholkonsentrasie tot en met 'n konsentrasie van ongeveer 1 tot 1.2 massa% nadat die ekwilibrium adsorbeerladings relatief konstant gebly het. Die alkoholkoolstofkettinglengte het minimale effek op adsorpsie gehad, met sommige gevalle wat toenemende tempo van adsorpsie vir die korter ketting alkohole vertoon het.

Wanneer die adsorpsie van 'n 1-alkohol in 'n enkel- en binêre komponentsisteem (met die spesifieke 1-alkohol wat 'n gelyke aanvanklike konsentrasie in beide sisteme het) vergelyk word, is die adsorbeerlading van die 1-alkohol in die binêre komponentsisteem merkbaar minder as in die korresponderende enkelkomponentsisteem. Vervolgens is antagonistiese/kompeterende gedrag gevind om oorwegend in die aanvanklike adsorbeerkonsentrasiebestek van 1 tot 1.5 massa% te wees.

Vir die enkel- en binêre komponentsisteme is die Redlich-Peterson (R^2 > 0.96) en Uitgebreide Freundlich modelle (R^2 > 0.85 vir meeste sisteme) gevind om die beste korrelasie van die ekwilibrium data te gee, onderskeidelik. Die binêre komponent isotermmodelle, het egter swakker korrelasie van die data gegee. Die enkel- en binêre komponent adsorpsiekinetika is gevind om baie soortgelyk aan mekaar te wees, met die pseudo-tweede-orde model wat ’n goeie korrelasie van die kinetiese data (R^2 > 0.96 vir meeste sisteme) gee. Die intrapartikel diffusiemodel was amper net so gepas vir die data.

Die adsorpsie van enkel- en binêre 1-alkohole van n-dekaan deur geaktiveerde alumina adsorbeermiddels te gebruik, is gevind om ’n tegnies uitvoerbare proses te wees, met adsorpsie voorgestel om gedomineer te word deur ’n swakker chemisorpsie, en kompeterende adsorpsie wat korter koolstofketting alkohole effens verkies.

ACKNOWLEDGEMENTS

First and foremost, I would like to express my gratitude to my supervisor, Prof. Cara E. Schwarz. Thank you for sharing your knowledge with me, and for your support and guidance throughout my project. Thank you also for believing in me and for giving me the opportunity to grow as a person.

Thank you to the Department of Chemical Engineering for the financial resources and support which enabled me to complete my master's studies.

My parents, Lea and André Bosman, thank you for providing me with the opportunity to pursue my educational ambitions, but in particular for teaching me the value of hard work and perseverance in the pursuit of ones goals and helping me when I needed it along the way. I cannot thank you enough for all the encouragement, love and support you have given me. Thank you also to Ouma, Catharine van der Merwe, and Oupa, Maans Bosman, for your continued love and support throughout my studies.

My brother, Handré Bosman, thank you for your unending motivation, your friendship and for being my biggest supporter. You have been nothing but a blessing in my life and for that I am truly thankful.

Sunel Nortjé, thank you for always being there. For always lending a shoulder or an ear, for your willingness to help and your continuous encouragement. Thank you also to my other friends, especially Jomaré Groenewald, and the Separations Technology research group for all your support.

Dr L.J. du Preez and Prof. S. Bradshaw, thank you for sharing your knowledge with me and for taking an interest in my work. The workshop and technical staff in the Department of Chemical Engineering, thank you for your endless support. Your hard work and eagerness to assist was noted with gratitude.

Lastly, I would like to express my sincere gratitude to Garland Lee Poil for being an inspiration and a light in my life. Thank you for your advice, words of wisdom and most importantly your endless support and encouragement. Thank you for being there every step of the way. I will never be able to thank you enough.

CONTENTS

NOMENCLATURE

Abbreviations & Acronyms

1-alcohol(s)	Primary alcohol(s)
1-D	1-decanol
1-H	1-hexanol
1-O	1-octanol
AA	Activated alumina
AA-F220	Activated Alumina F220
Al	Alumina
ARE	Average relative error
BET	Brunauer-Emmett-Teller
BJH	Barrett, Joyner & Halenda
DFT	Density functional theory
EDX	Energy-dispersive X-ray
EMT	External mass transfer
FM	Freundlich model
GC	Gas chromatograph(y)
GUM	Guide to the expression of uncertainty in measurement
H_{Al}	Hydrogen in alcohol molecule
HPLC	High-pressure liquid chromatography
HYBRID	Hybrid error function
IC	Initial adsorbate concentration
IPD	Intra-particle diffusion
LM	Langmuir model
LPGA	Low pressure gas adsorption
MPSD	Marquardt's percentage standard deviation
O_{Al}	Oxygen in alcohol molecule
O_s	Oxygen on adsorbent surface
P1	Pseudo-first-order model
P2	Pseudo-second-order model

PN	Pseudo-nth-order model
R-P	Redlich-Peterson
RPM	Redlich-Peterson model
SAE	Sum of absolute errors
SCD	Selexsorb CD®
SCDx	Selexsorb CDx®
SEM	Scanning electron microscope
Si	Silica
SM	Sips model
SSE	Sum of squares of errors
STP	Standard temperature and pressure
XRD	X-ray Diffraction

Symbols

Δ	Uncertainty parameter (uncertainty calculations), application specific
ΔH	Heat of adsorption, kJ.mol^{-1}
a_{RP}	Redlich-Peterson model constant, (mL.mg^{-1})$^{(1/n)}$
C_{bulk}	Adsorbate concentration in the bulk solution, mol.m^{-3}
C_e	Equilibrium adsorbate concentration, mg.mL^{-1}
C_o	Initial adsorbate concentration, mg.mL^{-1} / mass%
$C_{surface}$	Adsorbate concentration on the adsorbent surface, mol.m^{-3}
C_t	Adsorbate concentration at time *t*, mg.mL^{-1} / mass%
E_a	Activation energy, kJ.mol^{-1}
f(t)	Function of time
k_1	Pseudo-1st-order rate constant, min^{-1}
k_2	Pseudo-2nd-order rate constant, g.(mg.min)$^{-1}$
k_c	Mass transfer coefficient, m.s^{-1}

K_F	Freundlich constant, $(mg.g^{-1})(mL.mg^{-1})^{1/n}$
k_{IP}	Intra-particle diffusion rate constant, $mg.(g.min^{0.5})^{-1}$
K_L	Langmuir constant, $mL.mg^{-1}$
k_N	Pseudo-n^{th}-order rate constant, $g^{n-1}.mg^{1-n}.min^{-1}$
K_{RP}	Redlich-Peterson constant, $L.mg^{-1}$
K_S	Sips constant, $(mL.mg^{-1})^{(1/n)}$
$m_{adsorbate}$	Mass of the adsorbate, mg
$m_{adsorbent}$	Mass of the adsorbent, g
η	Interaction parameter (binary isotherm models), dimensionless
n	Number of data points (error functions, modelling), dimensionless
n	Reaction order (Pseudo-n^{th}-order kinetic model), dimensionless
n	Empirical regression parameter (Freundlich, Sips & Redlich-Peterson models), dimensionless
p	Number of regression parameters in model, dimensionless
p/p_o	Relative pressure, dimensionless
q	Adsorbent loading, $mg.g^{-1}$
$\bar{q}$	Average adsorbent loading, $mg.mg^{-1}$
q_e	Equilibrium adsorbent loading, $mg.g^{-1}$
q_{max}	Maximum monolayer adsorbent loading, $mg.g^{-1}$
q_t	Adsorbent loading at time *t*, mg/g^{-1}
R^2	Model correlation coefficient, dimensionless
$R_{q,i}$	Interaction effect parameter of component "*i*", dimensionless
S_n	Standard error (uncertainty calculations), application specific
t	Time, min
T	Temperature, °C (unless otherwise stated)
V	Volume, mL

W	Adsorbent pore diameter/width, nm
W_{EMT}	Radial external mass transfer flux, mol.$(m^2.s)^{-1}$
x	Correlative model parameter (Extended Freundlich model), dimensionless
X	Mass fraction, dimensionless
y	Correlative model parameter (Extended Freundlich model), dimensionless
z	Correlative model parameter (Extended Freundlich model), dimensionless
α	Initial adsorption rate constant (Elovich model), mg.$(g.min)^{-1}$
α	Significance level (uncertainty calculations), dimensionless
β	Surface coverage correlative Elovich model parameter, $g.mg^{-1}$
ε_P	Adsorbent porosity, dimensionless
θ	Boundary layer effect parameter (Intra-particle diffusion model), $mg.g^{-1}$
θ	Fractional adsorbent surface coverage parameter (Extended Langmuir model), dimensionless
ρ	Density, $kg.m^{-3}$

Subscripts & Superscripts

1	Component 1 in the binary component system
2	Component 2 in the binary component system
bin	Binary
exp	Experimentally measured
i	Component “i”
j	Component “j”
pred	Predicted via a model
sin	Single

Chapter 1: Introduction

1.1 Background

Surface active agents, generally referred to as surfactants, are amphiphilic molecules which means that they comprise both hydrophilic (affinity to water) as well as lipophilic (affinity to fats) properties [1], [2]. Surfactants consist of two distinct parts: a non-polar hydrophobic backbone, typically a hydrocarbon chain of approximately eight to 18 carbon atoms; and, a polar hydrophilic part [1]. Surfactants are used in several industries including but not limited to: petroleum; detergents; pharmaceuticals; lubricants, adhesives and paints; minerals processing; and, food processing [3], [4].

Initially, surfactants were typically produced from renewable resources, *i.e.* oils derived from plants and animals, however, currently they are predominantly produced from petrochemical feedstocks [3]. Petrochemical feedstocks contain alcohols which are passed through processes such as ethoxylation and alkylation to produce different types of surfactants [2]. One of the steps in the production of these surfactants is the grafting of an hydroxyl group onto an alkane hydrocarbon chain [5]. In practice, reactions very seldom have a one hundred percent conversion which results in unreacted alcohols being present in the intermediate alkane product stream. It is undesirable to have unreacted alcohols present in the alkane stream in downstream steps which necessitates the removal of these alcohols [6]. Distillation is a satisfactory method for separating alcohols and alkanes; however, achieving perfect separation tends to be difficult and typically very energy intensive with large-scale distillation columns, partly as a result of the boiling points of some alcohols and alkanes being very similar. For this reason, an energy-efficient separation technique is required to remove the alcohol contaminants remaining in the alkane stream after distillation.

Energy-efficient separation techniques, such as adsorption, are currently being employed more often in industry. Adsorption is the process of diffusion of a molecule (adsorbate) from a bulk solution onto the surface of a solid particle (adsorbent) where it adheres to the surface of the solid particle either through physical forces or chemical bonds [7]. Several adsorbents such as activated carbon, activated alumina, silica gels and zeolites can be used depending on the application [7]. Adsorption is typically used for the removal of small quantities of contaminants from chemical, gas or water streams. Since the alkane stream in question typically only contains small amounts of alcohols, adsorption may be a feasible method for the purification of this stream. Figure 1.1-1 provides an indication of the possible use of adsorption within the surfactant production line.

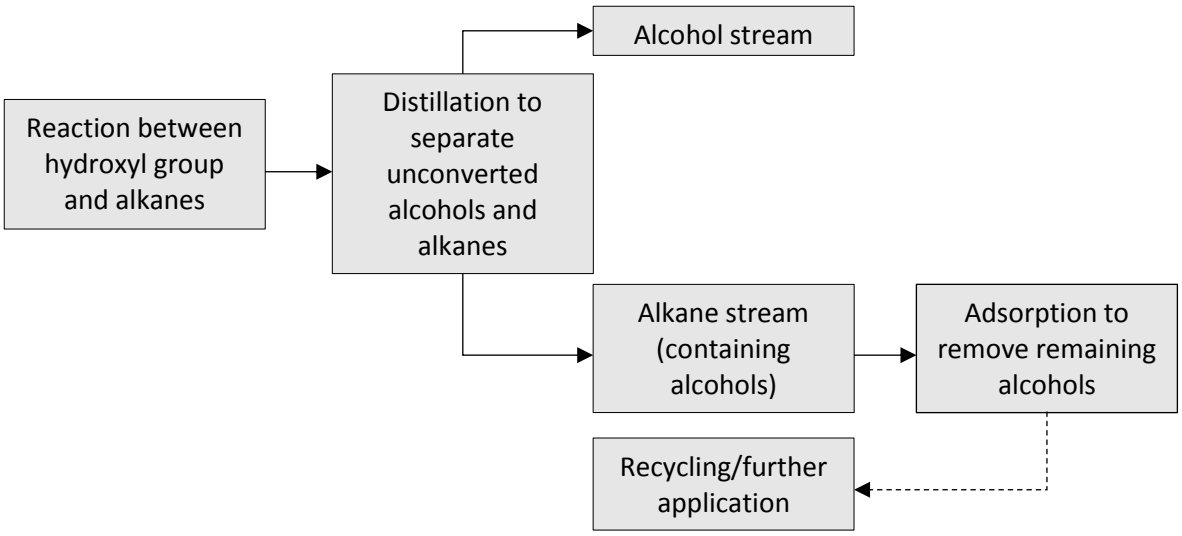

Figure 1.1-1: Process flow diagram indicating the function of adsorption in the surfactant production line

A recent study was conducted by Groenewald [8] to investigate the single component adsorption behaviour of 1-alcohols from an alkane solvent. The systems investigated in the study were composed of either 1-hexanol, 1-octanol or 1-decanol in a n-decane solvent and the adsorbents used were Activated Alumina F220, Selexsorb CDx® and Selexsorb CD®; all different types of activated alumina. Upon investigation, Groenewald [8] found that adsorption was in fact a technically viable process for the removal of a single 1-alcohol (of abovementioned 1-alcohols) from n-decane.

The study by Groenewald [8], however, only investigated the single component adsorption of these 1-alcohols from n-decane. Studies like that of Guojie *et al.* [9] suggest that the adsorption behaviour of multicomponent alcohol systems is typically significantly different than that of their corresponding single alcohol systems. Since the alcohol-alkane streams produced in industry generally consist of various alcohols, it is important to also investigate multicomponent adsorption behaviour to determine the viability of adsorption as a method of purification for this specific application. An understanding of multicomponent adsorption of alcohol-alkane systems can therefore be very useful in industries such as the surfactant industry.

1.2 Problem Statement

Limited open research and data on the adsorption of 1-alcohols from n-alkanes exist. The available research and data mainly pertain to single component adsorption and not multicomponent adsorption; however, it is multicomponent adsorption that is predominantly employed in industry. A need therefore exists for an improved comprehension of the multicomponent adsorption of 1-alcohols from n-alkanes.

1.3 Research Objectives

The aim of this study is to gain knowledge and insight on the single and binary component adsorption of 1-alcohols from a n-alkane by using various industrially relevant activated alumina adsorbents. This aim will be satisfied through the following objectives:

(i) Measurement and investigation of single (one 1-alcohol) and binary (two 1-alcohols) component adsorption data for several 1-alcohol systems, using various activated alumina adsorbents.
   a. Comparison of the alcohol adsorption ability of three activated alumina adsorbents;
   b. Investigation of the effect of temperature on the adsorption of alcohols;
   c. Investigation of the effect of initial alcohol concentration on the adsorption of alcohols;
   d. Investigation of the effect of alcohol carbon chain length on the adsorption of alcohols;
   e. Comparison of single and binary component adsorption of alcohols; and,
   f. Investigation of possible interaction in the binary component adsorption of alcohols from an alkane.

(ii) Modelling of the equilibrium data for the single and binary component adsorption of 1-alcohols from an alkane using various activated alumina adsorbents.
   a. Modelling of single component adsorption data with various equilibrium isotherms;
   b. Modelling of binary component adsorption data with various equilibrium isotherms.

(iii) Modelling of the kinetic data for the single and binary component adsorption of 1-alcohols from an alkane using various activated alumina adsorbents.
   a. Modelling of single component adsorption data with various kinetic models;
   b. Modelling of binary component adsorption data with various kinetic models.

1.4 Research Approach

Both kinetic as well as equilibrium adsorption data were measured. This was done using a bench-scale batch experimental setup.

The data obtained from the experiments were compared at different temperatures, initial concentrations and alcohol chain lengths to determine the effect of changes in these variables. The data were modelled with various equilibrium isotherms, such as the Langmuir and Freundlich isotherms, to investigate the equilibrium behaviour of the different systems. The kinetics were investigated by modelling the experimental data with various kinetic models such as the pseudo-first and second-order models and the Intra-particle diffusion model.

The single and binary component adsorption results were compared to better comprehend the differences and the possible interaction in binary component systems. Collectively, this provided for a fair understanding

of the binary component adsorption behaviour and how it differs or compares to single component adsorption behaviour of 1-alcohols from an alkane.

1.5 Scope and Limitations

This study will build on the data and research of abovementioned study conducted by Groenewald [8]. Therefore, the same alcohol-alkane systems as investigated by Groenewald [8], *i.e.* 1-hexanol, 1-octanol and 1-decanol as 1-alcohol adsorbates and n-decane as solvent, will be investigated in this study. The adsorbents will also be the same as those used by Groenewald [8]: Activated Alumina F220, Selexsorb CDx® and Selexsorb CD®. Some of the data measured by Groenewald [8] will be used to allow for comparison with the data measured in this study as well as for the binary component equilibrium modelling. For this reason, the experimental setup in this study will also be similar to that used by Groenewald [8].

The alcohols and alkane as well as the adsorbents that will be used were selected such as to allow the current study to build on the available data for these systems. In addition to expanding the data and knowledge for these systems, the alcohols and alkanes are also relevant to the petrochemical industry, readily available and within an acceptable price range. The activated alumina adsorbents were also selected such as to expand available data on these specific systems. In addition, the use of activated alumina adsorbents has become increasingly more common for the adsorption of organic compounds, therefore aligning with this study. The alumina adsorbents selected are also specially formulated for the adsorption of organic compounds, amongst others.

As mentioned, adsorption equilibrium and kinetic behaviour will be investigated, by using a bench-scale batch adsorption setup. In practice, however, adsorption is generally done by use of adsorption columns. The adsorption process is therefore not only dependent on the adsorbate concentration and time, but also on the spatial variation within the column, described by adsorption dynamics [10]. Adsorption columns and dynamics, however, is beyond the scope of this study.

It is also important to note that this study focuses on the fundamental understanding of the adsorption process itself, *i.e.* investigating whether 1-alcohols can be adsorbed from an alkane using activated alumina and the behaviour of such systems, and not on the financial viability of such adsorption applications nor the regeneration of the investigated adsorbents.

1.6 Thesis Chapter Overview

Chapter 2 consists of a literature review and relevant theory on adsorption, adsorbents, the effects of different variables on adsorption, interaction in binary component systems, and equilibrium and kinetic models.

Chapter 3 provides an outline of the materials and methods used in study, with emphasis on the experimental design, analytical methods, reproducibility of data and uncertainty analysis.

Chapter 4 entails the adsorbent characterisation which investigates and compares the physical properties, such as surface area, pore volume and pore structure of the adsorbents investigated.

Chapter 5 addresses objective (i) and therefore encompasses the experimental results of the study, including the investigation and comparison of the alcohol adsorption abilities of the different adsorbents, investigation of the effects of different variables on the adsorption of alcohols from an alkane, a comparison of single and binary component adsorption behaviour and the investigation of possible interaction in binary component systems.

Chapter 6 discusses objective (ii) which provides insight into the equilibrium modelling of the systems investigated, by fitting various equilibrium isotherm models on the data.

Chapter 7 pertains to objective (iii) which entails the adsorption kinetic modelling of the alcohol-alkane systems, with emphasis on the rate-limiting step(s) of the various single and binary component systems.

Lastly, Chapter 8 encapsulates the findings of this study under ‘Conclusions’ and provides recommendations for future work.

Chapter 2: Literature Review

2.1 Adsorption Overview

Adsorption, a surface phenomenon [11], is the process of diffusion of a liquid or gas molecule (adsorbate) from a bulk solution to the surface of a solid particle (adsorbent) where it adheres to the surface of the solid particle either through physical forces or chemical bonds [7].

Since adsorption is a surface process, it can be quantified by surface concentration. The surface area of an adsorbent is, however, a difficult property to measure which results in adsorption typically being quantified as adsorbent loading [10]. Adsorbent loading is denoted by Equation 2.1-1 with q the adsorbent loading, $m_{adsorbate}$ the mass of adsorbate adsorbed and $m_{adsorbent}$ the mass of the adsorbent.

$$q = \frac{m_{adsorbate}}{m_{adsorbent}} \qquad [\ 2.1\text{-}1\ ]$$

Equation 2.1-1 can be rearranged and simplified to Equation 2.1-2, with V the volume of the solution, C_o (mg.mL^{-1}) the initial adsorbate concentration and C_t (mg.mL^{-1}) the adsorbate concentration at time t.

$$q_t = \frac{(C_o - C_t)V}{m_{adsorbate}} \qquad [\ 2.1\text{-}2\ ]$$

2.1.1 Adsorption Process

The adsorption process comprises three distinct steps [12], [13]:

(i) External mass transfer from the bulk solution, through the external boundary layer and onto the external surface of the adsorbent;

(ii) Intra-particle diffusion of the adsorbate from the external surface of the adsorbent, into the adsorbent pores and to the active adsorption sites; and,

(iii) Settling of the adsorbate molecules at active adsorption sites.

According to Worch [10], the first step described above can be further divided: (i) External mass transfer from the bulk solution to the external boundary layer surrounding the adsorbent particle; and, (ii) Mass transfer through the external boundary layer to the surface of the adsorbent.

2.1.1.1 *External Mass Transfer (EMT)*

External mass transfer (EMT) is the movement of adsorbate molecules from the bulk solution, over the external boundary layer surrounding the adsorbent and onto the external surface of the adsorbent [7] (Figure 2.1-1).

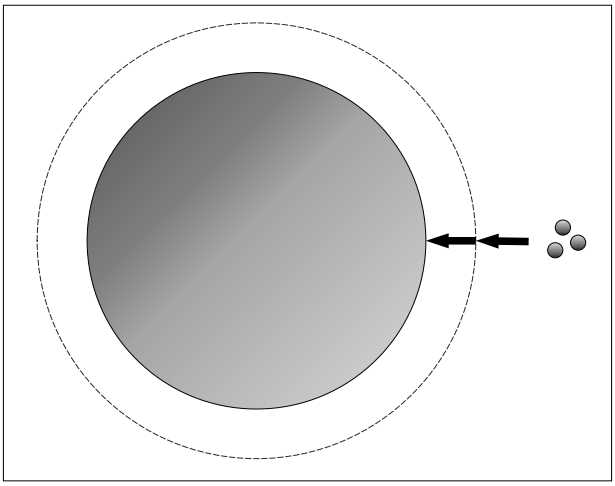

Figure 2.1-1: EMT of the adsorbate molecules from the bulk solution, over the external boundary layer (represented by the dotted line) surrounding the adsorbent particle and onto the surface of the adsorbent.

Several studies have established that mass transfer is predominantly a result of concentration gradient and that the rate of mass transfer has a very strong correlation to the surface area normal to the direction of movement [7]. Before equilibrium is reached, the adsorbate concentration on the adsorbent surface will always be less than the adsorbate concentration in the bulk solution which results in a driving force for EMT of the adsorbate particles through the external boundary layer [14]. The rate of EMT is therefore primarily dependent on the concentration gradient over the external boundary layer as well as the thickness of the boundary layer [12]. Equation 2.1-3 denotes the radial EMT flux with k_c being the mass transfer coefficient and C_{bulk} and $C_{surface}$ being the adsorbate concentration in the bulk solution and on the adsorbent surface respectively [12].

$$W_{EMT} = k_c(C_{bulk} - C_{surface}) \qquad [\ 2.1\text{-}3\ ]$$

EMT is very dependent on physical factors such as stirring speed of the bulk solution. A higher stirring speed will result in a thinner boundary layer and will enhance diffusion to and through the boundary layer [10].

2.1.1.2 *Intra-particle Diffusion (IPD)*

IPD is the movement of adsorbate particles from the external surface of the adsorbent into and through the pores of the adsorbent. Diffusion is a result of various driving forces such as concentration gradient, pressure, temperature and external forces [7]. In adsorption, IPD is predominantly a result of concentration gradient within the adsorbent particle itself [7] (Figure 2.1-2).

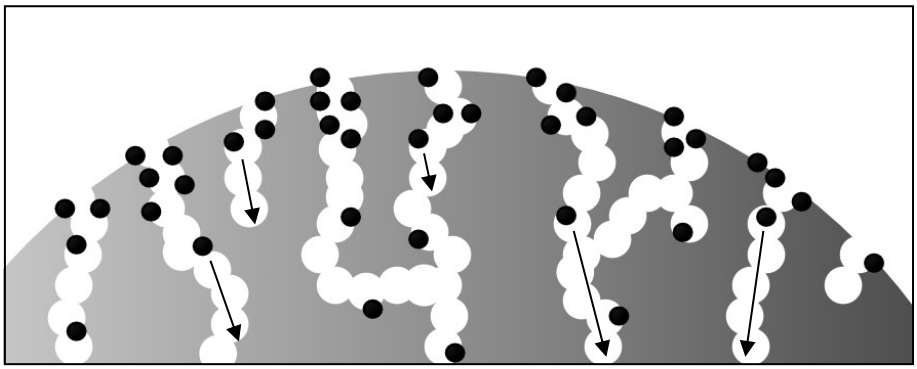

Figure 2.1-2: Intra-particle diffusion of adsorbate molecules from a high concentration on the adsorbent surface to a low concentration at the active adsorption sites inside the adsorbent pores

IPD can either be categorised as volume or surface diffusion, or a combination of both volume and surface diffusion [7], [15], [16]. Several studies have reported that surface diffusion is the predominant form of IPD [17].

2.1.1.2.1 Pore Volume Diffusion

Pore volume diffusion generally refers to the movement of adsorbate molecules through the liquid inside the adsorbent pores [18]. Porous adsorbents typically comprise macropores, mesopores and micropores. If this is the case, the macropores are used as transport pores for the adsorbate molecule to reach the micropores [19]. Movement of adsorbate molecules through the macropores is generally through pore volume diffusion [19].

In the case of the adsorbent pores having diameters markedly greater than that of the adsorbate molecules, the movement of these molecules can be attributed to collisions between the adsorbate molecules and the solvent molecules: molecular diffusion [18]. In the case of the adsorbent pores having diameters in the same range as that of the adsorbate molecules, the movement is attributed not only to collisions between the adsorbate and the solvent molecules but also to collisions between the adsorbate molecules and the adsorbent surface. It is important to note that in the latter case the collisions between the adsorbate molecules and the adsorbent surface will be predominant [18], [19]. During the last stages of diffusion, the adsorbate molecules migrate into the micropores of the adsorbent. Often the size of the adsorbate molecules are very close to that of the micropores, restricting movement of these molecules [19].

2.1.1.2.2 Surface Diffusion

Surface diffusion is the movement of an adsorbate molecule from one adsorption site to another. Surface diffusion is also referred to as surface hopping [20]. Okazaki *et al*. [21] proposed four different hopping mechanisms (Figure 2.1-3):

(i) Hopping from an unoccupied site to an unoccupied site;

(ii) Hopping from an unoccupied site to an occupied site;

(iii) Hopping from an occupied site to an unoccupied site; and

(iv) Hopping from an occupied site to an occupied site.

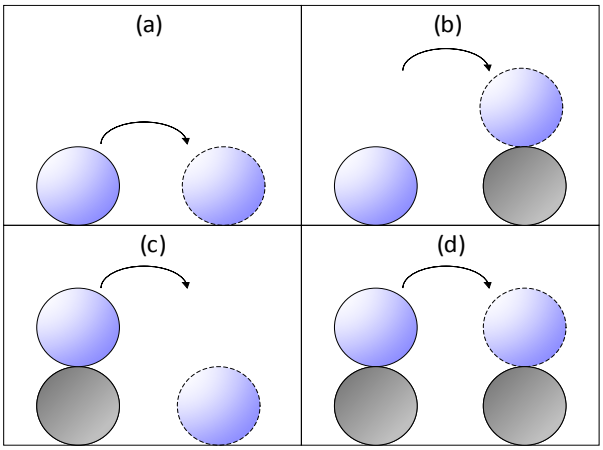

Figure 2.1-3: Surface diffusion hopping mechanisms as proposed by Okazaki et al.; Hopping of adsorbate molecule from: (a) an unoccupied site to an unoccupied site; (b) an unoccupied site to an occupied site; (c) an occupied site to an unoccupied site; and, (d) an occupied site to an occupied site (redrawn from [21])

Surface diffusion or surface hopping is highly dependent on the surface energy fluctuations of the adsorbent, that is, "the heat of adsorption and the activation energy of migration" [19]. In the case of the activation energy dividing two adjacent active sites being less than the heat of adsorption, the possibility exists for an adsorbate molecule to hop from one active site to another [19] (Figure 2.1-4).

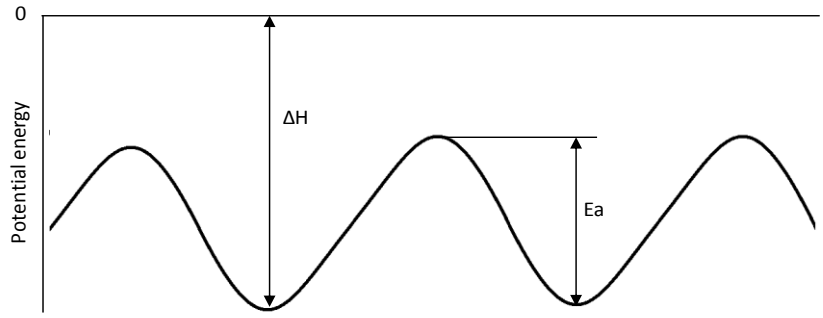

Figure 2.1-4: Energy distribution on the surface of porous adsorbents (ΔH denotes the heat of adsorption and E_a the activation energy) (redrawn from [19])

2.1.1.3 *Equilibrium Reaching Adsorption Stage*

Final adsorption in this study refers to the adsorbate molecules settling at an active adsorption site within the pores of the adsorbent. Adhesion of the adsorbate to the adsorbent surface can either be a result of physical forces or chemical bonds that form between the adsorbate and the adsorbent surface [7].

2.1.1.3.1 Chemical Adsorption

Adhesion through chemical bonds is called chemisorption [7]. Chemisorption is generally stronger than physisorption with an enthalpy of adsorption of between approximately -40 and -400 kJ.mol^{-1} [11]. Due to the large enthalpy of adsorption, bonds will not easily break due to adsorbate molecule vibrations. This essentially deems chemisorption an irreversible process at low temperatures such as room temperature [11]. Weak chemisorption, however, can be a reversible process in some cases. Chemisorption occurs in monolayer since the adsorbate and adsorbent surface need to be in contact for a chemical bond to form [22]. Therefore, after all vacant adsorption sites on the adsorbent surface have bonded with adsorbate molecules, the process of chemisorption will cease [22].

2.1.1.3.2 Physical Adsorption

Adhesion as a result of physical forces is referred to as physisorption [7]. These physical forces are van der Waals forces: attraction between the adsorbate and the adsorbent as a result of weak electrostatic interactions [11]. Physisorption can only occur if the adsorbate molecules connect the adsorbent surface at an energy low enough for the adsorbent to partially absorb some of the energy and for the rest to dissipate as heat, thereby allowing the adsorbate molecule to adhere to the adsorbent surface [11], [20]. If the energy with which the adsorbate connects the surface is too high, the adsorbate molecule will bounce off [11]. As a result of the concomitant low energy of physisorption (enthalpy of approximately -20 kJ.mol^{-1}) , the process is typically unstable [11].

Similar to any surface, adsorbent surfaces have energy fluctuations with troughs and peaks [20]. The troughs of the periodic energy fluctuations act as active adsorption sites and the adsorbate molecules adhere to these sites (Figure 2.1-5).

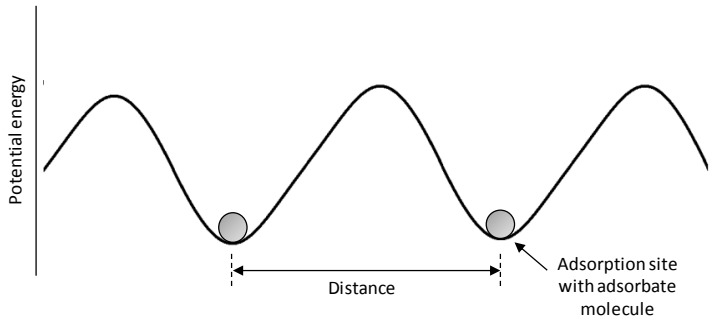

Figure 2.1-5: Schematic diagram of the energy fluctuations on an ideal adsorbent surface (redrawn from [20]).

Localised adsorption, *i.e*. one adsorbate molecule per active adsorption site, occurs when the distance between two adjacent troughs are notably greater than the diameter of the adsorbate molecule [20]. Physisorption allows for multilayer adsorption however as expected, the strength of adsorption significantly

decreases with increasing number of adsorbate layers [7]. According to a study conducted by Mohamed [23], multilayer adsorption typically occurs in the macro- and mesopores of adsorbents.

2.2 Adsorbents

A vast number of different adsorbents are being used in adsorption applications today. Adsorbents are chosen based on several properties such as: polarity; surface functional groups; surface area; pore volume; pore structure; and, pore size. Some of the most widely used adsorbents in use today are activated carbon, silica gel, zeolites and activated alumina.

2.2.1 Types of Adsorbents

2.2.1.1 *Activated Carbon*

Activated carbon is a treated material that can be derived from a vast number of carbonaceous sources. These sources include materials such as coal, wood, organic waste material, nut shell and petroleum residues [7], [24]. Treatment of these materials includes either physical or chemical activation, whereby the porosity of the material is enhanced [25].

Activated carbon is generally considered to be nonpolar (hydrophobic), however, depending on the initial source from which the adsorbent was derived, activated carbon may sometimes have oxygen functional groups present on its surface [22]. This causes a slight polarity, which means activated carbon may also be organophilic in some cases [22], [26]. Due to its hydrophobic/organophilic nature, activated carbon is often used for applications such as removing organic contaminants from water, however, since it is a very effective adsorbent it is also used for various other applications such as gas purification, solvent recovery and air purification [19], [22], [26].

2.2.1.2 *Silica Gel*

Silica gel typically comes in the form of milky white, glassy beads and essentially has the chemical formula of $SiO_2.nH_2O$. This adsorbent can be produced through various processes, one being through the "coagulation of a colloidal solution of silicic acid" [20]. Silica gel is highly polar and hydrophilic, due to hydroxyl functional groups present on its surface [19]. As a result of the hydrophilicity of silica gel, it is most widely used as a desiccant, *i.e.* for the removal of water [19], [20].

2.2.1.3 *Zeolites*

Zeolites are "porous crystalline aluminosilicates" [20]. These adsorbents can either be manufactured synthetically or in some cases found naturally, however, synthetically manufactured zeolites are more widely used due to their specificity [20]. The pore structure of the adsorbent is dependent on the crystal lattice and is therefore uniform with no pore size distribution [20].

Zeolites contain both alumina as well as silica in varying ratios, however, with a Si/Al ratio never lower than 1 [22]. Should the separation application require the adsorbent to be highly polar or have a high affinity for water, the zeolite adsorbent will be alumina rich, whereas if the application requires the adsorbent to be more hydrophobic, the adsorbent will be more silica rich since silica in its pure form is nonpolar [22].

2.2.1.4 *Activated Alumina (AA)*

AA is essentially porous aluminum oxide (Al_2O_3) [22]. It is most commonly derived from bauxite ($Al_2O_3.3H_2O$) which is a rock typically consisting of hydrated aluminum oxides and aluminum hydroxides such as diaspore (α-AlO(OH)), gibbsite (γ-$Al(OH)_3$) and boehmite (γ-AlO(OH)) [19], [27]. The aluminum hydroxides are extracted from the bauxite through the Bayer process after which it is thermally dehydrated and recrystallized at high temperatures [28]. Different forms of AA can be manufactured with the most widely used form being the γ-alumina due to its high porosity, large surface area and resistance to high temperatures [19].

AA is typically produced in the form of white spherical beads. It is known to be very resilient as it does not change form (soften, disintegrate, swell or shrink) when placed in a solvent [27]. According to Bowen *et al*. [29], several studies have reported that the structure of AA either comprises "agglomerates of spherical particles, fibrils and/or plate-like layers". The structure of the AA adsorbent is highly dependent on the raw materials from which it is derived and the method used to synthesise the adsorbent [30]. Similarly, the physical properties of AA are also dependent on the method of synthesis and the activation method used. Table 2.2-1 summarises the physical properties of different examples of AA, as obtained from literature.

Table 2.2-1: Physical properties of activated alumina

Properties	[19]	[7]	[31]
Specific surface area (m^2/g)	150-500	320	200-300
Pore radius (nm)	1.5-6	1-7.5	1.8-3
Porosity	0.4-0.76	0.5	0.7-0.77
Particle density (g/cm^3)	0.8-1.8	1.25	0.65-1

AA is highly polar and typically has numerous functional groups present on its surface [22]. It can be tailored for a specific application: AA used for the adsorption of oxygenates typically have a low sodium content and high Lewis acidity which allows for Lewis bases such as alcohols to interact with the surface of the adsorbent [32]. AA can be used for several applications with two being the removal of water content from gas streams, *i.e*. used as a desiccant, and the removal of organics from hydrocarbon streams [19], [22].

2.2.2 Project Specific Adsorbents

The use of AA for the adsorption of organic compounds has become increasingly more common, partly due to its versatility and resilience.

The adsorbents investigated in this study were provided by BASF through the UDEC Group. BASF manufactures several adsorbents including alumina, silica and alumina-silica gels. Among others, BASF has two alumina ranges: F200 and Selexsorb®. For this study, three adsorbents were selected from these ranges: Activated Alumina F220 (AA-F220), Selexsorb CDx® (SCDx) and Selexsorb CD® (SCD).

2.2.2.1 *Activated Alumina F220* [33]

AA-220 is generally used as a desiccant, *i.e.* for the drying of various gas and liquid streams. AA-F220 is also known to be very polar. Therefore, it has a very high affinity for polar compounds and will preferentially adsorb the highest polarity molecules. When AA-F220 comes in contact with a solution containing n-decane and 1-alcohols, it should in theory preferentially adsorb the 1-alcohols since these are the polar compounds in the solution. This is in line with the focus of this study which hypothesises that AA-F220 would be a suitable adsorbent.

AA-F220 has serval benefits associated with it. These benefits include its uniform ball size, high crush strength, low abrasion and high adsorptive capacity. AA-F220 has a good cyclic stability meaning it allows for regeneration of the adsorbent [33] and can therefore yield a long lifespan.

2.2.2.2 *Selexsorb CDx®* [34]

SCDx is Al_2O_3 combined with a proprietary modifier. The SCDx adsorbent is specifically formulated for the adsorption of polar organic compounds. These polar organic compounds include:

(i) Sulfur-based molecules (mercaptans, sulfides, disulfides and thiophenes);
(ii) Nitrogen-based molecules (nitriles, amines, amides and pyridines); and,
(iii) Oxygenated hydrocarbon molecules (alcohols, glycols, aldehydes, ketones, ethers and peroxides).

BASF's SCDx is also custom-formulated for the removal of oxygen-based organic contaminants from liquid hydrocarbon streams. The current study essentially focuses on the removal of oxygenated hydrocarbons, *i.e.* 1-alcohols, from a hydrocarbon solvent, *i.e.* n-decane. In theory, SCDx should therefore be a suitable adsorbent for the systems that will be investigated in this study.

2.2.2.3 ***Selexsorb CD®*** [35]

Similar to SCDx, SCD is also Al_2O_3 with a proprietary modifier. The SCD adsorbent is specifically formulated for the adsorption of polar compounds. These include:

(i) Water;
(ii) Oxygenated hydrocarbons (alcohols, aldehydes, ketones, ethers and peroxides);
(iii) Mercaptans;
(iv) Sulfides; and,
(v) Nitrogen-based molecules (ammonia, amines and nitriles).

Similar to SCDx, one of the more specific custom applications for SCD is the adsorption of oxygenated organic compounds, such as alcohols, from hydrocarbon feed streams produced in industries such as the petroleum industry. This is in line with the focus of this study. Therefore, SCD should in theory also be suitable for the systems that will be investigated in this study.

2.3 Adsorption of Organics

Little open data exist on the adsorption of 1-alcohols from an alkane using AA adsorbents. There is, however, one study that specifically investigated the single component adsorption of 1-alcohols from n-decane using various alumina adsorbents. This study was conducted by Groenewald [8]. The systems investigated were 1-hexanol, 1-octanol and 1-decanol in an n-decane solvent, using AA-F220, SCDx an SCD as adsorbents. Adsorption was investigated for various initial adsorbate concentrations and temperatures.

After an extensive literature review, no open data were found (to the author's knowledge) investigating the binary component adsorption of 1-alcohols from n-decane using abovementioned three adsorbents; thus, introducing a lacuna which this study will attempt to fill. The study conducted by Groenewald [8] also provides data and findings upon which this study can build. Expanding the initial adsorbate concentration and temperature ranges for the single component adsorption could also further contribute to the data of these specific systems.

2.4 Variables Influencing Adsorption

Adsorption is dependent on several variables such as operating temperature, the initial concentration of adsorbate in the bulk solution and the properties of the specific adsorbate. The effect of these variables on the adsorption of 1-alcohols from n-decane was also investigated by Groenewald [8], which allows for further research to build upon the knowledge gained in that study.

2.4.1 Temperature

The effect of temperature on any adsorption process is dependent on the specific system, *i.e.* whether adsorption occurs through chemisorption or physisorption.

Chemisorption is (mostly) exothermic and governed by strong valence forces between adsorbate molecules and the adsorbent [12]. According to Le Chatelier's principle, adsorption will decrease with an increase in temperature [12]. For chemisorption systems, however, it has been widely reported that adsorption first increases with an increase in temperature up to a certain maximum temperature, after which it then obeys Le Chatelier's principle and starts to decrease. This is due to the activation energy associated with chemisorption. At low temperatures, kinetics controls the adsorption process since the system does not possess the required activation energy for chemisorption. As temperature increases the energy of the system increases allowing for more adsorbate molecules to achieve the activation energy required to break the intramolecular bonds, and form bonds with the adsorbent surface, which in turn results in an increase in adsorbent loading [36]. When a temperature is reached that provides sufficient energy to the system, thermodynamics will start to govern the adsorption process and Le Chatelier's principle will be obeyed [36]. Thus, a decrease in adsorbent loading is observed for an increase in temperature.

Physisorption is also an exothermic process governed by weak Van der Waals forces [12]. According to Le Chatelier's principle, adsorption for physisorption systems will decrease with increasing temperature [12]. Figure 2.4-1 depicts how temperature typically affects a physisorption and chemisorption system.

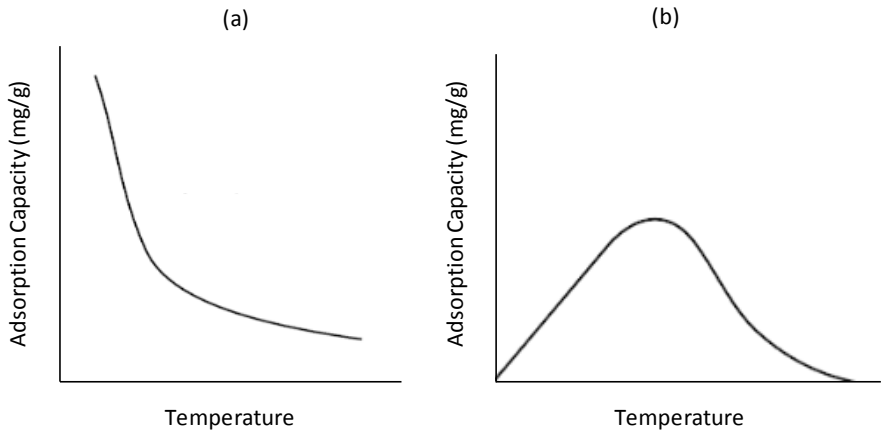

Figure 2.4-1: Typical effect of temperature on the equilibrium adsorbent loading of a (a) physisorption; and, (b) chemisorption system (redrawn from [36])

For the single component systems containing either 1-hexanol, 1-octanol or 1-decanol in n-decane, Groenewald [8] found that adsorption of these alcohols increased with an increase in temperature, in the range of 25°C to 35°C, and reported that 35°C was the optimum temperature for achieving maximum equilibrium adsorbent loadings. This allows for further research, to determine whether adsorbent loadings

will increase for temperatures beyond the range investigated by Groenewald [8] or whether adsorbent loadings for these 1-alcohols will start to decrease in accordance with Figure 2.4-1 when increasing the temperature above 35°C.

2.4.2 Initial Adsorbate Concentration (IC)

In liquid systems, the concentration of the adsorbate in the bulk solution is of much importance. The adsorbate concentration acts as a driving force for mass transfer [14]. It has been widely reported that adsorbent loading increases with increasing initial adsorbate concentration up to a certain point; this is generally attributed to adsorbent saturation and/or interaction between the adsorbed molecules and the molecules remaining in the bulk solution.

Groenewald [8] reported an increase in 1-alcohol adsorption for an increase in initial alcohol concentration in the concentration range of 0 to 2 mass% (200 mL solution). Further investigation may reveal whether adsorption will continue to increase when increasing initial alcohol concentration beyond the range investigated by Groenewald or whether it will start to plateau at some initial adsorbate concentration.

2.4.3 Alcohol Chain Length

The chain length of alcohols can have an effect on the adsorption process due to a change in size of the adsorbate molecules and due to possible changes in the behaviour of the alcohols in the bulk solution.

As the chain length of an alcohol increases, the size of the molecule also increases which in turn affects its movement through the pores of the adsorbent. This has been reported in several studies including that of Hsieh and Teng [37] where they showed that a smaller sized adsorbate exhibited a greater adsorbent loading when compared to a larger sized adsorbate. The smaller sized adsorbate was thought to experience less interference when diffusing through the micropores of the adsorbent, hence resulting in better adsorption [37].

Groenewald [8] established that 1-hexanol adsorbed the most effectively from n-decane, when compared to 1-octanol and 1-decanol. The research, however, does not report on the effect of carbon chain length for combinations of 1-alcohols which reveals a lacuna, allowing for further research. Based on the knowledge gained from the study conducted by Groenewald [8], it is expected that binary combinations of 1-alcohols with shorter combined carbon chain lengths exhibit better adsorption than combinations of 1-alcohols with longer combined chain lengths.

2.5 Interaction Effect in Binary Component Systems

In a multicomponent adsorption system, the adsorbates in the solution can either interact with one another or adsorb without interaction. A means of identifying the type of interaction in a multicomponent system is

comparing the equilibrium adsorbent loading of a component in a single component system (q_e) with that of the same component in a multicomponent system ($q_{e,i}$) while maintaining a constant initial concentration for that specific adsorbate. This is denoted by the interaction parameter, $R_{q,i}$ (Equation 2.5-1).

$$R_{q,i} = \frac{q_{e,i}}{q_e} \qquad [\ 2.5\text{-}1\ ]$$

Adsorbate-adsorbate interaction is typically divided into three categories [38], [39]:

(i) Synergistic interaction: The equilibrium adsorbent loading of component "*i*" is greater in the multicomponent system than in the single component system, *i.e.* $R_{q,i} > 1$.

(ii) Antagonistic interaction: The equilibrium adsorbent loading of component "*i*" is less in the multicomponent system than in the single component system, *i.e.* $R_{q,i} < 1$, thereby implying competitive adsorption.

(iii) Non-interaction: The presence of additional adsorbates has no effect on the adsorbent loading of component "*i*", *i.e.* $R_{q,i} = 1$.

The interaction effect in multicomponent systems have been widely investigated. Several studies have investigated the interaction effect for wastewater streams containing metal ions and dyes [40]. In a study conducted by Moreno-Pérez *et al.* [40], it was proved that the presence of AB25 dye enhanced the adsorption of metal ions thereby resulting in synergistic interaction, whereas some other dyes had an antagonistic effect on the adsorption of metal ions. Clegg *et al.* [41] investigated the synergistic and competitive aspects of the adsorption of polyethylene glycol and polyvinyl alcohol onto Na-Bentonite and found that the presence of polyethylene glycol enhanced the adsorption of polyvinyl alcohol, suggesting synergistic adsorption. Another study by Fu *et al.* [42] investigated the effects of alcohols and hydrocarbons on the adsorption of sulfonate surfactants onto alumina from a water solvent. This study reported that the presence of dodecane significantly increased the adsorption of surfactants, whereas it decreased with the addition of propanol [42]. According to this study, the alcohols decreased the adsorption of the sulfonate surfactants as a result of enhancing the attractive forces between the surfactant and the water solvent [42]. Unfortunately, to the author's knowledge, no work has been done on the interaction effect in an adsorption system comprising 1-alcohols, an alkane and AA. This introduces another lacuna, potentially to be filled by this study.

2.6 Adsorption Equilibrium Modelling

Equilibrium adsorbent loading can be predicted through the use of adsorption isotherm models [10]. According to the literature review, the most widely employed isotherm models are the Langmuir and Freundlich models [43], [44]. Equilibrium isotherm models are merely used to correlate and predict adsorption data and the information obtained from isotherms, *i.e.* verification of concomitant assumptions, is speculative and should be investigated further [18].

2.6.1 Single Component Adsorption

For the single component adsorption, four isotherm models were investigated in this study: Langmuir, Freundlich, Sips and Redlich-Peterson.

2.6.1.1 *Langmuir Isotherm Model (LM)*

The LM was first introduced by Irvin Langmuir in 1918 for the adsorption of gasses onto glass, mica and platinum [43]. The LM is generally used to describe monolayer adsorption onto an ideal adsorbent surface and is based on the kinetic principle that the rate of adsorption onto the surface of the adsorbent is equal to the rate of desorption from the surface [20].

The model is denoted by Equation 2.6-1, with q_e and q_{max} the equilibrium and maximum adsorbent loadings respectively (q_{max} is the adsorbent loading for complete monolayer adsorbent surface coverage), K_L the Langmuir or affinity constant and C_e the equilibrium adsorbate concentration in the bulk solution. For the derivation of LM, refer to Do [20] or Tien [18].

$$q_e = \frac{q_{max} K_L C_e}{1 + K_L C_e} \qquad [\ 2.6\text{-}1\ ]$$

The LM is based on the following assumptions [18], [20], [22]:

(i) The adsorbent surface is energetically homogenous, *i.e.* the heat of adsorption is constant for all adsorption sites on the adsorbent surface;
(ii) Only monolayer adsorption occurs;
(iii) Each active adsorption site is occupied by one adsorbate molecule only; and,
(iv) The adsorbed adsorbate molecules do not interact.

2.6.1.2 *Freundlich Isotherm Model (FM)*

FM was one of the first empirical mathematical approximations for the modelling of equilibrium adsorption data, used by Freundlich [44]. This model is typically used to model adsorption onto energetically heterogenous surfaces and is widely reported to be suitable for the description of organics from aqueous solutions [20]. In addition, the FM is generally used for non-ideal reversible adsorption systems [45].

The FM is denoted by Equation 2.6-2 with K_F the Freundlich constant and n an empirical parameter. Both K_F and n are temperature dependent: K_F as well as n decrease with increasing temperature [20]. The parameter, n, is indicative of adsorption intensity, *i.e.* $n > 1$ suggests favourable adsorption whereas $n < 1$ suggests poor adsorption [46]. Very high values of n, *i.e*. approaching 10, suggests an irreversible adsorption process, since the adsorbate concentration has to drop very low for the adsorbate molecules to desorb after adsorption [20]. Refer to Do [20] for a derivation of FM.

$$q_e = K_F C_e^{\frac{1}{n}} \qquad [\ 2.6\text{-}2\ ]$$

The FM is based on the following assumptions [20]:

(i) The adsorbent surface is energetically heterogenous: the active adsorption sites with identical adsorption energy are grouped together;

(ii) There is no interaction between the groups of adsorption sites; and,

(iii) Each adsorption site is only occupied by one adsorbate molecule.

Though widely applied, FM is limited in its use: it can only be used below the saturation concentration since the model does not have a limit on the adsorbent loading, *i.e.* the adsorbed phase can increase to infinity with increasing adsorbate concentration which is not an accurate description [19], [20].

2.6.1.3 *Sips Isotherm Model (SM)*

The SM, also referred to as the Langmuir-Freundlich isotherm, was first proposed by Sips in 1948 [47]. The SM is similar to the LM but incorporates the *n*-parameter of the FM. Sips proposed this model in order to incorporate a limit on the adsorbent loadings determined by the FM [20]. It is generally applied to heterogenous systems [45]. Additionally, the SM is widely used for the description of hydrocarbon adsorption onto activated carbon [18].

The SM is denoted by Equation 2.6-3 with K_s the Sips constant which is related to the energy of adsorption and *n* a parameter related to the heterogeneity of the specific adsorbent [48]: should *n* be unity, SM simplifies to the LM which indicates that the adsorbent surface is homogenous [49].

$$q_e = \frac{q_{max} C_e^{\frac{1}{n}}}{1+(C_e)^{\frac{1}{n}}} \qquad [\ 2.6\text{-}3\ ]$$

2.6.1.4 *Redlich-Peterson Isotherm Model (RPM)*

The RPM was first introduced by Redlich and Peterson in 1959 [50]. This is a three-parameter isotherm incorporating the characteristics of both the LM ad FM [45]. Since this isotherm incorporates both the LM and FM characteristics, it can be applied to both energetically homogenous as well as heterogenous adsorbent surfaces.

The RPM is denoted by Equation by 2.6-4 with K_{RP} and a_{RP} the Redlich-Peterson constants and *n* the model exponent. For *1/n* = 1 the model simplifies to LM, therefore K_{RP}/a_{RP} becomes equal to the monolayer maximum adsorption capacity (q_{max}) as determined by LM and for very high concentrations the model simplifies to FM [48]. Consequently, the model is not constrained to monolayer adsorption, but can represent monolayer or multilayer adsorption [51].

$$q_e = \frac{K_{RP} C_e}{1 + a_{RP} (C_e)^{\frac{1}{n}}} \qquad [\ 2.6\text{-}4\ ]$$

2.6.1.5 *Comparison of Single Component Isotherm Models*

Figure 2.6-1 depicts the LM, FM, SM as well as RPM isotherms in their typical form. The most notable difference is between the LM and FM where it is clear that the LM reaches an equilibrium stage, whereas the FM continues to increase with increasing adsorbate concentration, as discussed in Section 2.6.1.2. The SM and RPM are dependent on the specific system being modelled and can therefore change form, *i.e*. it can look more like the LM or more like the FM. These two isotherms will, nonetheless, look relatively similar to one another for a specific set of data.

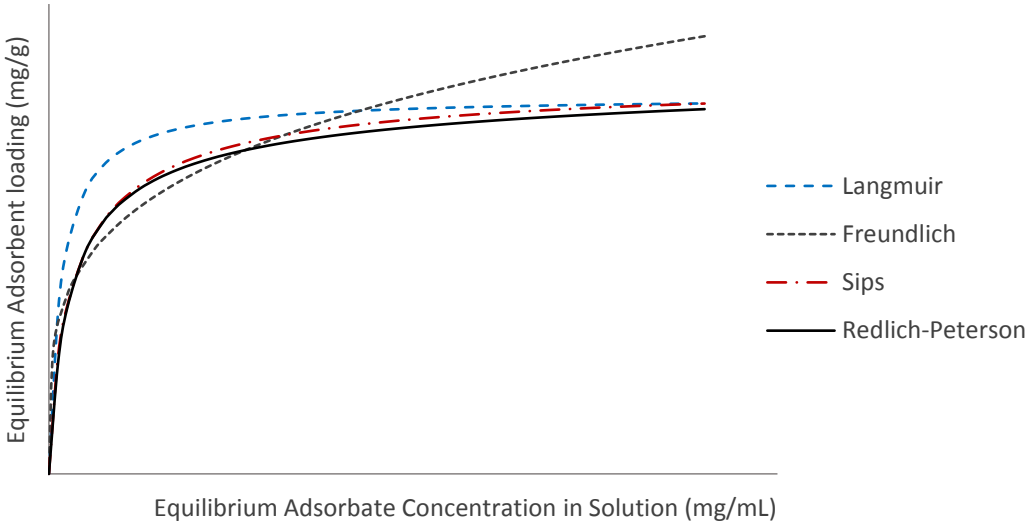

Figure 2.6-1: Typical form of the Langmuir; Freundlich; Sips; and, Redlich-Peterson isotherm models

Little research exists on the adsorption equilibrium modelling of 1-alcohols from alkanes by using AA as adsorbent. A few isotherm models reported for the prediction of adsorption data using AA include a Langmuir/BET model [52] as well as a proposed multilayer model [53] for water vapour adsorption, LM for the adsorption of sulphur from model oil [54] and fluoride from drinking water [55] and both the LM and FM isotherms for the adsorption of arsenite and arsenate also from drinking water [56], [57]. These are, however, not truly comparable with the systems investigated in this study.

2.6.2 Binary Component Adsorption

Several studies have reported that the adsorption behaviour of binary component systems are notably different than that of the corresponding single component systems [9]. In the case of multicomponent adsorption, single component isotherms are not satisfactory for describing the adsorption process as there are many factors which they do not account for [58]. The primary factor being interference and possible

competition for adsorption sites [59]. Competitive adsorption typically occurs when two or more adsorbates compete for the same active adsorption site, whereas non-competitive adsorption is typically when one adsorbate in a mixture of more than one only settles at active adsorption sites not occupied by another adsorbate. Competitive adsorption depends on many factors with one of the most important factors being the rate of adsorption of the respective adsorbates in the multicomponent mixture [60].

Some of the most commonly used multicomponent adsorption isotherm models are:

(i) Different forms of the Langmuir isotherm model;

(ii) Extended Freundlich isotherm model;

(iii) Sips model for multicomponent systems; and,

(iv) Redlich-Peterson models for multicomponent systems.

Multicomponent systems are not only dependent on the equilibrium adsorbate concentration of one adsorbate, but on that of various different adsorbates. This is indicated by a summation in the models, which recognises the presence of more than one adsorbate. The summation present in the models discussed below represents components "*i*" through "*j*" in the system.

2.6.2.1 ***Langmuir Isotherm Model***

Various forms of the LM have been developed for the description of multicomponent, and in some cases, specifically binary component adsorption systems.

2.6.2.1.1 Non-modified Competitive Langmuir Model

The Non-modified LM was suggested by Markham and Benton [61] in 1931 for the adsorption of gas mixtures onto silica. The model for the different components in a multicomponent system is expressed by Equation 2.6-5, with the same assumptions as for the pure component LM.

$$q_{e,i} = \frac{(q_{i,max} K_{L,i} C_{e,i})}{1+\sum K_{L,j} C_{e,j}} \qquad [\ 2.6\text{-}5\ ]$$

The parameter $q_{max,i}$ and the Langmuir constant, $K_{L,i}$, are obtained from the single component adsorption systems of the respective adsorbates [62]. By using the single component adsorption system parameters, interaction between the adsorbates as well as between the adsorbate molecules and the adsorbent surface is neglected to some extent [58], [63]. As mentioned, the K_L parameter in the LM corresponds to the affinity of the specific adsorbate which may be affected in a solution with more than one adsorbate resulting in inaccurate predictions [62].

This model also assumes that all adsorption sites are equally accessible to all adsorbate molecules. Wurster *et al.* [64] pointed out that the Non-modified LM would therefore not provide an accurate characterisation

of a binary component adsorption system should adsorption of one adsorbate in the solution occur at adsorption sites not accessible to the other adsorbate in the solution. A study conducted by Allen *et al.* [65] suggested that this model provides relatively accurate predictions at higher adsorbent loadings, but cannot be used to predict lower monolayer capacities of components in binary systems. Allen *et al.* [65] also pointed out that the assumptions on which the Non-modified LM is based were invalid for the adsorption of basic dyes onto peat which resulted in the model not being a good fit. The assumptions of the Non-modified LM should therefore be carefully validated when applying this model.

Even though this model is widely used due to its simplicity, it has been indicated by Broughton [66] that this model is only thermodynamically consistent for the case where the adsorbent loadings of the different adsorbates are equal. This statement was verified by both Ruthven [22] and Lim *et al.* [67] who proved that the Non-modified LM approach does not comply with the Gibbs-Duhem thermodynamic relationship should the adsorbent loadings for the respective adsorbates not be equal.

2.6.2.1.2 Extended Langmuir Model with Adjusted Binary Parameters

A previous study conducted by Kurniawan *et al.* [62] on the adsorption of dyes suggested a new mathematical model which incorporates the fractional loading of the respective adsorbates on the adsorbent surface. The Extended LM is denoted by Equation 2.6-6 with the model parameters determined with Equations 2.6-7 through 2.6-9.

$$q_{e,i} = \frac{q_{\max(bin)} K_{L,i(bin)} C_{e,i}}{1+\sum K_{L,j(bin)} C_{e,j}} \qquad [\ 2.6\text{-}6\ ]$$

$$q_{\max(bin)} = q_{\max,1(\sin)}\theta_1 + q_{\max,2(sin)}\theta_2 \qquad [\ 2.6\text{-}7\ ]$$

$$K_{L,1(bin)} = K_{L,1(\sin)} e^{-\frac{\theta_2}{\theta_1}} \qquad [\ 2.6\text{-}8\ ]$$

$$K_{L,2(bin)} = K_{L,2(sin)} e^{-\frac{\theta_1}{\theta_2}} \qquad [\ 2.6\text{-}9\ ]$$

The parameter θ corresponds to the fractional adsorbent surface coverage, *i.e.* fractional loading, and the selectivity of each respective adsorbate [68]. Since the different adsorbate molecules compete for active adsorption sites, θ adjusts the single component parameters (q_{max} and K_L) accordingly to incorporate the effect of interaction in a binary system [62], [68]. The model is fitted to the binary experimental data to determine θ_i. Competition for active adsorption sites theoretically decreases the adsorbate affinity which in turn results in lower affinity constants (K_L) for adsorbates in the binary component system in comparison to the corresponding single component systems [69].

2.6.2.1.3 Modified Langmuir Isotherm Model

In 1975, Mathews and Crittenden [70] suggested the Modified LM, denoted by Equation 2.6-10 with η the interaction parameter. The interaction parameter was incorporated to provide a correlation between single and binary component adsorption data while accounting for interaction between adsorbates in the adsorbed phase.

$$q_{e,i} = \frac{q_{i,max} K_{L,i} \left(\frac{C_{e,i}}{\eta_i}\right)}{1 + \sum K_{L,j} \left(\frac{C_{e,j}}{\eta_j}\right)} \qquad [\ 2.6\text{-}10\ ]$$

Single component Langmuir parameters, $q_{i,max}$ and $K_{L,i}$, may not accurately describe the interaction between the adsorbates, and the adsorbates and adsorbent, necessitating the interaction parameter [71]. The interaction parameter is specific to each component and adjusts the equilibrium concentration based on the amount of each species in the solution [71]. This parameter is determined by fitting the model to the multicomponent adsorption data.

Even though the Modified LM has been reported to provide relatively accurate predictions for adsorbate compounds with similar adsorbent loadings, Choy *et al.* [72] points out that there are several weaknesses associated with this model; one being the weak theoretical foundation of η. Nonetheless, Choy *et al.* [72] also reported a notable improvement in predicting adsorption data of acid dyes onto activated carbon by the Modified LM over the Non-modified LM and the Extended LM.

2.6.2.2 *Extended Freundlich Isotherm Model*

The Extended FM is an empirical relation proposed by Fritz and Schlunder [73]. As for the pure component adsorption isotherm, the Extended FM is typically applied to heterogenous adsorption systems with interaction between molecules in the adsorbed phase [38]. Equation 2.6-11 denotes the model with *x, y* and *z* the correlative binary system parameters and $K_{F,i}$ and n_i parameters derived from the respective corresponding single component FM isotherms [73].

$$q_{e,i} = \frac{K_{F,i} C_{e,i}^{n_i + x_i}}{C_{e,i}^{x_i} + y_i C_{e,j}^{z_i}} \qquad [\ 2.6\text{-}11\ ]$$

2.6.2.3 *Extended Sips Isotherm Model*

The Extended SM is typically used for heterogenous adsorption systems [22], [38]. As for the pure component SM, the model simplifies to a multicomponent LM at higher concentrations as a result of the parameter *n* approaching unity. This can be indicative of the heterogeneity of the system. Though this model typically fits the data of heterogenous systems well, it is not constrained to heterogeneous systems as it comprises both characteristics of the LM as well as FM.

The Extended SM is denoted by Equation 2.6-12 with $q_{max,i}$ and $K_{s,i}$ obtained from the respective single component SM isotherms [22]. The parameter n is obtained from fitting the model to multicomponent adsorption data.

$$q_{e,i} = \frac{q_{ma,i} K_{S,i} C_{e,i}^{\frac{1}{n}}}{1+\sum_{j=1}^{n} K_{S,i} C_{e,i}^{\frac{1}{n}}} \qquad [\ 2.6\text{-}12\ ]$$

2.6.2.4 *Multi-component Redlich-Peterson Isotherm*

The RPM can be applied to a large adsorbate concentration range [38]. Similar to the RPM for single component adsorption, this isotherm is a hybrid and as a result does not obey ideal monolayer adsorption [45]. According to some studies, this isotherm can be used to describe systems exhibiting either monolayer or multilayer adsorption [51].

2.6.2.4.1 Non-modified Competitive Redlich-Peterson Isotherm Model

The model is denoted by Equation 2.6-13 with the RPM constant (K_{RP}) and the other model constants (a_{RP}, n) obtained from the corresponding single component RPM isotherms of the respective adsorbates [38]. A draw-back of the Non-modified RPM is that it does not have an interaction parameter.

$$q_{e,i} = \frac{K_{RP,i} C_{e,i}}{1+\sum_{j=1}^{n}\left(a_{RP,j} C_{e,j}^{\frac{1}{n_j}}\right)} \qquad [\ 2.6\text{-}13\ ]$$

2.6.2.4.2 Modified Competitive Redlich-Peterson Isotherm Model

To account for the Non-modified RPM not having an interaction parameter, an interaction parameter has been incorporated to produce the Modified RPM [38]. The model is denoted by Equation 2.6-14 with η_i the interaction parameter specific to each adsorbate. Similar to the Non-modified RPM, K_{RP}, a_{RP} and n are also obtained from the corresponding single component models with the interaction parameter obtained by fitting the model to multicomponent adsorption data [38].

$$q_{e,i} = \frac{K_{RP,i}\left(\frac{C_{e,i}}{\eta_i}\right)}{1+\sum_{j=1}^{n}\left(a_{RP,j}\left(\frac{C_{e,j}}{\eta_j}\right)^{\frac{1}{n_j}}\right)} \qquad [\ 2.6\text{-}14\ ]$$

2.6.2.5 *Binary Equilibrium Isotherm Graph*

Binary equilibrium isotherms are slightly different than single component isotherms since they are dependent not only on the equilibrium concentration of one component but on two, as shown in the isotherm models discussed above. Binary isotherm graphs are therefore not two-dimensional, but three-

dimensional (3-D) graphs (Figure 2.6-2). In this case, the example is a Modified LM for a mixture of two components, *i.e.* component 1 and component 2.

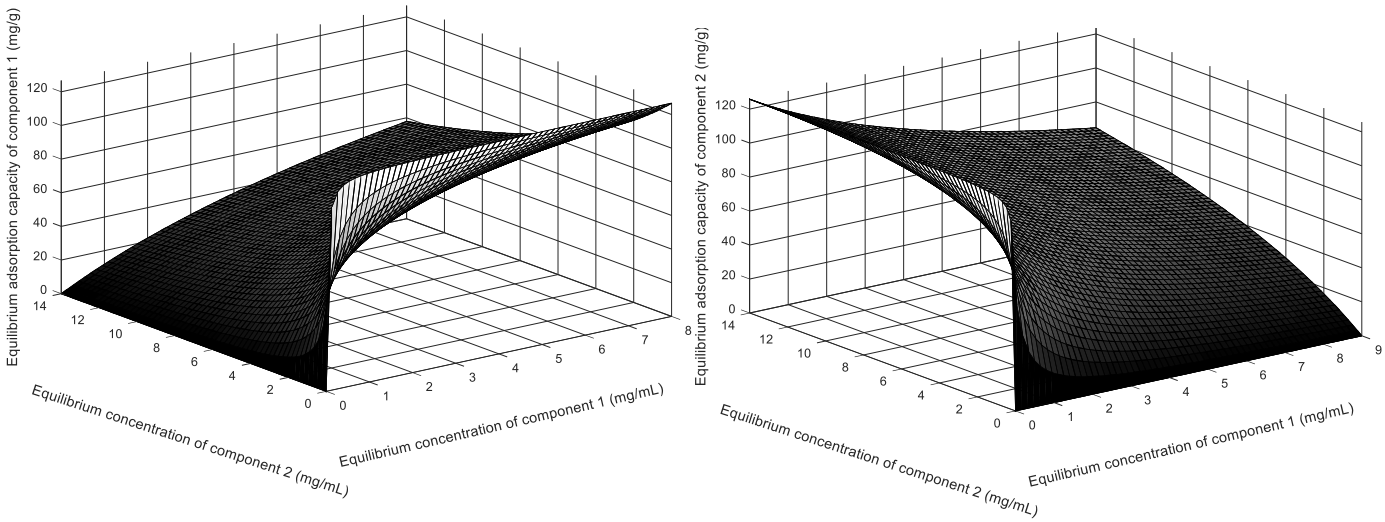

Figure 2.6-2: Typical binary component isotherm graphs (Modified Langmuir model as example) for component 1 (left) and component 2 (right) in a binary component system

To the author's knowledge no open data exist on the binary component adsorption equilibrium modelling of systems comprising 1-alcohols and an alkane using AA adsorbents. The study conducted by Groenewald [8] allows for this study to build on the single component equilibrium modelling, to use the single component data measured by Groenewald [8] and investigate the binary component equilibrium modelling of systems comprising 1-alcohols and an n-alkane.

2.7 Adsorption Kinetics

Adsorption kinetics are the "time dependence of the adsorption process" [10]. Kinetic models are used to describe the increase in adsorbent loading with time or the decrease in adsorbate concentration in the bulk solution as a function of time (Equation 2.7-1). It is generally also used to determine the rate-limiting step(s) of the adsorption process [10].

$$q = f(t); C_{adsorbate} = f(t) \qquad [\ 2.7\text{-}1\ ]$$

The experimental adsorption data typically generate a kinetic curve similar to that provided in Figure 2.7-1.

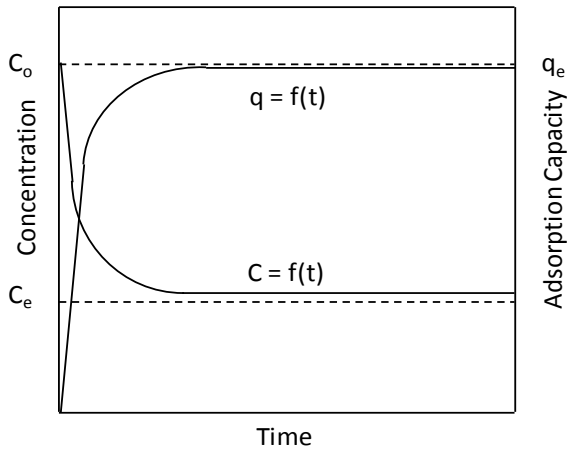

Figure 2.7-1: Typical adsorption kinetic curve, with the solid lines representing the change in adsorbate concentration and adsorbent loading and the dotted lines representing the equilibrium adsorbate concentration (bottom) and equilibrium adsorbent loading (top) (redrawn from [10])

Most kinetic models generally have several concomitant assumptions. These assumptions include [10]:

(i) Constant temperature;

(ii) Perfect mixing of the bulk solution;

(iii) Mass transfer within the adsorbent particle can be described as diffusion; and,

(iv) The adsorbent particles are spherical.

In principle, the rate-limiting step(s) of kinetic models are assumed. When fitting a kinetic model to the experimental data, the assumption is either verified or discarded [10]. This provides information on the rate-limiting mechanism(s) of the adsorption process as well as useful kinetic parameters.

2.7.1 Adsorption Kinetic Models

The adsorption kinetic models are based on the assumption that the rate-limiting step of the overall adsorption process is the settling of adsorbate molecules at active sites on the adsorbent surface [13], [74]. Although not always the case, this is typically true when the adsorption occurs through chemisorption [13]. Though these models are widely used to determine the rate-limiting step(s) in the adsorption process, Khamizov *et al*. [75] argued that the pseudo-order models alone cannot be used for the determination of the kinetic mechanism, or rate-limiting step. This was also verified by studies conducted by Simonin [76] and Qiu *et al.* [77].

2.7.1.1 *Pseudo-order Models*

Generally, the pseudo-first-order (P1) and pseudo-second-order (P2) models are derived from the LM, discussed in Section 2.6.1.1 [74], [78]. The LM's concomitant assumptions are therefore transferred to P1 and P2. The shared assumptions for these two models are [18], [20], [22]:

(i) The adsorbent surface is energetically homogenous;

(ii) Only monolayer adsorption occurs;

(iii) Each active adsorption site is occupied by one adsorbate molecule only; and,

(iv) The adsorbed adsorbate molecules do not interact.

When comparing P1 and P2, various studies have shown that P2 is generally more accurate in describing adsorption kinetics [76]. In a study conducted by Ho [79], it was suggested that experimental adsorption data typically obey P2 when the initial adsorbate concentration is relatively low whereas P1 is more generally employed for higher initial adsorbate concentration systems. This is also clear from the theoretical derivations of P1 and P2, as pointed out by Aziziam [78].

In a study conducted by Leyva-Ramos *et al.* [80], it was pointed out that kinetic adsorption models have limited use: in that study, and several others, the rate constants obtained from the models had no apparent trend with the variation of operating conditions and parameters such as equilibrium adsorbent loading, temperature, adsorbent particle size and stirring speed. This suggests that the experimentally obtained rate constants are therefore only applicable to the specific experimental setup and set of operating conditions and thus not valid for any other experimental setup [10].

2.7.1.1.1 Pseudo-first-order model (P1)

P1 was first proposed by Lagergren [81] in 1898 to describe the kinetics of the adsorption of ocalic and malonic acid onto charcoal. The model is based on the surface reaction denoted by Equation 2.7-2. Should this reaction be changed to a reversible reaction, the Langmuir kinetic model would be applicable and no longer P1 [13]. This would be the case if the effect of desorption cannot be neglected.

$$site + adsorbate \rightarrow site.adsorbate \qquad [\ 2.7\text{-}2\ ]$$

The surface reaction (Equation 2.7-2) is assumed to follow a first-order rate equation [13]. The P1 is therefore expressed by Equation 2.7-3, with q_t and q_e denoting adsorbent loading at time t and at equilibrium respectively, k_1 the P1 rate constant and t denoting time.

$$q_{t,i} = q_{e,i}\left(1 - e^{-k_{1,i}t}\right) \qquad [\ 2.7\text{-}3\ ]$$

A theoretical derivation employed by Azizian [78] suggests that k_1 is not the intrinsic rate constant but rather a combination of the adsorption and desorption rate constants and also a linear function of initial adsorbate concentration, C_o. According Azizian [78], P1 tends to best describe the kinetics of systems with relatively high initial adsorbate concentration; this is shown by Azizian's [78] derivation and has also been proven by several other studies including that of Ho and McKay [82].

2.7.1.1.2 Pseudo-second-order model (P2)

Two researchers had a contribution towards P2. The model was first proposed by Blanchard in 1983 for the removal of heavy metals from water by using natural zeolites, after which it was further developed by Ho in 1995 [83]. P2 can be expressed by Equation 2.7-4 with k_2 the P2 rate constant. Azizian [78] provides a detailed theoretical derivation of P2.

$$q_{t,i} = \frac{k_{2,i} q_{e,i}^2 t}{1 + k_{2,i} q_{e,i} t} \qquad [\ 2.7\text{-}4\ ]$$

When referring to the theoretical derivation by Azizian [78], it is clear that k_2 is a complex function of the initial concentration of adsorbate in the bulk solution (C_o). According to Azizian [78], P2 tends to best describe the kinetics of systems with low initial adsorbate concentration. As mentioned, this has been proven by several studies including a study conducted by Al-Ghouti *et al*. [84] where P2 was the best overall kinetic model and also exhibited greater correlation of the data at lower initial adsorbate concentrations.

2.7.1.1.3 Pseudo-nth-order Model (PN)

The PN model is typically used for the adsorption of metal ions onto activated carbon [85]. The surface reaction is assumed to follow a rate equation of order *n*. PN is expressed by Equation 2.7-5 with k_n the PN rate constant [85].

$$q_{t,i} = q_{e,i} - \left(q_{e,i}^{1-n_i} - (1-n_i) k_{n,i} t\right)^{\frac{1}{1-n_i}} \qquad [\ 2.7\text{-}5\ ]$$

Since the order of the surface reaction is not defined and depends solely on the adsorption data, this model sometimes fits kinetic data better than P1 or P2. Even though the model typically fits kinetic data well, literature has reported the parameters associated with this model to be slightly dubious, with the kinetic constant (k_n) very sensitive to variations in the order of the surface reaction.

2.7.1.2 ***Elovich Model***

The Elovich kinetic model was first proposed by Zeldovich [86] for the adsorption of carbon monoxide onto manganese dioxide. It is typically used to describe the kinetics of activated chemisorption processes [13]. The model is given in Equation 2.7-6 with α the initial chemisorption rate and β a parameter relating to the surface coverage and activation energy of the specific adsorption process [87].

$$q_{t,i} = \left(\frac{1}{\beta_i}\right) \ln(\alpha_i \beta_i t) \qquad [\ 2.7\text{-}6\ ]$$

According to Rudzinski *et al.* [88], the Elovich kinetic model and the LM are very closely related: should the Elovich kinetic model succeed in describing the adsorption kinetic data, it is very likely that the adsorption process will also follow the LM.

2.7.1.3 *Comparison of Adsorption Kinetic Models*

Figure 2.7-2 compares the typical form of the different adsorption kinetic models discussed in this section. Note that the form of PN is dependent on the order of the model and can therefore differ from that represented in Figure 2.7-2.

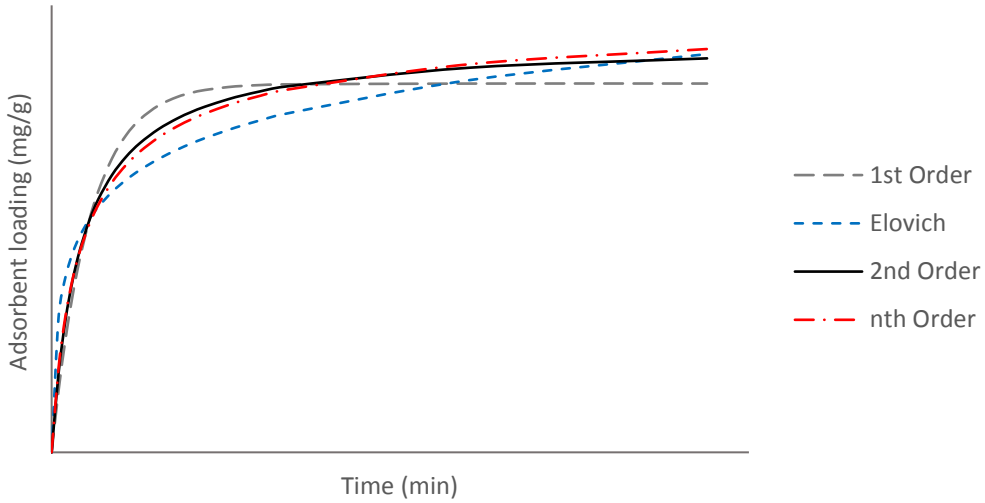

Figure 2.7-2: Typical form of the Pseudo-first-order; Pseudo-second-order; Pseudo-nth-order; and, Elovich kinetic models

Groenewald [8] applied three kinetic models to the data of the investigated alcohol-alkane systems; these models included P1 and P2. These models were found to fit the data relatively well, with correlation coefficients greater than approximately 0.94 on average. Groenewald [8] also found that P2 correlated the data better than P1, which hypothesises that P2 will also outperform P1 in this study. In addition to abovementioned models, Groenewald [8] also investigated IPD model.

2.7.2 Intra-particle Diffusion Model

For diffusional models, the rates of EMT and IPD are taken into account and the surface reaction is assumed to be "instantaneous" [80]. According to several studies this is the case and IPD is the rate-controlling step of the adsorption process [7], [19], [74].

One of the most widely used adsorption mechanism models is the IPD model [89]. This model was first introduced by Weber and Morris [89] for a study on the batch adsorption of alkyl benzene sulfonates onto activated carbon. The model is denoted by Equation 2.7-7 with k_{IP} the IPD rate constant and θ a constant associated with the external boundary layer thickness [89]; a greater value of θ typically indicates a significant external boundary layer effect [90].

$$q_t = k_{IP} t^{0.5} + \theta \qquad [\ 2.7\text{-}7\ ]$$

The Weber-Morris plot is constructed by plotting q_t versus $t^{0.5}$ [89]. This model is often used incorrectly, when fitting a single straight line through the adsorption kinetic data [91]. Adsorption is a multistage process generally exhibiting a curvilinear plot, therefore segment analysis should be employed [91]. This plot often generates two or in some cases three distinct linear segments [13], [92]. Should the plot provide a single linear segment, the process is generally solely controlled by IPD; however, in the case of more than one linear segment, the rate at which the adsorbate is adsorbed is controlled by more than one process, *i.e*. EMT and/or IPD (Figure 2.7-3) [92], [93]. In the event of the Weber-Morris plot exhibiting three linear segments, the first linear segment is generally linked to EMT, the second linear segment to IPD and the third linear segment to the equilibrium reaching stage [94], [95].

An extension of the IPD linear segment through the *y*-axis provides a measure of the boundary layer thickness, *i.e.* the effect of the external boundary layer [90], [96]. Should this linear segment pass through the origin, it indicates that the effect of the external boundary layer is insignificant and that EMT is not the rate-controlling step [95]. This is typically the case in well-agitated systems. The Weber-Morris plot could also exhibit slight curvature of the data points; according to several studies, including that of McKay *et al.* [96] and Asfour *et al.* [97], curvature could be attributed to the effects of EMT.

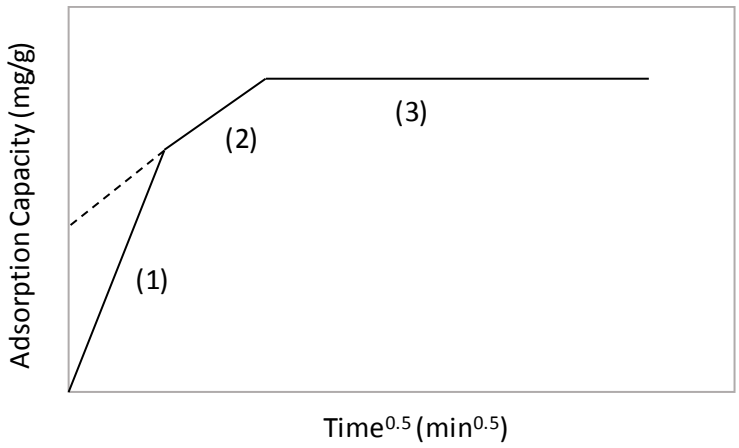

Figure 2.7-3: Typical Weber-Morris plot with three distinct stages: (1) External mass transfer stage; (2) intra-particle diffusion stage; and, (3) equilibrium reaching stage (extension of intra-particle diffusion plot indicates effect of external boundary layer)

In the study conducted by Groenewald [8], the IPD model was applied to the data of alcohol-alkane systems. The nonlinear form of the model was used and overall it was found to provide a good fit to the data (R^2 > 0.95) [8].

Chapter 3: Materials and Methods

3.1 Overview

The objective of this chapter is to provide the necessary information on the materials and methods used in this study, in order to better understand the experimental adsorption data measured. This chapter will discuss the experimental design and analysis protocol which includes the experimental and analytical procedures, materials and setup. Also discussed in this chapter is the reproducibility of experimental data, uncertainty analysis as well as data and data processing.

3.2 Experimental Design

Various adsorption experiments were conducted with the aim of determining the change in alcohol concentration in the bulk solution as well as on the adsorbent surface. To achieve all objectives of this study, two sets of experiments were conducted: kinetic experiments and equilibrium experiments. Figure 3.2-1 depicts the reasoning behind the experimental design and what was investigated using each set of data.

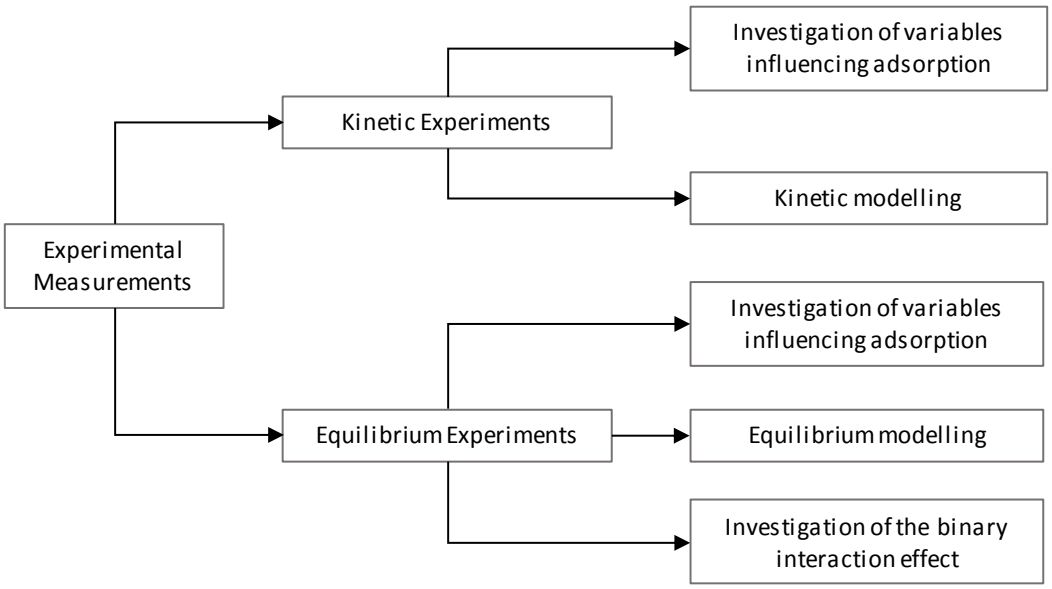

Figure 3.2-1: Schematic diagram of the experimental design and the reason for each set of experiments

3.2.1 Experimental Procedure

Abovementioned sets of experiments were conducted following the same procedure with the only difference being the kinetic experiments were sampled at various time intervals whereas the equilibrium experiments were only sampled at the beginning and the end of each run, as will be discussed below. The same experimental procedure was followed for the single and binary component adsorption experiments and a full factorial experimental design was considered.

The adsorption experiments were conducted using a bench-scale water bath, 500 mL glass beakers and a magnetic stirring plate. The temperature in the water bath was set to a specified temperature of either 25 or 45°C after which it was allowed to reach the specified temperature. The 500 mL beakers together with a magnetic stirrer in each respective beaker were weighed and the weights were recorded. After weighing the beakers, 200 mL of an alcohol (1-hexanol, 1-octanol and/or 1-decanol) and n-decane solution of specified concentration (0.3-3.3 mass%) was added to the beaker. The beakers containing the alcohol-alkane solutions and the magnetic stirrers were weighed again and the weights recorded. The beakers containing the solutions were immersed in the water bath and allowed to reach the specified temperature. While the solutions were heating up in the water bath, the mesh adsorbent baskets were weighed after which 10 g of adsorbent (Selexsorb CDx®, Selexsorb CD® or Activated Alumina F220) was added to each of the respective mesh adsorbent baskets. After the solutions had reached the specified temperature the mesh adsorbent baskets were lowered into the beakers and the water bath was closed. The magnetic stirring plate was switched on at 350 rpm and the system was allowed to reach equilibrium for approximately 23 hours and 30 minutes. Preliminary experiments were conducted to determine this approximate time of equilibrium. The results and a discussion of these preliminary experiments are provided in Appendix A (Section A.1.1, p129). During this time, samples of the solutions were taken. Each sample volume was 200 µL and it was taken with a pipette through sample ports in the water bath cover. The sample ports were closed with plugs when not in use in between samples so as to prevent evaporation of the solutions. For the kinetic experiments, samples were taken at 0, 15, 30, 150, 240, 360, 480, 1380, 1395, 1410 and 1415 minutes respectively. For the equilibrium experiments, samples were taken at the beginning and the end (at the equilibrium time) of each experimental run. Thus, at 0 minutes and at 1380, 1395, 1410, 1415 minutes. The samples were transferred into dedicated 2 mL glass sample vials and marked accordingly.

In comparison to the volume of the bulk solution, the sample volume of 200 µL was small enough not to disturb the adsorption process, *i.e.* 11 samples of 200 µL each equal approximately 1.1% of the total bulk solution for each kinetic experimental run. This was verified by comparing the adsorption data when taking 80 µL samples and 200 µL.

Table 3.2-1 and Table 3.2-2 encapsulate the single component and binary component experimental variables, respectively. A step-by-step experimental procedure is provided in Appendix A (Section A.1.2, p130).

Table 3.2-1: Single component adsorption experimental variables

Temperature	***Alcohol-alkane systems***	***Adsorbents***	***Initial Alcohol Concentration Range***
45°C	1-hexanol + n-decane 1-octanol + n-decane 1-decanol + n-decane	AA-F220 SCDx® SCD®	0.3-2 mass%

Table 3.2-2: Binary component adsorption experimental variables

Temperature	***Alcohol-alkane systems***	***Adsorbents***	***Initial Alcohol Concentration Range***
25 & 45°C	1-hexanol + 1-decanol + n-decane 1-hexanol + 1-octanol + n-decane 1-octanol + 1-decanol + n-decane	AA-F220 SCDx® SCD®	0.3-3.3 mass%

The single component experiments were only conducted at 45°C, since these experiments had already been conducted at 25°C by Groenewald [8]. Groenewald investigated the temperature range of 25°C to 35°C, therefore a slightly higher temperature of 45°C was selected to build on the existing data. For the binary component experiments, however, experiments were conducted at 25°C and 45°C since the equilibrium modelling of the binary component data requires both the single as well as the binary component data and two temperatures were required to allow for comparison. The two temperatures were selected such that it was within the typical temperature range investigated in adsorption studies, *i.e.* approximately 25°C to 50°C [62], [90], [98]–[100], to avoid additional cooling or excessive heating of the systems.

Since data obtained from the study by Groenewald [8] were used, the exact same adsorbates and adsorbents, solution volume and adsorbent mass were used with a slightly expanded initial alcohol concentration range. The initial alcohol concentration range was selected such that its upper limit was slightly higher than that investigated by Groenewald [8], but so as to also be less than the typical alcohol contaminant make-up in surfactant/petrochemical alcohol-alkane streams.

3.2.2 Gas Chromatography Analysis Procedure

All 200 µL samples obtained from the experimental measurements were prepared for GC analysis in order to determine the concentration of each sample. An internal standard, which was 20 µL of 1-pentanol, was added to each of the samples and weighed with a 5-decimal balance. The samples containing the 1-pentanol internal standard were diluted with the same solvent as was used in the calibration of the GC method, *i.e*. HPLC grade methanol. This concluded the sample preparation. The prepared samples were inserted into the GC for analysis with the GC system automatically analysing 50 samples in series. The data provided by the GC were used to determine the mass percentage of each of the alcohols in the original alcohol and n-decane solutions used in the adsorption experiments.

A step-by-step procedure of the GC calibration is outlined in Appendix A (Section A.1.3, p132) and for a detailed analysis protocol, also refer to Appendix A (Section A.1.4, p133).

3.2.3 Experimental Setup

A bench-scale batch adsorption setup was used in this study (Figure 3.2-2). The setup consisted of a water bath that was maintained at constant temperature by use of a heater with a circulation system. The water bath had a frame on the inside in which the beakers containing the alcohol-alkane solutions were mounted. The cover of the water bath had sample ports and hooks for the adsorbent mesh baskets to hang from. Underneath the water bath was a magnetic stirring plate which ensured constant mixing of the alcohol-alkane solutions. Images of the experimental setup are provided in Appendix A (Section A.1.5, p135).

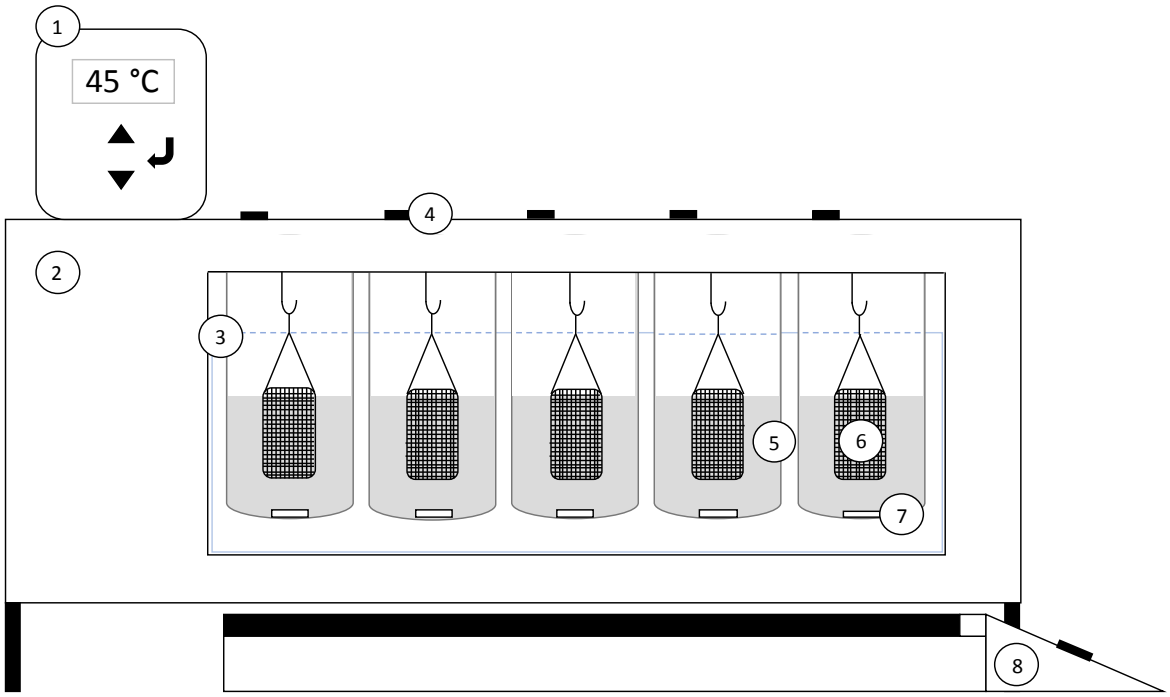

Figure 3.2-2: Schematic diagram of experimental setup ((1) Heater with circulation pump; (2) Water bath; (3) Water at specified temperature; (4) Plugs in sample ports in water bath lid; (5) 500 mL glass beaker containing alcohol-alkane solution; (6) Mesh basket with adsorbent; (7) Magnetic stirrer bar; and, (8) Magnetic stirring plate)

3.2.4 Materials

The adsorbents that were used are summarised in Table 3.2-3. These adsorbents are specially formulated for the adsorption of organic compounds, among others. The adsorbents were manufactured by BASF Chemical Company and supplied by UDEC.

Table 3.2-3: Adsorbent specifications [1]

Adsorbent	***Chemical Composition***	***Bulk Density (kg/m³)***	***Particle Size (mm)***	***Manufacturer***
Selexsorb® CDx	95.1% Al_2O_3	665	3.2 (1/8”)	BASF
Selexsorb® CD	95.1% Al_2O_3	697	3.2 (1/8”)	BASF
AA-F220	93% Al_2O_3	785	3.2 (1/8”)	BASF

The chemicals used for the adsorption experiments are summarised in Table 3.2-4. These chemicals are relevant to the surfactant/petrochemical industry, have the potential to provide a good base understanding of the adsorption behaviour of 1-alcohols in an n-alkane and are within an acceptable price range for the given project.

Table 3.2-4: Specifications of chemicals used for experiments [2, 3]

Name	***Formula***	***Structure***	***Product Number***	***Manufacturer***	***Purity***
1-hexanol	$C_6H_{14}O$	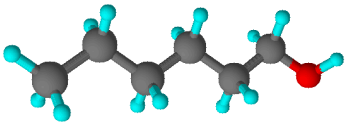	H13303	Sigma-Aldrich	98%
1-octanol	$C_8H_{18}O$	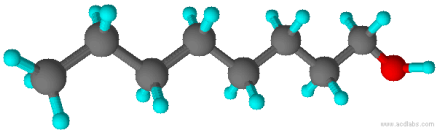	472328	Sigma-Aldrich	≥ 99.0%
1-decanol	$C_{10}H_{22}O$	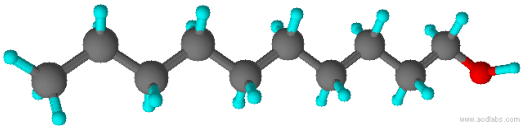	W236500	Sigma-Aldrich	≥ 98.0%
n-decane	$C_{10}H_{22}$	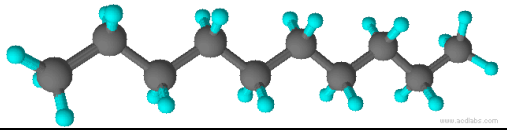	30570	Sigma-Aldrich	≥ 95.0%

The chemicals that were used for sample analysis are summarised in Table 3.2-5. These were similar to those used by Groenewald [8] to ensure consistency and reproducibility of the experimental results.

[1] *The physical properties summarised here are that stipulated in each respective adsorbent’s material data sheets, as provided by BASF* [33]–[35].

[2] *Key: grey = carbon; blue = hydrogen; and, red = oxygen*

[3] *Molecule structures constructed with ACD Labs/ChemSketch Software*

Table 3.2-5: Specifications of chemicals used for analysis

Name	*Formula*	*Structure*	*Product Number*	*Manufacturer*	*Purity*
1-pentanol	$C_5H_{12}O$	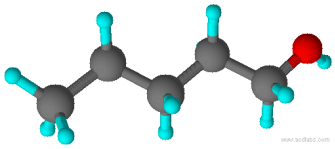	398268	Sigma-Aldrich	≥ 99.0%
methanol	CH_3OH	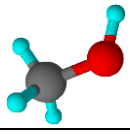	34860	Sigma-Aldrich	≥ 99.9 %

3.3 Reproducibility of Experimental Data

Reproducibility experiments were performed to ensure the same results were obtained from this study as were obtained by Groenewald [8]. The data obtained by repeating some of the experimental runs conducted by Groenewald [8] were very similar, which deemed the data from this study reproducible (Figure 3.3-1). It can, however, be observed that adsorption seem to have been slightly better in this study than for the study conducted by Groenewald [8]. These slight differences in experimental values were within the uncertainty range and can be attributed to the use of a slightly lower water bath in the current study (solutions and magnetic stirrer bars less than approximately 5mm closer to magnetic stirring plate) as well as a different magnetic stirring plate. Additional reproducibility data are provided in Appendix A (Section A.2.1, p136).

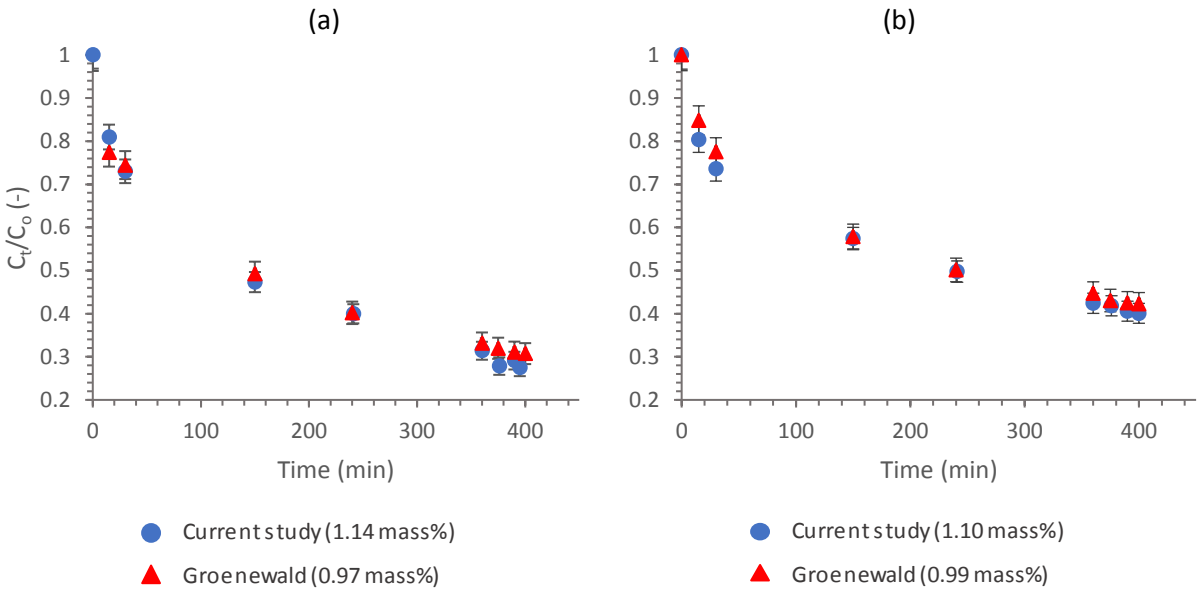

Figure 3.3-1: Comparison of concentration decay plots for current study and a study conducted by Groenewald [8] for the single component adsorption of (a) 1-hexanol onto Selexsorb CD®; and, (b) 1-octanol onto Selexsorb CDx® (T = 35°C; initial concentration (IC) as indicated on graphs)

As shown, the data obtained with the experimental setup used in this study were comparable to that obtained by Groenewald [8]. However, to ensure that these systems were mixing effectively, some additional experiments were conducted after investigating the reproducibility of the data. These experiments included adding baffles to the beakers and investigating the effect on adsorbent loading. The solutions containing baffles and magnetic stirrer bars exhibited no significant increase (or decrease) in the adsorbent loadings as compared to solutions at the same conditions containing only magnetic stirrer bars and no baffles. Thus, indicating effective mixing using only the magnetic stirrer bars and no baffles. Consequently, all experiments were conducted without baffles. A brief discussion is provided in Appendix A (Section A.2.2, p137).

3.4 Uncertainty Analysis

An uncertainty analysis was conducted based on the concentrations as measured by the GC. The measurement uncertainty comprised two components:

(i) The uncertainty as determined from the repeat experimental runs; and,

(ii) The uncertainty of the GC repeat samples.

The uncertainty parameter of each respective concentration was determined using the student's t-statistic, a significance level of 0.05 and the standard error of five repeat measurements. This was done for each of the different binary system adsorbates, and for one of the single component systems, 1-hexanol, since the error for the single component systems was relatively small and consistent comparatively. From there onwards the rule of error propagation was used to determine the uncertainty parameter of each consequent calculated value.

The average concentration uncertainty of the single component 1-hexanol system used to determine the uncertainty for all single component systems was 1.64% of the specific concentration. For the binary component systems, the concentration uncertainties were determined for both components alone (component 1 and component 2) as well as for the binary mixture since the binary component data are presented in both ways throughout this thesis (Table 3.4-1). An outline of the uncertainty calculation methodology, and the repeatability data used for the uncertainty analysis are provided in Appendix B (p139).

Table 3.4-1: Average Concentration Uncertainties of Various Binary Component Systems

Binary Component System	**Average Concentration Uncertainty (%)**			
	1-hexanol	***1-octanol***	***1-decanol***	***Binary Mixture***
1-hexanol + 1-decanol	6.55	-	4.08	3.28
1-hexanol + 1-octanol	3.73	2.99	-	2.33
1-octanol + 1-decanol	-	9.76	7.58	5.67

The temperature of the systems also slightly deviated from the specified temperature at times. The relative error in the temperature was determined to be 0.05°C for the experimental runs at 25°C and 0.03°C for the experimental runs at 45°C. These relative errors were small and insignificant with regards to influencing adsorption over a period of 23 hours and 30 minutes.

3.5 Data & Data Processing

All data measured in this study are provided in Appendix C (p146). For each respective results chapter, *i.e.* Chapters 5 through 7, a calculation methodology pertaining to the work discussed in that chapter is provided in the corresponding appendices, as indicated in those chapters. These include methodologies on the determination of the normalised liquid concentration at time *t*, C_t/C_o, (Equation 3.5-1) as well as the adsorbent loading, q (Equation 3.5-2).

$$\frac{C_t}{C_o} = \frac{\left(\frac{m_{alcohol\ in\ solution}}{V_{solution}}\right)_t}{\left(\frac{m_{alcohol\ in\ solution}}{V_{solution}}\right)_o} \qquad [\ 3.5\text{-}1\ ]$$

$$q = \frac{m_{alcohol\ adsorbed}}{m_{adsorbent}} \qquad [\ 3.5\text{-}2\ ]$$

Since a vast number of systems have been investigated, only some of the processed data graphs are provided in the body of this thesis, with the rest of the graphs provided in Appendix D (p185) for further reference.

Chapter 4: Adsorbent Characterisation

4.1 Overview

The objective of this chapter is to investigate and compare the physical properties of the three different adsorbents used in this study. The three adsorbents are:

(i) Activated Alumina F220 (AA-F220);

(ii) Selexsorb CDx® (SCDx); and,

(iii) Selexsorb CD® (SCD).

The information obtained here will ultimately aide in gaining more insight into the findings in subsequent results chapters.

4.2 Physical Properties

The physical properties investigated include the surface area and pore volume, as well as the pore structure and composition of each adsorbent. Additional information/theory on the physical properties of adsorbents is provided in Appendix E (Section E.1, p214).

4.2.1 Surface Area & Pore Volume

The surface area and pore volume of the adsorbents were investigated through low pressure gas adsorption (LPGA), with nitrogen as the adsorptive medium. This was done with a 3Flex instrument (accelerated surface area and porosimetry system) from the Micromeritics Instrument Corporation. Table 4.2-1 summarises the surface area of the adsorbents. It can be observed that SCDx and SCD proved to have the greatest single point as well as Brunauer-Emmett-Teller (BET) surface areas, with that of AA-F220 being slightly less. As determined with the Density Functional Theory (DFT) Model, SCDx's micropore structure constitutes approximately 68% of its total surface area and SCD's approximately 58%. The micropore structure of AA-F220, however, constitutes the smallest part of its surface area with its external surface area constituting 44% and its mesopore structure constituting approximately 33% of the total surface area.

Table 4.2-1 also provides the pore volumes of the different adsorbents. With the exception of the pore volume as determined by the single point adsorption method, the three adsorbents proved to have very similar total pore volumes. The micropore volume of the respective adsorbents were determined to be 0.049, 0.114 and 0.090 cm^3/g for AA-F220, SCDx and SCD, respectively (DFT Model). The micropore volume therefore constitutes approximately 13, 28 and 24% of the total pore volume of AA-F220, SCDX and SCD, respectively (DFT Model).

The average adsorption pore diameters of AA-F220, SCDx and SCD, as determined with the BET method, were 48.179, 42.890 and 46.104 Å and the average micropore diameters, as determined with the Horvath-Kawazoe method, were 10.879, 7.972 and 8.480 Å, respectively. The mesopore volume of AA-F220 was determined to be slightly greater than that of SCDx and SCD and the macropore volume constituted less than 1% of the total pore volume in all three adsorbents.

Table 4.2-1: LPGA results for blank AA-F220, SCDx and SCD

Properties	***Activated Alumina F220***	***Selexsorb CDx®***	***Selexsorb CD®***
Surface Area			
Single point surface area (m^2/g)	321.988	464.489	407.356
BET surface area (m^2/g)	334.335	466.008	408.284
BJH Adsorption cumulative surface area of pores between 10 Å and 4000 Å width (m^2/g)	335.768	262.380	283.737
BJH Desorption cumulative surface area of pores between 17 Å and 3000 Å width (m^2/g)	384.924	272.382	305.632
Pore Volume			
Single point adsorption total pore volume (cm^3/g)	0.403	0.500	0.471
Single point desorption total pore volume (cm^3/g)	0.404	0.500	0.471
BJH adsorption cumulative pore volume (cm^3/g)	0.357	0.370	0.370
BJH desorption cumulative pore volume (cm^3/g)	0.419	0.405	0.411
Pore Size			
Adsorption average pore diameter (Å)	48.179	42.890	46.104
Desorption average pore diameter (Å)	48.308	42.890	46.104
BJH adsorption average pore width (Å)	42.560	56.384	52.137
BJH desorption average pore width (Å)	43.530	59.484	53.772

The adsorption-desorption isotherms, as obtained from the LPGA analysis, are provided in Figure 4.2-1. The adsorption-desorption isotherms for all three adsorbents seem to resemble Type IV BET isotherms. According to IUPAC [101], this indicates multilayer adsorption of the nitrogen adsorptive gas with capillary condensation at the high pressures. H3 hysteresis can be observed for SCDx and SCD, suggesting “plate-like particles” with “slit-shaped pores” [101]. For AA-F220, however, H2 hysteresis was observed in its adsorption-desorption isotherm, suggesting that the pore sizes of this adsorbent are not well defined [101].

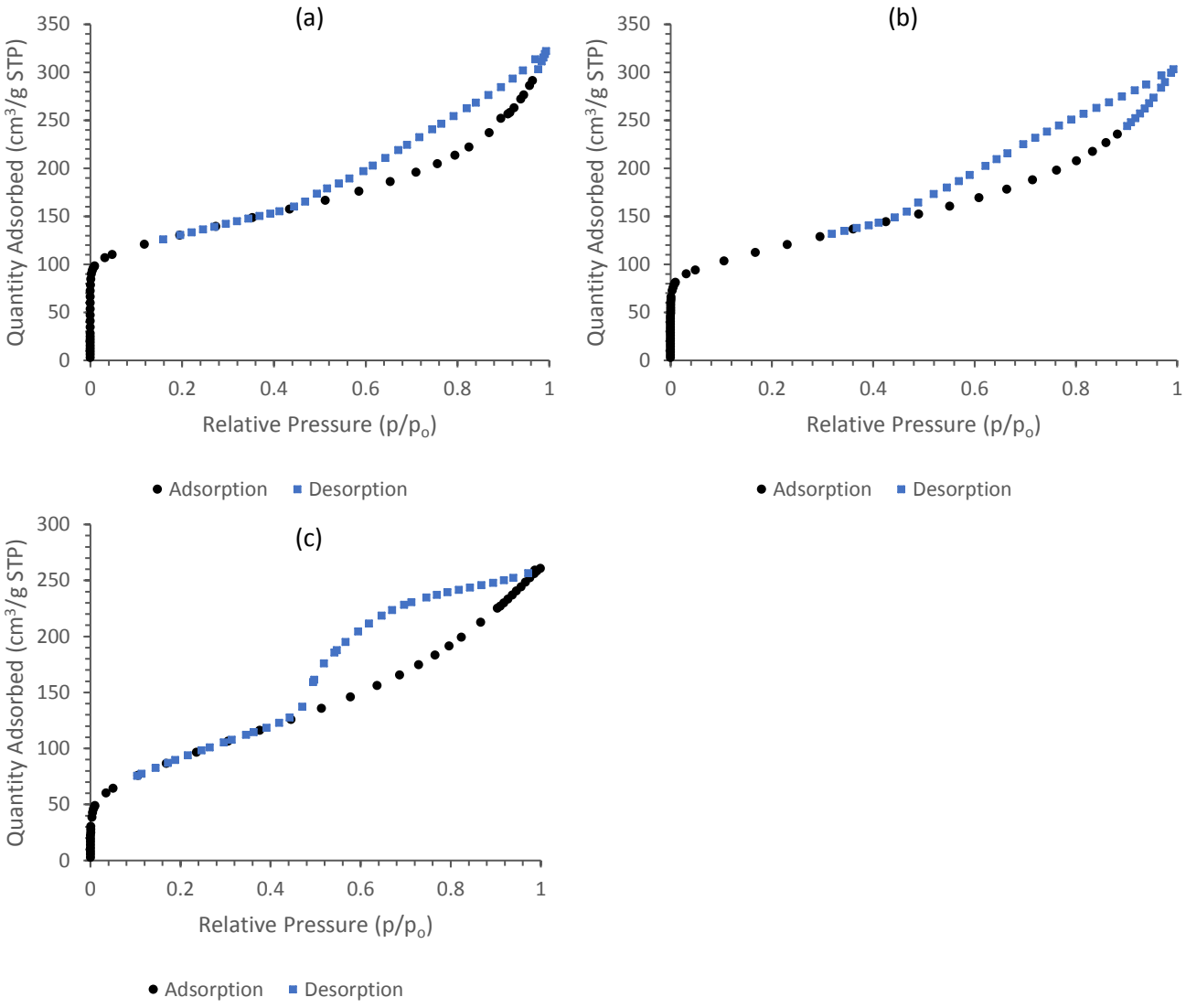

Figure 4.2-1: BET adsorption-desorption isotherms for (a) Selexsorb CDx®; (b) Selexsorb CD®; and, (c) Activated Alumina F220

The Barrett, Joyner and Halenda (BJH) pore size distributions are depicted in Figure 4.2-2. From these it can be observed that all three adsorbents predominantly consist of micropores and mesopores.

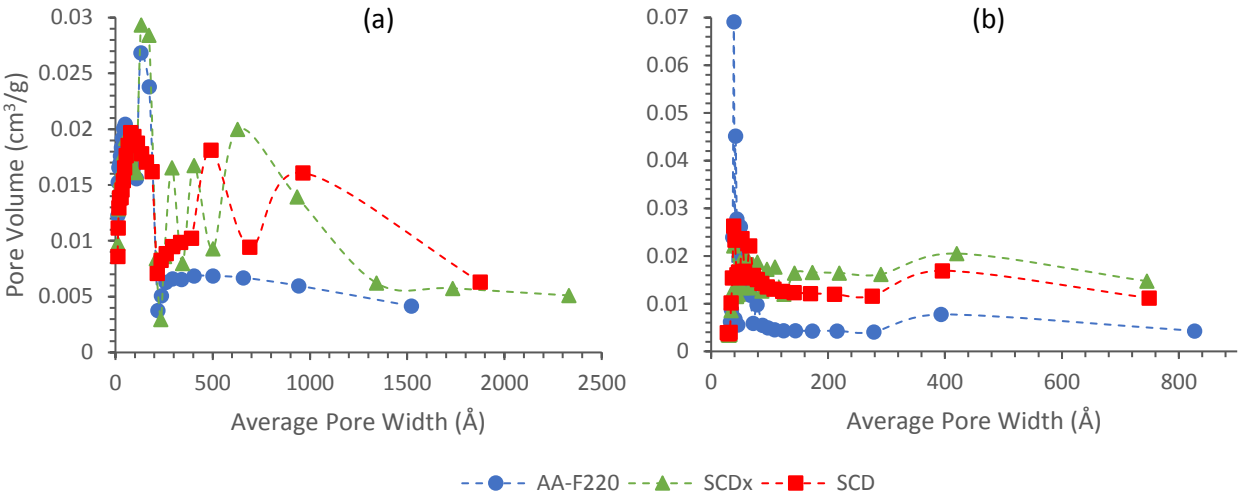

Figure 4.2-2: BJH (a) adsorption; and, (b) desorption pore size distributions

4.2.2 Pore Structure

Scanning electron microscope (SEM) images were taken of the blank adsorbents to investigate the structure of these adsorbents. Two sets of SEM images are provided: one set more to the centre of the adsorbent and one set more to the outer part of the adsorbent closer to the external surface (Figure 4.2-3). The reason for this is to illustrate the change in pore structure in the radial direction of the adsorbents.

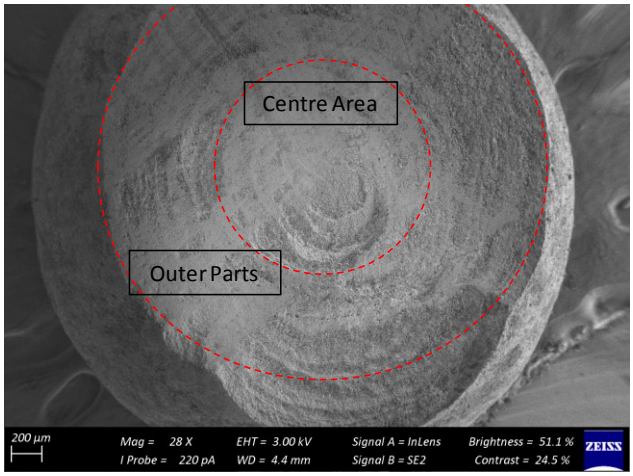

Figure 4.2-3: SEM image of sectioned Activated Alumina F220 indicating the location of the centre and the outer part of the adsorbent where the two sets of SEM images were taken

The centre area of the adsorbents investigated appeared to be a lot denser than the outer parts of the adsorbents (Figure 4.2-4). This indicates that the large macro- and mesopores are situated more to the outer parts of the adsorbents closer to the surface, while the smaller meso- and micropores are situated more to the centre of the adsorbents. The macro- and larger mesopores are thus aptly referred to as transport pores

since adsorbate molecules would have to pass through them to reach the micropore structure of the adsorbents. Refer to Appendix E (Section E.2, p216) for all SEM images.

(a) (b)

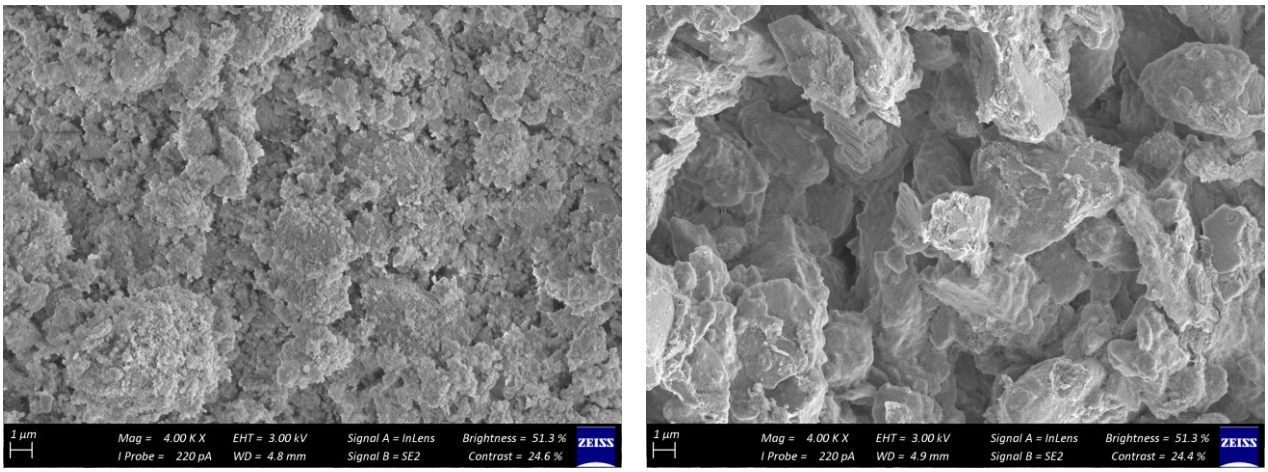

Figure 4.2-4: SEM images of blank Activated Alumina F220 (a) close to the centre of the adsorbent bead; and, (b) close to the surface area, i.e. the outer parts of the adsorbent bead

Bowen *et al.* [29] reported that depending on the synthesis of AA adsorbents, these adsorbents typically have a layered "platelike" structure or a more granular structure, *i.e.* "agglomerates of spherical particles". SEM images of different magnifications for each of the three adsorbents investigated are provided in Figure 4.2-5 through Figure 4.2-7. It can be observed from these images that AA-F220 (Figure 4.2-5) have pores visibly larger than that of SCDx (Figure 4.2-6) and SCD (Figure 4.2-7). SCDx and SCD are also much more granular in structure.

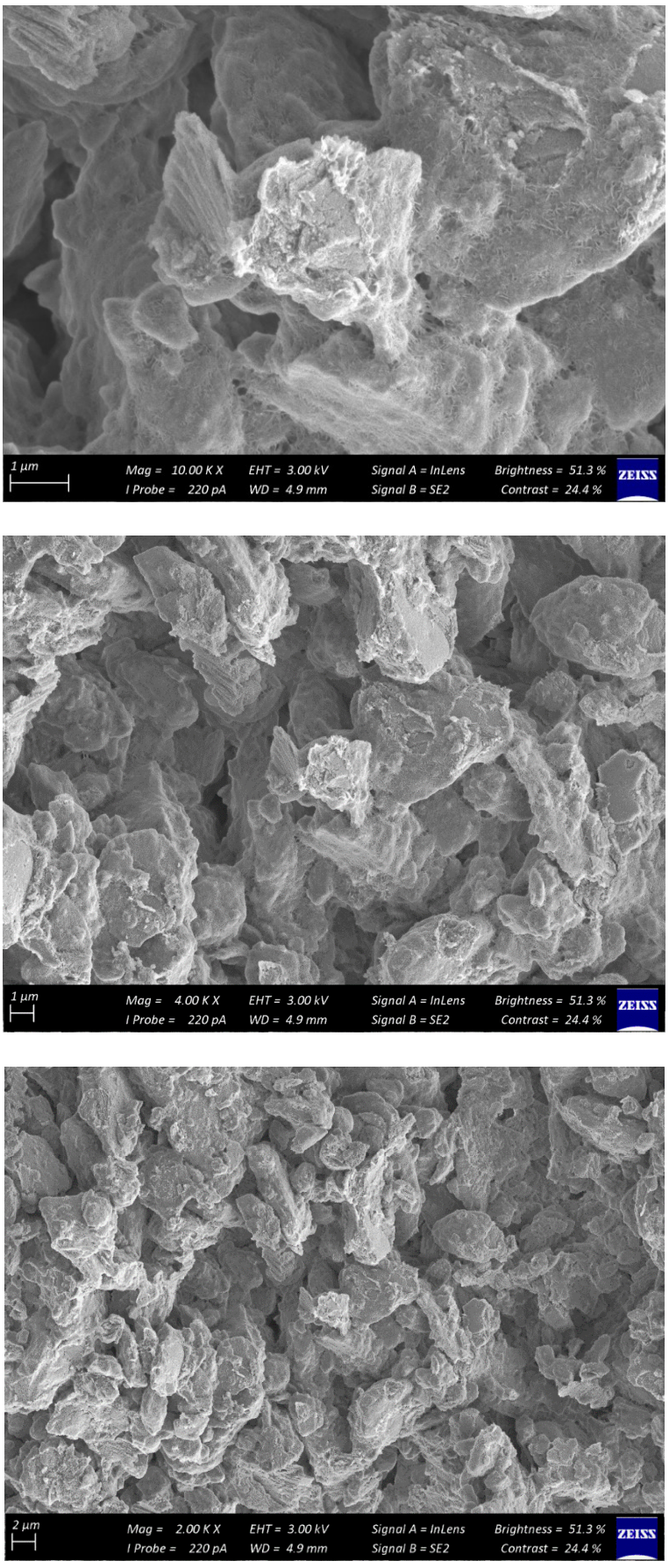

Figure 4.2-5: Different magnification SEM images of blank Activated Alumina F220 at the outer parts of the adsorbent bead

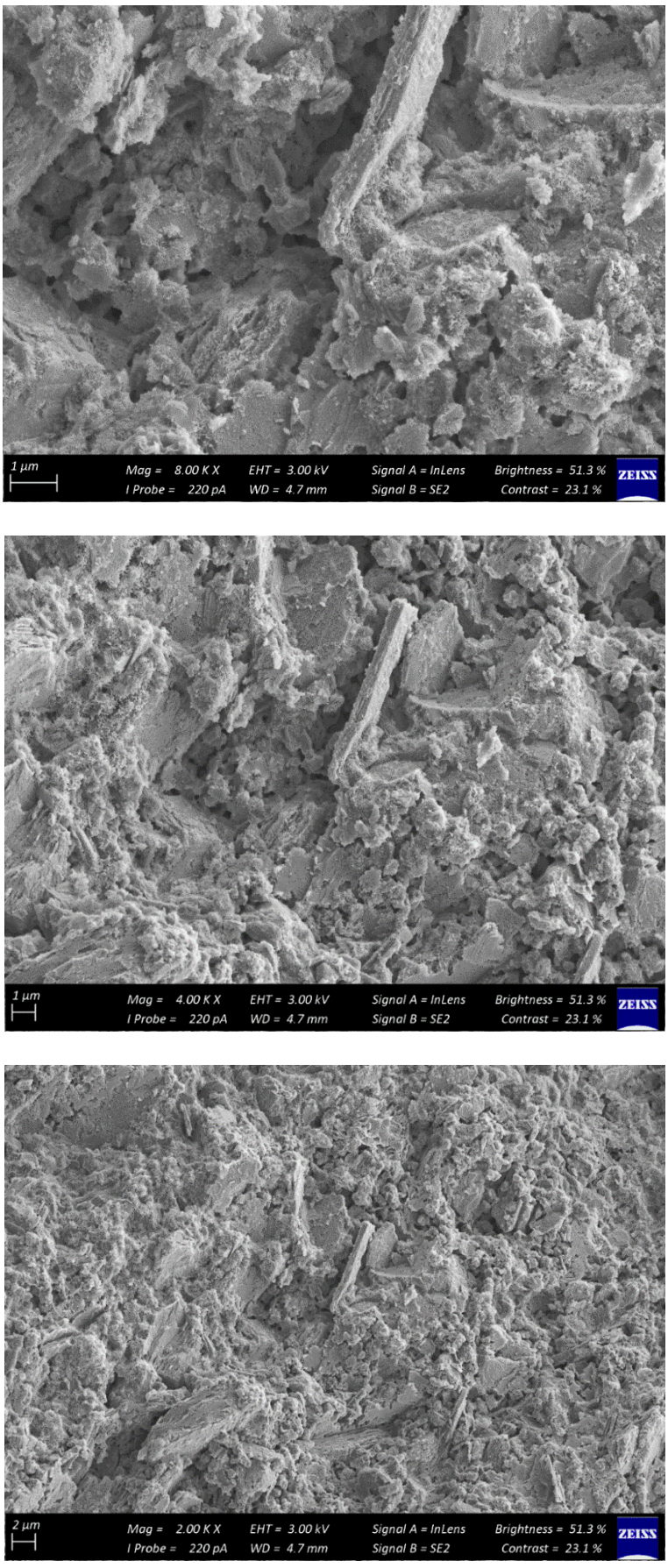

Figure 4.2-6: Different magnification SEM images of blank Selexsorb CDx® at the outer parts of the adsorbent bead

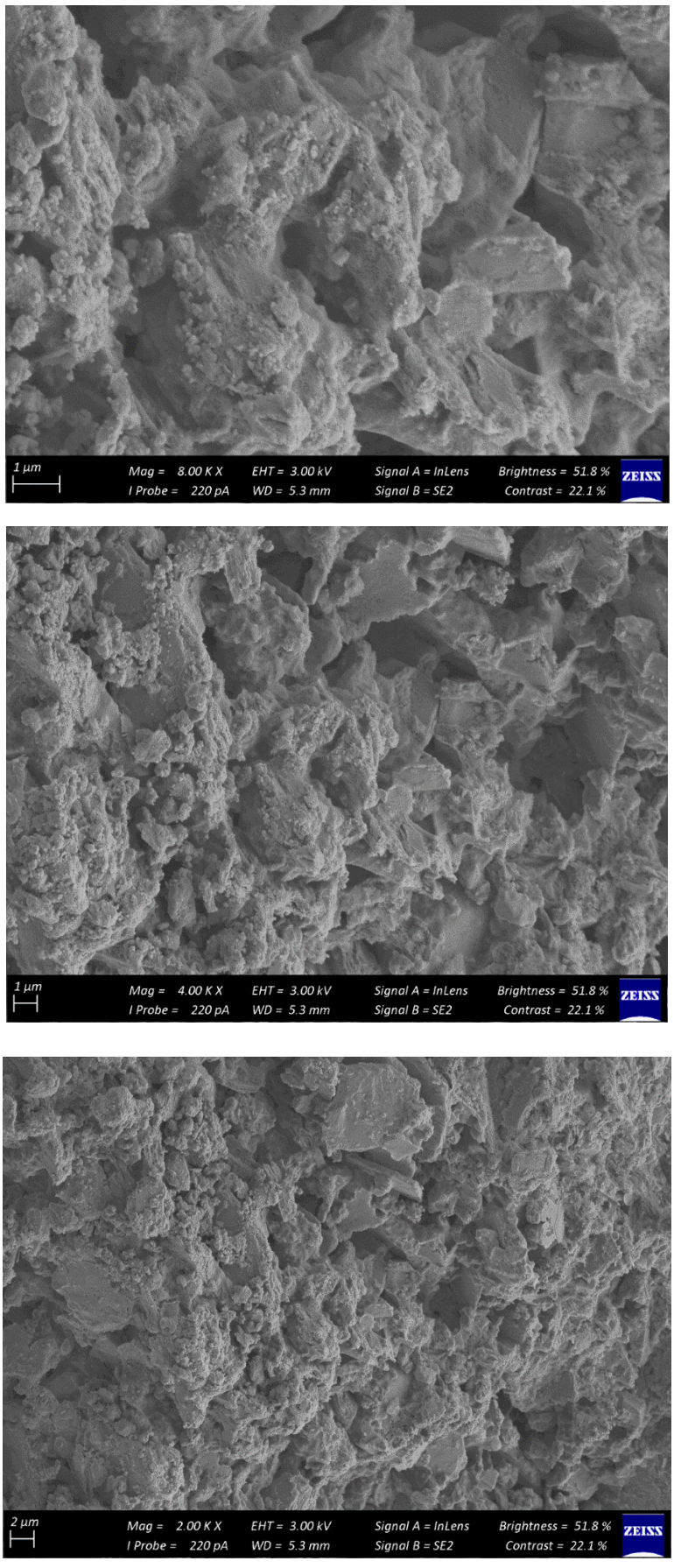

Figure 4.2-7: Different magnification SEM images of blank Selexsorb CD® at the outer parts of the adsorbent bead

4.2.3 Adsorbent Composition

An energy-dispersive X-ray (EDX) analysis was conducted on the three respective adsorbents to determine the elemental composition of these adsorbents before adsorption (Table 4.2-2). The composition was investigated at 150 different positions on the adsorbent particles and the average of these results was assumed as the composition. A brief methodology on the determination of the adsorbent compositions is provided in Appendix E (Section E.3.1, p219).

As expected, SCDx and SCD have relatively similar compositions whereas the composition of AA-F220 differs markedly. AA-F220 only has trace amounts of carbon with no sodium or silica. SCDx and SCD have a relatively large amount of silica with trace amounts of carbon and sodium. The combined composition of elemental aluminium and oxygen (the building blocks of AA) for AA-F220, SCDx and SCD is 96.9, 85.2 and 89.9 mass%, respectively. The composition of these adsorbents could also have been analysed with X-ray Diffraction (XRD), however, XRD was not considered in this study. For the detailed EDX analysis results refer to Appendix E (Section E.3.2, p220).

Table 4.2-2: EDX results for Activated Alumina F220, Selexsorb CDx® and Selexsorb CD® [4]

Element (mass%)	***Adsorbents***		
	Activated Alumina F220	***Selexsorb CDx®***	***Selexsorb CD®***
Aluminium (Al)	47.5	41.9	43.7
Oxygen (O)	49.5	43.3	46.1
Sodium (Na)	0.0	1.7	1.3
Carbon (C)	3.0	2.8	2.3
Silica (Si)	0.0	10.3	6.6

4.3 Chapter Summary

The objective of this chapter was to investigate the surface area and pore volume, pore structure and composition of three different AA adsorbents.

A BET analysis showed that SCDx and SCD have similar surface areas to AA-F220 but contain micropore volumes greater than that of AA-F220. SEM images showed that the pore structure of SCDx and SCD are more similar to one another than to that of AA-F220. Furthermore, SCDx and SCD have a more granular structure than AA-F220. Though the adsorbent compositions were determined to be fairly similar, the EDX analysis indicated that SCDx and SCD contain a large percentage of silica whereas AA-F220 does not.

[4] *The reported EDX analysis results are only accurate to one decimal place, as indicated in the equipment manual.*

Chapter 5: Adsorption Experimental Results

5.1 Overview

This chapter addresses objective (i) of this thesis. The objective of this chapter is therefore to investigate the experimental adsorption data obtained in this study. Firstly, the alcohol adsorption ability of various alumina adsorbents will be compared after which the effect of several variables on adsorption will be investigated. Lastly, the single and binary component adsorption behaviour will be compared after which binary interaction will be investigated.

5.2 Experimental Measurements

Various sets of data were measured in this study. The change in adsorbate concentration in the bulk solutions was measured with time. This allowed for the determination of the percentage adsorbate adsorbed from the solutions as a function of time as well as the adsorbent loading of each respective system. In this chapter, several parameters will be used to discuss the data and results obtained. These parameters include normalised adsorbate concentrations (C_t/C_o) and adsorbent loading (q_t). An outline of the calculation methodology of these parameters is provided in Appendix F (Section F.1, p227).

Nine different single component systems were investigated (adsorbate-adsorbent combinations). This was done at one temperature (45°C) using three different initial adsorbate concentrations. In addition, nine different binary component systems were investigated. This was done at two temperatures (25°C and 45°C), also using three different initial adsorbate concentrations. The time profiles of all systems investigated in this study, are provided in Appendix D (p185).

In this chapter, only the data measured in this study will be discussed and not the data measured by Groenewald [8]. This means that the single component data at a temperature of 45°C will be discussed and the binary component data both at 25°C and 45°C will be discussed.

5.3 Comparison of Various Activated Alumina Adsorbents

Firstly, the three adsorbents were compared based on their ability to remove alcohol adsorbates from n-decane. All three adsorbents proved to be technically viable as they all exhibited the ability to separate the 1-alcohols from the n-decane solvent.

5.3.1 Single Component Adsorption

Figure 5.3-1 depicts the concentration decay profiles of 1-hexanol, 1-octanol and 1-decanol at various initial concentrations using the three different adsorbents investigated. From these graphs it can be observed that

the adsorbents performed relatively similar. For the single component adsorption of 1-hexanol and 1-octanol, however, SCD seemed to slightly outperform AA-F220 at the equilibrium time with SCDx performing very similar to SCD in most cases (within the margin of error). For the system depicted in Figure 5.3-1a, SCD was able to remove approximately 77.0% of the 1-hexanol from the n-decane, while SCDx and AA-F220 removed 72.3% and 66.6%, respectively. For the system containing 1-octanol (Figure 5.3-1b), SCD removed 50.8% of the 1-octanol from the n-decane while SCDx and AA-F220 removed 50.0% and 47.3%, respectively at the equilibrium time of 1410 minutes. SCD and SCDx performing slightly better than AA-F220 at equilibrium may be attributed to the difference in micropore surface area, as these two adsorbents have micropore surface areas markedly greater than that of AA-F220.

For the systems containing 1-decanol (Figure 5.3-1c), the adsorbents performed more similar with little distinction in the percentage alcohol removed at equilibrium (within uncertainty range). The bond lengths of 1-hexanol, 1-octanol and 1-decanol are 11.18, 14.26 and 17.34 Å, respectively. Micropores are typically classified as having a pore width of less than 20 Å [101]. Since 1-decanol has a bond length closer to the upper limit of the size of micropores, it was expected that more of the 1-decanol molecules (than the 1-hexanol and 1-octanol molecules) would be excluded from the micropore structure based on size. SCDx and SCD therefore essentially had less surface area in the micropore structure available to 1-decanol, which would explain why SCDx and SCD did not necessarily outperform AA-F220 for the adsorption of 1-decanol like it did for the systems containing 1-hexanol and 1-octanol.

At times prior to equilibrium, AA-F220 seemed to outperform SCDx and SCD for all systems investigated. It can be observed in Figure 5.3-1 that the blue markers representing AA-F220 are below those representing SCDx an SCD at most of the time stamps between 0 and approximately 360 minutes. This indicates that AA-F220 adsorbed the 1-alcohols slightly faster than SCDx and SCD. According to Worch [10], equilibrium adsorbent loading is more closely related to internal surface area, therefore SCDx and SCD performed marginally better at equilibrium for some of the systems, while adsorption kinetics is more closely related to external surface area. As mentioned in Chapter 4 (Section 4.2.1), AA-F220's external surface area and mesopore structure constitute most of its total surface area and its external surface area is also markedly greater than that of SCDx and SCD. AA-F220 therefore has a much larger surface area readily available to the alcohol adsorbate molecules without much interference of diffusion through the transport pores. As the SEM images also showed, the transport pores of AA-F220 are visibly larger than those of SCDx and SCD which results in more adsorbate molecules reaching active adsorption sites within a shorter time period. The largest part of SCDx and SCD's surface areas are within their micropore structures, therefore the adsorbate molecules first needed to diffuse through the transport pores to reach the active sites situated inside these adsorbents' micropore structures.

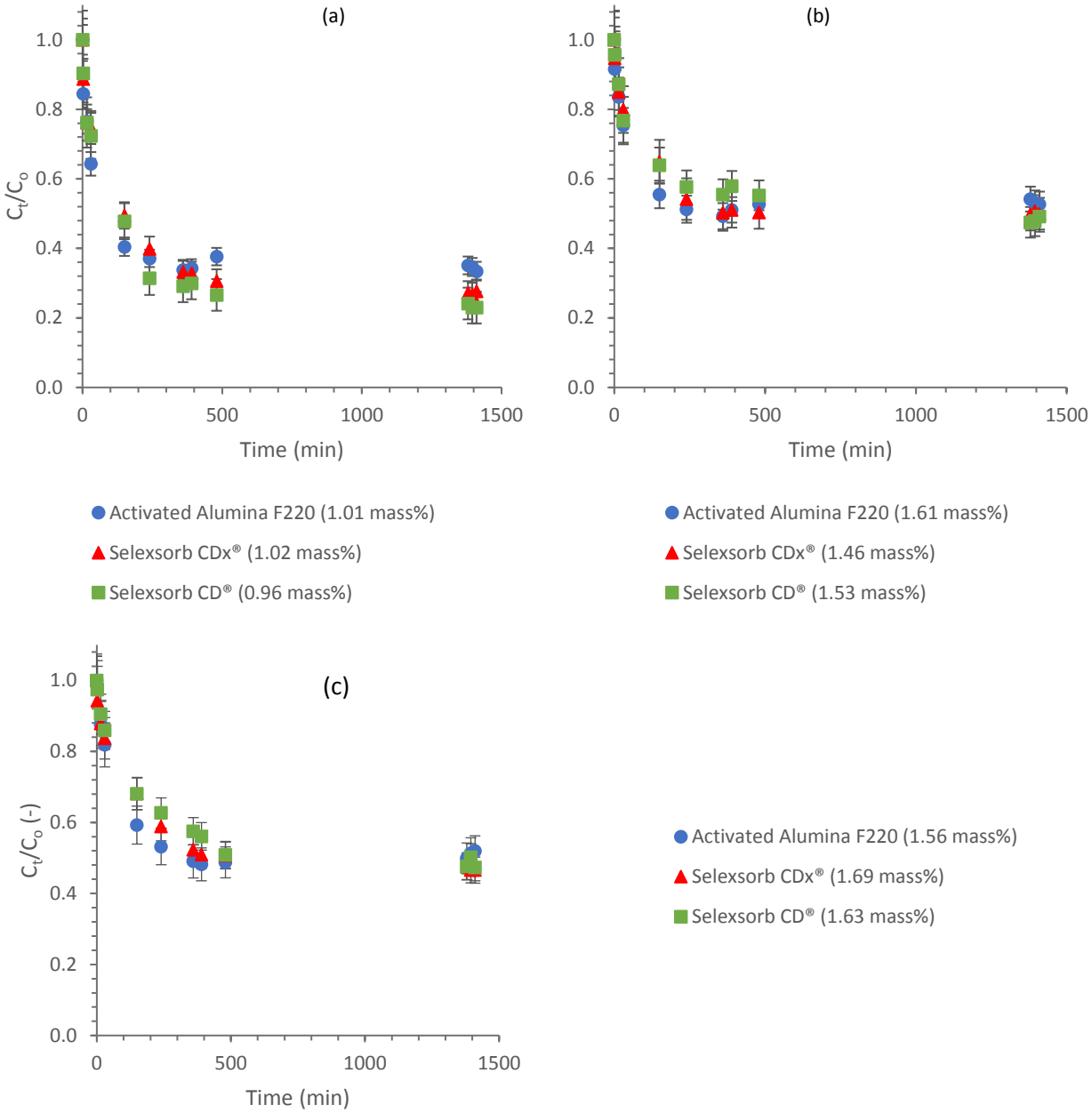

Figure 5.3-1: Comparison of adsorbents for the single component adsorption of (a) 1-hexanol (IC as indicated); (b) 1-octanol (IC as indicated); and, (c) 1-decanol (IC as indicated) (T = 45°C)

All of the abovementioned trends were evident throughout for the investigated systems with initial adsorbate concentrations of approximately 1 mass% and higher, however, for the systems with initial adsorbate concentrations less than approximately 1 mass%, this trend was not consistent. Refer to Appendix D (p185) for the concentration decay graphs of all other systems investigated.

Above findings were contradictory to that reported by Groenewald [8], where it was found that AA-F220 exhibited the best alcohol adsorption ability in an alcohol-alkane system when compared to SCDx and SCD. Groenewald [8] did, however, report that as temperature was increased in the range of 25°C to 35°C, SCDx and SCD exhibited enhanced adsorption in some cases. This could explain why SCDx and SCD marginally

outperformed AA-F220 in this study at 45°C, as a higher temperature would provide more energy to more adsorbate molecules to diffuse into the micropore structure and reach available adsorption sites.

The equilibrium adsorbent loadings of the adsorbents (at given conditions) are encapsulated in Table 5.3-1. Note that the ranges are to account for the uncertainties in these adsorbent loadings.

Table 5.3-1: Equilibrium adsorbent loadings of various activated alumina adsorbents (T = 45°C)

Adsorbates	***Adsorbent loadings (mg/g)***		
	AA-F220	*SCDx*	*SCD*
1-hexanol	115-119	117-121	117-121
1-octanol	111-115	114-118	117-121
1-decanol	114-118	116-120	116-120

5.3.2 Binary Component Adsorption

For the binary component systems, several different trends were observed. For the binary component systems of 1-hexanol and 1-octanol, SCDx and SCD marginally outperformed AA-F220 at equilibrium, both at both 25°C and 45°C and all initial adsorbate concentrations (Figure 5.3-2 a and b). This was to be expected since most of the 1-hexanol and 1-octanol adsorbate molecules would enter the micropore structure of SCDx and SCD which is markedly greater than that of AA-F220. There was one anomaly at 25°C and an initial adsorbate concentration of approximately 1 mass% where this trend was not observable.

At both 25°C as well as 45°C, AA-F220 appeared to outperform SCDx and SCD at equilibrium for the systems containing a mixture of 1-hexanol and 1-decanol (Figure 5.3-2 c and d). The equilibrium adsorbent loadings obtained by AA-F220 was more comparable to SCDx and SCD for the single component adsorption of 1-decanol due to partial size exclusion of the 1-decanol molecules in SCDx and SCD.

For most of the binary component systems investigated, AA-F220 seemed to either perform relatively similar to SCDx and SCD (within the uncertainty margin) or marginally outperform SCDx and SCD for a short period of time prior to the equilibrium time, *i.e.* in the period of 0 to approximately 30 minutes. This can be attributed to the larger external surface area of AA-F220, as discussed for the single component adsorption (Section 5.3.1).

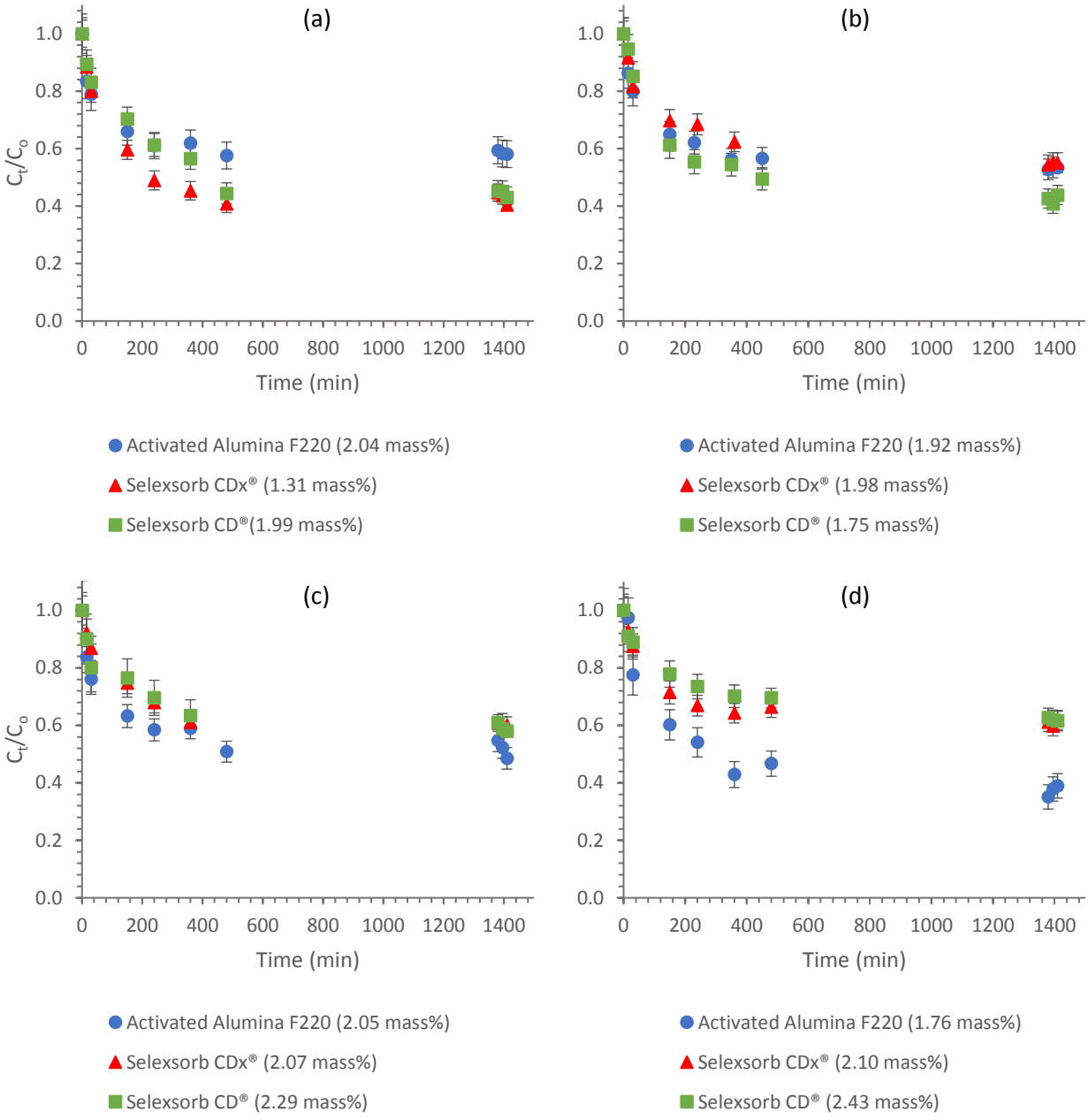

Figure 5.3-2: Comparison of adsorbents for the total binary component adsorption of a (a) 1-hexanol + 1-octanol (50:50) mixture (T = 45°C); (b) 1-hexanol + 1-octanol (50:50) mixture (T = 25°C); (c) 1-hexanol + 1-decanol (50:50) mixture (T = 45°C); and, (d) 1-hexanol + 1-decanol (50:50) mixture (T = 25°C) (IC as indicated)

For binary component systems the maximum adsorbent loadings of the various AA adsorbents are much more complex to determine as there are several contributing factors, such as the interaction between the adsorbates. This will be discussed in greater detail later in this chapter. It is interesting to note nonetheless, that the equilibrium adsorbent loadings of the binary component mixtures (at given conditions) were found to be somewhat greater than for the single component systems (Table 5.3-2) .

Table 5.3-2: Equilibrium adsorbent loadings of various activated alumina adsorbents when adsorbing binary (equimass) 1-alcohol mixtures (T = 45°C)

Adsorbates	***Adsorbent loadings (mg/g)***		
	AA-F220	*SCDx*	*SCD*
1-hexanol + 1-decanol	128-132	130-134	130-134
1-hexanol + 1-octanol	128-132	126-130	138-142
1-octanol + 1-decanol	128-132	127-131	138-142

5.4 Variables Influencing Adsorption

After investigation of the adsorbents, several variables were investigated based on their effect on the adsorption of 1-alcohols from n-decane. The variables that will be discussed in this section are initial adsorbate concentration, temperature, and alcohol carbon chain length.

5.4.1 Temperature

For the majority of the single component systems, increasing the temperature resulted in a corresponding increase in the equilibrium adsorbent loading (Figure 5.4-1a & b). For the binary component systems using AA-F220, no discernible trend could be identified with regards to the equilibrium adsorbent loadings at different temperatures. For SCDx and SCD, the majority of the systems and initial adsorbate concentrations exhibited enhanced equilibrium adsorbent loadings at the higher temperature of 45°C (Figure 5.4-1c & d) with the exception of some cases exhibiting relatively equal equilibrium adsorbent loadings with differences of less than approximately 7 mg/g (*e.g.* the systems summarised in Table C.1-29 (p161) and Table C.1-32 (p163), Appendix C).

As depicted in Figure 5.4-1, the systems operating at 45°C adsorbed markedly more of the respective adsorbates within a shorter period of time. When referring to Figure 5.4-1c for example, it can be observed that to achieve an adsorbent loading of approximately 90 mg/g, the system at 45°C required 150 minutes whereas the system at 25°C required 360 minutes.

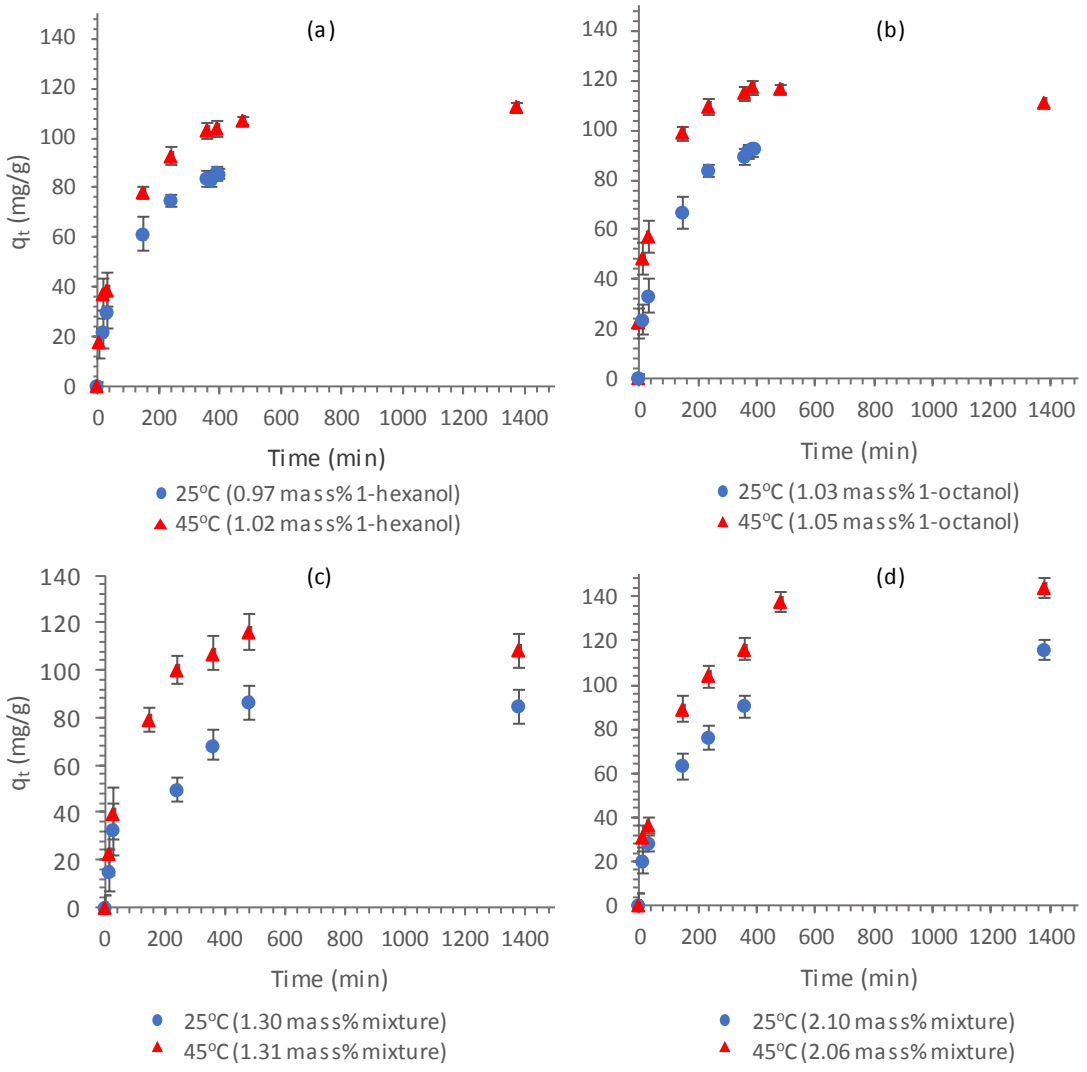

Figure 5.4-1: Time profiles for the (a) single component adsorption of 1-hexanol (Selexsorb CDx®); (b) single component adsorption of 1-octanol (Activated Alumina F220); (c) binary component adsorption of a 1-hexanol + 1-octanol total mixture (Selexsorb CDx®); and, (d) binary component adsorption of a 1-octanol + 1-decanol mixture (Selexsorb CD®) (25°C single component data obtained from [8]) [5]

An increase in adsorption when increasing the temperature may be attributed to an increase in energy in the systems; increased energy would provide adsorbate molecules with the required energy to break intramolecular bonds and form bonds with the adsorbent surfaces in the case of chemisorption [36], thereby increasing adsorbent loadings, and also provide the necessary energy for adsorbate molecules to diffuse through the adsorbent pore structures, especially the micropore structures, which would increase the adsorption kinetics. Increased energy would allow for more collisions between different adsorbate molecules as well as adsorbate molecules and the adsorbent surfaces [18], [19], resulting in better diffusion through

[5] *The single component data at 25°C measured by Groenewald* [8] *had an equilibrium time of 390 min, therefore at this temperature no data points are present at 1410 min (the equilibrium time used in this study). Groenewald* [8]*, however, argued that a period of 390 min was sufficient time to reach equilibrium, making these values comparable with the data measured in this study.*

the pore structure of the adsorbents. Since AA-F220 contains less of a micropore structure as compared to SCDx and SCD, it may partially explain why no definitive increase in the total equilibrium adsorbent loading was exhibited in some of the binary component systems when increasing the temperature, *e.g*. the binary system of 1-hexanol and 1-octanol with initial concentration of approximately 2 mass% onto AA-F220 (Appendix C, Table C.1-27, p155 and Table C.1-20, p157). The relatively equal equilibrium adsorbent loadings at different temperatures, as exhibited by some of the binary component systems using AA-F220, SCDx and SCD, could also be due to increased adsorbate-adsorbate interaction between the respective adsorbates at higher temperatures, resulting in slightly lower adsorption. This will be discussed in more detail in Section 5.6.

Several studies have reported AA adsorbents to perform better at higher temperatures. Ruthven [22] pointed out that AA has enhanced adsorbent loading for water vapour at higher temperatures, hence the reason for AA commonly being used as a desiccant at elevated temperatures [52]. A study conducted by Mtaallah *et al.* [102] also proved that the removal efficiency of cadmium from wastewater by using AA, increased with an increase in temperature from 10 to 40^{o}C. For systems similar to the ones investigated in this study, Groenewald [8] reported an increase in adsorption for an increase in temperature in the temperature range of 25^{o}C to 35^{o}C, which concurs with the findings of this study.

As discussed in Section 2.4.1, temperature has different effects on physisorption and chemisorption processes which allows for temperature to be applied in attempting to distinguish between these two types of adsorption. In this study, most cases exhibited an increase in adsorbent loadings with an increase in temperature, which could be indicative of chemisorption. However, since some cases exhibited relatively equal equilibrium adsorbent loadings, *i.e.* equilibrium loadings differing less than approximately 7 mg/g, or a slight decrease in adsorbent loadings with increasing temperature (*e.g.* the binary system of 1-hexanol and 1-decanol onto AA-F220 (Appendix C, Table C.1-12, p153 and Table C.1-15, p154) as well as the binary system of 1-hexanol and 1-decanol onto SCD (Appendix C, Table C.1-48, p171 and Table C.1-51, p172), both with initial alcohol concentrations of approximately 3 mass%), it may suggest a possible combination of chemisorption and physisorption.

A study conducted by Cai and Sohlberg [103] on the adsorption of alcohols onto AA found that alcohols were chemisorbed. In abovementioned study, an AA cluster ($Al_{48}O_{72}$) was used to represent an AA adsorbent with methanol, ethanol, propanol and isopropanol used as adsorbates. Two different adsorbent bonding sites were investigated: (i) A site where the oxygen atom on the adsorbent surface had an adjacent cationic aluminium vacancy (Site A); and, (ii) A site where the oxygen on the adsorbent surface did not have an adjacent vacancy (Site B) [103]. For chemisorption to take place on Site A, only the alcohol functional group hydrogen (H_{al}) is required to interact with the oxygen on the adsorbent surface (O_s), *i.e.* hydrogen bonding

[103]. For chemisorption to occur at Site B, however, H_{al} has to interact with O_s while the oxygen from the alcohol functional group (O_{al}) is also required to interact with the aluminium cation (Al) on the adsorbent surface [103]. According to Zhou and Snyder [104], η- and γ-alumina adsorbents contain cation vacancies, meaning for the adsorbents investigated in this study (γ-alumina adsorbents), adsorption is more likely to take place on Site A. According to the results found in this study and that reported in the study by Cai and Sohlberg [103], it is speculated that adsorption of 1-alcohols onto AA-F220, SCDx and SCD occurred through some form of chemisorption. Groenewald [8], however, reported that AA-F220, SCDx as well as SCD containing 1-alcohol adsorbates (spent adsorbents after adsorption) could be regenerated at temperatures of 185 and 205°C. This would suggest weak chemisorption in the case of chemisorption, with the possibility of weak chemisorption in combination with physisorption. A typical configuration of the chemisorption of an alcohol onto AA is pictured in Figure 5.4-2.

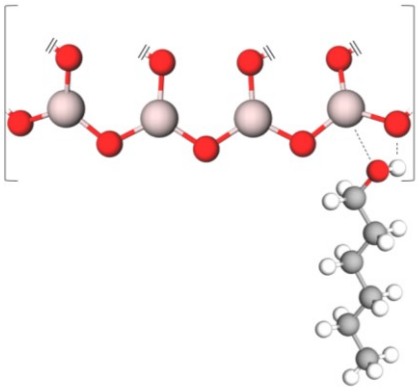

Figure 5.4-2: A typical configuration of the chemisorption of an alcohol (in this case 1-hexanol) onto activated alumina, Al_2O_3 (partial representation), with the dashed lines indicating the interaction between H_{al} and O_s, and O_{al} and Al (redrawn from [103]) [6]

SEM images of the respective adsorbents were taken before and after adsorption of the alcohol adsorbates (Figure 5.4-3, Figure 5.4-4 and Figure 5.4-5). Using the scanning-electron microscope, several different adsorbent beads were investigated at the same relative positions on the beads before and after adsorption, to ensure that the findings from the SEM images were representative of all the adsorbent beads. These images were compared to see if any changes could be observed after adsorption, and it was found that there were slight differences in the images albeit on a small scale. The reason for these differences is uncertain and the magnification and resolution of the SEM images are not on a molecular level, however, it is speculated that it may be indicative of chemisorption that took place during the adsorption process.

SEM analysis can only be done on dry samples; thus, the adsorbents were dried (at 30°C) before analysis. It is thought that most, if not all, physisorbed material would desorb from the adsorbent surface during the

[6] *Image constructed with MolView software*

drying process and the remainder (should any material remain on the surface) would desorb during SEM analysis when the adsorbent particles are degassed. Chemisorbed material, however, should hypothetically not desorb at such low temperatures. As mentioned, AA adsorbents are very resilient and do not shrink or swell in solution, they also do not disintegrate, change form or break easily [27]. This would suggest that the changes in the SEM images from before and after adsorption were not structural changes, but rather possible chemical changes as a result of chemical bonds that formed between the alcohol adsorbates and the adsorbent surfaces. This supports the argument of possible chemisorption occurring.

(a) (b)

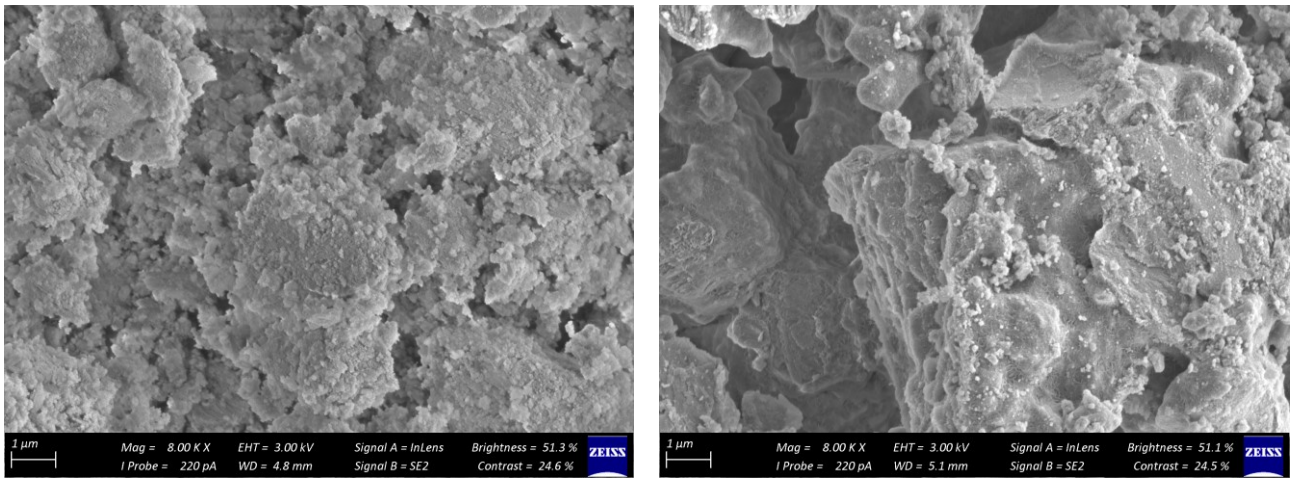

Figure 5.4-3: Activated Alumina F220 SEM images (a) before; and, (b) after adsorption

(a) (b)

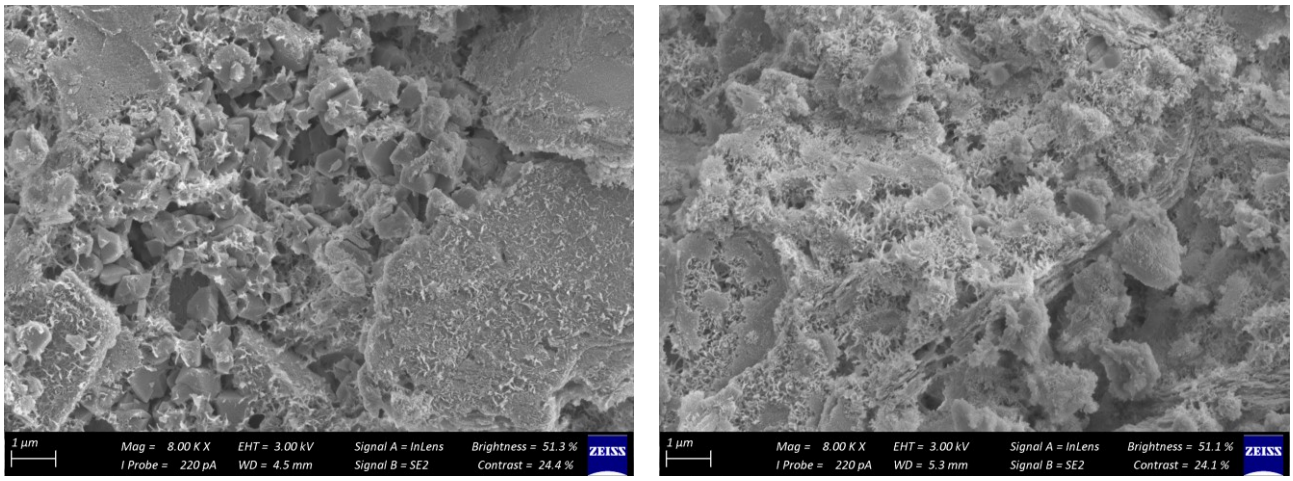

Figure 5.4-4: Selexsorb CDx® SEM images (a) before; and, (b) after adsorption

(a) (b)

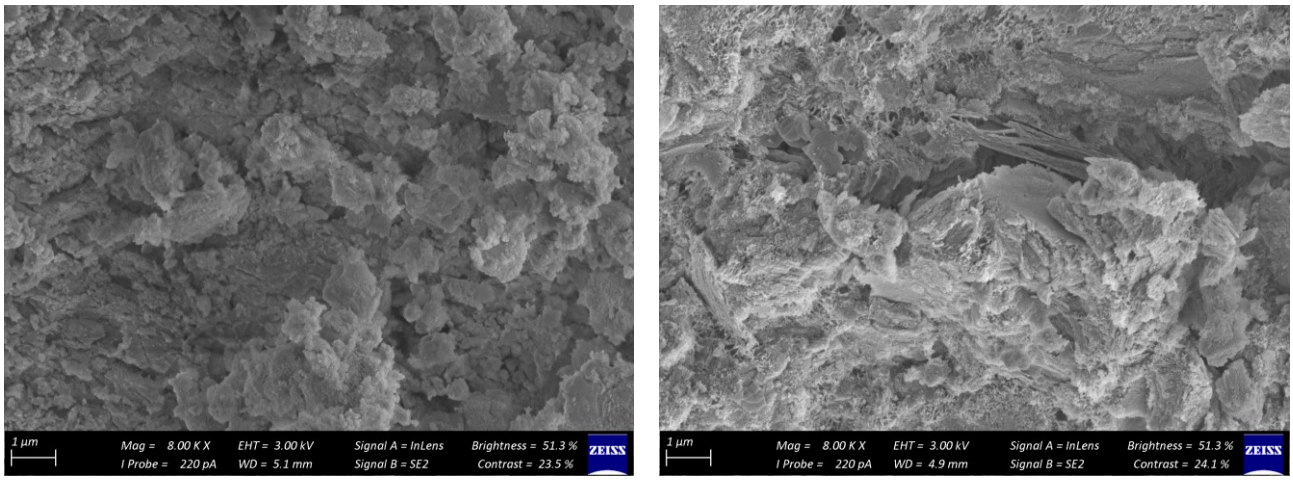

Figure 5.4-5: Selexsorb CD® SEM images (a) before; and, (b) after adsorption

5.4.2 Initial Adsorbate Concentration (IC)

As expected, initial adsorbate concentration had quite a significant effect on the adsorption process. Compared to the other variables investigated (in the ranges considered in this study), it was observed that initial adsorbate concentration had the most pronounced effect on both the single as well as the binary component adsorption systems.

Within the investigated concentration range, adsorbent loading increased with increasing initial adsorbate concentration for both the single and binary component systems. Increasing adsorbent loading with increasing initial adsorbate concentration is to be expected, since the concentration gradient between the liquid phase and the solid phase is greater; this in turn results in a more significant driving force for adsorption [105]. With an increased number of adsorbate molecules, the high energy sites on the adsorbents will be filled first, after which the lower energy sites will progressively also be filled [84].

For most systems, the increase in adsorption was not indefinite which was also to be expected. Typically, the adsorbent loading will not increase indefinitely with increasing initial adsorbate concentration, since the adsorbent might reach its saturation capacity. For most single component systems, excluding the anomalies of 1-decanol onto SCDx and 1-hexanol onto SCD (Appendix D, Section D.1, p186), the adsorbent loading of the systems started to plateau for initial concentrations greater than approximately 1-1.2 mass%. This trend was observed for most of the single component systems. Some of these systems are provided in Figure 5.4-6. As depicted, little to no increase in the equilibrium adsorbent loadings was exhibited when increasing the initial adsorbate concentrations beyond 1.10 (Figure 5.4-6a), 1.18 (Figure 5.4-6b), 1.02 (Figure 5.4-6c) and 1.05 mass% (Figure 5.4-6d), for the different systems respectively.

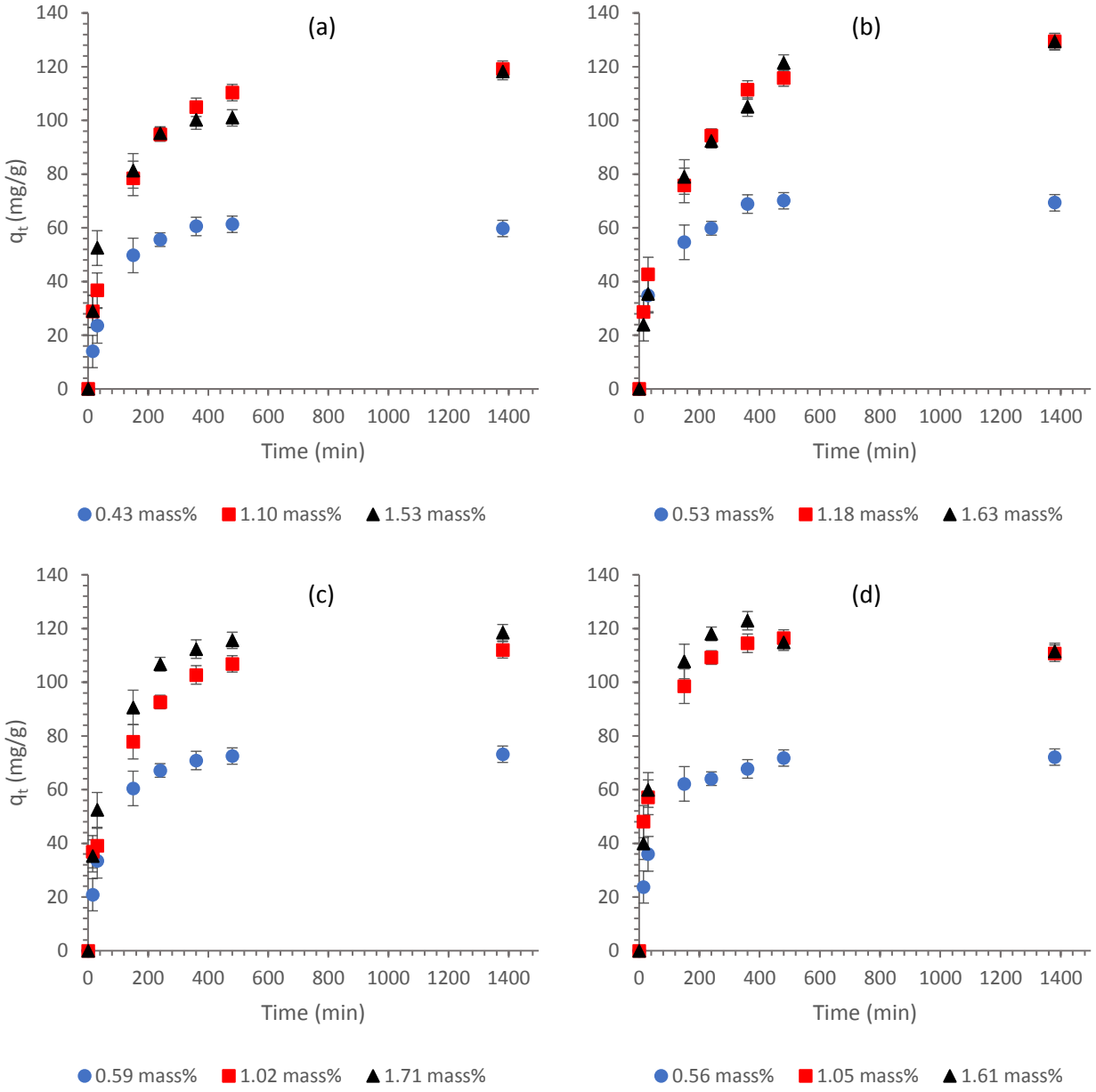

Figure 5.4-6: Time profiles for the single component adsorption of (a) 1-octanol onto Selexsorb CD®; (b) 1-decanol onto Selexsorb CD®; (c) 1-hexanol onto Selexsorb CDx®; and, (d) 1-octanol onto Activated Alumina F220, with different initial adsorbate concentrations (T = 45°C)

The results obtained in this study for the single component systems, concur with those of other studies including a study conducted by Mtaallah *et al.* [102] on the adsorption of cadmium onto AA, and a study by Srivastav *et al.* [54] on "adsorptive desulfurization by activated alumina". In both these studies they found that the initial adsorbate concentration of the adsorbate in the solution, cadmium and sulfur respectively, had an appreciable effect on the adsorbent loading of the AA when varying the concentration from 10 to 100 $mg.mL^{-1}$ for the cadmium system [102] and 100 to 1000 $mg.mL^{-1}$ for the desulfurization system [54]. In addition, Groenewald [8] also reported an increase in adsorption for an increase in initial adsorbate concentration for systems similar to the single component systems investigated here

Similar to that of the single component systems, the increase in equilibrium adsorbent loading with increase in initial adsorbate concentration was not indefinite for the binary component systems either, and started to plateau for concentrations greater than approximately 1.2 mass% for the vast majority of these systems (Figure 5.4-7). Anomalies were observed for the systems of 1-hexanol + 1-decanol onto AA-F220 and 1-hexanol + 1-octanol onto SCD at 25°C, and 1-hexanol + 1-octanol onto SCDx at 45°C (Appendix D, Section D.2, p195) where this trend was not exhibited.

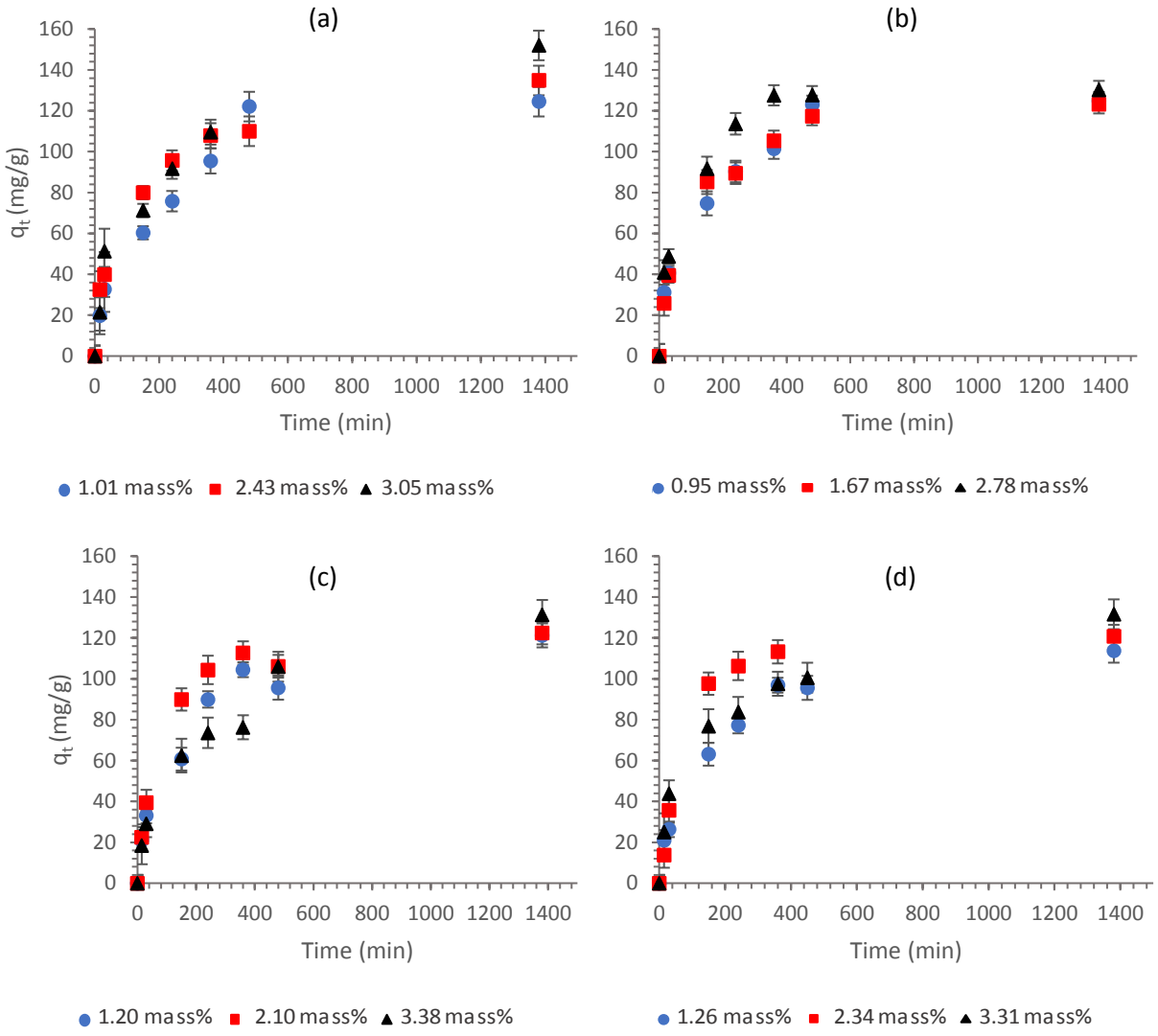

Figure 5.4-7: Time profiles of the binary component adsorption of a 50:50 mixture of (a) 1-hexanol and 1-decanol onto Selexsorb CD® (T = 45°C); (b) 1-octanol + 1-decanol onto Selexsorb CDx® (T = 45°C); (c) 1-hexanol + 1-decanol onto Selexsorb CDx® (T = 25°C); and, (d) 1-octanol + 1-decanol onto Selexsorb CDx® (T = 25°C), with different initial adsorbate concentrations

In addition to the adsorbents possibly achieving saturation capacity, the adsorbent loading not increasing for greater initial adsorbate concentrations could also possibly be ascribed to adsorbate-adsorbate interaction. According to Cai and Sohlberg [103], adsorbed alcohol molecules adjacent to one another may start to

interact as the adsorbent approaches saturation capacity. In the case of H_{al} interacting with O_s, O_{al} and O_s will come into close proximity and may start to repel one another. This in turn impedes adjacent alcohol molecules from achieving the desired configuration for chemisorption and can limit the adsorbent loading of the system [103].

5.4.3 Alcohol Chain Length

The effect of alcohol carbon chain length on adsorption was investigated through:

(i) Investigation and comparison of the single component adsorption of 1-alcohols;

(ii) Comparison of the adsorption of various respective 1-alcohols in a binary component system; and,

(iii) Investigation and comparison of the adsorption of different binary combinations of 1-alcohols.

5.4.3.1 *Effect of Alcohol Chain Length on Single Component Adsorption*

Firstly, the adsorption of single component systems was investigated. The alcohol carbon chain length proved to have a very small to no influence on the equilibrium adsorption of these single component systems as the equilibrium adsorption of the different 1-alcohols was relatively equal comparatively (and within the uncertainty range), when using either of the adsorbents and initial concentrations investigated (Figure 5.4-8).

Though the effect of the alcohol chain length was not as pronounced on the equilibrium adsorption, the vast majority of the single component systems at various initial adsorbate concentrations exhibited marginally better adsorption for the two shorter chain alcohols, 1-hexanol and 1-octanol as compared to 1-decanol, during a short period of time prior to the total equilibrium time. This can be observed in the examples provided, where the blue and red markers are below the green markers in the time period of 0 minutes to approximately 400 minutes (Figure 5.4-8). This was especially pronounced in the time period of 0 minutes to 30 minutes for the systems using AA-F220 (Figure 5.4-8c) where decidedly more of the 1-hexanol and 1-octanol adsorbates were adsorbed as compared to the amount of 1-decanol adsorbed in this time. This indicates that 1-hexanol and 1-octanol were adsorbed slightly faster than 1-decanol which may be attributed to the shorter chain alcohols diffusing into the pore structures of the various adsorbents with less hindrance than the longer chain alcohol, 1-decanol.

The study conducted by Groenewald [8] found that when comparing the single component adsorption of 1-hexanol, 1-octanol and 1-decanol onto AA, 1-hexanol seemed to adsorb slightly better than the other two alcohols. However, the equilibrium adsorbent loadings of these three alcohols were also reported to be relatively equal comparatively, which coincides with the findings in this study [8].

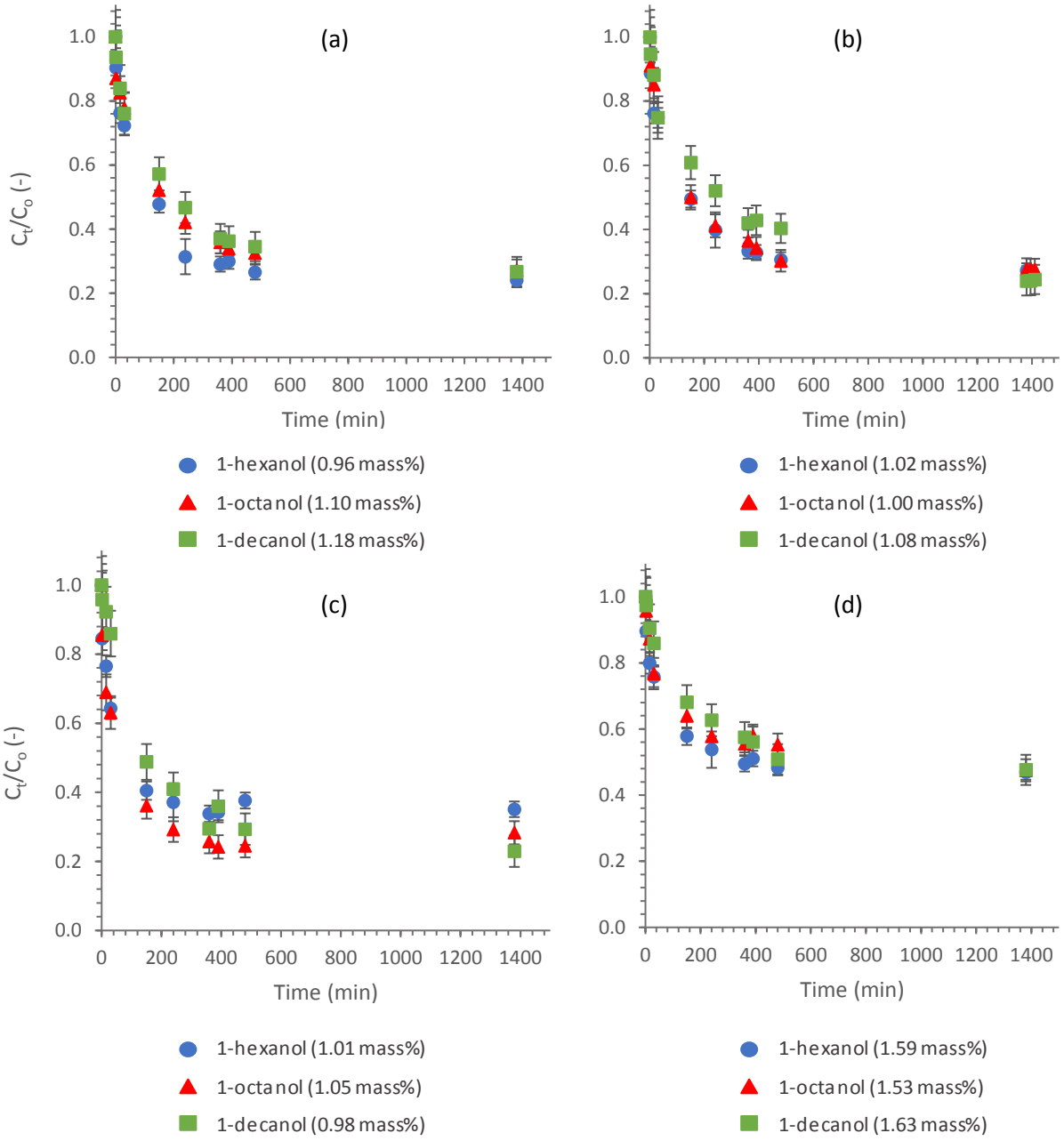

Figure 5.4-8: Concentration decay profiles for the single component adsorption of various 1-alcohols onto (a) Selexsorb CD®; (b) Selexsorb CDx®; (c) Activated Alumina F220; and, (d) Selexsorb CD® (different IC than system in a) (IC as indicated; T = 45°C)

5.4.3.2 *Effect of Alcohol Chain Length on the Adsorption of an Alcohol in a Binary Component System*

The selectivity parameter was used to determine the effect of alcohol carbon chain length on the adsorption of the 1-alcohols in a binary component system. Selectivity was investigated by comparing the ratio of the liquid phase initial concentration of the alcohols to the ratio of the solid phase concentration of the different alcohols at equilibrium, *i.e.* the adsorbent loading of the alcohols at equilibrium. This was done to determine the affinity and preference of the adsorbents for specific alcohols [106] and to determine the effect of alcohol carbon chain length on adsorption. A similar method has been used by numerous other studies to determine

the affinity for a specific adsorbate. These studies include that of Moreno-Pérez *et al.* [40] for the study of heavy metals and acid blue 25 onto activated carbon, and Hernández-Hernández *et al.* [106] for the study of heavy metals onto stratified bone char.

The selectivity graphs of two systems are provided in Figure 5.4-9. Should the ratio of the adsorbent loadings be on the straight line depicted, the ratio of alcohols in the solution at the start of the experimental run is equal to the ratio of alcohol adsorbed at equilibrium. This would suggest that the adsorbent has an equal affinity for both alcohols. Should the adsorbent loading ratio be above the straight line, the adsorbent exhibits a preference for the shorter chain alcohol and vice versa. From Figure 5.4-9 it can be observed that the shorter chain alcohols in the binary mixtures were preferentially adsorbed, since the ratios are predominantly above the straight line. The data points indicating this finding are, however, within the uncertainty margin.

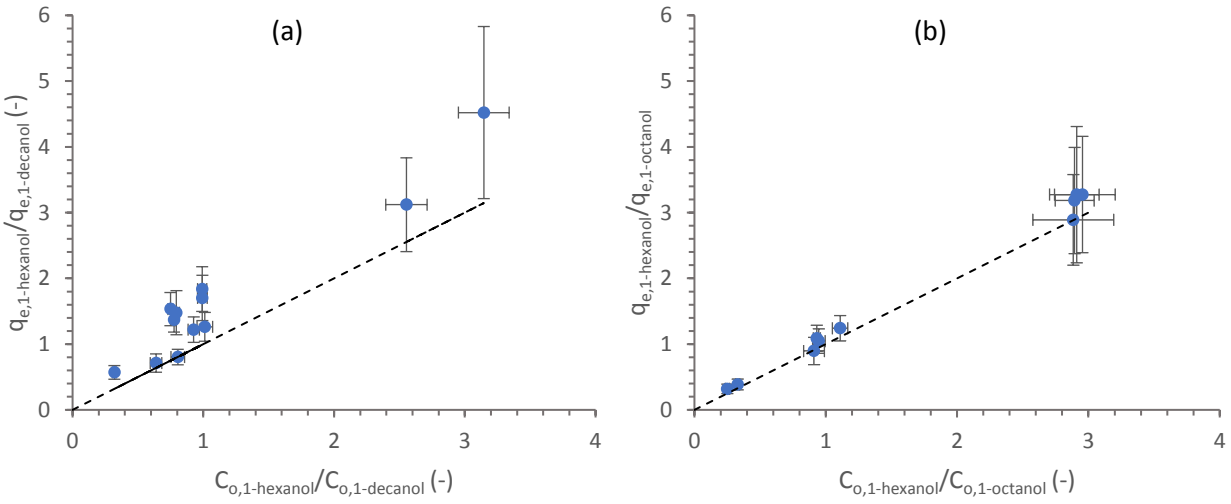

Figure 5.4-9: Comparison of initial liquid phase adsorbate concentration ratio and equilibrium adsorbent loading ratio in a binary component system of (a) 1-hexanol and 1-decanol (Selexsorb CDx®; T = 45°C); and, (b) 1-hexanol and 1-octanol (Activated Alumina F220; T = 25°C)

For the binary systems of 1-hexanol and 1-octanol (Figure 5.4-9b), and 1-octanol and 1-decanol, the various adsorbents only exhibited a small inclination towards the shorter chain alcohol. For the binary system comprising 1-hexanol and 1-decanol (Figure 5.4-9a), preference for the shorter chain alcohol was somewhat more pronounced, however, still within the uncertainty margin. This seemed to be the case for the majority of the systems investigated (at both temperatures, using all adsorbents) and is due to the difference in the carbon chain length of 1-hexanol and 1-decanol being double that of the difference in the other binary alcohol systems.

5.4.3.3 *Effect of Combined Alcohol Chain Length in Binary Component Adsorption*

The effect of the combined chain length in the binary component mixtures, *i.e.* the mixture of the two alcohols, was much more unclear. The equilibrium adsorbent loadings of the respective binary component systems appeared to be relatively equal, with the loadings having differences within the error margin (Figure 5.4-10). In many cases, the binary component systems containing 1-hexanol exhibited greater adsorbent loadings at times prior to equilibrium (0 to approximately 400 minutes), than the one system not containing 1-hexanol, *i.e.* the system of 1-octanol + 1-decanol (Figure 5.4-10). This was to be expected, since the combined carbon chain lengths of the two systems containing 1-hexanol were less than the system not containing 1-hexanol. These differences in adsorption were, however, very small and within the uncertainty range for most of these cases.

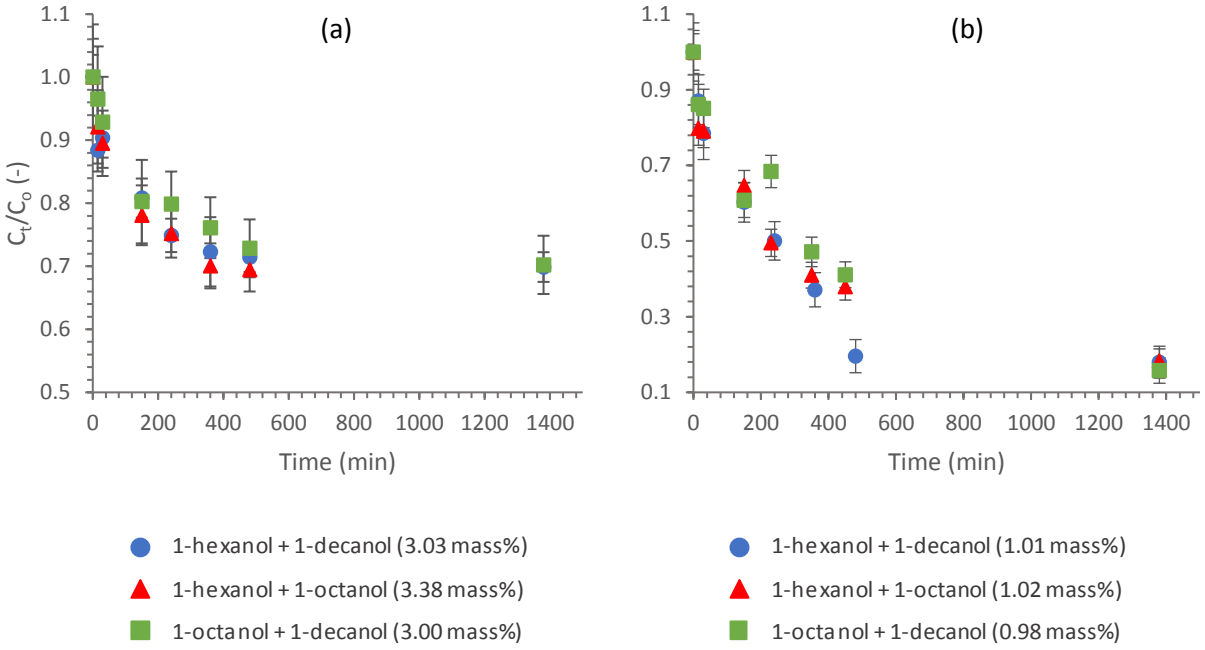

Figure 5.4-10: Concentration decay profiles for the binary component adsorption of various 1-alcohol mixtures (50:50) onto Selexsorb CD® at (a) 45°C; and, (b) 25°C (IC as indicated) [7]

The effect of the carbon chain length observed for the abovementioned systems (Sections 5.4.3.1, 5.4.3.2 and 5.4.3.3) can be attributed to the size of the adsorbate molecules and pore structure of the various adsorbents, and possibly also to the polarity of the different chain length alcohols.

As the carbon chain length of the alcohols increases, the molecule size increases. As mentioned in Chapter 4 (Section 4.2.1), the average pore diameters of AA-F220, SCDx and SCD are 48.179, 42.890 and 46.104 Å respectively. The total bond lengths of 1-hexanol, 1-octanol and 1-decanol are 11.18, 14.26 and 17.34 Å

[7] *The y-axis scales of the two graphs have been adjusted in order to provide a clearer representation of the data/trends*

respectively [8]. The average micropore diameters of AA-F220, SCDx and SCD are 10.879, 7.972 and 8.480 Å, respectively. This indicates that overall the adsorbents have pore sizes large enough to accommodate the adsorbates investigated, however, with possible size exclusion of some of the adsorbate molecules in the micropore structures. As reported in a study by Hsieh and Teng [37], however, it is possible that smaller sized adsorbate molecules are adsorbed more effectively due to less interference when diffusing through the pores of the adsorbent. This may explain why the shorter chain alcohols in this study adsorbed marginally better in some cases.

For the adsorption of alcohols from alkanes using AA, polarity is very significant; AA is polar, thereby attracting the polar end of the alcohol molecules and not the non-polar alkane molecules. As the chain length of the alcohols increases, the polar part of the molecule, *i.e.* the OH^- functional group, becomes a smaller part of the molecule. Since the longer chain alcohols are therefore slightly less polar than the shorter chain alcohols, it is possible that adsorption of the latter would be more effective than that of the former.

5.5 Comparison of Single and Binary Component Adsorption

To investigate the adsorption behaviour of single and binary component systems the following were compared (all with equal initial adsorbate concentration):

(i) Adsorption of a 1-alcohol in single component system (*e.g*. adsorption of alcohol "*A*" in a system containing only alcohol "*A*" in solution);

(ii) Adsorption of the same 1-alcohol in a binary component system (*e.g*. adsorption of alcohol "A" in a system containing alcohols "*A*" and "*B*" in solution); and,

(iii) Adsorption of a binary component mixture comprising the same 1-alcohol as in (i) and (ii), together with another 1-alcohol (*e.g*. adsorption of the mixture of alcohols "*A*" and "*B*" in solution).

For the systems investigated in this study, it was shown that the total fraction of 1-alcohol adsorbates adsorbed from the bulk solution at equilibrium, of a system comprising a single 1-alcohol adsorbate and a mixture comprising two 1-alcohol adsorbates were relatively equal, *i.e.* within 15% of one another for this specific system (Figure 5.5-1). In some cases, the equilibrium fraction of the binary alcohol mixture adsorbed even surpassed that of the single component system albeit by a small margin.

It was observed that even though a relatively equal fraction of the binary component mixture and single component system (of equal initial adsorbate concentration) was adsorbed at equilibrium, the adsorption of a single component within a binary component mixture (with the single component in the binary mixture having the same initial concentration as the single component system), was notably poorer than in a

corresponding single component system (Figure 5.5-1). This may be due to the different adsorbates in the binary component mixture competing for active adsorption sites on the adsorbent surface, as will be discussed in Section 5.6. This trend was evident for most cases, *i.e.* different AA adsorbents, temperatures and different adsorbate systems, with some of the lower initial concentration systems (approximately 0.5 mass%) exhibiting slightly different behaviour, where the fraction adsorbed of the single 1-alcohol in the binary component system became more comparable to that of the single component system.

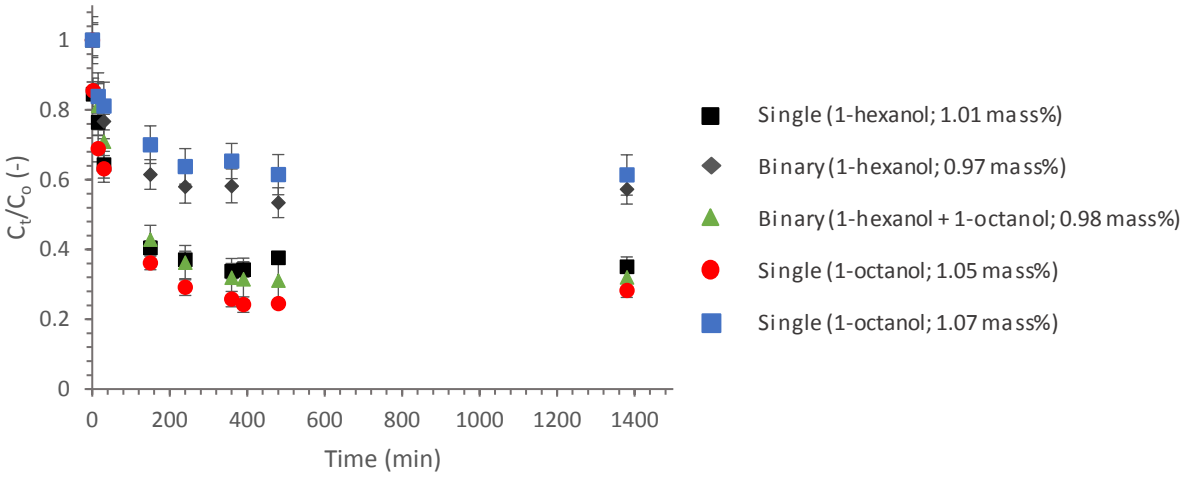

Figure 5.5-1: Concentration decay profiles for the adsorption of a single component, a single component in a 50:50 binary mixture (comprising 1-hexanol + 1-octanol) as well as a total 50:50 binary mixture (comprising 1-hexanol + 1-octanol) all with approximately the same initial concentration, onto Activated Alumina F220 (T = 45°C) [8]

At times prior to the equilibrium time (0 minutes to approximately 300 minutes), the adsorbent loading of the binary component mixtures appeared to be the average of the adsorbent loadings associated with that system's corresponding single component systems. This can be observed in Figure 5.5-2 where the blue markers, representing the adsorbent loadings of the total binary component mixtures, are positioned in between those of the corresponding single component systems, *i.e.* the black and red markers. This can also be seen for the systems depicted in Figure 5.5-1 (green markers representing the binary component mixtures positioned in between the black and red markers representing the corresponding single component systems) and was the case for most of the systems investigated.

[8] *Key to the legend of the graph: Binary (1-hexanol; 1.03 mass%) = 1.03 mass% of 1-hexanol in a 50:50 binary mixture; Binary (1-hexanol + 1-decanol; 1.08 mass%) = 1.08 mass% of a binary mixture comprising 1-hexanol and 1-decanol; etc.*

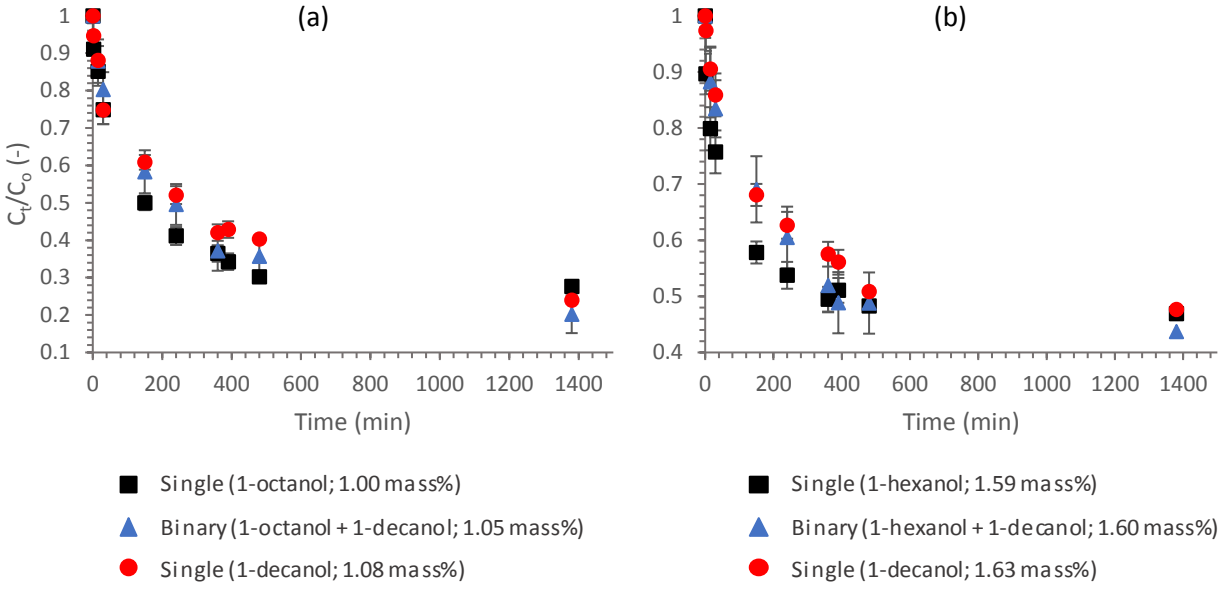

Figure 5.5-2: Comparison of the concentration decay profiles of several binary component mixtures and their corresponding single component systems, using (a) Selexsorb CDx®; and, (b) Selexsorb CD® (IC as indicated; T = 45°C)

This observation suggests that the adsorption behaviour of a 50:50 binary component mixture of 1-alcohols (in the time period of 0 to approximately 300 minutes), could potentially be approximated by the single component system of an alcohol with carbon chain length equal to the average of the two alcohols present in the binary component system. For instance, the binary component adsorption behaviour of a mixture comprising 1-hexanol and 1-decanol, could potentially be approximated with the single component adsorption of 1-octanol (Figure 5.5-3).

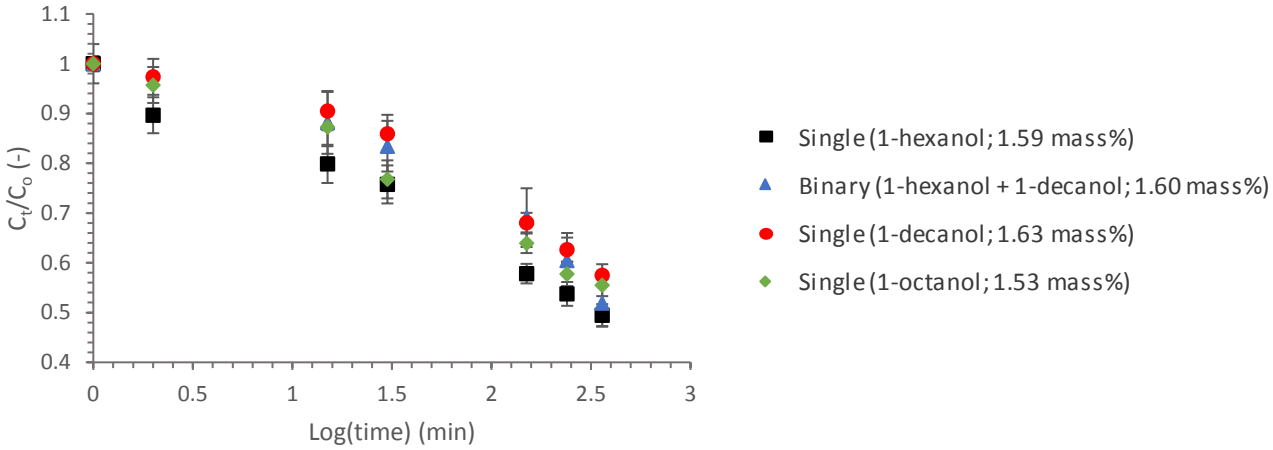

Figure 5.5-3: Comparison of the concentration decay profile of a binary component mixture, its corresponding single component systems as well as a single component system of an alcohol with carbon chain length equal to the average of that of the alcohols in the binary component mixture (Selexsorb CD®; IC as indicated; T = 45°C)

5.6 Interaction Effect in Binary Component Systems

Ultimately, to better comprehend the differences in the single and binary component adsorption behaviour, the interaction in the binary component systems was investigated.

As discussed in Chapter 2 (Section 2.5), adsorbate-adsorbate interaction in a multicomponent adsorption system is typically divided into either synergistic interaction; antagonistic interaction; or, non-interaction [38], [39]. The interaction parameter is denoted by $R_{q,i}$, and represents the ratio of the binary component equilibrium adsorbent loading to the single component equilibrium adsorbent loading. A calculation methodology is provided in Appendix F (Section F.2.1, p230).

For the binary component system of 1-hexanol and 1-decanol, it was observed that the interaction parameter corresponding to 1-decanol deviated from unity more than that of 1-hexanol (Figure 5.6-1). This suggests that the presence 1-decanol had less of an influence on the adsorption of 1-hexanol (interaction parameters closer to 1), whereas the presence of 1-hexanol had a notable influence on the adsorption of 1-decanol. The interaction parameters being less than 1, is indicative of antagonistic adsorption. For the system of 1-hexanol and 1-decanol, adsorption of the longer chain alcohol, 1-decanol, was affected decidedly more negatively at the higher temperature of 45°C (Figure 5.6-1b) suggesting increased competition between the respective adsorbates.

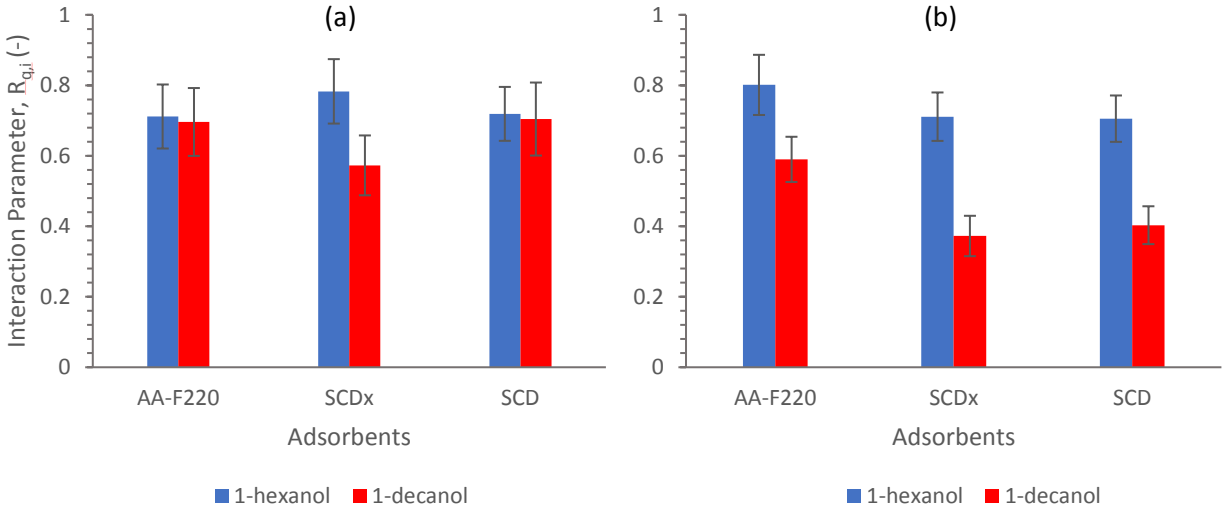

Figure 5.6-1: Comparison of the interaction parameters corresponding to 1-hexanol and 1-decanol in a binary component system at (a) 25°C; and, (b) 45°C (component IC = 1 mass%) [9,10]

For the binary component system of 1-hexanol and 1-octanol, the two components seem to have had much more of an equal effect on one another compared to the other two binary mixtures investigated (Figure 5.6-2). These two components exhibited interaction parameters relatively equal to one another and well within the uncertainty range for most cases. This indicates that even though both components exhibited antagonistic interaction, the adsorption of one of the two components were not affected appreciably more negatively than the other when in the binary mixture. The interaction parameters for the binary mixtures (initial adsorbate concentration of approximately 1 mass%) ranged from 0.73 to 0.90 at 25°C and 0.55 to 0.88 at 45°C. Antagonistic adsorption was predominant for the initial adsorbate concentration range of 1 to 1.5 mass% when using any one of the adsorbents investigated. As for the systems containing 1-hexanol and 1-decanol, here also adsorption of the longer chain alcohol was affected more adversely at the higher temperature of 45°C as compared to 25°C.

[9] *The initial adsorbate concentration is not necessarily precisely 1 mass% but has an error margin associated with it (this is also relevant to Figure 5.6-2 and Figure 5.6-3).*

[10] *For the determination of the interaction parameters at 25°C, single component data measured by Groenewald* [8] *were used together with binary component data measured in this study (this is also relevant to Figure 5.6-2 and Figure 5.6-3).*

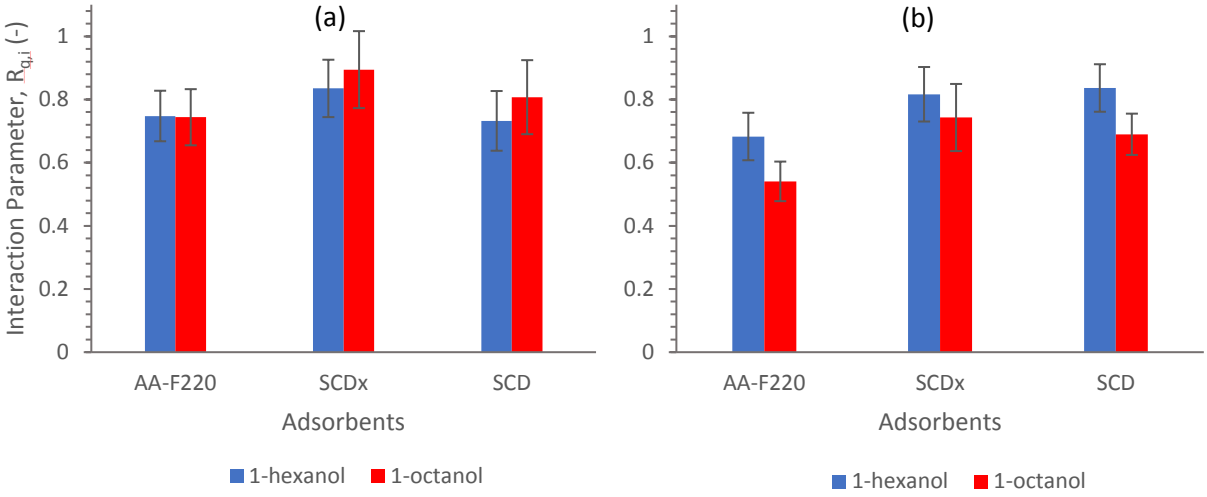

Figure 5.6-2: Comparison of the interaction parameters corresponding to 1-hexanol and 1-octanol in a binary component system at (a) 25°C; and, (b) 45°C (component IC = 1 mass%)

For the binary component system of 1-octanol and 1-decanol, the interaction parameters corresponding to 1-decanol again deviated from unity more than that of 1-octanol (Figure 5.6-3). This suggests that the presence of 1-octanol had a more pronounced effect on the adsorption of 1-decanol than the other way around. Similar to the binary systems comprising 1-hexanol and 1-decanol, and 1-hexanol and 1-octanol, antagonistic adsorption was predominant in the initial concentration range of 1 to 1.5 mass% for all adsorbents and temperatures investigated. As depicted in Figure 5.6-3, the interaction parameters for this binary component system ranged from approximately 0.56 to 0.85 at 25°C and 0.52 to 0.74 at 45°C, again suggesting increased antagonistic interaction at the higher temperature.

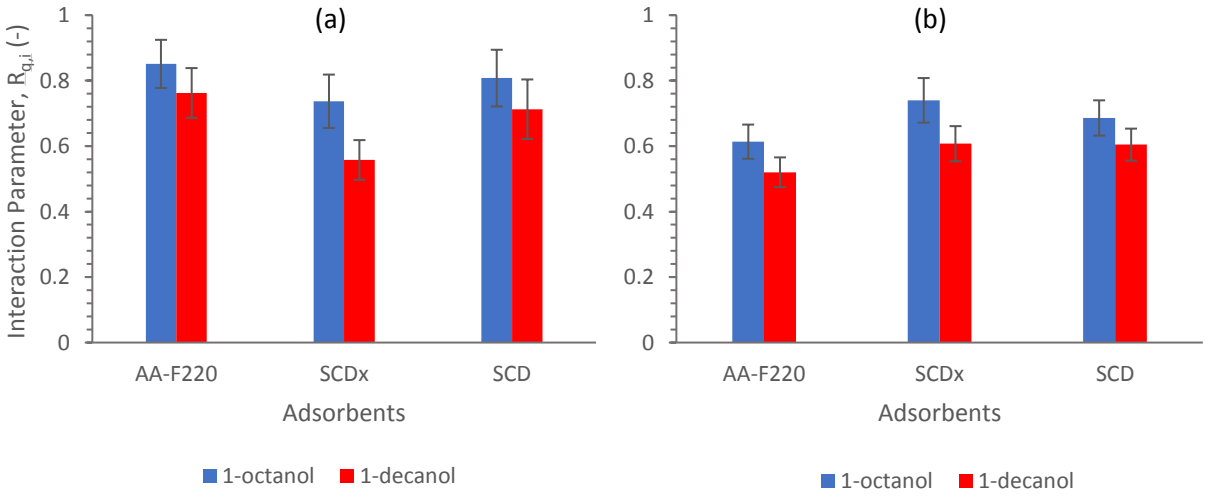

Figure 5.6-3: Comparison of the interaction parameters corresponding to 1-octanol and 1-decanol in a binary component system at (a) 25°C; and, (b) 45°C (component IC = 1 mass%)

It is thought that the antagonistic adsorption observed for these systems could possibly be ascribed to either one or both of the following [107]:

(i) Adsorbates competing for the same active adsorption sites; and/or,

(ii) Pore blocking.

Generally, reduction in adsorbent loading for multicomponent systems containing lower molecular weight adsorbates is likely to be a result of direct competition for adsorption sites [107]. For multicomponent systems containing heavier adsorbates, however, pore blocking is more likely to be the cause since the heavier adsorbate molecules adsorb in the larger transport pores thereby impeding movement of other adsorbates into the smaller pores of the adsorbents or even completely blocking the pores [107]. Yang *et al.* [108], suggested that adsorbates with molecular weight less than 200 g/mol be considered "low molecular weight" adsorbates. In this study, the highest molecular weight adsorbate investigated was 1-decanol, with a molecular weight of 158 g/mol. Consequently, it can be assumed that the reduction in adsorbent loading of the respective adsorbates investigated, pointing to antagonistic adsorption, was more due to direct competition for adsorption sites. Pore blocking, nonetheless, is not impossible for the systems investigated, and may well have occurred within the micropore structure of the adsorbents in some cases.

Competition between two adsorbates for an active adsorption site is highly dependent on the rate of adsorption of the respective adsorbates [60]. It will be shown in Chapter 7, that the rate constant associated with some of the kinetic models predominantly increased with decreasing alcohol chain length. The shorter chain alcohols therefore adsorbed faster than the longer chain alcohols, thereby occupying more of the active adsorption sites faster. This could explain why the longer chain alcohols were more adversely affected by the presence of a shorter chain alcohol than vice versa.

At the lowest investigated initial alcohol concentration of 0.5 mass%, the systems behaved somewhat different than at the higher concentrations, with some of the systems exhibiting interaction parameters close to or marginally greater than unity. This suggests that the interaction between the adsorbates might have been less at lower initial concentrations with the possibility of synergistic interaction in some instances. Given that the synergistic interaction cases were within the uncertainty margin, the likelihood of synergistic adsorption is almost negligible. Many of these systems also indicated that the shorter chain alcohols were affected more negatively by the presence of a longer chain alcohol at this initial adsorbate concentration, however, the differences in these interaction parameters were within the uncertainty margin for most of these cases. Refer to Appendix F (Section F.2.2, p231) for the interaction effect graphs of the 0.5 mass% initial concentration cases.

5.7 Chapter Summary

The objective of this chapter was to discuss the experimental adsorption data obtained in this study.

This was done through the measurement and investigation of the adsorption data of three single component alcohol-alkane systems, using three different AA adsorbents, at three different initial adsorbate concentrations. In addition to the single component systems, the data of three binary component alcohol-alkane systems were measured and investigated, using three different alumina adsorbents, at two temperatures and three initial adsorbate concentrations.

The alcohol adsorption abilities of the various alumina adsorbents were investigated. For the single component adsorption of 1-hexanol and 1-octanol, SCD and SCDx proved to have marginally greater alcohol adsorbent loadings than AA-F220, however, for the adsorption of 1-decanol, the three adsorbents performed relatively equal. For the binary component adsorption of 1-hexanol + 1-octanol and 1-octanol + 1-decanol, SCDx and SCD again seemed to marginally outperform AA-F220, however, for the binary component adsorption of 1-hexanol + 1-decanol, AA-F220 achieved slightly greater adsorbent loadings than SCDx and SCD.

The effect of several variables on adsorption was investigated. It was established that temperature influenced the equilibrium adsorbent loading of the systems investigated; for most systems an increase in temperature produced a corresponding increase in adsorption. This, in addition to literature findings and observations made from SEM images taken before and after adsorption suggested that adsorption occurred through weak chemical bonds with the possibility of physisorption not being excluded entirely.

Initial adsorbate concentration proved to have a very pronounced effect on the equilibrium adsorbent loading of all the single as well as binary component systems. Adsorbent loading increased with an increase in initial adsorbate concentration up to a concentration of approximately 1-1.2 mass% after which it remained relatively constant.

Carbon chain length and binary combinations of different chain length alcohol adsorbates only marginally effected the equilibrium adsorbent loading of the adsorbents in the single and binary component systems respectively, with the shorter chain alcohols adsorbing slightly better than the longer chain alcohols in some single component systems. Though within the uncertainty range, selectivity parameters suggested that the shorter chain alcohols in binary component mixtures also adsorbed somewhat better than the longer chain alcohols.

When comparing single and binary component adsorption behaviour, the binary alcohol mixtures had adsorption efficacies relatively equal to that of the single alcohol systems. Adsorption of a component in a

binary alcohol mixture, however, proved to be appreciably poorer than adsorption of a component in a corresponding single component system.

Finally, the interaction effect in the binary component systems was investigated. For the initial adsorbate concentration range of 1 to 1.5 mass%, antagonistic adsorption, *i.e.* competitive adsorption, was predominant for al systems investigated at both 25°C as well as 45°C, with adsorption of the longer chain alcohols in the binary component mixtures being inhibited more by the presence of a shorter chain alcohol, than vice versa.

Collectively, above findings aided in gaining more insight into the adsorption of 1-alcohols from n-decane when using AA as adsorbent. The adsorption data of various systems were measured and discussed addressing and fulfilling objective (i) of this study.

Chapter 6: Adsorption Equilibrium Modelling

6.1 Overview

This chapter addresses objective (ii) of this research study. The objective of this chapter is therefore to apply various equilibrium isotherm models to single and binary component alcohol-alkane systems, using the three AA adsorbents introduced in previous chapters, and to identify the most suitable isotherm models for correlation of the adsorption data.

6.1.1 Isotherm Modelling

Modelling of the equilibrium isotherms was done using the non-linear minimisation method. For this method, the Solver Add-in package in Microsoft Excel® was used together with the Hybrid fractional error function (HYBRID) [51], [65] (Equation 6.1-1).

$$HYBRID = \frac{100}{n-p}\sum_{i=1}^{n}\left(\frac{\left(q_{e,exp}-q_{e,pred}\right)_i^2}{q_{e,exp}}\right)_i \qquad [\ 6.1\text{-}1\ ]$$

Where, n Number of data points;

p Number of regression parameters in specific model;

$q_{e,exp}$ Experimentally determined adsorbent loading at equilibrium (*mg/g*); and,

$q_{e,pred}$ Model predicted adsorbent loading at equilibrium (*mg/g*).

In order to identify the most suitable model, the correlation coefficient (R^2) [109] and Marquardt's percentage standard deviation (MPSD) [51], [65], [110] were determined and compared for each model. The correlation coefficient is denoted by Equation 6.1-2 and the MPSD by Equation 6.1-3.

$$R^2 = \frac{\sum\left(q_{e,pred}-\overline{q_{e,exp}}\right)^2}{\sum\left(q_{e,pred}-\overline{q_{e,exp}}\right)^2+\sum\left(q_{e,pred}-q_{e,exp}\right)^2} \qquad [\ 6.1\text{-}2\ ]$$

$$MPSD = 100\left(\sqrt{\frac{1}{n-p}\sum_{i=1}^{n}\left(\frac{\left(q_{e,exp}-q_{e,pred}\right)_i^2}{q_{e,exp}}\right)_i}\right) \qquad [\ 6.1\text{-}3\ ]$$

Ultimately, models presenting a high correlation coefficient (close to 1) and a low MPSD value (close to 0) were deemed suitable models. Reasoning behind the use of the HYBRID function is provided in Appendix G (Section G.1, p234).

6.2 Single Component Adsorption

This section aims to model single component adsorption data with equilibrium isotherm models[11]. The single component alcohol-alkane systems were modelled by use of four different adsorption isotherm models (Table 6.2-1).

Table 6.2-1: Single component adsorption isotherm models

Isotherm Models		
Langmuir Isotherm (LM)	$q_e = \frac{q_{max} K_L C_e}{1+K_L C_e}$	[43]
Freundlich Isotherm (FM)	$q_e = K_F C_e^{\frac{1}{n}}$	[44]
Sips Isotherm (SM)	$q_e = \frac{q_{max} K_s (C_e)^{\frac{1}{n}}}{1+K_s (C_e)^{\frac{1}{n}}}$	[47]
Redlich-Peterson Isotherm (RPM)	$q_e = \frac{K_{RP} C_e}{1+a_{RP} (C_e)^{\frac{1}{n}}}$	[50]

6.2.1 Single Component Adsorption Results

For the investigated adsorption systems, the correlation coefficients determined for some of the models were very similar. Consequently, the MPSD of the different models was also determined and used to identify the most suitable model for each system.

The single component adsorption data used for the equilibrium modelling are provided in Appendix C (Section C.2.1, p179).

6.2.1.1 *Activated Alumina F220*

Table 6.2-2 summarises the isotherm model parameters for the single component adsorption of 1-hexanol, 1-octanol and 1-decanol onto AA-F220. When comparing the correlation coefficients and MPSD values for each of the systems, it seemed as though the Freundlich model was the least suitable, whereas the remaining three isotherm models were equally suitable for the description of these systems.

For the LM, the values of the affinity constant, K_L, appeared to increase with an increase in temperature. This suggests that the affinity of AA-F220 towards all three of the respective adsorbates increased with increasing

[11] *The single component model parameters provided for the temperature of 25°C have been determined from the data of a study conducted by Groenewald, with some additional data points measured in this study added to the data sets* [8]. *The parameters at 45°C, however, have been obtained from data measured in this study.*

temperature. Similar to the LM, the Sips constants, K_s, also indicated a higher affinity towards the adsorbates at the higher temperature, which is concordant with the findings in Chapter 5, Section 5.4.1.

The *n*-parameters obtained for the FM were markedly greater than unity, indicating favourable adsorption [46]. For the SM and the RPM, the *n*-parameters were relatively close to unity indicating an inclination towards the LM.

Table 6.2-2: Equilibrium isotherm model parameters for the adsorption of a single alcohol from n-decane onto Activated Alumina F220

Isotherm Parameters	***25°C***			***45°C***		
	1-hexanol	***1-octanol***	***1-decanol***	***1-hexanol***	***1-octanol***	***1-decanol***
Langmuir Isotherm						
K_L *(mL.mg^{-1})*	1.90	1.19	2.69	5.26	5.21	1.91
q_{max} *(mg.g^{-1})*	123	120	112	107	115	133
R^2	0.99	1.00	0.87	0.99	0.99	0.98
MPSD (%)	2.21	0.68	5.56	4.61	5.13	7.30
Freundlich Isotherm						
K_F *(mg.g^{-1})(mL.mg^{-1})$^{1/n}$*	73.0	66.3	81.1	81.9	88.8	84.6
n (-)	3.54	3.74	5.81	6.20	6.31	4.54
R^2	0.96	0.98	0.92	0.98	0.98	0.96
MPSD (%)	5.25	3.57	4.33	7.09	6.42	10.37
Sips Isotherm						
K_s *(mL.mg^{-1})$^{(1/n)}$*	0.91	1.08	2.00	7.09	3.67	4.00
q_{max} *(mg.g^{-1})*	160	126	118	105	119	121
n (-)	1.54	1.14	0.80	0.83	0.96	0.80
R^2	1.00	1.00	0.82	0.99	0.99	0.97
MPSD (%)	1.02	0.00	8.35	4.46	4.19	1.94
Redlich-Peterson Isotherm						
K_{RP} *(L.mg^{-1})*	1.13	2.32	0.99	0.54	0.38	0.14
a_{RP} *(mL.mg^{-1})$^{(1/n)}$*	14.3	34.2	11.9	4.95	2.92	0.54
n (-)	1.37	1.35	1.21	0.99	0.97	0.73
R^2	1.00	0.98	0.94	1.00	0.99	0.97
MPSD (%)	1.13	3.52	3.99	4.60	5.02	4.48

6.2.1.2 *Selexsorb CDx®*

Table 6.2-3 summarises the isotherm model parameters for the single component adsorption of 1-hexanol, 1-octanol and 1-decanol onto SCDx. The MPSD criterion shows that as for AA-F220, the FM was the least suitable model for the description of these systems. The LM, SM and RPM had similar correlation coefficients and MPSD values which indicated that these models were equally suitable.

According to Table 6.2-3, there was no apparent difference in the Langmuir affinity constants, K_L, for the two different temperatures. For the SM there was a difference in the affinity constants for the two temperatures, however, without any discernible trend.

Similar to AA-F220, the SM and RPM *n*-parameters determined for SCDx were also relatively close to unity, indicating an inclination towards the LM rather than the FM.

Table 6.2-3: Equilibrium isotherm model parameters for the adsorption of a single alcohol from n-decane onto Selexsorb CDx®

Isotherm Parameters	***25°C***			***45°C***		
	1-hexanol	***1-octanol***	***1-decanol***	***1-hexanol***	***1-octanol***	***1-decanol***
Langmuir Isotherm						
K_L $(mL.mg^{-1})$	1.83	1.42	3.22	1.95	2.16	3.64
q_{max} $(mg.g^{-1})$	101	88.5	86.6	136	124	145
R^2	0.99	0.99	0.95	0.97	0.99	1.00
MPSD (%)	0.00	3.88	5.69	9.65	4.90	2.02
Freundlich Isotherm						
K_F $(mg.g^{-1})(mL.mg^{-1})^{1/n}$	74.4	54.3	64.8	83.6	79.2	102
n (-)	8.12	4.73	7.75	4.03	4.16	4.93
R^2	0.96	1.00	0.89	0.94	0.97	0.99
MPSD (%)	0.00	1.00	8.83	13.66	8.10	4.19
Sips Isotherm						
K_s $(mL.mg^{-1})^{(1/n)}$	1.84	1.10	4.00	1.93	2.38	2.59
q_{max} $(mg.g^{-1})$	101	94.0	85.0	136	121	153
n (-)	1.03	0.90	0.80	1.00	0.93	1.26
R^2	1.00	0.97	0.96	0.97	0.99	1.00
MPSD (%)	0.00	6.74	5.01	9.66	4.89	1.52
Redlich-Peterson Isotherm						
K_{RP} $(L.mg^{-1})$	0.96	8.76	0.98	0.23	0.23	0.67
a_{RP} $(mL.mg^{-1})^{(1/n)}$	12.2	161	13.0	1.50	1.72	5.03
n (-)	1.11	1.27	1.05	0.94	0.95	1.06
R^2	0.99	1.00	0.89	0.98	0.97	1.00
MPSD (%)	0.00	1.02	5.92	9.06	4.77	1.13

6.2.1.3 *Selexsorb CD®*

For the adsorption systems of 1-hexanol, 1-octanol and 1-decanol onto SCD, the isotherm model parameters are summarised in Table 6.2-4. However, not as clear at 25°C, it is evident at 45°C that the MPSD values of the FM were appreciably greater than that of the other three isotherm models. Consequently, the LM, SM and RPM were better suited for the description of these systems.

The effect of temperature on the affinity constants of both the LM and SM (K_L, K_S) were inconclusive. Correspondingly, the Freundlich *n*-parameters also varied without any clear trend with regards to temperature. These Freundlich *n*-parameters were notably greater than unity implying favourable adsorption [46]. The *n*-parameters corresponding to the SM isotherm deviated from unity more for the systems using SCD as adsorbent than for the systems using AA-F220 and SCDx as adsorbents. The *n*-parameters corresponding to the RPM, however, were very close to unity, suggesting an inclination towards the LM.

Table 6.2-4: Equilibrium isotherm model parameters for the adsorption of a single alcohol from n-decane onto Selexsorb CD®

Isotherm Parameters	***25°C***			***45°C***		
	1-hexanol	***1-octanol***	***1-decanol***	***1-hexanol***	***1-octanol***	***1-decanol***
Langmuir Isotherm						
K_L *(mL.mg^{-1})*	3.66	0.99	2.98	3.52	5.45	2.18
q_{max} *(mg.g^{-1})*	100	97.8	89.5	127	126	146
R^2	1.00	0.98	0.86	0.99	0.99	0.99
MPSD (%)	1.76	4.65	9.05	5.10	4.66	4.60
Freundlich Isotherm						
K_F *(mg.g^{-1})(mL.mg^{-1})$^{1/n}$*	73.4	51.5	64.7	91.2	94.3	94.4
n (-)	5.72	3.60	6.12	5.10	5.35	4.33
R^2	1.00	1.00	0.86	0.96	0.94	0.96
MPSD (%)	2.08	1.27	9.02	12.2	13.9	10.7
Sips Isotherm						
K_s *(mL.mg^{-1})$^{(1/n)}$*	1.77	1.10	1.76	7.44	8.87	3.90
q_{max} *(mg.g^{-1})*	118	95.0	103	118	122	133
n (-)	1.80	0.90	1.72	0.64	0.80	0.61
R^2	1.00	0.98	0.86	1.00	0.99	1.00
MPSD (%)	0.00	5.55	8.99	3.00	3.94	0.02
Redlich-Peterson Isotherm						
K_{RP} *(L.mg^{-1})*	0.60	1.43	0.45	0.38	0.53	0.22
a_{RP} *(mL.mg^{-1})$^{(1/n)}$*	6.86	26.6	5.85	2.71	3.76	1.09
n (-)	1.09	1.36	1.08	0.94	0.92	0.84
R^2	1.00	1.00	0.86	0.98	1.00	1.00
MPSD (%)	0.00	1.45	8.94	4.33	2.98	0.80

6.2.2 Single Component Adsorption Discussion

The LM, SM and RPM all appeared to be suitable for the description of the systems of 1-hexanol, 1-octanol and 1-decanol onto the three different adsorbents, with the FM proving to be less adequate at both 25°C and 45°C. This finding was made through evaluation of the correlation coefficients and MPSD values of each isotherm model and further established by visual representation of the investigated models fitted onto the

experimental data. From Figure 6.2-1, it is clear that FM was the least suitable model; initially it overpredicts, thereafter underpredicts and finally continues to increase as opposed to the experimental data. As shown, the SM and RPM were virtually indistinguishable in their ability to predict the equilibrium data and the LM also fitted the data equally well. However, when considering all abovementioned criteria to identify the most suitable model, the RPM was found to be slightly superior with correlation coefficients (R^2) predominantly greater than 0.96. This trend was evident for all the single component systems measured, *i.e.* 1-hexanol, 1-octanol and 1-decanol in n-decane, at both temperatures, using any one of the three adsorbents. It should be noted, however, that the RPM and SM are both three-parameter models whereas the LM and FM are two-parameter models, therefore the RPM and SM were expected to have higher correlation coefficients.

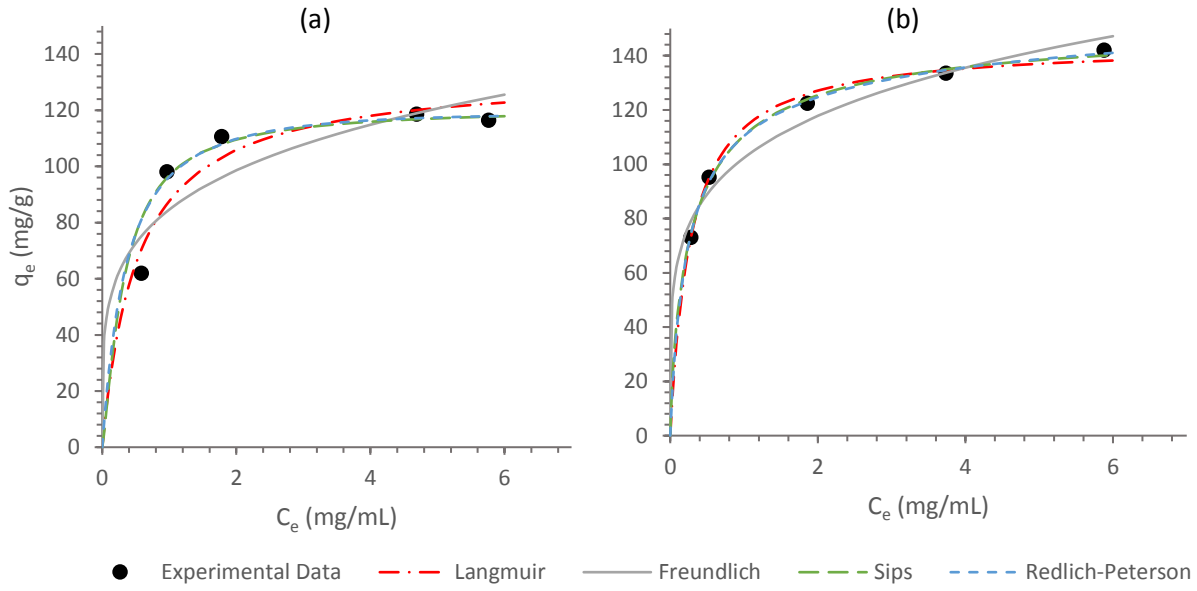

Figure 6.2-1: Equilibrium models on the single component adsorption of (a) 1-decanol onto Activated Alumina F220; and, (b) 1-decanol onto Selexsorb CDx® (T = 45°C)

Even though the FM was identified to be the least suitable model for the single component systems investigated in this study, the *n*-parameters could still be used as a guideline of adsorption intensity since the correlation coefficients of these isotherms were still relatively high. These *n*-parameters were greater than unity for all the systems investigated, indicating favourable adsorption [46]. They were, however, markedly less than 10, suggesting that the adsorption of these alcohols was reversible [20]. Consequently, the adsorption of these 1-alcohols onto the investigated AA adsorbents can be assumed to have been through weak chemisorption since strong chemisorption is essentially irreversible [11]. Adsorption occurring through weak chemisorption can be considered a positive aspect of this specific separation process since the possibility exists for the alumina adsorbents to be regenerated and used in more than one adsorption cycle, resulting in a prolonged lifespan.

The RPM being identified as the most suitable isotherm model for all the single component systems could possibly provide information on whether the adsorption occurred in monolayer or multilayer, as well as the heterogeneity of the systems. As mentioned, the *n*-parameters of the RPM were close to unity. This indicates that the RPM was inclined towards the LM rather than the FM. The LM is associated both with monolayer adsorption and an energetically homogenous system, whereas the Freundlich isotherm is linked to an energetically heterogenous adsorption system [18]–[20], [22]. Since the RPM was more inclined towards the LM, it suggests that these adsorption systems were more energetically homogenous than heterogenous [18]–[20], [22]. Note that the isotherm models provide an indication of the heterogeneity of the systems but do not indicate the source of homogeneity or heterogeneity. It could therefore either be attributed to the adsorbent particle structure, or the energetic properties of the adsorbent and/or adsorbate [20].

Several studies have reported the RPM not to be constrained by monolayer adsorption [51]. Since for the systems investigated, the RPM was merely inclined to the LM but not entirely representative thereof, it may point to monolayer adsorption with some additional layers forming after the monolayer capacity of the adsorbents had been achieved [45]. Should this be the case, the additional adsorbate layers that formed would have been through physisorption in the meso- and macropores of the adsorbents, since the size of the adsorbate molecules and the adsorbent micropores would not have allowed for multilayer adsorption in the micropore structures of the adsorbents.

6.3 Binary Component Adsorption

This section aims to investigate the use of single component isotherm parameters in binary component isotherm models to correlate and possibly predict binary component adsorption data as this would greatly simplify the process of binary component adsorption modelling. As discussed in Chapter 2 (Section 2.6.2), the isotherm models use the single component isotherm parameters together with some binary model parameters regressed from the binary component adsorption data. Only the binary component isotherm parameters (regression parameters) and the correlation coefficients are provided in this section. Refer to Section 6.2 for the single component isotherm parameters. Table 6.3-1 encapsulates the models employed in this section.

Since there exists very little to no knowledge (to the author's knowledge) on the equilibrium adsorption behaviour of binary alcohol-alkane systems using AA adsorbents, a vast number of isotherm models were investigated. These models were compared as follows:

(i) Different forms of the same base isotherm, *i.e.* different forms of the LM and RPM; and,

(ii) Isotherms with the same number of regression parameters, *i.e.* the Modified LM, Extended LM and the Modified RPM were compared based on their 2-parameter nature.

Note that although these isotherm models were compared and the more suitable ones identified, it does not necessarily mean that these models were adequate in describing the systems. It only means that these isotherms were better suited when compared to the others in that specific category (as categorised above). After the isotherm models in each category were compared, a model was identified as the overall best model.

Table 6.3-1: Binary component adsorption isotherm models

Isotherm Models		
Langmuir Isotherm		
Non-modified Competitive Langmuir Isotherm	$q_{e,i} = \frac{(q_{i,max} K_{L,i} C_{e,i})}{1+\sum K_{L,j} C_{e,j}}$	[61]
Extended Langmuir Isotherm	$q_{e,i} = \frac{q_{\max(bin)} K_{L,i(bin)} C_{e,i}}{1+\sum K_{L,j(bin)} C_{e,j}}$	[62]
Modified Langmuir Isotherm	$q_{e,i} = \frac{q_{i,max} K_{L,i} \left(\frac{C_{e,i}}{\eta_i}\right)}{1+\sum K_{L,j} \left(\frac{C_{e,j}}{\eta_j}\right)}$	[70]
Freundlich Isotherm		
Extended Freundlich Isotherm	$q_{e,i} = \frac{K_{F,i} C_{e,i}^{n_i+x_i}}{C_{e,i}^{x_i}+\gamma_i C_{e,j}^{z_i}}$	[73]
Sips Isotherm		
Extended Sips Isotherm	$q_{e,i} = \frac{q_{max,i} K_{S,i} C_{e,i}^{\frac{1}{n}}}{1+\sum_{j=1}^{n} K_{S,i} C_{e,i}^{\frac{1}{n}}}$	[22]
Redlich-Peterson Isotherm		
Non-modified Competitive Redlich-Peterson Isotherm	$q_{e,i} = \frac{K_{RP,i} C_{e,i}}{1+\sum_{j=1}^{n} \left(a_{RP,j} C_{e,j}^{\frac{1}{n_j}}\right)}$	[38]
Modified Competitive Redlich-Peterson Isotherm	$q_{e,i} = \frac{K_{RP,i} \left(\frac{C_{e,i}}{\eta_i}\right)}{1+\sum_{j=1}^{n} \left(a_{RP,j} \left(\frac{C_{e,j}}{\eta_j}\right)^{\frac{1}{n_j}}\right)}$	[38]

6.3.1 Binary Component Adsorption Results

The binary component data used for the modelling in this section are provided in Appendix C (Section C.2.2, p180).

6.3.1.1 *Comparison of Different Forms of the Same Base Isotherm Models*

The LM is one of the most widely used adsorption isotherm models, with various forms used for the description of multicomponent adsorption equilibrium. In this study, three forms were investigated: (i) Non-modified LM; (ii) Modified LM; and, (iii) Extended LM. The adequacy of these models is depicted in Figure 6.3-1, with the vast majority of the systems investigated exhibiting similar behaviour.

As expected, overall the Non-modified LM were the least suitable in predicting the data for the systems investigated. Since this model does not incorporate an interaction parameter, the components in the binary component system are assumed to behave exactly like that of the single component system, without any interaction between the different alcohols. As established (Section 5.6), however, this was not the case which deemed this model inadequate. The Non-modified LM is also based on several assumptions such as all adsorption sites being equally accessible to all adsorbate molecules which might not be the case for these systems [64]. Lastly, it has been pointed out by several studies that the Non-modified LM is only applicable to systems where the adsorbent loadings of both components are equal, as this is a requirement for the model to be thermodynamically consistent [66]. As shown in Sections 5.3.1 and 5.4.3.1, the adsorbent loadings of the components were not always equal for these systems which would explain why this model was not adequate in correlating the data.

The Modified LM and Extended LM were relatively similar in their ability to correlate/predict the data, however, even though they provided better correlations than the Non-modified LM, they still fell short in accurately correlating the data for these systems. For the majority of the systems, the LM models all appeared to underpredict the equilibrium adsorbent loadings (Appendix G, Section G.2.1, p235). The Modified LM interaction parameter accounts for adsorbate-adsorbate interaction in the adsorbed phase [70], whereas the Extended LM contains a parameter accounting for the differences in the surface coverage of the different components [68]. For the systems investigated, these parameters alone seemed to be inadequate in describing the competitive nature of the binary systems.

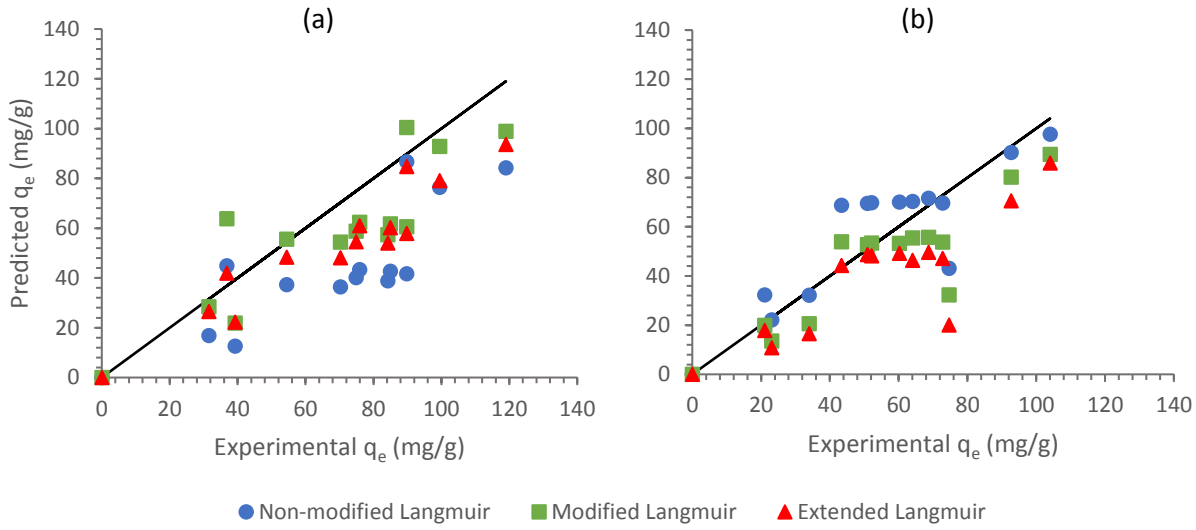

Figure 6.3-1: Predicted vs. experimental equilibrium adsorbent loadings for the comparison of different forms of the binary Langmuir isotherm model for the adsorption of a) 1-hexanol; and, b) 1-decanol in the system of 1-hexanol + 1-decanol (50:50 by mass) onto Activated Alumina F220 (T = 45°C)

The RPM for multicomponent adsorption is reported either as the Non-modified RPM or as the Modified RPM [38]. These two forms of the RPM were applied to the binary component adsorption data obtained. Overall, the Modified RPM proved to correlate the data of the investigated systems better than the Non-modified RPM which is to be expected for a reason similar to that explained for the Non-modified LM's inadequacy. This finding is pictured in Figure 6.3-2 where it is clear that the Non-modified RPM is not suitable in describing the data of these systems. This was evident for all the binary component systems investigated in this study (Appendix G, Section G.2.1, p235).

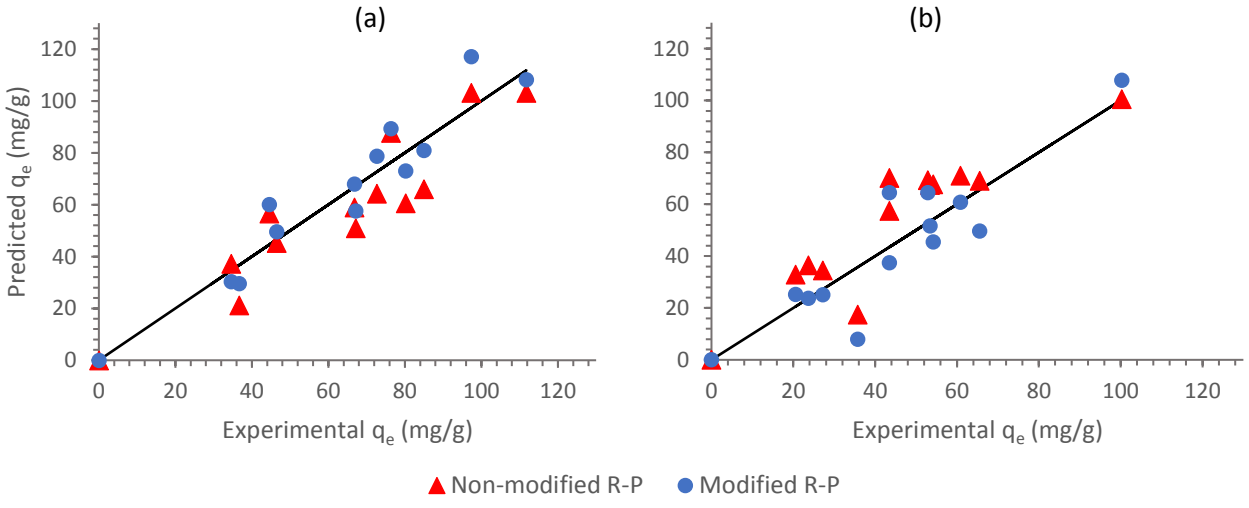

Figure 6.3-2: Predicted vs. experimental equilibrium adsorbent loadings for the comparison of different forms of the binary Redlich-Peterson isotherm model for the adsorption of a) 1-hexanol; and, b) 1-octanol in the system of 1-hexanol + 1-octanol (50:50 by mass) onto Selexsorb CDx® (T = 45°C)

Again, the more suitable model of the two, the Modified RPM, also did not correlate to the data particularly well. As for the multicomponent LM's, this may be attributed to the interaction parameter alone not being sufficient in describing the competitive nature of the systems investigated.

The models were also compared based on their number of regression parameters. The Modified LM, Extended LM and Modified RPM were therefore compared for each system, as they are all two-parameter models. No specific two-parameter model could, however, be distinguished as the most suitable model for all these systems and will therefore be discussed separately for each adsorbent and binary component system combination. As for identification of the most suitable forms of the LM and RPM models, the correlation coefficient of each model aided in identifying the most suitable two-parameter model for each system. These correlation coefficients together with the model parameters of each isotherm model, are provided in Sections 6.3.1.2 through 6.3.1.4.

6.3.1.2 *Activated Alumina F220*

Overall, the Extended FM proved to be the most suitable model for the description of all the binary component systems using AA-F220. Since this model comprises six regression parameters, it was expected that this model would provide a better mathematical correlation to the experimental data than the other isotherm models. This, however, gives the Extended FM an inequitable advantage over the other models. For this reason, the second most suitable models were also identified for each of the systems.

Of the two-parameter isotherms, the Extended LM and the Modified RPM seemed to be the most suitable at 25°C and 45°C respectively for the system of 1-hexanol and 1-decanol. Overall, the Extended SM and Modified RPM had the second highest correlation coefficients at 25°C and 45°C, respectively for the binary system of 1-hexanol and 1-decanol. For visual comparison, parity plots of the two-parameter models as well as the different forms of LM and RPM are provided in Appendix G (Section G.2.1.1, p236).

For the two-parameter isotherms, the Modified LM and the Modified RPM proved to have the highest correlation coefficients at 25°C (Figure 6.3-3) and 45°C respectively for the system of 1-hexanol and 1-octanol. The Extended SM had the second highest overall correlation coefficient. From Figure 6.3-3 it is clear that even though some models might have had higher correlation coefficients when compared to others, it does not necessarily mean that they can be used to describe the equilibrium behaviour of these systems.

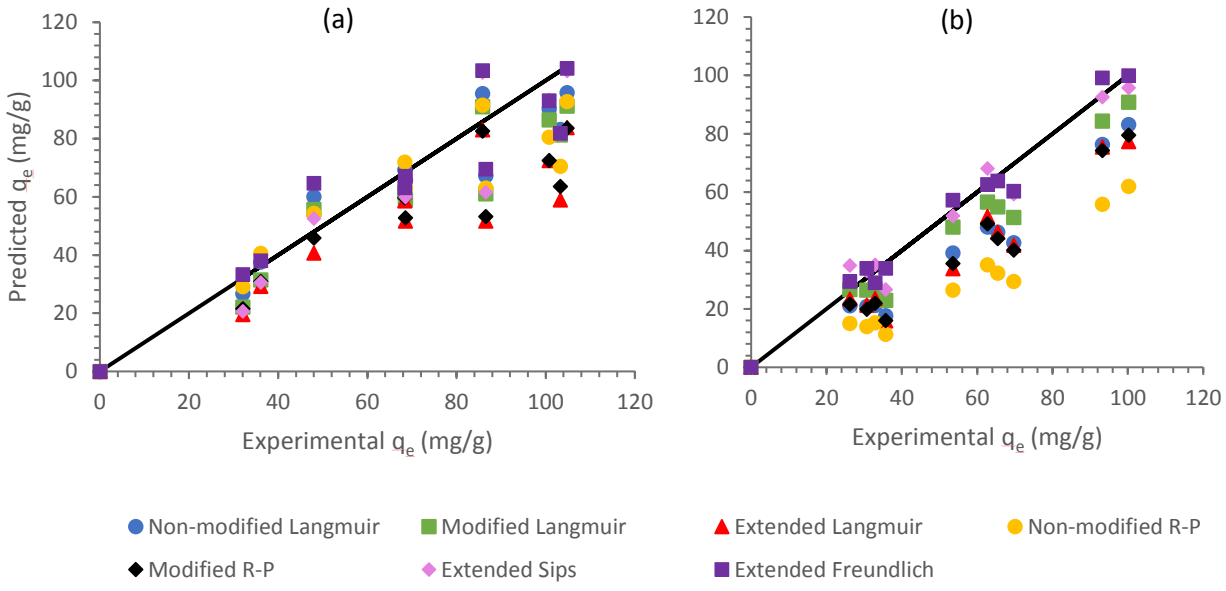

Figure 6.3-3: Predicted vs. experimental equilibrium adsorbent loadings for the comparison of different isotherm models for the adsorption of a) 1-hexanol; and, b) 1-octanol in the system of 1-hexanol + 1-octanol (50:50 by mass) onto Activated Alumina F220 (T = 25°C)

The Modified RPM proved to be the most suitable two-parameter isotherm at both temperatures for the system of 1-octanol and 1-decanol. The Modified RPM had the second highest overall correlation coefficient.

Table 6.3-2 summarises the isotherm parameters for the binary component adsorption onto AA-F220. It can be observed from Table 6.3-2 that the fractional coverage coefficient as obtained from the Extended LM, θ, was mostly greater for the shorter chain alcohol. This indicates that AA-F220 exhibited a marginally greater affinity for the shorter chain alcohol in the mixture [68].

The *n*-parameter for the Extended SM was relatively close to unity, however not as close as in the single component systems. This suggests that the behaviour of these systems was less inclined towards the LM than in the single component adsorption. The interaction parameters, *η*, for the Modified RPM deviated from unity more at 45°C than at 25°C. This suggested the possibility of increased interaction at the higher temperature.

Table 6.3-2: Equilibrium isotherm model parameters for the adsorption of a binary alcohol mixture from n-decane onto Activated Alumina F220 (the parameter subscript numbers correspond to the first or second component in the mixture as presented at the top, i.e. in a mixture of 1-H + 1-D, 1-H will be component 1 and 1-D will be component 2, with 1-H denoting 1-hexanol and 1-D denoting 1-decanol)

Isotherm Model Parameters	**Binary Alcohol Mixtures**					
	25°C			**45°C**		
	1-H + 1-D	**1-H + 1-O**	**1-O + 1-D**	**1-H + 1-D**	**1-H + 1-O**	**1-O + 1-D**
Non-modified Langmuir Isotherm						
R^2_1	0.53	0.87	0.57	0.61	0.69	0.78
R^2_2	0.35	0.78	0.80	0.77	0.83	0.56
Modified Langmuir Isotherm						
η_1 (-)	0.61	0.85	1.12	0.54	0.61	1.44
η_2 (-)	0.88	0.65	2.90	1.03	0.78	0.75
R^2_1	0.58	0.84	0.74	0.72	0.81	0.83
R^2_2	0.36	0.90	0.62	0.74	0.78	0.61
Extended Langmuir Isotherm						
θ_1 (-)	0.57	0.47	0.60	0.60	0.53	0.41
θ_2 (-)	0.43	0.53	0.40	0.40	0.47	0.59
$q_{max.bin}$ ($mg.g^{-1}$)	95.6	121	117	118	111	126
$K_{L1.bin}$ ($mL.mg^{-1}$)	1.74	0.63	0.62	0.96	2.14	1.26
$K_{L2.bin}$ ($mL.mg^{-1}$)	0.77	0.49	0.59	0.62	1.71	0.95
R^2_1	0.60	0.69	0.66	0.71	0.73	0.89
R^2_2	0.36	0.75	0.67	0.65	0.74	0.57
Extended Freundlich Isotherm						
x_1 (-)	0.87	0.34	0.82	0.72	1.16	0.94
y_1 (-)	0.63	0.17	0.22	0.53	0.41	0.77
z_1 (-)	0.41	1.15	1.07	0.55	1.00	0.72
x_2 (-)	0.87	0.67	0.44	0.79	0.83	0.14
y_2 (-)	0.16	0.24	0.12	0.19	0.52	0.22
z_2 (-)	2.26	1.35	1.46	1.56	1.34	1.23
R^2_1	0.91	0.89	0.97	0.91	0.97	0.94
R^2_2	0.63	0.98	0.95	0.87	0.90	0.73
Extended Sips Isotherm						
n (-)	1.19	1.01	0.79	1.13	0.70	1.51
R^2_1	0.65	0.87	0.62	0.57	0.89	0.63
R^2_2	0.61	0.96	0.87	0.70	0.82	0.55
Modified Redlich-Peterson Isotherm						
η_1 (-)	0.35	1.24	0.37	4.46	0.52	2.33
η_2 (-)	0.46	0.79	0.17	1.18	0.45	1.11
R^2_1	0.85	0.68	0.95	0.72	0.83	0.92
R^2_2	0.70	0.72	0.85	0.72	0.83	0.57
Non-modified Redlich-Peterson Isotherm						
R^2_1	0.63	0.78	0.95	0.71	0.88	0.62
R^2_2	0.46	0.55	0.46	0.66	0.77	0.61

As mentioned, the Extended FM seemed to be the most suitable model for the description of all these systems. For the binary component adsorption onto AA-F220, the Extended SM and Modified RPM appeared to be the best alternatives to the Extended FM. Figure 6.3-4 depicts the Extended FM for the system of 1-hexanol and 1-octanol onto AA-F220. The Modified RPM model (for the system of 1-hexanol and 1-octanol at 45°C) is provided in Appendix G (Section G.2.2.1, p246) to allow for comparison. Since the suitability of the isotherm models is difficult to evaluate using these 3-D isotherm graphs, the suitability of the models will from here onwards only be presented with parity plots. Examples of the 3-D isotherm graphs are, however, provided in Appendix G (Section G.2.2, p245), as indicated in the following sections.

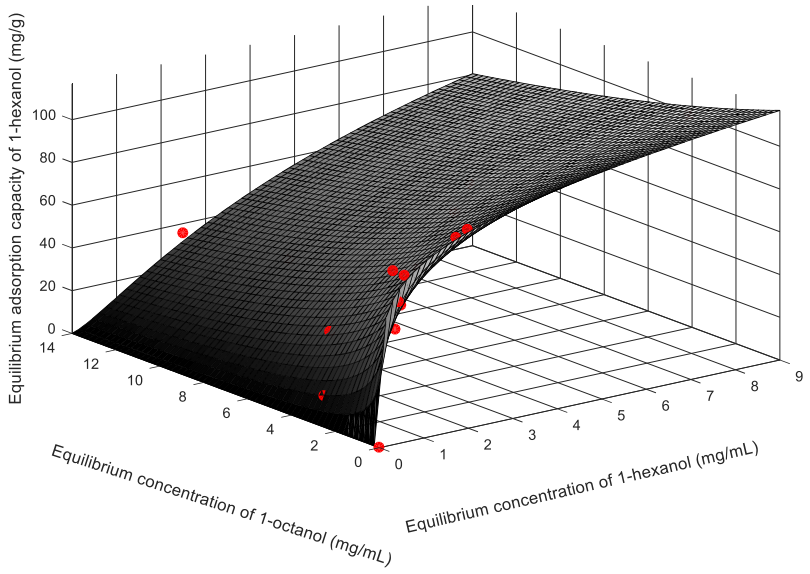

a) Extended Freundlich isotherm for 1-hexanol in a binary adsorption system of 1-hexanol + 1-octanol

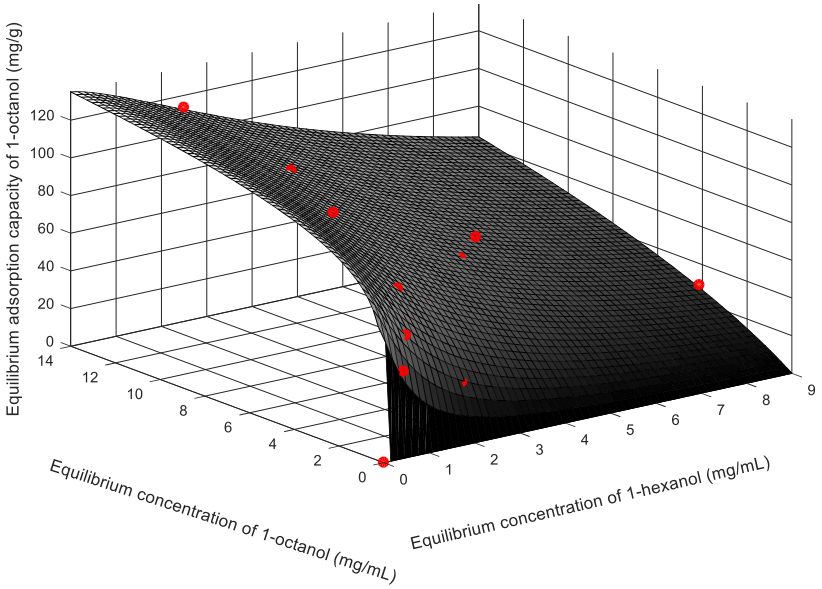

b) Extended Freundlich isotherm for 1-octanol in a binary adsorption system of 1-hexanol + 1-octanol

Figure 6.3-4: Extended Freundlich isotherms for the binary component adsorption of a) 1-hexanol; and, b) 1-octanol onto AA-F220 (T = 45°C)

6.3.1.3 ***Selexsorb CDx®***

The Extended FM proved to be the best overall model for the description of the adsorption of all the binary component systems using SCDx as adsorbent.

The Extended LM turned out to be the best two-parameter isotherm for the system comprising 1-hexanol and 1-decanol (Figure 6.3-5). Overall, the Extended SM had the second highest correlation coefficient.

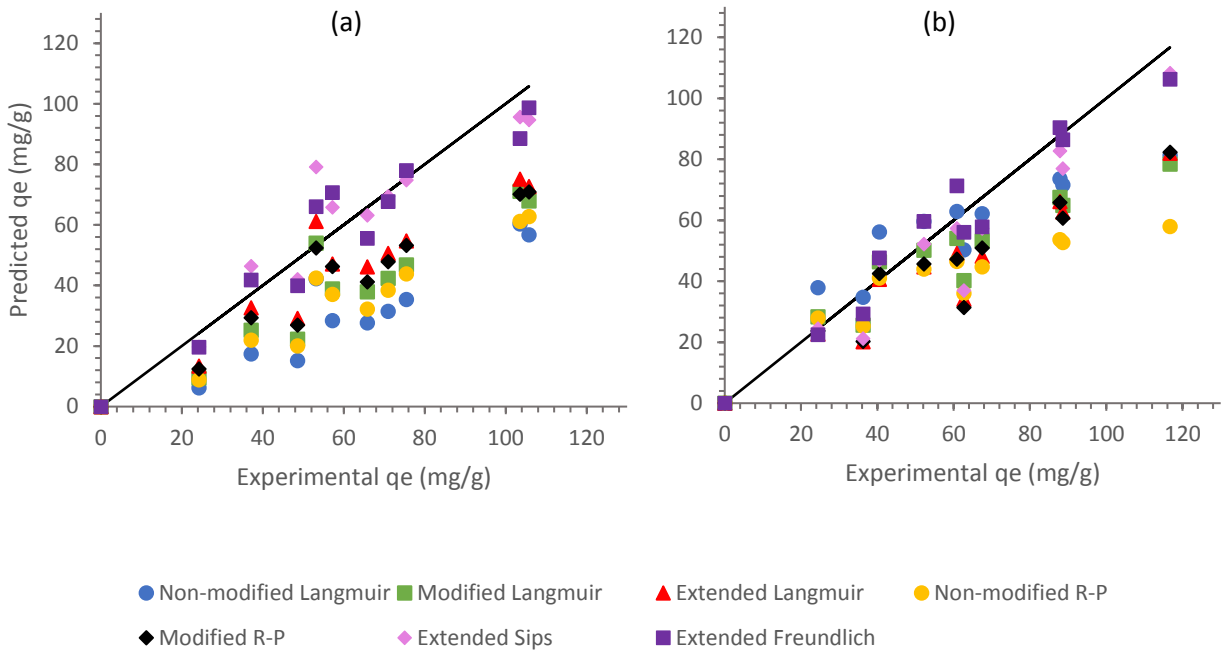

Figure 6.3-5: Predicted vs. experimental equilibrium adsorbent loadings for the comparison of different isotherm models for the adsorption of a) 1-hexanol; and, b) 1-decanol in the system of 1-hexanol + 1-decanol (50:50 by mass) onto Selexsorb CDx® (T = 25°C)

For the system of 1-hexanol and 1-octanol, the Modified RPM had the highest correlation coefficient among the two-parameter isotherms. Overall, the Extended SM and Modified RPM had the second highest correlation coefficients at 25°C and 45°C, respectively. For the parity plots of all systems using SCDx, refer to Appendix G (Section G.2.1.2, 239).

For the system of 1-octanol and 1-decanol, the Modified RPM and Extended LM proved to be the best two-parameter models at 25°C and 45°C, respectively. The Extended SM and Extended LM had the second highest overall coefficients at 25°C and 45°C.

Table 6.3-3 outlines the isotherm parameters for the binary component adsorption onto SCDx. It can be observed that the fractional coverage parameters provided by the Extended LM were greater for the shorter chain alcohol, similar to the parameters corresponding to the adsorption onto AA-F220. This is expected and indicates a slight preference of the shorter chain alcohol by the SCDx [68].

It can be observed from Table 6.3-3 that the *n*-parameters for the Extended Sips isotherm appreciably deviated from unity. This can possibly be attributed to the system deviating from Langmuir behaviour, *i.e*. not only exhibiting monolayer adsorption, but possibly exhibiting multilayer adsorption to some extent. Since the *n*-parameters were not as close to one, it is also possible that the adsorption was not completely homogenous [49].

Similar to AA-F220, the Extended FM proved to be the most suitable model for these systems. The Extended FM and SM 3-D graphs for the system of 1-hexanol and 1-octanol onto SCDx (at 45^{o}C) are provided in Appendix G (Section G.2.2.2, p247) to prove as examples for comparison. It is important to note that the alternative model, the Extended SM, still had very low correlation coefficients, which in turn deems it inadequate for the description of these systems.

Table 6.3-3: Equilibrium isotherm model parameters for the adsorption of a binary alcohol mixture from n-decane onto Selexsorb CDx® (the parameter subscript numbers correspond to the first or second component in the mixture as presented at the top, i.e. in a mixture of 1-H + 1-O, 1-H will be component 1 and 1-O will be component 2, with 1-H denoting 1-hexanol and 1-O denoting 1-octanol)

Isotherm Model Parameters	**Binary Alcohol Mixtures**					
	25°C			**45°C**		
	1-H + 1-D	**1-H + 1-O**	**1-O + 1-D**	**1-H + 1-D**	**1-H + 1-O**	**1-O + 1-D**
Non-modified Langmuir Isotherm						
R^2_1	0.53	0.64	0.49	0.55	0.74	0.68
R^2_2	0.69	0.44	0.78	0.69	0.76	0.61
Modified Langmuir Isotherm						
η_1 (-)	0.55	1.14	0.65	0.95	0.95	1.11
η_2 (-)	0.88	0.92	1.69	1.47	1.47	2.88
R^2_1	0.61	0.60	0.58	0.57	0.77	0.83
R^2_2	0.66	0.44	0.58	0.61	0.79	0.69
Extended Langmuir Isotherm						
θ_1 (-)	0.61	0.51	0.59	0.61	0.57	0.60
θ_2 (-)	0.39	0.49	0.41	0.39	0.43	0.40
$q_{max.bin}$ ($mg.g^{-1}$)	95.3	94.8	87.7	95.3	131	132
$K_{L1.bin}$ ($mL.mg^{-1}$)	0.96	0.69	0.72	0.96	0.92	1.10
$K_{L2.bin}$ ($mL.mg^{-1}$)	0.68	0.51	0.75	0.68	0.57	0.83
R^2_1	0.67	0.54	0.53	0.60	0.79	0.84
R^2_2	0.66	0.41	0.55	0.61	0.62	0.64
Extended Freundlich Isotherm						
x_1 (-)	0.94	1.02	1.85	1.06	0.00	0.73
y_1 (-)	0.78	0.19	0.10	0.28	0.42	0.57
z_1 (-)	0.77	1.33	1.66	1.03	0.29	0.68
x_2 (-)	0.93	1.05	1.02	0.98	0.53	0.08
y_2 (-)	0.27	0.14	0.07	0.06	0.67	0.52
z_2 (-)	1.75	1.68	1.84	2.37	1.11	0.80
R^2_1	0.91	0.79	0.86	0.83	0.74	0.87
R^2_2	0.95	0.44	0.88	0.82	0.86	0.71
Extended Sips Isotherm						
n (-)	0.98	0.78	0.52	0.75	1.35	2.60
R^2_1	0.89	0.75	0.54	0.53	0.63	0.49
R^2_2	0.89	0.49	0.89	0.71	0.75	0.63
Modified Redlich-Peterson Isotherm						
η_1 (-)	0.70	0.33	0.29	0.96	1.45	1.03
η_2 (-)	0.82	1.80	0.52	4.05	2.41	3.91
R^2_1	0.58	0.51	0.47	0.92	0.82	0.80
R^2_2	0.59	0.37	0.46	0.91	0.72	0.68
Non-modified Redlich-Peterson Isotherm						
R^2_1	0.55	0.45	0.77	0.53	0.78	0.51
R^2_2	0.49	0.29	0.46	0.61	0.76	0.61

6.3.1.4 ***Selexsorb CD®***

As for the binary component adsorption onto AA-F220 and SCDx, the Extended FM also proved to be the most suitable model for the description of these systems onto SCD.

For the system of 1-hexanol and 1-decanol onto SCD, the Modified LM proved to have the highest correlation coefficient for the two-parameter models. The Extended SM had the second highest overall. For the parity plots comparing these models when using SCD as adsorbent, refer to Appendix G (Section G.2.2.3, p249).

Similar to the system of 1-hexanol and 1-decanol, the Modified LM was the best among the two-parameter isotherms at both temperatures for the system comprising 1-hexanol and 1-octanol (Figure 6.3-6). Overall, the Modified LM and the Modified RPM had the second highest coefficients at 25°C and 45°C, respectively.

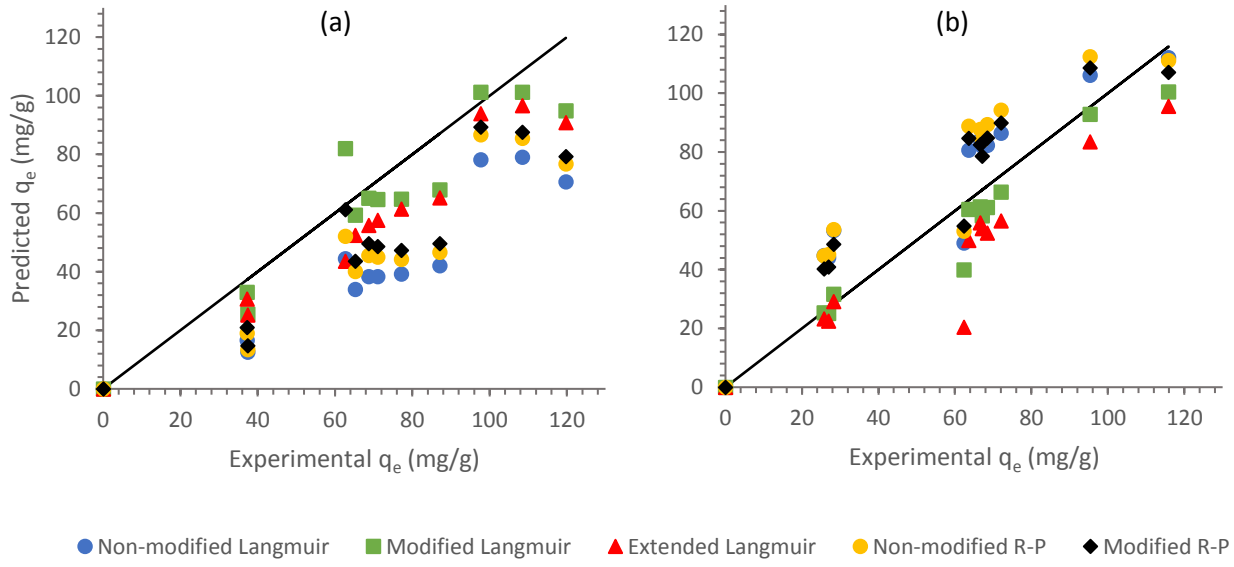

Figure 6.3-6: Predicted vs. experimental equilibrium adsorbent loadings for the comparison of different forms of the binary Langmuir and Redlich-Peterson isotherm models for the adsorption of a) 1-hexanol; and, b) 1-octanol in the system of 1-hexanol + 1-octanol (50:50 by mass) onto Selexsorb CD® (T = 45°C)

For the two-parameter isotherms, the Modified LM again was determined to be the best suit at 25°C, whereas the Modified RPM was the best suit at 45°C for the 1-octanol and 1-decanol system. Note, however, that the Modified LM and RPMs had correlation coefficients very close to one another at 45°C. At 25°C, the Extended SM had the overall second highest coefficients, while the Modified RPM was the most suitable alternative option at 45°C. Figure 6.3-7 portrays the predicted isotherm adsorbent loadings compared to the experimentally determined adsorbent loadings.

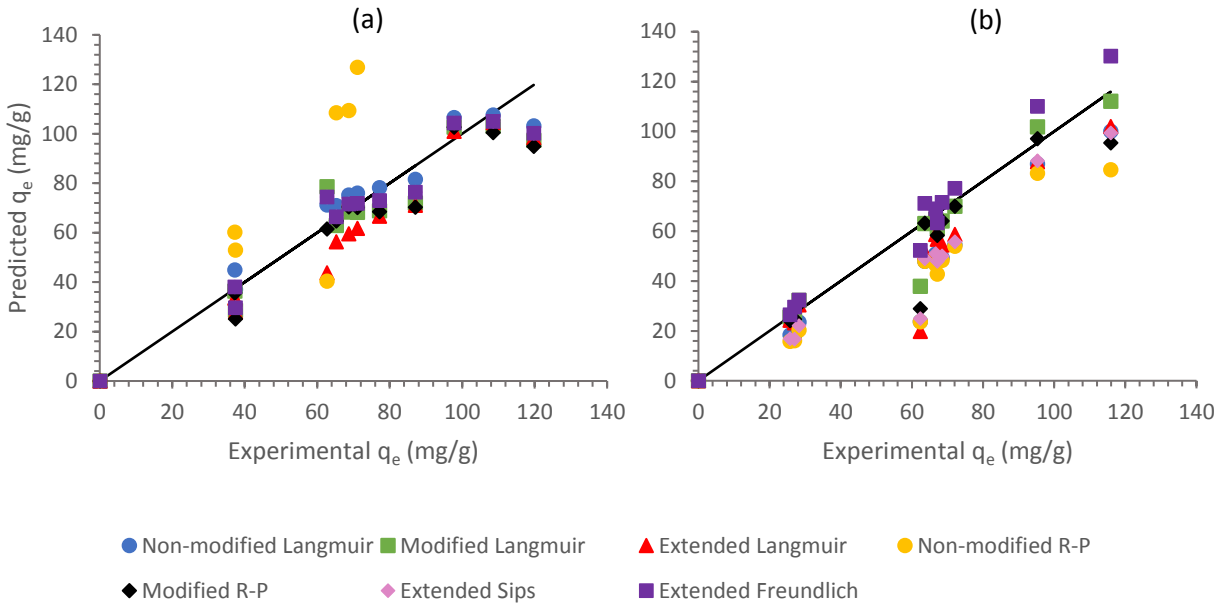

Figure 6.3-7: Predicted vs experimental equilibrium adsorbent loadings for the comparison of different isotherm models for the adsorption of a) 1-octanol; and, b) 1-decanol in a binary 1-octanol + 1-decanol mixture onto SCD (T = 45°C)

Table 6.3-4 provides the binary isotherm parameters for the systems of 1-hexanol and 1-decanol, 1-hexanol and 1-octanol, and, 1-octanol and 1-decanol onto SCD. The fractional surface coverage parameters determined from the Extended LM was determined to be somewhat greater for the shorter chain alcohol which indicates that more of the adsorbent surface is covered in the shorter chain alcohol.

The *n*-parameters associated with the Extended SM were relatively close to unity. This may suggest that the adsorption onto SCD was not completely energetically homogenous [49]. In addition, the possibility of multilayer adsorption to some extent exists [45].

The isotherm with the highest overall correlation coefficient was the Extended FM similar to the systems with AA-F220 as well as SCDx. For these systems, the alternative to the Extended FM would be the Extended SM or the Modified RPM. The correlation coefficients of these isotherms, however, were relatively low indicating their inadequacy to accurately correlate and/or predict the equilibrium adsorption data of these systems. The 3-D Extended FM and Modified RPM isotherm graphs, for the system of 1-hexanol and 1-decanol, are provided in Appendix G (Section G.2.2.3, p249).

Table 6.3-4: Equilibrium isotherm model parameters for the adsorption of a binary alcohol mixture from n-decane onto Selexsorb CD® (the parameter subscript numbers correspond to the first or second component in the mixture as presented at the top, i.e. in a mixture of 1-O + 1-D, 1-O will be component 1 and 1-D will be component 2, with 1-O denoting 1-octanol and 1-D denoting 1-decanol)

Isotherm Model Parameters	**Binary Alcohol Mixtures**					
	25°C			**45°C**		
	1-H + 1-D	**1-H + 1-O**	**1-O + 1-D**	**1-H + 1-D**	**1-H + 1-O**	**1-O + 1-D**
Non-modified Langmuir Isotherm						
R^2_1	0.53	0.45	0.49	0.62	0.71	0.94
R^2_2	0.35	0.51	0.65	0.67	0.83	0.73
Modified Langmuir Isotherm						
η_1 (-)	0.61	0.52	0.59	0.08	0.08	0.39
η_2 (-)	0.88	0.19	1.59	0.18	0.18	0.27
R^2_1	0.58	0.50	0.60	0.76	0.86	0.90
R^2_2	0.36	0.72	0.58	0.52	0.91	0.94
Extended Langmuir Isotherm						
θ_1 (-)	0.57	0.42	0.62	0.52	0.60	0.44
θ_2 (-)	0.43	0.58	0.38	0.48	0.40	0.56
$q_{max.bin}$ ($mg.g^{-1}$)	95.6	98.7	94.6	95.0	127	137
$K_{L1.bin}$ ($mL.mg^{-1}$)	1.74	0.90	0.54	1.46	1.82	1.56
$K_{L2.bin}$ ($mL.mg^{-1}$)	0.77	0.49	0.58	1.00	1.19	0.98
R^2_1	0.60	0.44	0.54	0.59	0.85	0.90
R^2_2	0.36	0.57	0.52	0.64	0.72	0.77
Extended Freundlich Isotherm						
x_1 (-)	0.87	2.06	1.08	0.90	1.38	0.85
y_1 (-)	0.63	0.33	0.05	0.28	0.26	0.34
z_1 (-)	0.41	1.62	1.66	0.65	1.17	0.93
x_2 (-)	0.87	0.47	0.80	0.56	0.86	0.58
y_2 (-)	0.16	0.04	0.14	0.08	0.47	0.53
z_2 (-)	2.26	1.90	1.37	1.62	1.39	1.23
R^2_1	0.91	0.62	0.83	0.79	0.98	0.97
R^2_2	0.63	0.94	0.68	0.77	0.99	0.96
Extended Sips Isotherm						
n (-)	1.42	0.87	0.88	1.38	0.87	0.91
R^2_1	0.68	0.57	0.55	0.58	0.63	0.93
R^2_2	0.36	0.64	0.75	0.58	0.91	0.78
Modified Redlich-Peterson Isotherm						
η_1 (-)	0.37	0.05	0.80	1.60	0.34	1.68
η_2 (-)	1.41	0.16	0.21	1.24	0.62	1.06
R^2_1	0.83	0.66	0.58	0.77	0.95	0.90
R^2_2	0.39	0.86	0.65	0.81	0.94	0.86
Non-modified Redlich-Peterson Isotherm						
R^2_1	0.53	0.44	0.75	0.7	0.71	0.56
R^2_2	0.33	0.40	0.46	0.76	0.84	0.70

6.3.2 Binary Component Adsorption Discussion

As discussed in Section 6.3.1, the Extended FM proved to be the most suitable model for the correlation of the equilibrium adsorption data for all the binary component systems investigated. The FM had correlation coefficients (R^2) greater than approximately 0.85 on average. Since this model comprises six regression parameters, markedly more than the other models investigated, alternatives to the Extended FM were identified and the Modified RPM and Extended SM were found to be the best alternatives. This was the case for all three adsorbents and all systems.

Since the Extended FM was revealed to be the most suitable model, it may suggest that adsorption was not entirely energetically homogenous and that there was possible interaction between the molecules in the solid phase, *i.e.* the adsorbed molecules [38]. However, since the model comprises six regression parameters it is expected that this model be mathematically more fit than the others. Thus, the assumptions associated with the Extended FM cannot be verified with certainty. The Extended FM should therefore only be used for the correlation of the binary component adsorption data of these systems and perhaps not to investigate the equilibrium behaviour of these systems.

The Extended SM appeared to fit the data better than the Modified RPM at the lower temperature of 25°C, whereas the Modified RPM was more suitable at 45°C. As for the single component adsorption systems, the Modified RPM model could possibly suggest monolayer adsorption at first with some additional layers forming after the adsorbents had reached their maximum monolayer capacity [51]. The systems investigated are also presumptively more homogenous than heterogenous [20]. However, the correlation coefficients linked to these isotherm models were low and therefore caution should be taken when verifying the assumptions associated with these models. Overall, the multicomponent isotherm models investigated in this study did not provide good correlations of the data. The lack of fit of these models can possibly be attributed to the use of single component isotherm parameters for the modelling of binary component systems; this indicated that the interaction parameters incorporated in the binary component models were not sufficient for the correction of the single component data and for describing the competitive nature of the systems investigated.

The most notable difference between the single and the binary component systems was the affinity constant as determined by the LM (affinity constants as determined with the single component LM and the binary component Extended LM): the single component parameters were greater than that determined for the binary component systems. This was expected and can be attributed to possible interaction, *i.e.* competitive behaviour, in the binary component systems and a consequent decrease in affinity towards the respective adsorbates [69].

6.4 Chapter Summary

The objective of this chapter was to apply various equilibrium isotherm models to single and binary component alcohol-alkane systems, using the three AA adsorbents introduced in previous chapters, and to identify the most suitable isotherm models for correlation of the adsorption data.

For the single component systems, the RPM proved to be better suited than the rest of the models evaluated, whereas the FM was found to be the least suitable model. Conversely, the Extended FM presented to be the most suitable model for the correlation of the binary component adsorption data. The second-best models for the binary component systems were the Modified RPM and the Extended SM, which coincides with the single component findings. The correlation coefficients of the binary component models, however, were relatively low and the models provided poor correlation of the data.

According to the concomitant model assumptions, the single component systems appeared to exhibit monolayer adsorption with the possibility of multilayer adsorption not excluded entirely. It also seemed as though the systems were not completely energetically homogenous, even though they were more inclined to homogeneity than heterogeneity. It was revealed that adsorption occurred either by means of physisorption or weak chemisorption, but not through strong chemisorption. The findings in Chapter 5 (Section 5.4.1) suggested that weak chemisorption was predominant, which is concordant with the findings in this chapter.

The equilibrium data of both the single and binary component systems were modelled using various equilibrium isotherm models, and the most suitable isotherm models were identified. Objective (ii) of this study was therefore successfully addressed and in this chapter.

Chapter 7: Adsorption Kinetic Modelling

7.1 Overview

This chapter addresses objective (iii) of this research study. The objective of this chapter is thus to apply and identify suitable kinetic models for the correlation of the kinetic data of both single and binary component alcohol-alkane systems using AA adsorbents, in order to better comprehend the rate-limiting step(s) of the different systems.

7.1.1 Kinetic Models

The adsorption kinetic models typically assume the surface reaction to be rate-limiting. These models alone, however, do not provide enough certainty on the rate-limiting step(s) of a system and should be used in conjunction with other tests and investigations. Contrary to the adsorption models, the diffusional kinetic models assume the surface reaction to be instantaneous and the external mass transfer (EMT) and intra-particle diffusion (IPD) to be the slowest steps.

The adsorption kinetics were investigated using four different kinetic models (Table 7.1-1). In addition, a diffusional model was used to investigate the significance of the EMT and IPD. This was done for both the single and binary component systems.

Table 7.1-1: Kinetic models [12]

Models		
Adsorption Kinetic Models		
Pseudo-first-order Model (P1)	$q_{t,i} = q_{e,i}\left(1 - e^{-k_{1,i}t}\right)$	[81]
Pseudo-second-order Model (P2)	$q_{t,i} = \frac{k_{2,i}q_{e,i}^2 t}{1+k_{2,i}q_{e,i}t}$	[83]
Pseudo-nth-order Model (PN)	$q_{t,i} = q_{e,i} - \left(q_{e,i}^{1-n_i} - (1-n_i)k_{n,i}t\right)^{\frac{1}{1-n_i}}$	[85]
Elovich Model	$q_{t,i} = \left(\frac{1}{\beta_i}\right)\ln(\alpha_i\beta_i t)$	[86]
Diffusional Kinetic Model		
Intra-particle Diffusion Model (Weber-Morris)	$q_t = k_{IP}\sqrt{t} + \theta$	[89]

[12] *The subscript "i" accompanying some of the models shows that these specific models are applied to the data of each respective component, therefore two kinetic equations will exist for each of the binary component mixtures, i.e. one equation for each of the components in the mixture.*

7.1.2 Kinetic Modelling

The kinetic modelling was done following a methodology similar to that used for the equilibrium isotherm modelling in Chapter 6. Modelling of the kinetics and determination of the model parameters (model regression) was done by non-linear minimisation of the HYBRID error function [51], [65] using the Solver add-in package in Microsoft Excel®. By comparing the correlation coefficient [109] and MPSD value [51], [65], [110] of each model as well as by comparing the model calculated equilibrium adsorbent loading with the experimentally measured equilibrium adsorbent loading, the most suitable models were identified for each adsorption system. The modelling methodology is outlined in Appendix H (Section H.1, p252).

7.2 Single Component Adsorption

This section aims to gain knowledge on the single component adsorption kinetics of several systems. In this section, the single component adsorption parameters are provided and discussed for multiple kinetic models.

7.2.1 Kinetic Modelling Results

The model parameters of three different adsorbate systems at one initial concentration are provided in this section. The kinetics was, however, investigated at three different initial adsorbate concentrations and two temperatures for each of the different systems. The model parameters not provided in this section are provided in Appendix H (Section H.2, p253), as will be indicated.

7.2.1.1 *Activated Alumina F220*

Table 7.2-1 summarises the adsorption kinetics model parameters for the adsorption of 1-hexanol, 1-octanol and 1-decanol respectively from n-decane, using AA-F220. The model parameters pertaining to other initial adsorbate concentrations are provided in Appendix H (Section H.2.1, p253).

From Table 7.2-1 it can be observed that the rate constants of P1 (k_1) exhibited little variation for the different carbon chain length alcohols, whereas the rate constant as determined with P2 (k_2) predominantly exhibited a slight decrease with increasing alcohol carbon chain length. When referring to the Elovich model, the initial adsorption rate constants (α) also seemed to decrease with increasing carbon chain length, though more pronounced at 25°C as compared to 45°C. For both P1 and P2, the rate constants were less at the lower temperature of 25°C for most of the systems. In addition, the Elovich initial adsorption rate constants (α) were also appreciably lower at 25°C as compared to 45°C.

Also outlined in Table 7.2-1 are the parameters of the IPD model. All IPD models had a positive *y*-intercept (θ). This indicates that EMT had an effect on the rate of the adsorption process. It can also be observed that these *y*-intercept values were greater at 45°C than at 25°C suggesting that the effect of EMT was more pronounced at the higher temperature than at the lower temperature of 25°C. No discernible trends were

exhibited with regards to changes in the IPD rate constant (k_{IP}) when varying the alcohol carbon chain length and temperature.

It can be observed that the correlation coefficients of the investigated models were relatively similar (Table 7.2-1). The calculated and experimentally determined equilibrium adsorbent loadings for these systems compared well for P1 and P2. These values also compared well for PN, with the exception of some cases where the reaction order *n*, was notably greater than 2. The MPSD for both P1 and the Elovich model was also appreciably greater than for P2 and PN. Collectively, this suggests that P2 and PN were best suited for the description of the adsorption kinetics of these systems.

Table 7.2-1: Kinetic model parameters for the adsorption of a single alcohol onto Activated Alumina F220

	45°C			25°C		
Model Parameters	***1-hexanol***	***1-octanol***	***1-decanol***	***1-hexanol***	***1-octanol***	***1-decanol***
Initial Concentration (mass%)	***1.01***	***1.04***	***0.98***	***0.99***	***1.03***	***1.13***
$q_{e,exp}$ $(mg.g^{-1})$	98.5	113	111	97.2	91.7	94.8
Pseudo-first-order Model						
$q_{e,cal}$ $(mg.g^{-1})$	95.5	111	109	97.7	87.9	92.9
k_1 (min^{-1})	0.03	0.03	0.01	0.02	0.02	0.01
R^2	0.97	0.97	0.99	0.96	0.98	0.96
MPSD (%)	24.1	23.6	24.1	10.5	9.51	18.9
Pseudo-second-order Model						
$q_{e,cal}$ $(mg.g^{-1})$	100	117	126	115	104	112
k_2 $(x10^{-3}\ g.(mg.min)^{-1})$	0.45	0.40	0.07	0.15	0.16	0.10
R^2	0.98	0.98	0.99	0.98	0.99	0.97
MPSD (%)	21.2	18.0	23.5	6.98	5.23	14.3
Pseudo-nth-order Model						
n (-)	4.29	2.45	1.27	2.24	3.30	2.14
$q_{e,cal}$ $(mg.g^{-1})$	123	121	112	121	132	115
k_n $(x10^{-5}\ g^{n-1}.mg^{1-n}.min^{-1})$	0.00	5.26	219.1	4.23	0.02	5.13
R^2	0.97	0.98	1.00	0.98	1.00	0.97
MPSD (%)	17.0	17.0	23.4	6.72	4.0	14.0
Elovich Model						
β $(g.mg^{-1})$	0.08	0.06	0.06	0.04	0.05	0.05
α $(mg.(g.min)^{-1})$	31.0	31.7	6.74	4.44	3.96	3.46
R^2	0.94	0.95	0.88	0.98	1.00	0.96
MPSD (%)	13.9	10.4	74.2	6.16	4.42	13.6
Intra-particle Diffusion Model						
θ $(mg.g^{-1})$	72.9	70.9	37.4	4.73	28.6	15.5
k_{ip} $(mg/g.min^{0.5})$	1.32	2.34	3.15	5.66	3.30	4.07
R^2	0.97	0.97	0.83	1.00	0.92	1.00

7.2.1.2 *Selexsorb CDx®*

The kinetic model parameters for the single component adsorption of 1-hexanol, 1-octanol and 1-decanol using SCDx, are summarised in Table 7.2-2. AS for AA-F220, PN and P2 had the highest correlation coefficients and the lowest MPSD values. The predicted equilibrium adsorbent loadings of P2 and PN were also more comparable to the experimentally determined values, than those obtained with P1. The model parameters provided in Table 7.2-2 exhibited trends predominantly similar to those discussed for the systems using AA-F220 as adsorbent (Section 7.2.1.1). For the model parameters of these systems with other initial adsorbate concentrations, refer to Appendix H (Section H.2.2, p256).

Table 7.2-2: Kinetic model parameters for the adsorption of a single alcohol onto Selexsorb CDx®

	45°C			25°C		
Model Parameters	***1-hexanol***	***1-octanol***	***1-decanol***	***1-hexanol***	***1-octanol***	***1-decanol***
Initial Concentration (mass%)	***1.02***	***1.00***	***1.08***	***0.97***	***1.05***	***0.99***
$q_{e,exp}$ $(mg.g^{-1})$	112	108	123	84.4	72.7	85.2
Pseudo-first-order Model						
$q_{e,cal}$ $(mg.g^{-1})$	103	99.2	108	81.2	70.3	80.2
k_1 (min^{-1})	0.02	0.01	0.01	0.02	0.01	0.02
R^2	0.95	0.97	0.94	0.97	0.98	0.97
MPSD (%)	28.5	26.5	35.0	9.95	11.5	9.21
Pseudo-second-order Model						
$q_{e,cal}$ $(mg.g^{-1})$	113	111	118	96.5	84.4	95.1
k_2 $(x10^{-3}\ g.(mg.min)^{-1})$	0.21	0.16	0.10	0.16	0.17	0.18
R^2	0.98	0.99	0.97	0.99	0.99	0.99
MPSD (%)	24.5	22.0	25.2	5.87	7.68	5.41
Pseudo-nth-order Model						
n (-)	2.45	2.31	2.39	3.84	3.59	3.16
$q_{e,cal}$ $(mg.g^{-1})$	118	116	125	136	115	119
k_n $(x10^{-5}\ g^{n-1}.mg^{1-n}.min^{-1})$	2.56	3.57	1.37	0.00	0.01	0.05
R^2	0.98	0.99	0.97	1.00	0.99	0.99
MPSD (%)	23.4	22.6	24.1	4.10	6.77	4.15
Elovich Model						
β $(g.mg^{-1})$	0.06	0.06	0.06	0.05	0.06	0.05
α $(mg.(g.min)^{-1})$	17.31	11.5	9.56	3.53	2.87	3.59
R^2	0.96	0.95	0.94	1.00	0.99	0.99
MPSD (%)	17.34	29.4	35.1	4.98	8.33	4.17
Intra-particle Diffusion Model						
θ $(mg.g^{-1})$	75.2	39.8	21.0	22.3	18.8	21.2
k_{ip} $(mg/g.min^{0.5})$	1.44	2.91	3.55	3.28	2.84	3.34
R^2	0.99	0.98	0.90	0.98	0.96	0.93

7.2.1.3 *Selexsorb CD®*

Table 7.2-3 delineates the kinetic model parameters for the single component adsorption of 1-hexanol, 1-octanol and 1-decanol onto SCD. As for the adsorption of these systems onto AA-F220 and SCDx, P2 and PN again proved to have the highest correlation coefficients and the lowest MPSD values. Consequently, since the kinetic adsorption behaviour of the systems using SCD as adsorbent was similar to that of AA-F220 and SCDx, the model parameters provided in Table 7.2-3 also exhibited trends predominantly similar to those discussed for the systems using AA-F220 as adsorbent (Section 7.2.1.1). For the model parameters of these systems with other initial adsorbate concentrations, refer to Appendix H (Section H.2.3, p259).

Table 7.2-3: Kinetic model parameters for the adsorption of a single alcohol onto Selexsorb CD®

	45°C			25°C		
Model Parameters	***1-hexanol***	***1-octanol***	***1-decanol***	***1-hexanol***	***1-octanol***	***1-decanol***
Initial Concentration (mass%)	***0.96***	***1.10***	***1.18***	**0.98**	**1.02**	**1.08**
$q_{e,exp}$ $(mg.g^{-1})$	107	120	129	89.0	73.0	72.6
Pseudo-first-order Model						
$q_{e,cal}$ $(mg.g^{-1})$	98.7	110	116	81.8	70.1	67.9
k_1 (min^{-1})	0.02	0.01	0.01	0.02	0.01	0.01
R^2	0.96	0.95	0.95	0.95	0.97	0.96
MPSD (%)	26.6	30.3	29.0	11.4	12.7	13.1
Pseudo-second-order Model						
$q_{e,cal}$ $(mg.g^{-1})$	108	122	129	95.6	84.1	81.3
k_2 $(x10^{-3}\ g.(mg.min)^{-1})$	0.22	0.14	0.12	0.20	0.17	0.18
R^2	0.98	0.98	0.98	0.98	0.99	0.98
MPSD (%)	22.1	25.5	22.3	7.28	8.57	9.00
Pseudo-nth-order Model						
n (-)	3.08	2.38	2.71	3.08	3.65	2.26
$q_{e,cal}$ $(mg.g^{-1})$	117	129	143	117	116	85.6
k_n $(x10^{-5}\ g^{n-1}.mg^{1-n}.min^{-1})$	0.16	2.11	0.34	0.08	0.00	5.28
R^2	0.98	0.98	0.99	0.98	0.99	0.98
MPSD (%)	18.5	26.2	20.3	7.19	7.56	8.49
Elovich Model						
β $(g.mg^{-1})$	0.07	0.06	0.06	0.05	0.06	0.06
α $(mg.(g.min)^{-1})$	14.6	14.8	12.6	4.25	2.92	2.89
R^2	0.96	0.95	0.96	0.99	0.99	0.98
MPSD (%)	16.4	28.3	24.4	4.53	8.72	7.94
Intra-particle Diffusion Model						
θ $(mg.g^{-1})$	79.9	47.5	11.6	19.8	13.5	7.45
k_{ip} $(mg/g.min^{0.5})$	0.97	3.05	5.28	3.44	3.12	3.37
R^2	0.84	1.00	1.00	1.00	1.00	0.99

7.2.2 Kinetic Modelling Discussion

From the results provided in Section 7.2.1 it is clear that the different alcohol-alkane systems and different adsorbents investigated exhibited very similar kinetic behaviour throughout. For all single component systems investigated in this study, P2 and PN were identified as the most suitable kinetic models. These two models both had high correlation coefficients and low MPSD values, and their predicted equilibrium adsorbent loadings compared well with the experimentally determined adsorbent loadings. Several studies including one pertaining to the adsorption of sulphur from model oil have also reported P2 to best describe the adsorption kinetics of various materials onto AA [54] which substantiates the findings from this study.

Figure 7.2-1 provides a visual representation, representative of all the single component systems investigated at both temperatures and various initial adsorbate concentrations, of the different models and their suitability to correlate the experimental data. From Figure 7.2-1 it can be observed that P2 and PN seemed to describe the data almost equally well, whereas P1 and the Elovich model were inadequate in describing the data. Initially, the Elovich model seemed to underpredict the data whereas P1 predicted a very rapid initial uptake of adsorbate after which it underpredicted the equilibrium adsorbent loading. Collectively, this indicates that even though the correlation coefficients of P1 and the Elovich model compared well with those of P2 and PN, they were not suitable for correlating the kinetic adsorption data of the investigated single component systems, and thus P2 or PN should be applied instead. Since PN is a three-parameter model and P2 a two-parameter model, P2 was assumed to be superior in this study with correlation coefficients (R^2) greater than 0.96 on average.

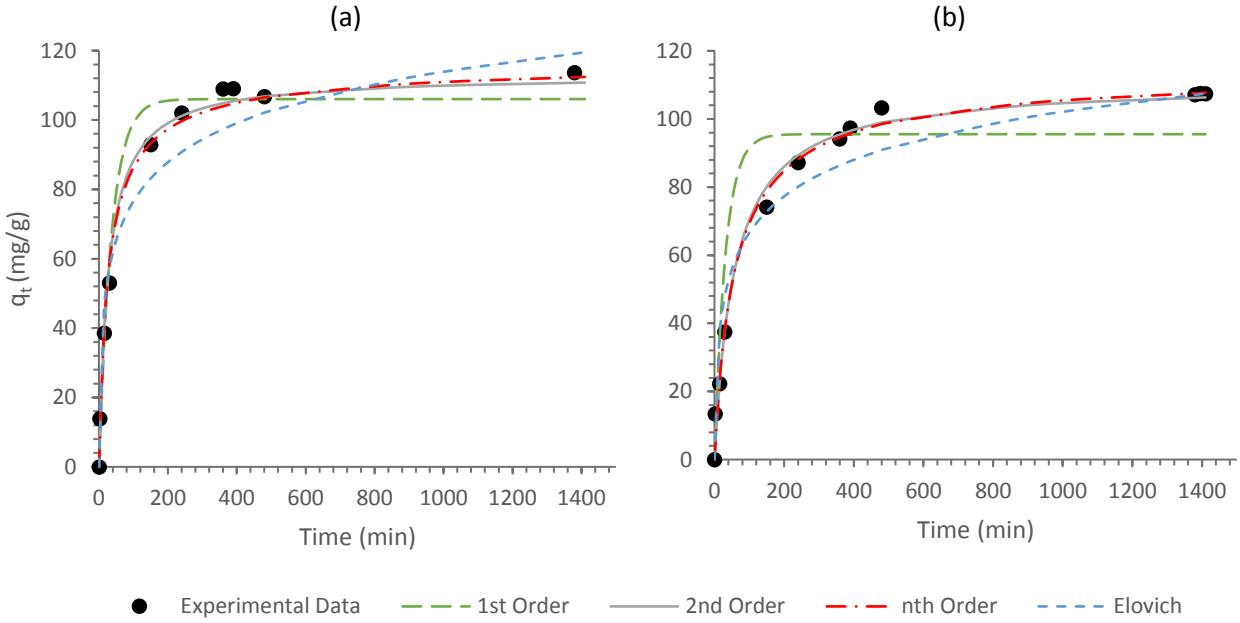

Figure 7.2-1: Kinetic adsorption models for the adsorption of (a) 1-hexanol onto Activated Alumina F220 (IC = 1.51 mass%); and, (b) 1-octanol onto Selexsorb CDx® (IC = 1.00 mass%) (T = 45°C)

From the model parameters of P2, it was observed that the kinetic constant (k_2) exhibited very little changes for the different adsorbents. Nonetheless, k_2 predominantly decreased with increasing alcohol chain length which coincides with the findings discussed in Chapter 5 (Section 5.4.3). This suggests that attachment of the shorter chain alcohols to the adsorbent surface was faster than for the longer chain alcohols, *i.e.* a faster surface reaction. In theory, as shown in a theoretical P2 derivation by Azizian [78], the observed P2 rate constant is a complex function of initial adsorbate concentration. At 25°C, k_2 predominantly decreased with increasing initial adsorbate concentration; a finding reported by several studies [84]. At 45°C, however, no discernible relationship was observed between k_2 and initial adsorbate concentration. This may be attributed to the complex competing effects of increased driving force with increased initial adsorbate concentration, the interaction between adsorbed molecules and adsorbate molecules in the bulk solution (discussed in Chapter 5, Section 5.4.2) as well as the energy distribution of active adsorption sites. For lower initial adsorbate concentrations, only the high energy adsorptions sites will be filled, resulting in a higher rate constant; whereas, at higher concentrations more of the lower energy sites will be filled, resulting in a lower rate constant [84]. When varying the system temperature from 25°C to 45°C, the P2 rate constant was found to increase for the majority of the systems investigated. This was to be expected and coincides with the findings in Chapter 5 (Section 5.4.1), as an increase in temperature would provide the necessary energy for the breaking of intramolecular bonds and the formation of new bonds with the adsorbent surface [12]. In turn, the molecules at the higher temperature would be able to react with the adsorbent surface faster than those at a lower temperature [12].

Of interest is the fact that the initial adsorption rate parameter (α) as obtained with the Elovich model, also increased with increasing temperature which concurs with the findings from P2. These initial adsorption rate constants were marginally greater for most systems using AA-F220 as adsorbent, as compared to the systems using SCDx and SCD. This may be attributed to AA-F220's large external surface area as compared to that of SCDx and SCD. Initial adsorbate concentration did not seem to have a very pronounced effect on the initial adsorption rate parameter at 25°C with the values remaining relatively equal, however, at 45°C no discernible trend was exhibited. For all the single component systems, at both temperatures and various initial adsorbate concentrations, the Elovich initial adsorption rate parameter also decreased for an increase in alcohol carbon chain length, indicating that the shorter chain alcohols were adsorbed much faster in the initial stages of the adsorption process.

Many adsorption studies have used the pseudo-order kinetic models to determine the kinetic mechanism, *i.e.* the rate-limiting step(s), of an adsorption process. Thus, if P2 for example provided the best fit to the experimental data, the rate-limiting step of the process would be assumed to be the surface reaction. Several more recent studies, however, have argued that these models alone, specifically P2, cannot be used to determine the rate-limiting step with certainty [75]–[77]. Thus, P2 being the most suitable kinetic model for

the systems investigated here does not necessarily imply that the rate of adsorption of these systems was governed by a surface reaction. It is, however, indicative of possible chemisorption with a surface reaction of second order [13].

Ultimately, the IPD model was applied to the data to gain further insight into the adsorption mechanism of the investigated systems. The Weber-Morris plots (plots of the IPD model) of all the single component systems, at both temperatures, exhibited similar behavioural trends (Figure 7.2-2). These plots all exhibited three distinct phases in the adsorption process: EMT from the bulk solution over the boundary layer onto the adsorbent surface and instantaneous adsorption on the external surface of the adsorbent (0 to approximately 70 minutes); IPD (70 to approximately 400 minutes); and, the equilibrium reaching phase. Generally, EMT is faster than IPD [111]. However, from the Weber-Morris plots and the IPD model parameters, it was clear that IPD was not the sole rate-limiting step in the adsorption process. The boundary layer surrounding the adsorbent particles, *i.e.* EMT, was demonstrated to have had an effect since the *y*-intercepts of the IPD segment of the Weber-Morris plots were not equal to 0 [90]. These EMT effects were also found to be appreciably more pronounced at the higher temperature of 45°C than at 25°C. This, in turn, suggests that the rate of adsorption of all these single component systems, was controlled not only by IPD, but possibly also by EMT [94], [95].

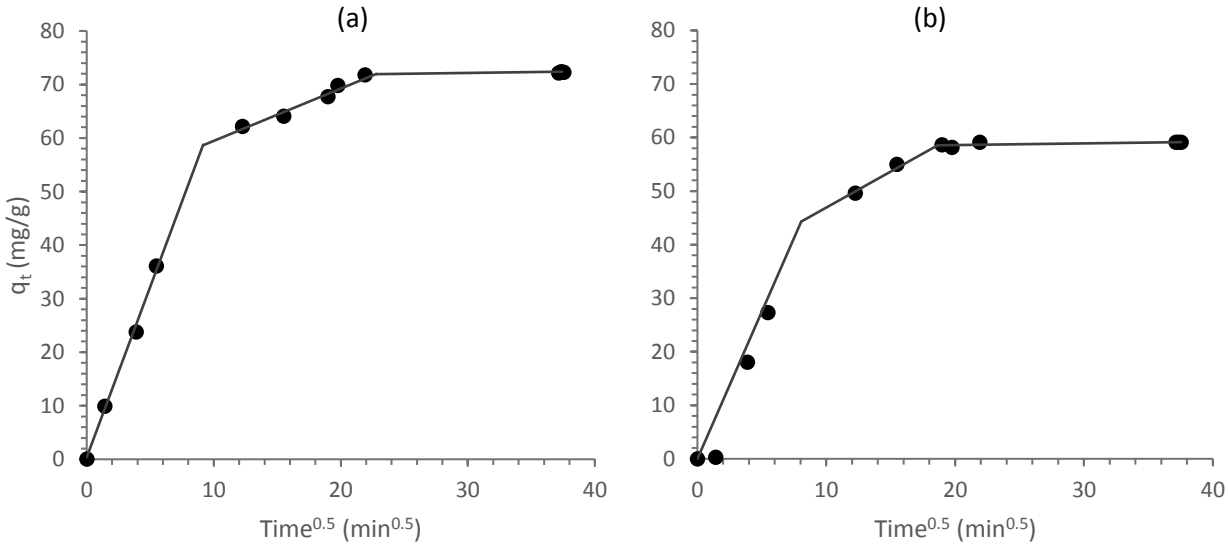

Figure 7.2-2: Intra-particle diffusion model (Weber-Morris plot) for the adsorption of (a) 1-octanol onto Activated Alumina F220 (IC = 0.56 mass%); and, (b) 1-hexanol onto Selexsorb CD® (IC = 0.43 mass%) (T = 45°C)

Collectively, these findings indicate that the rate of adsorption of these single component systems possibly depended not only on IPD and EMT, but also on the surface reaction to some extent. This, however, could not be confirmed with certainty and further investigation is required. It should be noted that very few studies have reported the surface reaction to be rate-limiting, with some studies only reporting a combination of the

two, *i.e.* chemical-diffusion, to be rate-limiting [112]. A study conducted by Groenewald [8] on the adsorption of 1-alcohols onto AA-F220, SCDx and SCD suggested that the rate of adsorption was predominantly diffusion limited with some cases being limited by the surface reaction. Ho and McKay [82], however, pointed out that "the effects of transport phenomena and chemical reactions are often experimentally inseparable", making it very difficult to correctly distinguish between these two.

7.3 Binary Component Adsorption

In this section the binary component adsorption parameters are provided and discussed for multiple kinetic models. Note that as for the single component adsorption section, the parameters are only provided for one initial concentration. The binary component adsorption kinetics was, however, investigated at several initial adsorbate concentrations. Binary component kinetic model parameters at various other adsorbate concentrations are provided in Appendix H (Section H.3, 262).

It should be noted that the kinetic adsorption models were fitted to the data of each respective adsorbate component in the binary mixtures, therefore the model parameters are provided for the components in the mixtures and not for the total mixture. The IPD model, however, was fitted to the data of the total binary mixtures.

7.3.1 Kinetic Modelling Results

7.3.1.1 *Activated Alumina F220*

Table 7.3-1 summarises the kinetic model parameters for the binary component adsorption of alcohol mixtures (50:50 by mass) onto AA-F220. These model parameters (for systems using AA-F220 as adsorbent) at various other initial adsorbate concentrations are provided in Appendix H (Section H.3.1, p262).

For all three binary alcohol mixtures, 1-hexanol and 1-decanol, 1-hexanol and 1-octanol, as well as 1-octanol and 1-decanol, the two most suitable kinetic models were identified as P2 and PN. The correlation coefficients of these models proved to be the highest in comparison the that of P1 and the Elovich model and the MPSD values determined for P2 and PN were also less than those determined for P1 and the Elovich model for most of the binary component systems. The equilibrium adsorbent loadings determined with P2 were much more comparable to the experimentally measured equilibrium loadings with P1 slightly underpredicting and PN slightly overpredicting these equilibrium adsorbent loadings. Consequently, P2 was identified as the most suitable model for correlation of the kinetic data of these binary component systems.

Table 7.3-1: Kinetic model parameters for the adsorption of binary alcohol mixtures onto Activated Alumina F220

Model Parameters	**Binary Systems**											
	45°C						**25°C**					
	1-H	**1-D**	**1-H**	**1-O**	**1-O**	**1-D**	**1-H**	**1-D**	**1-H**	**1-O**	**1-O**	**1-D**
Initial Concentration (mass%)	**0.95**	**1.10**	**0.97**	**1.07**	**1.02**	**1.17**	**0.82**	**0.94**	**0.93**	**0.98**	**1.01**	**0.95**
$q_{e,exp}$ $(mg.g^{-1})$	74.8	72.8	65.0	62.2	67.4	68.5	57.4	55.1	68.5	65.5	77.1	60.9
Pseudo-first-order Model												
$q_{e,cal}$ $(mg.g^{-1})$	69.5	66.6	63.1	58.3	65.0	66.5	53.7	59.0	63.1	60.4	74.6	61.6
k_1 (min^{-1})	0.03	0.03	0.03	0.03	0.02	0.02	0.01	0.00	0.03	0.02	0.01	0.00
R^2	0.96	0.89	0.98	0.95	0.98	0.97	0.95	0.90	0.95	0.96	0.99	0.99
MPSD (%)	7.33	14.2	6.22	10.5	5.90	7.49	21.1	236	8.54	10.7	14.0	15.2
Pseudo-second-order Model												
$q_{e,cal}$ $(mg.g^{-1})$	75.2	72.2	67.2	62.4	70.6	72.4	61.9	78.5	68.4	67.1	83.8	72.9
k_2 $(x10^{-3}\ g.(mg.min)^{-1})$	0.41	0.43	0.55	0.60	0.35	0.31	0.15	0.03	0.45	0.28	0.11	0.06
R^2	0.99	0.94	0.99	0.98	0.99	0.98	0.96	0.86	0.99	1.00	1.00	0.98
MPSD (%)	5.53	10.4	3.37	6.46	2.89	5.22	25.9	236	4.15	4.53	7.42	21.4
Pseudo-nth-order Model												
n (-)	2.29	3.61	1.91	3.61	1.91	3.61	1.57	1.35	2.92	2.36	2.04	1.10
$q_{e,cal}$ $(mg.g^{-1})$	77.6	86.2	66.7	86.2	66.7	86.2	57.7	60.7	75.9	70.3	84.3	62.2
k_n $(x10^{-5}\ g^{n-1}.mg^{1-n}.min^{-1})$	11.8	0.03	79.3	0.03	79.3	0.03	88.6	74.6	0.84	5.96	8.86	298
R^2	0.99	0.95	0.99	0.92	0.98	0.95	0.96	0.88	0.99	1.00	1.00	0.99
MPSD (%)	5.67	8.64	3.39	13.2	10.8	15.1	23.9	245	3.01	3.62	7.34	16.0
Elovich Model												
β $(g.mg^{-1})$	0.09	0.09	0.11	0.12	0.09	0.08	0.08	0.08	0.10	0.09	0.06	0.08
α $(mg.(g.min)^{-1})$	7.80	9.64	12.5	12.7	5.15	4.62	1.31	0.92	7.71	3.54	2.01	1.08
R^2	0.96	0.94	0.94	0.97	0.94	0.92	0.95	0.95	0.97	0.98	0.98	0.97
MPSD (%)	10.7	8.85	9.50	6.63	10.6	11.5	16.9	25.6	6.98	6.43	11.8	10.7

It can be observed from Table 7.3-1 that the P2 rate constant (K_2) marginally increased with increasing combined alcohol chain length. For most systems this rate constant was also greater for the shorter chain alcohol in the binary component systems than for the longer chain alcohol. The P2 rate constant seemed to increase with increasing temperature whereas the P1 rate constant exhibited no such trend. The Elovich model initial adsorption rate constant (α) also proved to be greater for the shorter chain alcohols in the binary mixtures and increased with increasing temperature.

The IPD model parameters when using AA-F220, are provided in Table 7.3-2. It can be observed that the value of the y-intercept (θ) was significant throughout all systems investigated with it being greater at the higher temperature of 45°C. This indicates that EMT as well as IPD had an influence on the rate of adsorption of these binary component systems. These IPD model parameters at various other initial adsorbate concentrations are provided in Appendix H (Section H.3.1, p262).

Table 7.3-2: Intra-particle diffusion model parameters for the adsorption of a binary alcohol mixture onto Activated Alumina F220

Intra-particle Diffusion Model Parameters	***Binary Alcohol Mixtures***					
	45°C			**25°C**		
	1-H + 1-D	**1-H + 1-O**	**1-O + 1-D**	**1-H + 1-D**	**1-H + 1-O**	**1-O + 1-D**
Initial Concentration (mass%)	2.05	2.04	2.19	1.76	1.92	1.96
θ *(mg.g^{-1})*	70.5	79.1	54.8	38.0	51.1	4.2
k_{ip} *(mg/g.min$^{0.5}$)*	3.41	2.26	4.45	2.91	3.91	5.77
R^2	0.83	0.81	1.00	0.78	0.98	0.98

7.3.1.2 *Selexsorb CDx®*

Table 7.3-3 outlines the kinetic model parameters for the binary component adsorption of 50:50 alcohol mixtures onto SCDx. These model parameters (for systems using SCDx as adsorbent) at various other initial adsorbate concentrations are provided in Appendix H (Section H.3.2, p269).

For the description of the kinetic behaviour of all three alcohol mixtures onto SCDx, P2 and PN were identified as the most suitable models. It can be observed that P2 and PN predominantly had the greatest correlation coefficients and the lowest MPSD values when compared to that of P1 and the Elovich model. As for the systems using AA-F220, P2 also best predicted the equilibrium adsorbent loadings of the various systems. The kinetic behaviour of these systems and the trends exhibited by the model parameters were similar to those discussed for AA-F220 (Section 7.3.1.1).

Table 7.3-3: Kinetic model parameters for the adsorption of binary alcohol mixtures onto Selexsorb CDx®

Model Parameters	**Binary Systems**											
	45°C						**25°C**					
	1-H	***1-D***	***1-H***	***1-O***	***1-O***	***1-D***	***1-H***	***1-D***	***1-H***	***1-O***	***1-O***	***1-D***
Initial Concentration (mass%)	***1.03***	***1.04***	***0.76***	***0.75***	***0.76***	***0.92***	**1.04**	**1.06**	**1.00**	**0.98**	**1.16**	**1.18**
$q_{e,exp}$ $(mg.g^{-1})$	80.9	44.0	66.8	53.5	60.7	63.1	70.9	52.2	73.0	60.9	59.4	56.4
Pseudo-first-order Model												
$q_{e,cal}$ $(mg.g^{-1})$	73.0	45.6	63.2	51.6	55.8	58.4	66.1	49.2	65.9	52.4	59.3	57.5
k_1 (min^{-1})	0.02	0.01	0.01	0.01	0.01	0.01	0.01	0.01	0.01	0.02	0.01	0.01
R^2	0.93	0.97	0.98	0.99	0.96	0.95	0.97	0.97	0.94	0.89	1.00	0.98
MPSD (%)	13.5	29.3	11.2	7.51	10.3	16.0	8.50	8.78	13.1	13.8	2.02	35.8
Pseudo-second-order Model												
$q_{e,cal}$ $(mg.g^{-1})$	81.2	52.2	70.3	58.3	62.5	65.3	73.8	55.6	74.5	59.5	65.2	65.6
k_2 $(x10^{-3}\ g.(mg.min)^{-1})$	0.25	0.12	0.23	0.20	0.26	0.20	0.22	0.22	0.19	0.32	0.24	0.12
R^2	0.98	0.94	1.00	0.98	1.00	0.99	1.00	0.98	0.98	0.97	0.98	0.94
MPSD (%)	7.41	38.1	6.46	8.12	3.59	8.69	3.64	7.48	9.97	8.54	8.08	43.7
Pseudo-nth-order Model												
n (-)	3.72	1.65	2.10	1.23	2.10	1.23	2.13	1.60	2.92	3.80	0.99	1.03
$q_{e,cal}$ $(mg.g^{-1})$	101	47.6	71.2	52.7	71.2	52.7	75.0	52.5	85.3	75.3	59.3	57.7
k_n $(x10^{-5}\ g^{n-1}.mg^{1-n}.min^{-1})$	0.01	56.8	15.4	421	15.4	421	12.5	110	0.28	0.01	1362	685
R^2	0.99	0.94	0.99	0.99	0.94	0.89	1.00	0.98	0.99	0.99	1.00	0.98
MPSD (%)	4.35	37.5	6.37	6.43	12.8	19.4	3.75	7.12	10.6	5.77	2.02	36.3
Elovich Model												
β $(g.mg^{-1})$	0.07	0.10	0.08	0.09	0.09	0.09	0.08	0.10	0.07	0.10	0.09	0.08
α $(mg.(g.min)^{-1})$	4.93	0.88	3.10	1.59	2.50	2.27	2.91	1.62	2.53	2.98	2.30	1.20
R^2	0.98	0.92	0.96	0.93	0.98	0.98	0.97	0.95	0.98	0.99	0.91	0.92
MPSD (%)	5.18	13.7	9.84	14.3	6.55	7.91	8.50	11.9	10.5	5.50	13.9	19.5

Table 7.3-4 provides the IPD model parameters for the binary component adsorption using SCDx. From these parameters it is clear that the effect of EMT was significant at both temperatures, since the *y*-intercepts (θ) were not equal to zero.

Table 7.3-4: Intra-particle diffusion model parameters for the adsorption of a binary alcohol mixture onto Selexsorb CDx®

Intra-particle Diffusion Model Parameters	***Binary Alcohol Mixtures***					
	45°C			**25°C**		
	1-H + 1-D	**1-H + 1-O**	**1-O + 1-D**	**1-H + 1-D**	**1-H + 1-O**	**1-O + 1-D**
Initial Concentration (mass%)	2.07	1.51	1.67	2.10	1.98	2.34
θ *(mg.g^{-1})*	29.7	55.9	22.2	49.9	47.4	69.7
k_{ip} *(mg/g.min$^{0.5}$)*	4.31	2.85	4.35	3.37	3.27	2.31
R^2	0.97	0.98	1.00	0.97	0.89	0.99

7.3.1.3 *Selexsorb CD®*

As for the systems using SCDx as adsorbent, these binary component systems also exhibited kinetic behaviour similar to when using AA-F220. The trends in the model parameters of these systems were therefore also relatively similar to those discussed for AA-F220.

Table 7.3-5 provides the kinetic model parameters for the binary component adsorption of 50:50 (by mass) alcohol mixtures using SCD as adsorbent. These model parameters (for systems using SCD as adsorbent) at various other initial adsorbate concentrations are provided in Appendix H (Section H.3.3, p276).

Similar to when using AA-F220 and SCDx as adsorbents, P2 and PN were also identified as most suitable models for the description of the kinetic behaviour of all three alcohol mixtures onto SCD. This was clear from the correlation coefficients, MPSD values and comparisons of the model determined equilibrium adsorbent loadings to the experimentally measured equilibrium loadings. As for the systems using SCDx as adsorbent, these binary component systems also exhibited kinetic behaviour similar to when using AA-F220. The trends in the model parameters of these systems were therefore also relatively similar to those discussed for AA-F220.

Table 7.3-5: Kinetic model parameters for the adsorption of binary alcohol mixtures onto Selexsorb CD®

Model Parameters	**Binary Systems**											
	45°C						**25°C**					
	1-H	***1-D***	***1-H***	***1-O***	***1-O***	***1-D***	***1-H***	***1-D***	***1-H***	***1-O***	***1-O***	***1-D***
Initial Concentration (mass%)	***1.11***	***1.18***	***0.91***	***1.08***	***1.00***	***1.07***	**1.22**	**1.21**	**0.80**	**0.95**	**1.09**	**1.01**
$q_{e,exp}$ $(mg.g^{-1})$	88.0	52.1	85.4	81.1	74.1	70.5	79.9	57.2	53.8	54.9	63.1	48.3
Pseudo-first-order Model												
$q_{e,cal}$ $(mg.g^{-1})$	76.6	43.2	81.0	78.7	69.6	66.4	70.9	51.5	81.0	78.7	59.8	46.3
k_1 (min^{-1})	0.02	0.02	0.01	0.01	0.01	0.01	0.01	0.01	0.01	0.01	0.01	0.01
R^2	0.88	0.82	0.93	0.98	0.96	0.96	0.93	0.93	0.97	0.98	0.97	0.97
MPSD (%)	15.5	20.6	25.4	16.9	17.7	17.6	16.1	24.9	22.8	8.910	18.6	19.3
Pseudo-second-order Model												
$q_{e,cal}$ $(mg.g^{-1})$	86.2	49.7	86.1	87.2	76.9	74.4	79.7	56.0	86.1	87.2	65.7	73.7
k_2 $(x10^{-3}\ g.(mg.min)^{-1})$	0.27	0.40	0.15	0.11	0.17	0.13	0.18	0.21	0.15	0.11	0.15	0.14
R^2	0.95	0.92	0.94	0.98	0.98	0.98	0.98	0.96	0.98	1.00	0.98	0.77
MPSD (%)	11.1	15.5	15.8	8.64	9.55	11.7	8.89	15.6	30.4	7.52	10.9	41.4
Pseudo-nth-order Model												
n (-)	3.00	3.23	2.86	2.83	2.86	2.83	2.95	2.67	2.86	2.83	3.24	3.41
$q_{e,cal}$ $(mg.g^{-1})$	92.0	55.7	106	106	106	106	92.7	60.7	106	106	79.3	62.6
k_n $(x10^{-5}\ g^{n-1}.mg^{1-n}.min^{-1})$	0.35	0.34	0.14	0.15	0.14	0.15	0.18	1.32	0.14	0.15	0.05	0.04
R^2	0.95	0.94	0.96	0.98	0.95	0.91	0.99	0.97	0.97	0.99	0.99	0.99
MPSD (%)	10.5	13.1	18.9	9.17	15.1	18.8	8.95	13.1	33.3	8.30	8.71	5.08
Elovich Model												
β $(g.mg^{-1})$	0.07	0.12	0.07	0.06	0.07	0.07	0.07	0.10	0.07	0.06	0.09	0.11
α $(mg.(g.min)^{-1})$	5.60	2.87	3.51	2.16	2.72	2.03	3.20	2.07	3.51	2.16	1.86	1.37
R^2	0.97	0.97	0.96	0.97	0.98	0.98	1.00	0.99	0.98	0.97	0.99	0.99
MPSD (%)	10.0	10.8	9.45	6.86	7.86	13.7	4.76	8.78	7.83	9.34	10.4	4.51

Table 7.3-6 summarises the IPD model parameters for the binary component adsorption using SCD. Similar to the systems with AA-F220 and SCDx, the EMT was found to have played a significant role in the adsorption process since the *y*-intercepts (θ) were not equal to zero.

Table 7.3-6: Intra-particle diffusion model parameters for the adsorption of a binary alcohol mixture onto Selexsorb CD®

Intra-particle Diffusion Model Parameters	***Binary Alcohol Mixtures***					
	45°C			**25°C**		
	1-H + 1-D	**1-H + 1-O**	**1-O + 1-D**	**1-H + 1-D**	**1-H + 1-O**	**1-O + 1-D**
Initial Concentration (mass%)	2.29	1.99	1.52	2.43	1.75	2.10
θ *(mg.g^{-1})*	(-0.77)	(-4.47)	21.9	43.9	55.9	13.0
k_{ip} *(mg/g.min$^{0.5}$)*	6.71	7.58	5.17	3.17	1.77	4.08
R^2	1.00	0.96	0.96	0.93	0.80	1.00

7.3.2 Kinetic Modelling Discussion

As presented in Section 7.3.1, all binary systems investigated were found to have exhibited very similar kinetic behaviour to one another with similar correlation coefficients, trends, rate constants *etc*. The most suitable kinetic models were identified as P2 and PN. Both these models had high correlation coefficients together with low MPSD values. As previously mentioned, however, PN is a three-parameter model whereas P2 is a two-parameter model. Thus, in this study P2 was assumed superior to PN, with correlation coefficients (R^2) greater than 0.96 on average, similar to the single component systems.

Figure 7.3-1 and Figure 7.3-2 depict the different kinetic models on two different systems at two different temperatures. The trends depicted (best and worst models) are representative of all the binary component systems investigated, at both temperatures and various initial adsorbate concentrations. It was apparent that P1 and the Elovich model where the least suitable for the description of the kinetic behaviour of both components in these systems. P2 and PN however appeared to fit the data fairly well. As shown, the Elovich model underpredicted at the start of the experimental run and overpredicted towards the end of the experimental runs for most systems. P1 on the other hand, overpredicted the data in the time period of approximately 200 to 400 minutes for the majority of the systems and appeared to slightly underpredict the equilibrium adsorbent loadings. On the contrary, PN seemed to slightly overpredict the equilibrium adsorbent loadings, with P2 proving to predict the most comparable equilibrium adsorbent loadings. The binary component kinetic behaviour compared well with that of the corresponding single component systems, exhibiting similar trends.

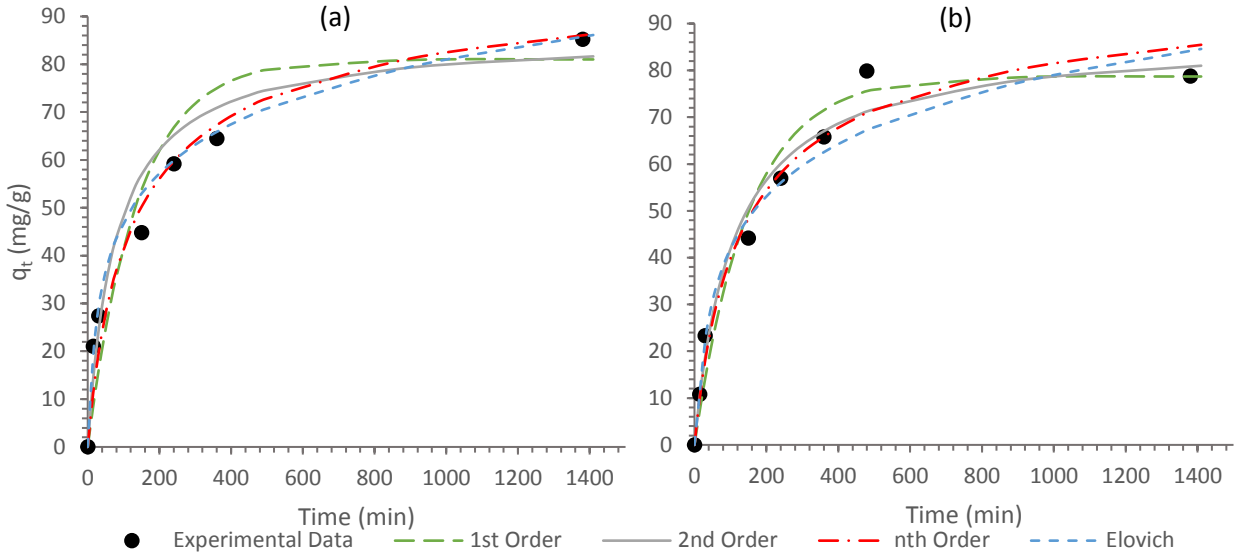

Figure 7.3-1: Kinetic adsorption models for the adsorption of a) 1-hexanol (IC = 0.91 mass%); and, b) 1-octanol (IC = 1.09 mass%) in a binary mixture of 1-hexanol and 1-octanol, onto Selexsorb CD® (T = 45°C)

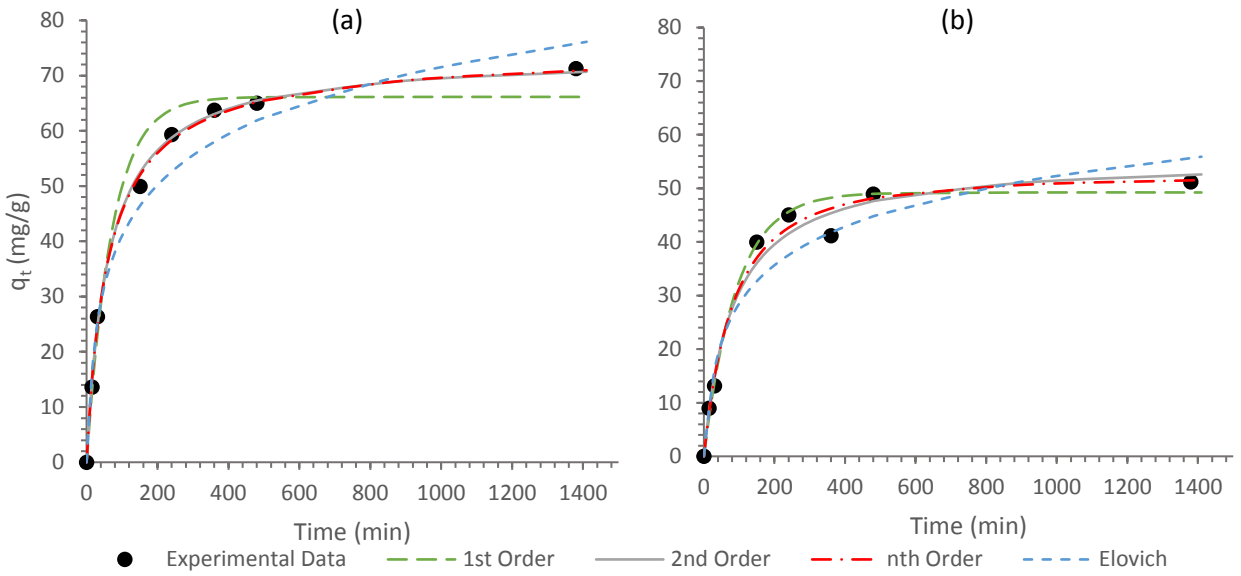

Figure 7.3-2: Kinetic adsorption models for the adsorption of a) 1-hexanol (IC = 1.04 mass%); and, b) 1-decanol (IC = 1.06 mass%) in a binary mixture of 1-hexanol and 1-decanol, onto Selexsorb CDx® (T = 25°C)

For the P2 rate constant (K_2), no apparent trend was observed when varying the initial adsorbate concentration, however, an increase in the rate constant was evident with an increase in temperature which was to be expected. For most of the binary component systems, the P2 rate constant was determined to marginally decrease with increasing alcohol chain length. Note that here "alcohol chain length" refers to the combined chain length of the two alcohols. When comparing the rate constants of the two alcohols in each binary component mixture, the constant associated with the shorter chain alcohol also seemed to be slightly higher than for the longer chain alcohol in most cases. This was to be expected and is in accordance with the

single component adsorption findings (Sections 7.2.1 and 7.2.2). This suggests that the shorter chain alcohol in a mixture of two alcohols would adsorb faster than the longer chain alcohol, giving the shorter chain alcohol somewhat of an advantage when competing for active adsorption sites. This may also explain why the adsorption of longer chain alcohols were affected more negatively in the presence of a shorter chain alcohol than vice versa (Chapter 5, Section 5.6).

The Elovich model also exhibited initial adsorption rate constants (α) marginally greater for the shorter chain alcohols in the binary systems, as compared to the longer chain alcohols. This suggests that initially the shorter chain alcohols in the binary mixtures were adsorbed faster than the longer chain alcohols; a finding evident throughout this study.

As for the single component systems, the IPD model was also investigated to aide in the determination of the rate-limiting step. It can be observed from Figure 7.3-3 that the IPD segments of the Weber-Morris plots do not pass through the origin and therefore indicates that IPD was not the sole rate-limiting step, but that EMT also had an effect on the rate of adsorption [90]. This trend was clear throughout for all the binary component systems, at both 25°C as well as 45°C. For the majority of the binary component systems, the boundary layer effect (θ) as determined with the IPD model was appreciably more pronounced at the higher temperature of 45°C, however, no discernible trend in the effect of the boundary layer was exhibited when varying the initial adsorbate concentrations or the different combinations of 1-alcohols. The IPD rate constant (K_{IP}) exhibited no apparent trend when varying the temperature from 25°C to 45°C, however, a corresponding increase in the rate constant was displayed for an increase in the initial adsorbate concentration in most cases; this may be ascribed to the increase in driving force [84].

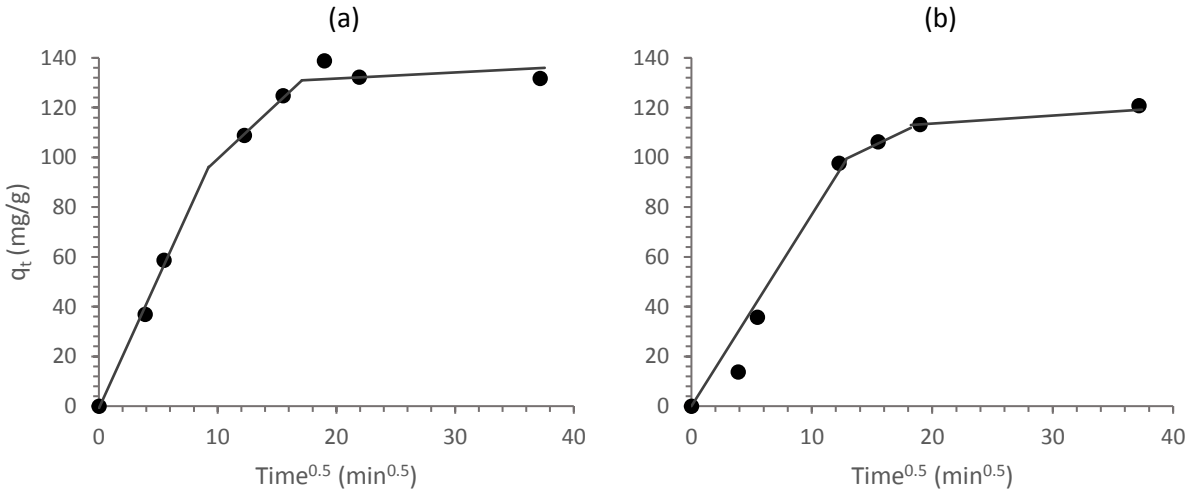

Figure 7.3-3: Intra-particle diffusion model (Weber-Morris plot) for the adsorption of a (a) 1-octanol and 1-decanol mixture onto Activated Alumina F220 (T = 45°C; mixture IC = 2.19 mass%); and, (b) 1-octanol + 1-decanol mixture onto Selexsorb CDx® (T = 25°C; mixture IC = 2.34 mass%)

As mentioned in Section 7.2.2, it cannot be assumed that the surface reaction is rate-limiting just because P2 was identified as the most suitable model. It can, however, be indicative of possible chemisorption [13]. Since both P2 and the IPD models were adequate in describing the data of the binary systems, the possibility exists that adsorption occurred through a complex mechanism influenced by IPD, EMT as well as the surface reaction. It is, however, difficult to distinguish between diffusion limited systems and chemisorption limited systems based only on the suitability of kinetic models, thus further investigation is required (discussed in Section 8.2.2, p118).

7.4 Comparison between Single and Binary Component Kinetics

In order to gain insight into the difference in behaviour between the adsorption of an alcohol in a single and binary component system, the most suitable kinetic model, P2, was compared for the single and binary component systems. Table 7.4-1 encapsulates the P2 model parameters for the adsorption of 1-octanol in a single component and two binary component systems as example. Here, it can be observed that the P2 rate constants of 1-octanol remained relatively constant in single and binary component systems. This was, however, not always the case with some rate constants differing significantly in the single and binary component systems.

Table 7.4-1: Comparison of pseudo-second-order model parameters of 1-octanol onto Selexsorb CD® in a single component system and in binary component systems (T = 45°C)

System	***1-octanol (single)***	***1-octanol in (1-H + 1-O)***	***1-octanol in (1-O + 1-D)***
Initial Concentration of 1-octanol (mass%)	1.10	1.09	1.00
$q_{e.cal}$ *(mg.g^{-1})*	122	87.2	77.0
k_2 *(x10^{-3} g.(mg.min)$^{-1}$)*	0.14	0.11	0.17

Interesting to note is that the initial adsorption rate parameter as determined with the Elovich model, was markedly greater for single component adsorption. This could possibly be attributed to interaction between the alcohol adsorbates in the binary system. Since the two adsorbates are now competing for the same adsorption sites, the initial adsorption may be slower in the binary component systems.

For both single and binary component adsorption, IPD as well as EMT appeared to have influenced the rate of alcohol adsorption. The main difference between the single and binary component adsorption as determined with the IPD model, was that the EMT of the binary component systems was found to be somewhat slower than for the single component systems.

7.5 Chapter Summary

The objective of this chapter was to apply and identify suitable kinetic models for the correlation of the kinetic data of both single and binary component alcohol-alkane systems using AA adsorbents, in order to better comprehend the rate-limiting step(s) of the different systems.

For the single component systems, five different models were applied to the kinetic data. P2 was found to be the most suitable model for correlation of the data. For the binary component systems, the same five kinetic models were applied to the data and again P2 was identified as the most suitable kinetics model. However, since the IPD model also provided good correlation, it was assumed that the rate-limiting step was a complex mechanism influenced by EMT, IPD and the surface reaction.

The shorter chain alcohols exhibited faster adsorption as compared to the longer chain alcohols and adsorption was somewhat faster at the higher temperature of 45°C. According to the Elovich model, the initial adsorption rate of 1-alcohol adsorbates in a single component system was also slightly faster than the adsorption of the same 1-alcohol adsorbates in a binary component system.

The kinetic data of all single and binary component systems were modelled using various kinetic models, and the most suitable kinetic models were identified for correlation of the data. Objective (iii) of this study was therefore successfully addressed in this chapter.

Chapter 8: Conclusions & Recommendations

8.1 Conclusions

The aim of this study was to gain knowledge and insight on the single and binary component adsorption of 1-alcohols from an alkane by using various industrially relevant AA adsorbents. This aim was achieved through the completion of three objectives: (i) measurement and investigation of experimental data; (ii) equilibrium modelling; and, (iii) kinetic modelling.

8.1.1 Adsorption Experimental Results

The first objective was to measure data to investigate the adsorption of several single and binary component 1-alcohol systems using various AA adsorbents.

8.1.1.1 *Experimental Measurements*

Kinetic and equilibrium data were measured for the single component adsorption of 1-hexanol, 1-octanol and 1-decanol from an n-decane solvent, using AA-F220, SCDx and SCD as adsorbents. The data were measured at one temperature (45°C) using three different initial adsorbate concentrations, to complement previously measured data at 25, 30 and 35°C. In addition to the single component data, kinetic and equilibrium data were also measured for three binary component systems: 1-hexanol + 1-decanol, 1-hexanol + 1-octanol as well as 1-octanol + 1-decanol. The binary component kinetic data were measured for equimass 1-alcohol mixtures. The same three adsorbents were used as for the single component adsorption experiments. The binary component adsorption data were measured at two different temperatures (25°C and 45°C) using various initial adsorbate concentrations.

8.1.1.2 *Comparison of Various Activated Alumina Adsorbents*

For the single component adsorption of 1-hexanol and 1-octanol, SCDx and SCD were found to perform slightly better than AA-F220, with equilibrium adsorbent loadings in the range of 110 to 130 mg/g at the conditions investigated. For the single component adsorption of 1-decanol, however, no distinction could be made between the three alumina adsorbents; all performing equally well. For the binary component adsorption of the systems comprising 1-hexanol + 1-octanol, and 1-octanol + 1-decanol, SCDx and SCD were found to marginally outperform AA-F220, while AA-F220 seemed to achieve slightly greater equilibrium adsorbent loadings for the binary component adsorption of 1-octanol + 1-decanol. At the given conditions, the overall equilibrium adsorbent loadings for the binary component systems were found to be somewhat greater than for the single component systems, *i.e.* in the range of 128 to 150 mg/g. Overall, the adsorbents

performed very similar with equilibrium adsorbent loadings very close to one another. Therefore, from an equilibrium perspective, no adsorbent was found to be superior.

8.1.1.3 *Variables Influencing Adsorption*

Temperature was found to have a notable effect on the adsorption of 1-alcohols from n-decane. For both the single as well as the binary component adsorption systems, increasing temperature proved to have a corresponding increase in the equilibrium adsorbent loading of the systems when varying the temperature from 25°C to 45°C; the effect of temperature on equilibrium adsorbent loading indicated that adsorption was occurring through chemical bonds rather than physical forces.

Of the three variables investigated (in the ranges considered), initial adsorbate concentration proved to have the most notable effect on the adsorption of 1-alcohols using AA adsorbents. For both single and binary component systems, adsorption increased for an increase in initial overall adsorbate concentration up to approximately 1.2 mass%. For initial adsorbate concentrations greater than 1 to 1.2 mass%, the equilibrium adsorbent loading was found to remain relatively constant for most systems.

It was demonstrated that the carbon chain length of the respective alcohols investigated had the least notable effect on the adsorption of these alcohols, for the ranges investigated. For the single component adsorption systems, a slight increase in adsorbent loading was exhibited for a decrease in alcohol chain length at times prior to the equilibrium time. For the binary component adsorption systems, the shorter chain alcohol in a binary system were found to adsorb marginally better than the longer chain alcohol in the same system.

8.1.1.4 *Comparison of Single and Binary Component Adsorption*

When comparing the total equilibrium adsorbent loadings of a binary component system comprising two 1-alcohols and its corresponding single component systems, each comprising one 1-alcohol (all with equal total initial adsorbate concentrations, *i.e.* the total 1-alcohol concentration of the binary component system equals the 1-alcohol concentration of the single component systems), it was found that these single and binary component systems performed relatively similarly. When comparing the equilibrium adsorbent loadings of a specific component within a binary component mixture (one of the 1-alcohols in the binary mixture) and the same 1-alcohol in a single component system (with the initial adsorbate concentration of the specific 1-alcohol equal in both systems), the 1-alcohol in the binary system exhibited adsorption notably poorer than the 1-alcohol in the single component system.

8.1.1.5 *Interaction Effect in Binary Component Systems*

For the initial adsorbate concentration range of 1 to 1.5 mass%, antagonistic/competitive behaviour was found to be predominant for all binary component systems, with adsorption of the longer chain alcohols

being inhibited somewhat more in the presence of a shorter chain alcohol than vice versa. This was found to be the case for all binary component systems, at both temperatures of investigation.

8.1.2 Adsorption Equilibrium Modelling

After investigation of the experimental results, equilibrium isotherm modelling was done for both the single and binary component systems.

It was found that all four isotherm models investigated provided a good correlation for the single component data, however, the RPM proved to be superior. For the binary component adsorption, the Extended FM was found to provide the best correlation of the data, with the modified RPM and Extended SM being the best alternatives to the Extended FM. Apart from the Extended FM, the isotherm models investigated did not provide good correlations of the adsorption data.

The RPM being the most compatible isotherm model for the single component systems suggest that: the systems were inclined to monolayer adsorption with the possibility of multilayer adsorption not being entirely excluded; the systems presented as more energetically homogenous than heterogenous; and, the model parameters suggest that physisorption and/or weak chemisorption occurred, but not strong chemisorption. Since the binary component isotherm models provided relatively poor correlations of the data, no model assumptions could be verified for the binary component systems.

8.1.3 Adsorption Kinetic Modelling

The equilibrium and kinetic behaviour of adsorption systems are often investigated together. Hence, the third objective entailed the kinetic modelling of the single and binary component adsorption data.

The adsorption kinetics for the single and binary component adsorption systems was found to be very similar. P2 was determined to provide the best correlation of the adsorption data with the IPD model also fitting the data well. It was therefore assumed that EMT, IPD as well as the surface reaction had an influence on the rate of adsorption. It was also found that some form of chemisorption was occurring, which coincides with the experimental results.

In this study, all three objectives were achieved, and a better overall understanding was gained on the single and binary component adsorption of 1-alcohols from an alkane solvent using AA adsorbents. The adsorption process was proposed to be dominated by weak chemisorption, with competitive adsorption favouring shorter carbon chain alcohols at initial alcohol concentrations greater than approximately 1 mass%.

8.2 Recommendations

Based on the findings from this study, several recommendations can be made for future work.

8.2.1 Experimental Design

In industry, adsorption is rarely done batch-wise as a result of large-scale operation. For this reason, it is recommended that these alcohol-alkane systems be investigated using a continuous column experimental setup. Packed-bed adsorption columns are widely investigated, however, the alcohol-alkane systems investigated in this study have not yet been investigated using such an experimental setup.

The adsorbents used in this study, all of which were AA adsorbents, proved to be a viable option for the adsorption of trace amounts of primary alcohols from n-decane. In order to compare the alcohol removal ability of AA with other market related adsorbents, it is recommended that other adsorbents also be investigated for these alcohol-alkane systems under the same conditions.

8.2.2 Adsorption Process

In this study, it was determined that adsorption was taking place through weak chemical bonds, *i.e.* weak chemisorption, or possibly a combination of weak chemisorption and physisorption. To further explore this finding, it is recommended that additional experimental conditions be added to the experimental design, including a number of different operating temperatures, *e.g.* 5 or more different temperatures. By investigating the adsorption behaviour at various operating temperatures, the heat of adsorption can be determined. If the heat of adsorption is in the range of approximately -40 $kJ.mol^{-1}$ to -400 $kJ.mol^{-1}$, it would verify the finding of chemisorption [11]. In this study, the heat of adsorption could not be determined with certainty, as only two operating temperatures were investigated. In addition, Temperature Programmed Desorption could be employed to investigate the molecules desorbing from the adsorbent surfaces in order to determine whether molecules adhered to the adsorbent surface through chemical bonds or physical forces.

Additionally, it was deduced that the rate of adsorption is dependent on EMT, IPD as well as on the surface reaction. This can be investigated further by testing the effect of different sized adsorbent beads on the rate of adsorption. Should the rate of adsorption change when varying the size of the adsorbent beads, diffusion is likely to be rate-limiting. The data can also be modelled with diffusion-chemisorption models.

8.2.3 Adsorption Modelling

As shown, the multicomponent isotherm models investigated provided relatively poor correlation of the data. It can be recommended that further work be done on these models in order to develop them to more accurately describe the competitive nature of the adsorption systems investigated.

References

[1] T. F. Tadros, *Surfactants*. London: Academic Press, 1984.

[2] R. Azarmi and A. Ashjaran, "Type and application of some common surfactants," *J. Chem. Pharm. Res.*, vol. 7, no. 2, pp. 632–640, 2015.

[3] M. K. Patel, A. Theiss, and E. Worrell, "Surfactant production and use in Germany: resource requirements and CO2 emissions," in *Resources, Conservation and Recycling*, vol. 25, Siegen, Germany, 1999, pp. 61–78.

[4] L. L. Schramm, E. N. Stasiuk, and D. G. Marangoni, "Surfactants and their applications," *Annu. Reports Prog. Chem. (Section C) Phys. Chem.*, vol. 99, pp. 3–48, 2003.

[5] H. Bahrmann, H. Bach, and G. D. Frey, "Oxo Synthesis," *Ullmann's Encycl. Ind. Chem.*, 2013.

[6] D. A. McKenzie, "Nonionic Surfactants," *J. Am. Oil Chem. Soc.*, vol. 55, no. 1, pp. 93–97, 1978.

[7] J. D. Seader, E. J. Henley, and D. K. Roper, *Separation Process Principles*, 3rd ed. USA: John Wiley & Sons, Inc., 2011.

[8] J. Groenewald, "Evaluation and comparison of the ability of three industrially relevant adsorbents to remove alcohol contaminants from an alkane solvent," University of Stellenbosch, Stellenbosch, 2019.

[9] W. Guojie, L. Shengbin, S. De Feyter, R. Feldman, J. E. Parker, and S. M. Clarke, "Behavior of binary alcohol mixtures adsorbed on graphite using calorimetry and scanning tunneling microscopy," *Langmuir*, vol. 24, no. 6, pp. 2501–2508, 2008.

[10] E. Worch, *Adsorption technology in water treatment: Fundamentals, processes, and modeling*. Berlin: Walter de Gruyter & Co, 2012.

[11] Y. Artioli, "The Chemistry of Adsorption," *Ecol. Process.*, pp. 60–65, 2008.

[12] H. S. Fogler, *Elements of chemical reaction engineering*, 4th ed. London: Pearson Education Limited, 2014.

[13] L. Largitte and R. Pasquier, "A review of the kinetics adsorption models and their application to the adsorption of lead by an activated carbon," *Chem. Eng. Res. Des.*, vol. 109, pp. 495–504, 2016.

[14] Y. A. Cengel and A. J. Ghajar, *Heat and Mass Transfer: Fundamentals & Application*, 5th ed. New York, NY: McGraw-Hill Education, 2015.

[15] R. Leyva-Ramos and C. J. Geankoplis, "Diffusion in liquid-filled pores of activated carbon," *Can. J. Chem. Eng.*, vol. 72, no. 2, pp. 262–271, 1994.

[16] T. S. Y. Choong, T. N. Wong, T. G. Chuah, and A. Idris, "Film-pore-concentration-dependent surface diffusion model for the adsorption of dye onto palm kernel shell activated carbon," *J. Colloid Interface Sci.*, vol. 301, no. 2, pp. 436–440, 2006.

[17] H. Komiyama and J. M. Smith, "Surface diffusion in liquid-filled pores," *AIChE J.*, vol. 20, no. 6, pp. 1110–1117, 1974.

[18] C. Tien, *Adsorption Calculations and Modeling*. Newton: Butterworth-Heineman, 1994.

[19] M. Suzuki, *Adsorption Engineering*, vol. 25. Amsterdam, Oxford, New York & Tokyo: Kodansha Ltd. & Elsevier Science Publishers, 1990.

[20] D. D. Do, *Adsorption Analysis: Equilibria and Kinetics*, 2nd ed. London: Imperial College Press, 1998.

[21] H. Tamon, M. Okazaki, and R. Toei, "Flow mechanism of adsorbate through porous media in presence of capillary condensation," *AIChE J.*, vol. 27, no. 2, pp. 271–277, 1981.

[22] D. M. Ruthven, "Physical Adsorption and the Characterization of Porous Adsorbents," in *Principles of Adsorption and Adsorption Processes*, vol. 19, John Wiley & Sons, Inc., 1984.

[23] E. F. Mohamed, "Removal of organic compounds from water by adsorption and photocatalytic oxidation," University of Toulouse, Toulouse, 2011.

[24] H. Marsh, *Activated Carbon*, 1st ed. Amsterdam: Elsevier Science & Technology, 2007.

[25] K. S. W. Sing *et al.*, "Reporting physisorption data for gas/solid systems wih special reference to the determination of surface area and porosity," *Pure Appl. Chem.*, vol. 57, p. 603, 1985.

[26] H. P. Boehm, "Some aspects of the surface chemistry of carbon blacks and other carbons," *Carbon N. Y.*, vol. 32, no. 5, pp. 759–769, 1994.

[27] K. Davis, "Material Review: Alumina (Al2O3)," *Sch. Dr. Stud. Eur. Union J.*, pp. 109–114, 2010.

[28] R. H. Doremus *et al.*, *Ceramic and Glass Materials*. New York, NY: Springer Science & Business Media, LLC, 2008.

[29] J. H. Bowen, R. Bowrey, and A. S. Malin, "A study of the surface area and structure of activated alumina by direct observation," *J. Catal.*, vol. 7, no. 3, pp. 209–216, 1967.

[30] H. Abou-Ziyan, D. Abd El-Raheim, O. Mahmoud, and M. Fatouh, "Performance characteristics of thin-multilayer activated alumina bed," *Appl. Energy*, vol. 190, pp. 29–42, 2017.

[31] J. Biswas, D. D. Do, P. F. Greenfield, and J. M. Smith, "Evaluation of bidisperse transport properties of a reforming catalyst using a diffusion cell," *Appl. Catal.*, vol. 32, no. C, pp. 217–234, 1987.

[32] R. T. Yang, *Adsorbents: Fundamentals and Applications*. New Jersey: John Wiley & Sons, Inc., 2003.

[33] BASF, "F-220, Activated Alumina for Liquid and Gas Drying: data sheet," 2009.

[34] BASF, "Selexsorb CDx, Alumina-based spherical adsorbent for the removal of polar compounds: data

sheet," 2009.

[35] BASF, "Selexsorb CD, Smooth spherical adsorbent for the removal of polar compounds: data sheet," 2009.

[36] R. Gopalan, D. Venkappayya, and S. Nagarajan, *Textbook of Engineering Chemistry*, 4th ed. New Delhi, India: VIKAS Publishing House Pvt Ltd, 2013.

[37] C. T. Hsieh and H. Teng, "Influence of mesopore volume and adsorbate size on adsorption capacities of activated carbons in aqueous solutions," *Carbon N. Y.*, vol. 38, no. 6, pp. 863–869, 2000.

[38] C. R. Girish, "Various Isotherm Models for Multicomponent Adsorption : a Review," *Int. J. Civ. Eng. Technol.*, vol. 8, no. 10, pp. 80–86, 2017.

[39] F. Wang, Y. Pan, P. Cai, T. Guo, and H. Xiao, "Single and binary adsorption of heavy metal ions from aqueous solutions using sugarcane cellulose-based adsorbent," *Bioresour. Technol.*, vol. 241, pp. 482–490, 2017.

[40] J. Moreno-Pérez, A. Bonilla-Petriciolet, C. J. Durán-Valle, R. Tovar-Gómez, M. del R. Moreno-Virgen, and V. Hernández-Montoya, "Analysis of synergistic and antagonistic adsorption of heavy metals and acid blue 25 on activated carbon from ternary systems," *Chem. Eng. Res. Des.*, vol. 93, pp. 755–772, 2014.

[41] F. Clegg, C. Breen, and Khairuddin, "Synergistic and competitive aspects of the adsorption of Poly (ethylene glycol) and Poly (vinyl alcohol) onto Na- Bentonite Synergistic and Competitive Aspects of the Adsorption of Poly (ethylene glycol) and Poly (vinyl alcohol) onto Na-Bentonite," *J. Phys. Chem. B*, vol. 118, no. 46, pp. 13268–13278, 2014.

[42] E. Fu, P. Somasundaran, and C. Maltesh, "Hydrocarbon and alcohol effects on sulfonate adsorption on alumina," *Colloids Surfaces A Physicochem. Eng. Asp.*, vol. 112, no. 1, pp. 55–62, 1996.

[43] I. Langmuir, "The adsorption of gases on plane surfaces of glass, mica and platinum," *J. Am. Chem. Soc.*, vol. 40, no. 9, pp. 1361–1403, 1918.

[44] H. M. F. Freundlich, "Over the adsorption in solution," *J. Phys. Chem.*, vol. 57, pp. 385–470, 1906.

[45] M. S. Podder and C. B. Majunder, "Studies on removal of As(III) and As(V) through their adsorption onto granular activated carbon/MnFe2O4 composite: isotherm studies and error analysis," *Compos. Interfaces*, vol. 23, no. 4, pp. 327–372, 2016.

[46] P. D. Húmpola, H. S. Odetti, A. E. Fertitta, and J. L. Vicente, "Thermodynamic analysis of adsorption models of phenol in liquid phase on different activated carbons," *J. Chil. Chem. Soc.*, vol. 58, no. 1, pp. 1541–1544, 2013.

[47] R. Sips, "Combined form of Langmuir and Freundlich equations," *J. Phys. Chem.*, vol. 16, pp. 490–495,

1948.

[48] S. N. C. Ramos *et al.*, "Modeling mono- and multi-component adsorption of cobalt(II), copper(II), and nickel(II) metal ions from aqueous solution onto a new carboxylated sugarcane bagasse," *Ind. Crops Prod.*, vol. 74, pp. 357–371, 2015.

[49] D. D. Do and R. G. Rice, "Applicability of the external-diffusion model in adsorption studies," *Chem. Eng. Sci.*, vol. 45, no. 5, pp. 1419–1421, 1990.

[50] O. Redlich and D. L. Peterson, "A useful adsorption isotherm," *J. Phys. Chem.*, vol. 63, pp. 1024–1026, 1959.

[51] N. Ayawei, A. N. Ebelegi, and D. Wankasi, "Review Article: Modelling and Interpretation of Adsorption Isotherms," *J. Chem.*, vol. 2017, 2017.

[52] R. Desai, M. Hussain, and D. M. Ruthven, "Adsorption of Water Vapor on Activated Alumina," *Can. J. Chem. Eng.*, vol. 70, pp. 699–706, 1992.

[53] K. Kotoh, M. Enouda, T. Matsui, and M. Nishikawa, "A Multilayer Model for Adsorption of Water on Activated Alumina in Relation to Adsorption Potential," *J. Chem. Eng.*, vol. 26, pp. 335–360, 1993.

[54] A. Srivastav and V. C. Srivastava, "Adsorptive desulfurization by activated alumina," *J. Hazard. Mater.*, vol. 170, no. 2–3, pp. 1133–1140, 2009.

[55] S. Ghorai and K. K. Pant, "Equilibrium, kinetics and breakthrough studies for adsorption of fluoride on activated alumina," *Sep. Purif. Technol.*, vol. 42, no. 3, pp. 265–271, 2005.

[56] T. F. Lin and J. K. Wu, "Adsorption of arsenite and arsenate within activated alumina grains: Equilibrium and kinetics," *Water Res.*, vol. 35, no. 8, pp. 2049–2057, 2001.

[57] T. S. Singh and K. K. Pant, "Equilibrium, kinetics and thermodynamic studies for adsorption of As(III) on activated alumina," *Sep. Purif. Technol.*, vol. 36, no. 2, pp. 139–147, 2004.

[58] S. Guo *et al.*, "A concurrent approach for process design and multicomponent adsorption modeling with local isotherms," *Chem. Eng. Sci.*, vol. 171, pp. 426–439, 2017.

[59] M. Turabik, "Adsorption of basic dyes from single and binary component systems onto bentonite: Simultaneous analysis of Basic Red 46 and Basic Yellow 28 by first order derivative spectrophotometric analysis method," *J. Hazard. Mater.*, vol. 158, no. 1, pp. 52–64, 2008.

[60] V. M. Gun'ko, "Competitive adsorption," *Theor. Exp. Chem.*, vol. 43, no. 3, pp. 139–183, 2007.

[61] E. C. Markham and A. F. Benton, "The Adsorption of Gas Mixtures by Silica," *J. Am. Chem. Soc.*, vol. 53, no. 2, pp. 497–507, 1931.

[62] A. Kurniawan, H. Sutiono, N. Indraswati, and S. Ismadji, "Removal of basic dyes in binary system by adsorption using rarasaponin-bentonite: Revisited of extended Langmuir model," *Chem. Eng. J.*, vol.

189–190, pp. 264–274, 2012.

[63] M. Ilić, D. Flockerzi, and A. Seidel-Morgenstern, "A thermodynamically consistent explicit competitive adsorption isotherm model based on second-order single component behaviour," *J. Chromatogr. A*, vol. 1217, no. 14, pp. 2132–2137, 2010.

[64] D. E. Wurster, K. A. Alkhamis, and L. E. Matheson, "Prediction of adsorption from multicomponent solutions by activated carbon using single-solute parameters," *Am. Assoc. Pharm. Sci.*, vol. 1, no. 3, p. E25, 2000.

[65] S. J. Allen, G. Mckay, and J. F. Porter, "Adsorption isotherm models for basic dye adsorption by peat in single and binary component systems," *J. Colloid Interface Sci.*, vol. 280, pp. 322–333, 2004.

[66] D. B. Broughton, "Adsorption isotherms for binary gas mixtures," *J. Ind. Eng. Chem.*, vol. 40, no. 8, pp. 1506–1508, 1948.

[67] B. G. Lim, C. B. Ching, and R. B. H. Tan, "Determination of competitive adsorption isotherms of enantiomers on a dual-site adsorbent," *Separations Technology*, vol. 5, no. 4. pp. 213–228, 1995.

[68] Q. Liu and Y. Gao, "Binary adsorption isotherm and kinetics on debittering process of ponkan (Citrus reticulata Blanco) juice with macroporous resins," *LWT - Food Sci. Technol.*, vol. 63, no. 2, pp. 1245–1253, 2015.

[69] F. E. Soetaredjo, S. Ismadji, S. P. Santoso, O. L. Ki, A. Kurniawan, and Y. H. Ju, "Recovery of catechin and epicatechin from sago waste effluent: Study of kinetic and binary adsorption isotherm studies," *Chem. Eng. J.*, vol. 231, pp. 406–413, 2013.

[70] A. P. Mathews, "Mathematical Modelling of Multicomponent Adsorption in Batch Reactors," University of Michigan, 1975.

[71] V. C. Srivastava, I. D. Mall, and I. M. Mishra, "Equilibrium modelling of single and binary adsorption of cadmium and nickel onto bagasse fly ash," *Chem. Eng. J.*, vol. 117, pp. 79–91, 2006.

[72] K. K. H. Choy, J. F. Porter, and G. McKay, "Langmuir isotherm models applied to the multicomponent sorption of acid dyes from effluent onto activated carbon," *J. Chem. Eng. Data*, vol. 45, no. 4, pp. 575–584, 2000.

[73] W. Fritz and E. U. Schlunder, "Simultaneous adsorption equilibria of organic solutes in dilute aqueous solutions on activated carbon," *Chem. Eng. Sci.*, vol. 29, p. 1279, 1974.

[74] W. Plazinski, J. Dziuba, and W. Rudzinski, "Modeling of sorption kinetics: The pseudo-second order equation and the sorbate intraparticle diffusivity," *Adsorption*, vol. 19, no. 5, pp. 1055–1064, 2013.

[75] R. K. Khamizov, D. A. Sveshnikova, A. E. Kucherova, and L. A. Sinyaeva, "Kinetic Models of Batch Sorption in a Limited Volume," *Russ. J. Phys. Chem. A*, vol. 92, no. 9, pp. 1782–1789, 2018.

[76] J. P. Simonin, "On the comparison of pseudo-first order and pseudo-second order rate laws in the modeling of adsorption kinetics," *Chem. Eng. J.*, vol. 300, pp. 254–263, 2016.

[77] H. Qiu, L. Lv, B. Pan, Q. Zhang, W. Zhang, and Q. Zhang, "Critical review in adsorption kinetic models *," *J. Zheijang Univ. Sci. A*, vol. 10, no. 5, pp. 716–724, 2009.

[78] S. Azizian, "Kinetic models of sorption: A theoretical analysis," *J. Colloid Interface Sci.*, vol. 276, no. 1, pp. 47–52, 2004.

[79] Y. S. Ho, "Review of second-order models for adsorption systems," *J. Hazard. Mater.*, vol. 136, no. 3, pp. 681–689, 2006.

[80] R. Leyva-Ramos, R. Ocampo-Pérez, J. V. Flores-Cano, and E. Padilla-Ortega, "Comparison between diffusional and first-order kinetic model, and modeling the adsorption kinetics of pyridine onto granular activated carbon," *Desalin. Water Treat.*, vol. 55, no. 3, pp. 637–646, 2015.

[81] S. Lagergren, "Zur Theorie der sogenannten Adsorption geloster Stoffe," *Chem. Eng. J.*, vol. 24, pp. 1–39, 1898.

[82] Y. S. Ho and G. McKay, "Pseudo-second order model for sorption processes," *Process Biochem.*, vol. 34, no. 5, pp. 451–465, 1999.

[83] Y. S. Ho, "Adsorption of Heavy Metals from Waste Streams by Peat," University of Birmingham, Birmingham UK, 1995.

[84] M. A. Al-Ghouti, M. A. M. Khraisheh, M. N. M. Ahmad, and S. Allen, "Adsorption behaviour of methylene blue onto Jordanian diatomite: A kinetic study," *J. Hazard. Mater.*, vol. 165, no. 1–3, pp. 589–598, 2009.

[85] A. G. Ritchie, "Alternative to the Elovich equation for the kinetics of adsorption of gases on solids," *J. Chem. Soc.*, vol. 73, pp. 1650–1653, 1977.

[86] Y. B. Zeldovich, "The oxidation of nitrogen in combustion and explosions," *Acta Physicochim.*, pp. 577–628, 1946.

[87] D. E. P. Sumalapao, J. R. Distor, N. Villarante, I. Ditan, N. T. Domingo, and L. F. Dy, "An error analysis on the biosorption kinetic models of biowaste adsorbent in an aqueous solution," *J. Math. Comput. Sci.*, vol. 6, no. 6, pp. 1157–1168, 2016.

[88] W. Rudzinski and W. Plazinski, "Kinetics of solute adsorption at solid/solution interfaces: A theoretical development of the empirical pseudo-first and pseudo-second order kinetic rate equations, based on applying the statistical rate theory of interfacial transport," *J. Phys. Chem. B*, vol. 110, no. 33, pp. 16514–16525, 2006.

[89] W. J. Weber and J. C. Morris, "Kinetics of Adsorption on Carbon from Solution," *J. Sanit. Eng. Div.*, vol.

89, no. 2, pp. 31–60, 1963.

[90] N. M. Mahmoodi, R. Salehi, and M. Arami, "Binary system dye removal from colored textile wastewater using activated carbon: Kinetic and isotherm studies," *Desalination*, vol. 272, no. 1–3, pp. 187–195, 2011.

[91] G. W. Kajjumba, S. Emik, A. Ongen, H. K. Ozcan, and S. Aydin, "Modelling of Adsorption Kinetic Processes - Errors, Theory and Application," *IntechOpen*, 2018. .

[92] V. Fierro, V. Torné-Fernández, D. Montané, and A. Celzard, "Adsorption of phenol onto activated carbons having different textural and surface properties," *Microporous Mesoporous Mater.*, vol. 111, no. 1–3, pp. 276–284, 2008.

[93] F. C. Wu, R. L. Tseng, and R. S. Juang, "Initial behavior of intraparticle diffusion model used in the description of adsorption kinetics," *Chem. Eng. J.*, vol. 153, no. 1–3, pp. 1–8, 2009.

[94] W. H. Cheung, Y. S. Szeto, and G. McKay, "Intraparticle diffusion processes during acid dye adsorption onto chitosan," *Bioresour. Technol.*, vol. 98, no. 15, pp. 2897–2904, 2007.

[95] N. Gandhi, D. Sirisha, and K. B. C. Sekhar, "Adsorption of Fluoride (F -) from Aqueous Solution by Using Pineapple (Ananas comosus) Peel and Orange (Citrus sinensis) Peel Powders," *Int. J. Bioremediation Biodegrad.*, vol. 4, no. 2, pp. 55–67, 2016.

[96] G. McKay, M. S. Otterburn, and A. G. Sweeney, "The removal of colour from effluent using various adsorbents," *Water Res.*, vol. 14, no. 1, pp. 15–20, 1980.

[97] H. M. Asfour, O. A. Fadali, M. M. Nassar, and M. S. El-Geundi, "Equilibrium studies on adsorption of basic dyes on hardwood," *J. Chem. Technol. Biotechnol.*, vol. 35 A, no. 1, p. 28, 1985.

[98] M. B. Desta, "Batch Sorption Experiments: Langmuir and Freundlich Isotherm Studies for the Adsorption of Textile Metal Ions onto Teff Straw (Eragrostis tef) Agricultural Waste," *J. Thermodyn.*, 2013.

[99] A. Regti, A. El Kassimi, M. R. Laamari, and M. El Haddad, "Competitive adsorption and optimization of binary mixture of textile dyes: A factorial design analysis," *J. Assoc. Arab Univ. Basic Appl. Sci.*, vol. 24, pp. 1–9, 2017.

[100] G. Atun and E. T. Acar, "Competitive adsorption of basic dyes onto calcite in single and binary component systems," *Sep. Sci. Technol.*, vol. 45, no. 10, pp. 1471–1481, 2010.

[101] IUPAC, "Recommendations for the characterization of porous solids," *Pure Appl. Chem.*, vol. 66, no. 8, pp. 1739–1758, 1994.

[102] S. Mtaallah, I. Marzouk, and B. Hamrouni, "Factorial experimental design applied to adsorption of cadmium on activated alumina," *J. Water Reuse Desalin.*, vol. 8, no. 1, pp. 76–85, 2017.

[103] S. Cai and K. Sohlberg, "Adsorption of alcohols on γ-alumina (110 C)," *J. Mol. Catal. A Chem.*, vol. 193, no. 1–2, pp. 157–164, 2003.

[104] R. -S Zhou and R. L. Snyder, "Structures and transformation mechanisms of the η, γ and θ transition aluminas," *Acta Crystallogr. Sect. B*, vol. 47, pp. 617–630, 1991.

[105] N. Özbay, A. Ş. Yargiç, R. Z. Yarbay-Şahin, and E. Önal, "Full factorial experimental design analysis of reactive dye removal by carbon adsorption," *J. Chem.*, vol. 2013, pp. 1–13, 2013.

[106] L. E. Hernández-Hernández, A. Bonilla-Petriciolet, D. I. Mendoza-Castillo, and H. E. Reynel-Ávila, "Antagonistic binary adsorption of heavy metals using stratified bone char columns," *J. Mol. Liq.*, vol. 241, pp. 334–346, 2017.

[107] D. R. Lin, L. J. Hu, B. S. Xing, H. You, and D. A. Loy, "Mechanisms of competitive adsorption organic pollutants on hexylene-bridged polysilsesquioxane," *Materials (Basel).*, vol. 8, no. 9, pp. 5806–5817, 2015.

[108] K. Yang, W. H. Wu, Q. F. Jing, W. Jiang, and B. S. Xing, "Competitive adsorption of naphthalene with 2,4-dichlorophenol and 4-chloroaniline on multiwalled carbon nanotubes," *Environ. Sci. Technol.*, vol. 44, pp. 3021–3027, 2010.

[109] K. V. Kumar, K. Porkodi, and F. Rocha, "Comparison of various error functions in predicting the optimum isotherm by linear and non-linear regression analysis for the sorption of basic red 9 by activated carbon," *J. Hazard. Mater.*, vol. 150, no. 1, pp. 158–165, 2008.

[110] B. Subramanyam and A. Das, "Linearised and non-linearised isotherm models optimization analysis by error functions and statistical means," *J. Environ. Heal. Sci. Eng.*, vol. 92, no. 12, 2014.

[111] W. Plazinski and W. Rudzinski, "Kinetics of adsorption at solid/Solution interfaces controlled by intraparticle diffusion: A theoretical analysis," *J. Phys. Chem. C*, vol. 113, no. 28, pp. 12495–12501, 2009.

[112] J. Simonin and J. Boute´, "Intraparticle diffusion-adsorption model to describe liquid / solid adsorption kinetics," *Rev. Mex. Ing. Quim.*, vol. 15, no. 1, pp. 161–173, 2016.

[113] JCGM/WG 1, *Evaluation of measurement data — Guide to the expression of uncertainty in measurement*. 2008.

[114] D. H. Everett, "Manual of Symbol and Terminology for Physico-chemical Quantities and Units, Appendix, Definitions, Terminology and Symbols in Colloid and Surface Chemistry," in *Pure & Appl. Chem.*, vol. 31, no. 4, 1972, p. 579.

[115] R. Brewer, *Fabric and Mineral analysis of Soils*. New York: John Wiley & Sons, 1964.

[116] J. Rouquerol *et al.*, "Recommendations for the characterization of porous solids," *Pure Appl. Chem.*,

vol. 66, no. 8, pp. 1739–1758, 1994.

[117] B. D. Zdravkov, J. J. Čermák, M. Šefara, and J. Janků, "Pore classification in the characterization of porous materials: A perspective," *Cent. Eur. J. Chem.*, vol. 5, no. 2, pp. 385–395, 2007.

Appendix A: Materials & Methods

Appendix Contents

A.1 Experimental Design

A.1.1 Preliminary Experiments to Determine the Time of Equilibrium

Experimental runs were conducted to determine the time required for the system to reach equilibrium. A known amount (10 g) of adsorbent was added to each respective alcohol-alkane system and samples were taken at different time stamps for a total of 30 hours (Figure A.1-1). Between 390 minutes and 1800 minutes, a slight change of 3.85, 1.27 and 1.75 mg/g was observed in the adsorbent loading for 1-decanol, 1-octanol and 1-hexanol respectively. These changes however were very small in comparison to the rapid changes at the start of the runs and within the average uncertainty of 3.83 mg/g. The changes were therefore considered insignificant. For the purposes of this study, equilibrium was assumed to be at approximately 23 hours and 30 minutes. As shown in Figure A.1-1, however, equilibrium seems to have been reached before 23 hours.

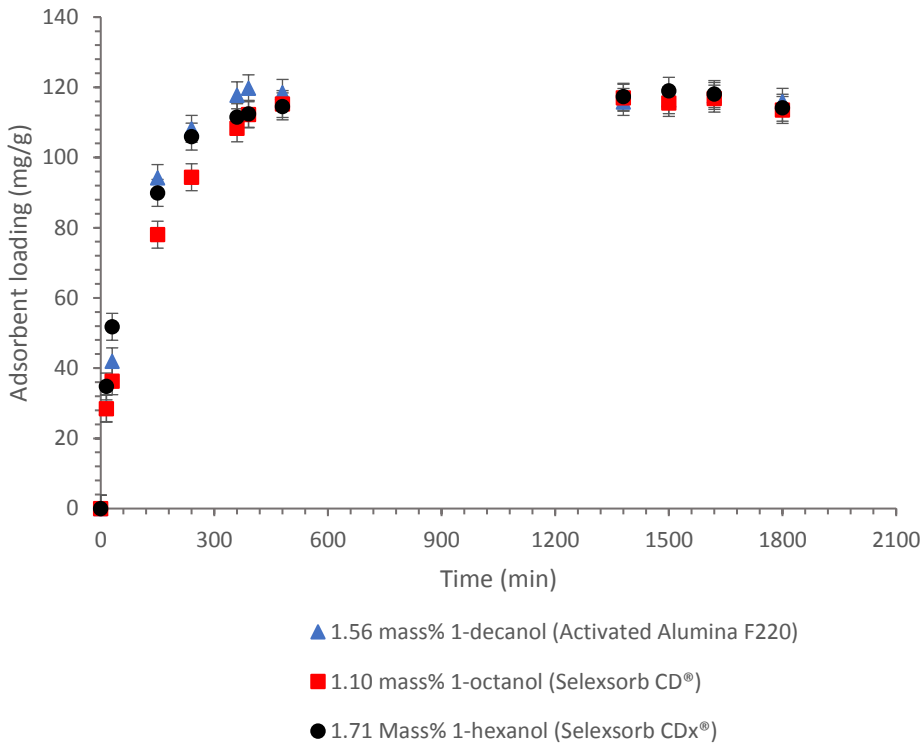

Figure A.1-1: Preliminary equilibrium experiments (T = 45°C)

A.1.2 Experimental Procedure

A.1.2.1 *Kinetic Adsorption Experiments*

1. Set the temperature of the water bath to specified temperature.
2. Add magnetic stirrer to 500ml beaker.
3. Weigh beaker containing magnetic stirrer.
4. Record weight.
5. Prepare alcohol-alkane solution by adding known amount of alcohol (1-hexanol, 1-octanol, 1-decanol) to the n-decane solvent.
6. Add 200ml of alcohol-alkane solution to 500ml beaker.
7. Weigh beaker containing alkane solvent and magnetic stirrer.
8. Record weight.
9. Be sure that the magnetic stirring plate is installed underneath the water bath and that enough water remains inside the bath.
10. Immerse beakers containing alcohol-alkane solution in water-bath.
11. Close lid of water-bath.
12. Switch on magnetic stirring plate and start stirring to the chosen speed (350 rpm).
13. Allow alcohol-alkane solutions to heat up to desired temperature.
14. While alcohol-alkane solutions are heating up inside the water-bath, weigh adsorbent mesh baskets.
15. Record weight.
16. Add a measured amount (10g) of the specific adsorbent (Selexsorb CDx®, Selexsorb CD®, Activated Alumina F220) to the adsorbent mesh baskets.
17. Measure temperature of alcohol-alkane solutions.
18. When alcohol-alkane solutions are at the desired temperature, lower adsorbent mesh baskets into the solutions.
19. Record time of first contact between adsorbent and alcohol-alkane solution.
20. Close lid of water-bath.
21. Allow beakers containing the alcohol-alkane solution to remain in the water bath while sampling at 0, 15, 30, 150, 240, 360, 480, 1380, 1395 and 1410 minutes. Sampling is done with a pipette and sample size is 200µL.
22. Transfer samples of the alcohol-alkane solution into dedicated 2 mL containers.
23. Mark each of the different containers accordingly.
24. After last sample, switch off water-bath and magnetic stirring plate.
25. Open lid of water-bath.
26. Remove adsorbent mesh baskets from water-bath.

27. Weigh each respective adsorbent mesh basket.
28. Record weight.
29. Remove beakers with remaining alcohol-alkane solution and dry the outside of the beakers.
30. Weigh each respective beaker containing alcohol-alkane solution and magnetic stirrer bar.
31. Record weight.
32. Transfer remaining alcohol-alkane solutions from beakers to Schott bottles.
33. Mark each of the different containers accordingly.
34. Discard spent adsorbent to designated containers.

A.1.2.2 *Equilibrium Adsorption Experiments*

1. Set the temperature of the water bath to specified temperature.
2. Add magnetic stirrer to 500ml beaker.
3. Weigh beaker containing magnetic stirrer.
4. Record weight.
5. Prepare alcohol-alkane solution by adding known amount of alcohol (1-hexanol, 1-octanol, 1-decanol) to the n-decane solvent.
6. Add 200ml of alcohol-alkane solution to 500ml beaker.
7. Weigh beaker containing alkane solvent and magnetic stirrer.
8. Record weight.
9. Be sure that the magnetic stirring plate is installed underneath the water bath and that enough water remains inside the bath.
10. Immerse beakers containing alcohol-alkane solution in water-bath.
11. Close lid of water-bath.
12. Switch on magnetic stirring plate and start stirring to the chosen speed (350 rpm).
13. Allow alcohol-alkane solutions to heat up to desired temperature.
14. While alcohol-alkane solutions are heating up inside the water-bath, weigh adsorbent mesh baskets.
15. Record weight.
16. Add a measured amount (10g) of the specific adsorbent (Selexsorb CDx®, Selexsorb CD®, Activated Alumina F220) to the adsorbent mesh baskets.
17. Measure temperature of alcohol-alkane solutions.
18. When alcohol-alkane solutions are at the desired temperature, lower adsorbent mesh baskets into the solutions.
19. Record time of first contact between adsorbent and alcohol-alkane solution.
20. Close lid of water-bath.

21. Allow beakers containing the alcohol-alkane solution to remain in the water bath while sampling at 0, 1380, 1395 and 1410 minutes. Sampling is done with a pipette and sample size is 200µL.
22. Transfer samples of the alcohol-alkane solution into dedicated 2 mL containers.
23. Mark each of the different containers accordingly.
24. After last sample, switch off water-bath and magnetic stirring plate.
25. Open lid of water-bath.
26. Remove adsorbent mesh baskets from water-bath.
27. Weigh each respective adsorbent mesh basket.
28. Record weight.
29. Remove beakers with remaining alcohol-alkane solution and dry the outside of the beakers.
30. Weigh each respective beaker containing alcohol-alkane solution and magnetic stirrer bar.
31. Record weight.
32. Transfer remaining alcohol-alkane solutions from beakers to Schott bottles.
33. Mark each of the different containers accordingly.
34. Discard spent adsorbent to designated containers.

A.1.3 Procedure for Gas Chromatography Calibration

1. Add specified volume, *i.e*. 10µL, 20µL, 30µL *etc.*, of each of the components (1-hexanol, 1-octanol, 1-decanol and n-decane) to be analysed by the GC to a 2mL sample vial.
2. Accurately weigh the mass of each of the different components and record.
3. Add specified volume (30µL) of internal standard (1-pentanol) using a pipette.
4. Accurately weigh the mass of the internal standard and record.
5. Fill the 2mL vial with solvent (methanol) using a pipette.
6. Accurately weigh the mass of the solvent and record.
7. Use the vortex to ensure the solution is thoroughly mixed.
8. With a pipette, transfer 200µL of the solution to a second 2mL vial.
9. Weigh the mass of the solution and record.
10. Fill the vial with solvent (methanol).
11. Weigh the mass of the solvent added and record.
12. Use the vortex to ensure the solution is thoroughly mixed.
13. Repeat steps 1-12 for several samples with different compositions of the same components (1-hexanol, 1-octanol, 1-decanol and n-decane).

A.1.4 Gas Chromatography Procedure

A.1.4.1 *Sample Preparation*

1. Accurately weigh sample to be prepared for GC analysis with 5-decimal balance.
2. Record sample weight.
3. Add specified volume (20µL) of internal standard (1-pentanol) to sample, using a pipette.
4. Accurately weigh the mass of the internal standard and record.
5. Fill the 2mL vial with solvent (methanol) using a pipette (approximately 1300 µL).
6. Use the vortex to ensure the solution is thoroughly mixed.
7. With a pipette, transfer 200µL of the solution to a second 2mL vial.
8. Fill the vial with solvent (methanol).
9. Use the vortex to ensure the solution is thoroughly mixed.

A.1.4.2 *Analysis Procedure*

1. Check pressure on the gas cylinder gauges and ensure sufficient flow to the GC.
2. Open gas valves to GC.
3. Switch on GC.
4. Switch on computer.
5. Open software.
6. Load specified method (file, load, method).
7. Wait for method to load and GC system to adjust accordingly.
8. Check that GC needle is loose and not obstructed.
9. Check if detector flame has ignited.
10. Insert blank solvent sample.
11. Do a single run on the blank solvent.
12. Check results to ensure blank sample is clean.
13. Insert samples into GC.
14. Load sequence for sampling.
15. Specify sample positions, sample names, method etc.
16. Run the GC and analyse samples.
17. After completion of the sample analysis, go to data analysis on the software and record all sample concentrations (mass of each component present in the sample).
18. Save the sample data.
19. Load the standby method (File, load, method).
20. Allow GC oven to cool down to approximately 40^{o}C.

21. Switch off GC.
22. Close gas flow to GC.
23. Remove sample vials from GC.

A.1.5 Experimental Setup

(a) (b)

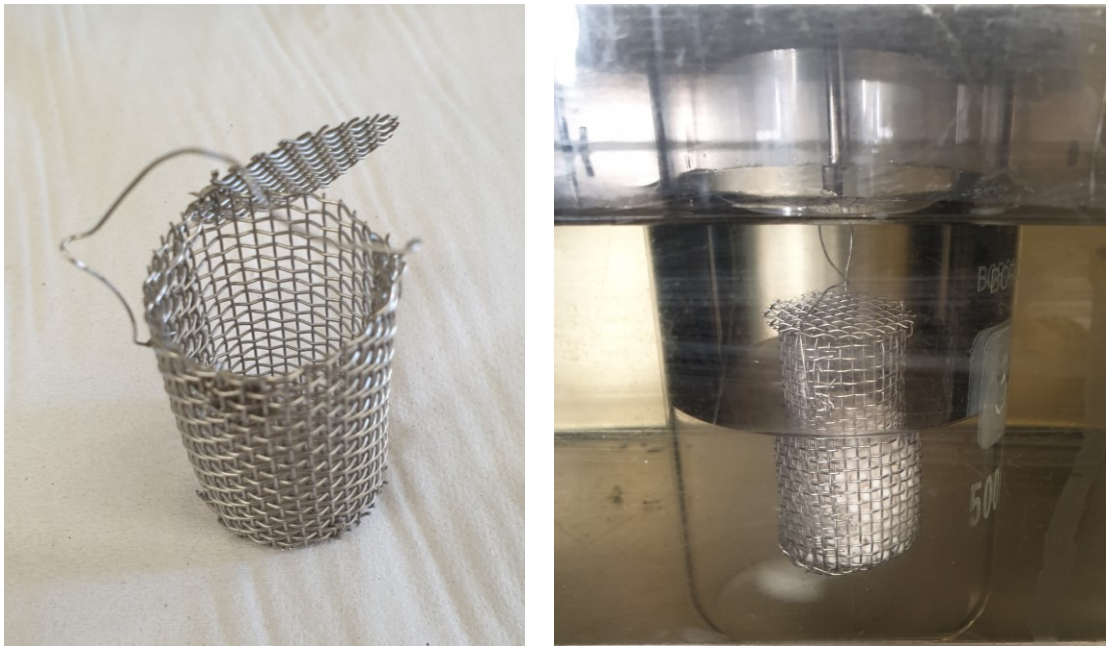

Figure A.1-2: (a) Mesh basket used for adsorbent; (b) Beaker containing alcohol-alkane solution with mesh basket containing adsorbent and magnetic stirrer bar, inside water-bath

Figure A.1-3: Experimental setup

A.2 Reproducibility of Experimental Data

A.2.1 Comparison with Previous Study

An experimental setup similar to the one used by Groenewald was used for the experiments conducted in this study [8]. To ensure that this experimental setup provided accurate data, some experimental runs conducted by Groenewald were repeated to compare the two sets of data. Figure A.2-1 compares the data obtained by Groenewald and the data obtained from this study [8]. These two sets of data were very similar comparatively, with the difference between the two sets within the margin of error which deemed the data obtained by this study reproducible.

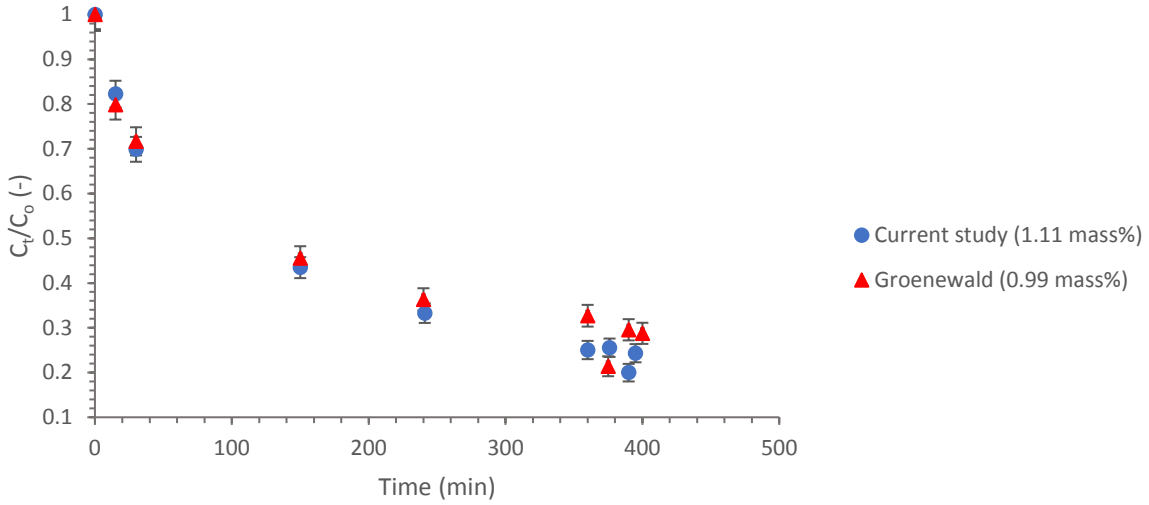

a) Concentration decay plots for the single component adsorption of 1-hexanol onto Selexsorb CDx®

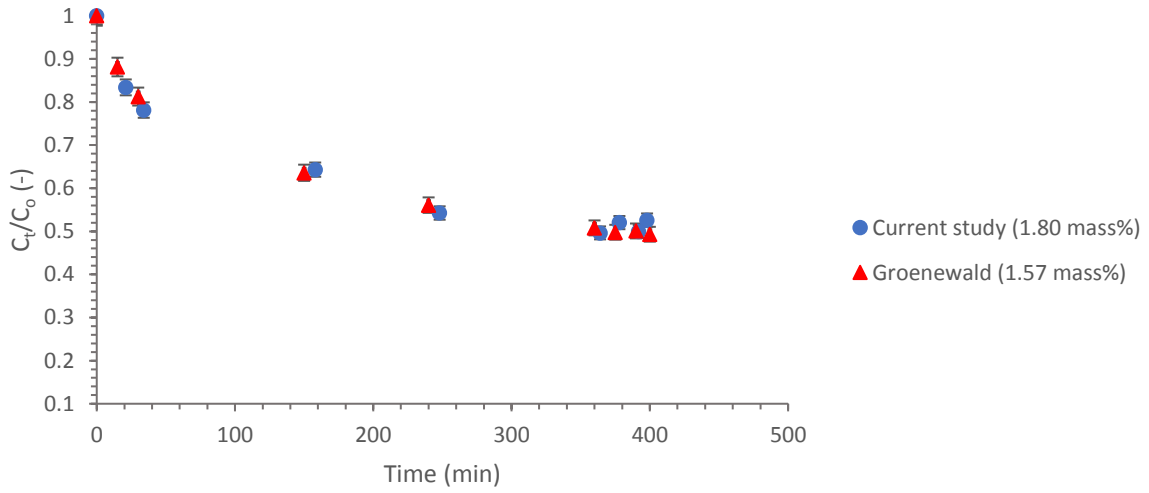

b) *Concentration decay plots for the single component adsorption of 1-octanol onto Activated Alumina F220*

Figure A.2-1: Comparison of concentration decay plots for current study and a study conducted by Groenewald [8] for the single component adsorption of (a) 1-hexanol onto Selexsorb CDx®; and, (b) 1-octanol onto Activated Alumina F220 (T = 35°C; IC as indicated on graphs)

A.2.2 Mixing in the System

When mixing a solution in a beaker by use of a magnetic stirring plate and stirrer bar, a vortex tends to form in the middle of the solution. This results in poor mixing of the solution. When adding the mesh basket containing the adsorbent to the beaker system, the vortex cannot form as the mesh basket impedes the mixing pattern. To determine the efficiency of the mixing, a baffle was designed and inserted into the system to compare the results with a system without baffles (Figure A.2-2).

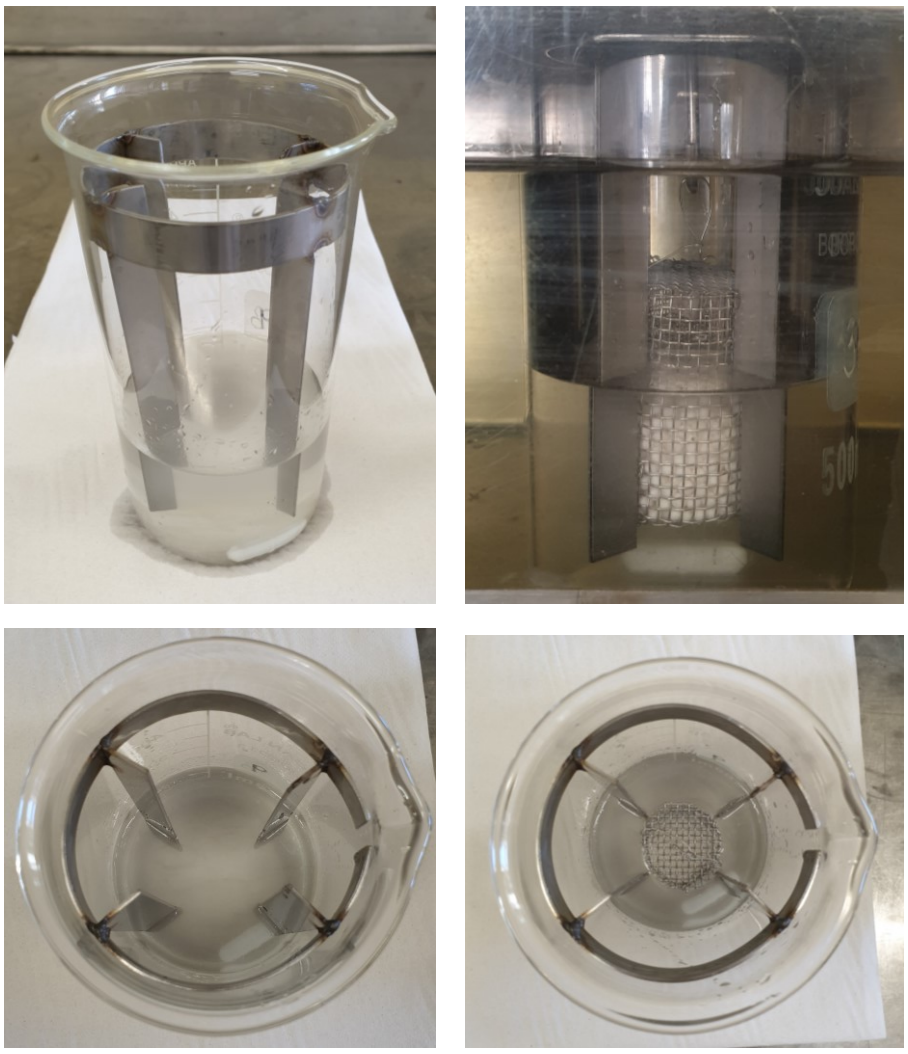

Figure A.2-2: Baffled adsorption system

The baffle is expected to impede the mixing pattern even more than the mesh basket, which should result in more contact time between the adsorbent particles and the solution. Should the equilibrium adsorbent loading of the system with the baffles be greater than the system without the baffles, poor mixing in the system without baffles can be assumed.

From Figure A.2-3 it can be observed that the baffles did not have a significant effect on the equilibrium adsorbent loading of the system. The difference was very small and well within the margin of error, as shown. This suggests that the setup used in this study provided for effective mixing without the baffles, with sufficient contact time between the adsorbent particles and the solution.

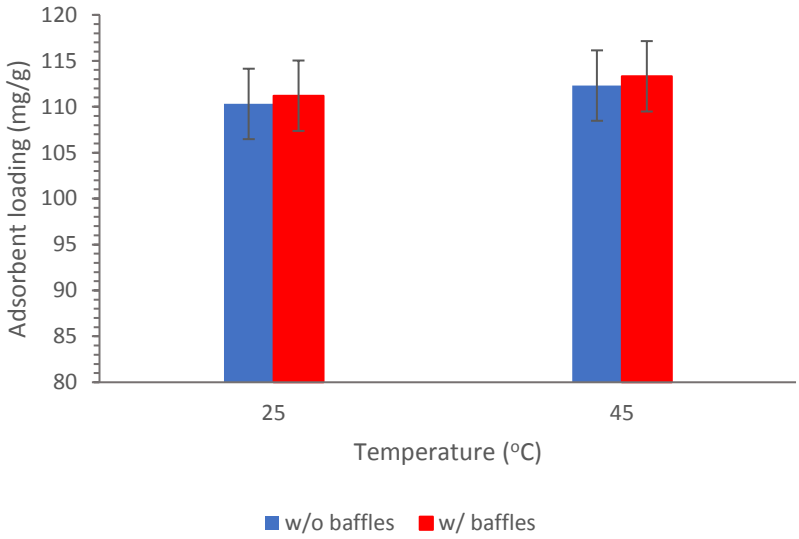

Figure A.2-3: Comparison of the equilibrium adsorbent loading (mg/g) for a system with baffles and a system without baffles

Appendix B: Uncertainty Analysis

Appendix Contents

B.1 Uncertainty Methodology

B.1.1 Measurement Uncertainty

The uncertainty parameter for the measured mass concentrations was determined using the standard error together with the two-tailed student's t-statistic and a significance level of 0.05 (Equation B.1-1).

$$\Delta_y = \pm t(\alpha, n-1)\, S_n \qquad [\text{B.1-1}]$$

Where, Δ_y Uncertainty parameter;

$t(\alpha,n\text{-}1)$ Student's t-statistic;

α Significance level (0.05);

n Number of repeats; and,

S_n Standard error.

The standard error was calculated by use of Equation B.1-2, with *s* denoting the standard deviation.

$$S_n = \frac{s}{\sqrt{n}} \qquad [\text{B.1-2}]$$

The uncertainty in the measured mass concentration however comprised two components: the uncertainty from the measurement of repeat runs as well as the uncertainty from the GC analysis of the samples. The combined uncertainty parameter for the concentration was therefore determined as follows:

$$\Delta_X^2 = \Delta_{X,measurement}^2 + \Delta_{X,analysis}^2 \qquad [\text{B.1-3}]$$

B.1.2 Uncertainty Propagation

In the event of a value being calculated from a direct measurement, the law of error propagation should be applied in order to determine the uncertainty of any consequent calculated value [113]. The propagated uncertainty was determined through a method proposed by The Guide to the Expression of Uncertainty in Measurement (GUM).

The uncertainty in calculated value, *y*, was determined through Equation B.1-4, using derivatives and direct measurement/analysis uncertainties.

$$y = f(X_1, \ldots X_n)$$

$$\Delta_y^2 = \sum_{i=1}^{n} \left(\left(\frac{df}{dX_i} \right) \Delta_{X_i} \right)^2 \qquad [\text{B.1-4}]$$

B.1.3 Sample Calculations

The single component system of 1-hexanol onto SCD (data provided in Table B.2-1) will be used to prove as example of the calculation methodology used to determine the uncertainty of measured values.

The average alcohol concentration was determined using Equation B.1-5.

$$X_{avg} = \frac{X_{run1}+X_{run2}+X_{run3}+X_{run4}+X_{run5}}{n} \qquad [\text{B.1-5}]$$

Therefore, at *t* = 150 min, the average alcohol concentration for this system was calculated to be:

$$X_{avg} = \frac{1.110+1.116+1.136+1.168+1.112}{5} = 1.129\ mass\%$$

After calculating the average concentration for the repeat samples, the standard deviation was calculated using Equation B.1-6.

$$s = \sqrt{\frac{\sum\left(X_{run\,i}-X_{avg}\right)^2}{n-1}} \qquad [\text{B.1-6}]$$

The standard deviation at *t* = 150 min, was therefore:

$$s = \sqrt{\frac{(1.110-1.129)^2+(1.116-1.129)^2+(1.136-1.129)^2+(1.168-1.129)^2+(1.112-1.129)^2}{5-1}} = 0.0244\ mass\%$$

The standard error was determined using Equation B.1-2 as follows:

$$S_n = \frac{s}{\sqrt{n}} = \frac{0.0244}{\sqrt{5}} = 0.0109\ mass\%$$

As mentioned, a significance level of 0.05 was used together with student's t-statistic to determine the uncertainty of the alcohol concentrations. This was done using the Microsoft Excel® statistics package. The measurement uncertainty at *t* = 150 min was therefore determined to be:

$$\Delta_{X,measurement} = \pm t(\alpha, n-1)\, S_n = \pm t\big(0.05, (5-1)\big)(0.0109) = 0.0303\ mass\%$$

Using the GC uncertainty (calculated similarly to be 0.00529 mass%), the combined uncertainty at *t* = 150 min was determined with Equation B.1-3.

$$\Delta_{X,150min} = \sqrt{0.0303^2 + 0.00529^2} = 0.03\ mass\%$$

B.2 Repeatability Data

B.2.1 Single Component System Data

Table B.2-1: Single component repeatability data (1-hexanol onto Selexsorb CD®; T = 25°C)

Time (min)	***Alcohol Concentration (mass%)***				
Run	***1***	***2***	***3***	***4***	***5***
0	1.59	1.59	1.60	1.59	1.59
15	1.40	1.41	1.45	1.40	1.38
30	1.32	1.37	1.31	1.35	1.35
150	1.11	1.12	1.14	1.17	1.11
240	1.00	1.00	1.01	0.98	0.99
360	0.94	0.93	0.92	0.92	0.90
480	0.93	0.91	0.92	0.91	0.90
1380	0.91	0.92	0.92	0.90	0.90
1385	0.90	0.91	0.91	0.90	0.91

B.2.2 Binary Component System Data

Table B.2-2: Binary component repeatability data for a) 1-hexanol; and, b) 1-decanol (1-hexanol + 1-decanol mixture onto Selexsorb CDx®; T = 25°C)

a) Binary repeatability data for 1-hexanol

Time (min)	***Alcohol Concentration (mass%)***				
Run	***1***	***2***	***3***	***4***	***5***
0	0.69	0.69	0.69	0.69	0.70
15	0.62	0.65	0.65	0.63	0.62
30	0.59	0.60	0.59	0.59	0.59
150	0.45	0.45	0.47	0.47	0.49
240	0.40	0.41	0.41	0.42	0.42
360	0.37	0.37	0.38	0.37	0.38
480	0.27	0.29	0.30	0.32	0.30
1380	0.27	0.29	0.30	0.32	0.30
1385	0.27	0.29	0.31	0.31	0.31

b) Binary repeatability data for 1-decanol

Time (min)	***Alcohol Concentration (mass%)***				
Run	***1***	***2***	***3***	***4***	***5***
0	0.97	0.97	0.96	0.96	0.95
15	0.87	0.90	0.90	0.89	0.86
30	0.83	0.88	0.85	0.88	0.87
150	0.73	0.74	0.72	0.75	0.76
240	0.68	0.68	0.63	0.68	0.68
360	0.65	0.65	0.61	0.62	0.64
480	0.50	0.54	0.50	0.51	0.52
1380	0.50	0.54	0.50	0.51	0.52
1385	0.49	0.52	0.49	0.49	0.51

Table B.2-3: Binary component repeatability data for a) 1-hexanol; and, b) 1-octanol (1-hexanol + 1-octanol mixture onto Selexsorb CDx®; T = 25°C)

a) Binary repeatability data for 1-hexanol

Time (min)	***Alcohol Concentration (mass%)***				
Run	***1***	***2***	***3***	***4***	***5***
0	0.89	0.89	0.92	0.92	0.91
15	0.82	0.82	0.84	0.82	0.80
30	0.79	0.81	0.82	0.80	0.77
150	0.67	0.68	0.67	0.67	0.69
240	0.57	0.61	0.57	0.57	0.58
360	0.58	0.59	0.61	0.56	0.57
480	0.49	0.51	0.52	0.50	0.50
1380	0.49	0.51	0.52	0.50	0.50
1385	0.48	0.49	0.51	0.51	0.49

b) Binary repeatability data for 1-octanol

Time (min)	***Alcohol Concentration (mass%)***				
Run	***1***	***2***	***3***	***4***	***5***
0	1.16	1.16	1.14	1.11	1.12
15	1.04	1.02	1.08	1.01	1.04
30	1.01	1.02	1.06	1.00	0.99
150	0.87	0.87	0.89	0.88	0.86
240	0.83	0.82	0.82	0.83	0.83
360	0.80	0.79	0.80	0.80	0.79
480	0.70	0.71	0.72	0.69	0.69
1380	0.70	0.71	0.72	0.69	0.69
1385	0.67	0.67	0.70	0.70	0.68

Table B.2-4: Binary component repeatability data for a) 1-octanol; and, b) 1-decanol (1-octanol + 1-decanol mixture onto Selexsorb CDx®; T = 25°C)

a) Binary repeatability data for 1-octanol

Time (min)	***Alcohol Concentration (mass%)***				
Run	***1***	***2***	***3***	***4***	***5***
0	0.34	0.33	0.32	0.32	0.32
15	0.30	0.27	0.28	0.28	0.28
30	0.27	0.26	0.26	0.26	0.27
150	0.21	0.19	0.19	0.19	0.19
240	0.17	0.16	0.16	0.16	0.15
360	0.16	0.15	0.14	0.14	0.14
480	0.14	0.14	0.13	0.13	0.13
1380	0.14	0.14	0.13	0.13	0.13

b) Binary repeatability data for 1-decanol

Time (min)	***Alcohol Concentration (mass%)***				
Run	***1***	***2***	***3***	***4***	***5***
0	0.52	0.51	0.48	0.49	0.51
15	0.45	0.43	0.46	0.46	0.46
30	0.41	0.41	0.42	0.40	0.42
150	0.32	0.32	0.33	0.32	0.29
240	0.27	0.28	0.27	0.28	0.25
360	0.24	0.25	0.25	0.25	0.23
480	0.22	0.21	0.20	0.22	0.20
1380	0.22	0.21	0.20	0.22	0.20

Appendix C: Experimental Adsorption Data

Appendix Contents

C.1 Kinetic Data

C.1.1 Single Component Systems

C.1.1.1 *Activated Alumina F220*

Table C.1-1: Kinetic data for the single component adsorption of 1-hexanol onto Activated Alumina F220 (T = 45°C)

	Initial Adsorbate Concentration (mass%)					
	0.84		*1.01*		*1.51*	
Time (min)	***Alcohol Concentration (mass%)***	***Alcohol Adsorbent Loading (mg/g)***	***Alcohol Concentration (mass%)***	***Alcohol Adsorbent Loading (mg/g)***	***Alcohol Concentration (mass%)***	***Alcohol Adsorbent Loading (mg/g)***
0	0.84	0.00	1.01	0.00	1.51	0.00
2	0.73	16.4	0.85	23.3	1.42	13.9
15	0.55	43.4	0.77	35.2	1.25	38.6
30	0.49	51.5	0.65	53.4	1.15	53.0
150	0.20	94.2	0.41	88.7	0.88	92.9
240	0.14	103	0.37	93.7	0.82	102
360	0.18	97.4	0.34	98.7	0.78	109
390	0.18	97.2	0.34	98.0	0.78	109
480	0.15	103	0.38	93.1	0.79	107
1380	0.16	99.9	0.35	96.9	0.75	114
1395	0.18	97.8	0.35	97.6	0.77	110
1410	0.22	92.1	0.34	99.4	0.80	106

Table C.1-2: Kinetic data for the single component adsorption of 1-octanol onto Activated Alumina F220 (T = 45°C)

	Initial Adsorbate Concentration (mass%)					
	0.56		*1.04*		*1.61*	
Time (min)	***Alcohol Concentration (mass%)***	***Alcohol Adsorbent Loading (mg/g)***	***Alcohol Concentration (mass%)***	***Alcohol Adsorbent Loading (mg/g)***	***Alcohol Concentration (mass%)***	***Alcohol Adsorbent Loading (mg/g)***
0	0.56	0.00	1.04	0.00	1.61	0.00
2	0.50	9.91	0.89	22.5	1.48	20.7
15	0.40	23.7	0.72	48.1	1.35	40.0
30	0.32	36.1	0.66	57.1	1.22	59.9
150	0.13	62.1	0.38	98.5	0.90	108
240	0.12	64.1	0.31	109	0.83	118
360	0.10	67.7	0.27	114	0.79	123
390	0.08	69.8	0.25	117	0.82	119
480	0.07	71.8	0.26	116	0.85	115
1380	0.07	72.1	0.30	111	0.87	111
1395	0.06	72.4	0.28	114	0.86	114
1410	0.06	72.3	0.27	114	0.85	115

Table C.1-3: Kinetic data for the single component adsorption of 1-decanol onto Activated Alumina F220 (T = 45°C)

	Initial Adsorbate Concentration (mass%)					
	0.49		*0.98*		*1.56*	
Time (min)	***Alcohol Concentration (mass%)***	***Alcohol Adsorbent Loading (mg/g)***	***Alcohol Concentration (mass%)***	***Alcohol Adsorbent Loading (mg/g)***	***Alcohol Concentration (mass%)***	***Alcohol Adsorbent Loading (mg/g)***
0	0.49	0.00	0.98	0.00	1.56	0.00
2	0.45	5.36	0.94	6.34	1.53	4.01
15	0.40	13.3	0.91	11.6	1.37	29.1
30	0.33	23.5	0.85	21.0	1.28	42.6
150	0.21	40.0	0.48	75.2	0.92	94.7
240	0.18	44.8	0.40	86.7	0.83	109
360	0.13	52.3	0.29	103	0.76	118
390	0.12	53.5	0.35	94.0	0.75	120
480	0.08	58.7	0.29	104	0.76	119
1380	0.08	58.9	0.23	113	0.78	117
1395	0.08	58.7	0.24	111	0.80	114
1410	0.08	59.6	0.23	112	0.81	112

C.1.1.2 *Selexsorb CDx®*

Table C.1-4: Kinetic data for the single component adsorption of 1-hexanol onto Selexsorb CDx® (T = 45°C)

	Initial Adsorbate Concentration (mass%)					
	0.59		*1.02*		*1.71*	
Time (min)	***Alcohol Concentration (mass%)***	***Alcohol Adsorbent Loading (mg/g)***	***Alcohol Concentration (mass%)***	***Alcohol Adsorbent Loading (mg/g)***	***Alcohol Concentration (mass%)***	***Alcohol Adsorbent Loading (mg/g)***
0	0.59	0.00	1.02	0.00	1.71	0.00
2	0.54	8.09	0.90	17.6	1.59	17.5
15	0.42	26.3	0.78	36.9	1.47	35.3
30	0.33	39.0	0.76	39.1	1.35	52.5
150	0.15	65.9	0.50	77.8	1.09	90.6
240	0.10	72.6	0.41	92.6	0.98	107
360	0.08	76.3	0.34	103	0.94	112
390	0.06	77.9	0.33	103	0.93	113
480	0.06	78.0	0.31	107	0.92	116
1380	0.06	78.7	0.28	112	0.90	118
1395	0.06	78.7	0.27	113	0.86	124
1410	0.06	78.4	0.28	111	0.87	123

Table C.1-5: Kinetic data for the single component adsorption of 1-octanol onto Selexsorb CDx® (T = 45°C)

	Initial Adsorbate Concentration (mass%)					
	0.44		*1.00*		*1.46*	
Time (min)	***Alcohol Concentration (mass%)***	***Alcohol Adsorbent Loading (mg/g)***	***Alcohol Concentration (mass%)***	***Alcohol Adsorbent Loading (mg/g)***	***Alcohol Concentration (mass%)***	***Alcohol Adsorbent Loading (mg/g)***
0	0.44	0.00	1.00	0.00	1.46	0.00
2	0.40	6.61	0.91	13.4	1.38	11.9
15	0.33	17.5	0.85	22.3	1.24	33.1
30	0.29	23.4	0.75	37.5	1.17	44.2
150	0.24	30.0	0.50	74.1	0.95	76.8
240	0.21	35.3	0.41	87.2	0.79	100
360	0.12	47.9	0.36	94.1	0.73	109
390	0.11	49.6	0.34	97.4	0.75	107
480	0.07	56.2	0.30	103	0.74	109
1380	0.06	56.9	0.28	107	0.73	110
1395	0.05	58.1	0.27	107	0.74	108
1410	0.05	58.1	0.27	107	0.73	110

Table C.1-6: Kinetic data for the single component adsorption of 1-decanol onto Selexsorb CDx® (T = 45°C)

	Initial Adsorbate Concentration (mass%)					
	0.54		*1.08*		*1.69*	
Time (min)	***Alcohol Concentration (mass%)***	***Alcohol Adsorbent Loading (mg/g)***	***Alcohol Concentration (mass%)***	***Alcohol Adsorbent Loading (mg/g)***	***Alcohol Concentration (mass%)***	***Alcohol Adsorbent Loading (mg/g)***
0	0.54	0.00	1.08	0.00	1.69	0.00
2	0.52	1.69	1.02	8.79	1.60	15.0
15	0.45	12.8	0.95	19.3	1.49	31.3
30	0.39	21.5	0.81	40.5	1.42	42.0
150	0.19	51.1	0.66	62.8	1.15	81.4
240	0.11	61.8	0.56	76.7	1.00	105
360	0.09	65.7	0.45	92.7	0.89	122
390	0.07	68.1	0.46	91.5	0.86	125
480	0.06	69.1	0.43	95.5	0.86	126
1380	0.03	73.5	0.26	121	0.80	134
1395	0.04	73.2	0.26	121	0.79	136
1410	0.05	71.4	0.26	121	0.79	136

C.1.1.3 *Selexsorb CD®*

Table C.1-7: Kinetic data for the single component adsorption of 1-hexanol onto Selexsorb CD® (T = 45°C)

	Initial Adsorbate Concentration (mass%)					
	0.43		*0.96*		*1.59*	
Time (min)	***Alcohol Concentration (mass%)***	***Alcohol Adsorbent Loading (mg/g)***	***Alcohol Concentration (mass%)***	***Alcohol Adsorbent Loading (mg/g)***	***Alcohol Concentration (mass%)***	***Alcohol Adsorbent Loading (mg/g)***
0	0.43	0.00	0.96	0.00	1.59	0.00
2	0.43	0.31	0.86	13.6	1.43	25.0
15	0.31	18.0	0.73	33.3	1.27	48.3
30	0.25	27.3	0.69	38.7	1.21	58.2
150	0.10	49.6	0.46	72.7	0.92	101
240	0.07	55.0	0.30	95.4	0.86	110
360	0.04	58.7	0.28	98.6	0.79	121
390	0.04	58.2	0.29	97.5	0.81	117
480	0.04	59.1	0.25	102	0.77	124
1380	0.04	59.1	0.23	106	0.75	127
1395	0.04	59.1	0.22	107	0.75	127
1410	0.04	59.1	0.22	107	0.75	126

Table C.1-8: Kinetic data for the single component adsorption of 1-octanol onto Selexsorb CD® (T = 45°C)

	Initial Adsorbate Concentration (mass%)					
	0.43		*1.10*		*1.53*	
Time (min)	***Alcohol Concentration (mass%)***	***Alcohol Adsorbent Loading (mg/g)***	***Alcohol Concentration (mass%)***	***Alcohol Adsorbent Loading (mg/g)***	***Alcohol Concentration (mass%)***	***Alcohol Adsorbent Loading (mg/g)***
0	0.43	0.00	1.10	0.00	1.53	0.00
2	0.40	4.79	0.96	21.4	1.46	9.93
15	0.34	13.9	0.91	28.8	1.33	29.0
30	0.27	23.5	0.86	36.7	1.17	52.5
150	0.09	49.7	0.57	78.4	0.98	81.2
240	0.05	55.6	0.46	94.7	0.88	95.1
360	0.02	60.5	0.40	105	0.85	100
390	0.01	61.1	0.37	108	0.88	94.8
480	0.01	61.3	0.36	110	0.84	101
1380	0.02	59.8	0.30	119	0.73	118
1395	0.02	59.9	0.30	119	0.73	117
1410	0.02	59.8	0.28	122	0.75	115

Table C.1-9: Kinetic data for the single component adsorption of 1-decanol onto Selexsorb CD® (T = 45°C)

	Initial Adsorbate Concentration (mass%)					
	0.53		*1.18*		*1.63*	
Time (min)	***Alcohol Concentration (mass%)***	***Alcohol Adsorbent Loading (mg/g)***	***Alcohol Concentration (mass%)***	***Alcohol Adsorbent Loading (mg/g)***	***Alcohol Concentration (mass%)***	***Alcohol Adsorbent Loading (mg/g)***
0	0.53	0.00	1.18	0.00	1.63	0.00
2	0.49	5.65	1.11	11.5	1.58	6.87
15	0.34	28.5	0.99	28.6	1.47	23.9
30	0.30	34.7	0.90	42.6	1.40	35.2
150	0.16	54.6	0.68	75.8	1.11	78.9
240	0.13	59.8	0.55	94.3	1.02	92.3
360	0.07	68.8	0.44	111	0.94	105
390	0.07	68.4	0.43	113	0.91	109
480	0.06	70.1	0.41	116	0.83	121
1380	0.06	69.3	0.32	129	0.77	129
1395	0.06	70.2	0.31	131	0.82	123
1410	0.05	71.2	0.34	125	0.77	130

C.1.2 Binary Component Systems

C.1.2.1 *Activated Alumina F220*

C.1.2.1.1 1-hexanol + 1-decanol

Table C.1-10: Kinetic data for the binary component adsorption of a 1-hexanol + 1-decanol mixture onto Activated Alumina F220 (T = 25°C; IC = 0.75 mass%)

Time (min)	*1-hexanol Concentration (mass%)*	*1-decanol Concentration (mass%)*	*Total Alcohol Concentration (mass%)*	*1-hexanol Adsorbent Loading (mg/g)*	*1-decanol Adsorbent Loading (mg/g)*	*Total Alcohol Adsorbent Loading (mg/g)*
0	0.41	0.34	0.75	0.00	0.00	0.00
15	0.33	0.27	0.60	12.0	10.3	22.3
30	0.34	0.26	0.61	10.1	11.4	21.5
150	0.16	0.11	0.27	38.1	33.9	72.0
240	0.13	0.11	0.24	42.4	34.4	76.8
360	0.10	0.03	0.13	47.2	46.0	93.2
480	0.09	0.02	0.11	48.4	48.6	97.0
1380	0.07	0.00	0.07	50.8	51.2	102
1395	0.07	0.00	0.07	51.1	51.2	102
1410	0.08	0.00	0.08	49.1	51.2	100

Table C.1-11: Kinetic data for the binary component adsorption of a 1-hexanol + 1-decanol mixture onto Activated Alumina F220 (T = 25°C; IC = 1.76 mass%)

Time (min)	*1-hexanol Concentration (mass%)*	*1-decanol Concentration (mass%)*	*Total Alcohol Concentration (mass%)*	*1-hexanol Adsorbent Loading (mg/g)*	*1-decanol Adsorbent Loading (mg/g)*	*Total Alcohol Adsorbent Loading (mg/g)*
0	0.82	0.94	1.76	0.00	0.00	0.00
15	0.78	0.94	1.72	4.33	0.32	4.65
30	0.63	0.74	1.37	19.5	20.8	40.3
150	0.42	0.64	1.06	40.6	30.8	71.4
240	0.42	0.53	0.95	40.6	41.7	82.3
360	0.29	0.46	0.76	53.9	48.5	102
480	0.38	0.44	0.82	44.5	51.1	95.6
1380	0.22	0.40	0.62	60.9	55.5	116
1395	0.25	0.42	0.67	58.2	53.2	111
1410	0.30	0.39	0.69	53.0	56.5	109

Table C.1-12: Kinetic data for the binary component adsorption of a 1-hexanol + 1-decanol mixture onto Activated Alumina F220 (T = 25°C; IC = 3.17 mass%)

Time (min)	***1-hexanol Concentra-tion (mass%)***	***1-decanol Concentra-tion (mass%)***	***Total Alcohol Concentra-tion (mass%)***	***1-hexanol Adsorbent Loading (mg/g)***	***1-decanol Adsorbent Loading (mg/g)***	***Total Alcohol Adsorbent Loading (mg/g)***
0	0.96	2.22	3.17	0.00	0.00	0.00
15	0.88	2.11	3.00	11.7	15.3	27.0
30	0.85	2.05	2.90	16.8	25.0	41.8
150	0.70	1.83	2.53	39.0	57.3	96.3
240	0.67	1.74	2.40	43.8	72.2	116
360	0.63	1.67	2.31	48.9	81.7	131
450	0.61	1.67	2.28	53.2	81.5	135
1380	0.59	1.66	2.25	54.8	83.9	139
1395	0.60	1.61	2.21	54.2	90.6	145
1410	0.58	1.58	2.16	57.2	95.0	152

Table C.1-13: Kinetic data for the binary component adsorption of a 1-hexanol + 1-decanol mixture onto Activated Alumina F220 (T = 45°C; IC = 0.92 mass%)

Time (min)	***1-hexanol Concentra-tion (mass%)***	***1-octanol Concentra-tion (mass%)***	***Total Alcohol Concentra-tion (mass%)***	***1-hexanol Adsorbent Loading (mg/g)***	***1-octanol Adsorbent Loading (mg/g)***	***Total Alcohol Adsorbent Loading (mg/g)***
0	0.35	0.57	0.92	0.00	0.00	0.00
15	0.27	0.39	0.66	12.4	27.6	40.0
30	0.20	0.44	0.64	22.2	20.2	42.5
150	0.10	0.16	0.26	37.5	61.6	99.1
240	0.09	0.12	0.22	38.4	67.7	106
360	0.05	0.07	0.13	44.0	75.1	119
480	0.08	0.07	0.15	39.9	76.1	116
1380	0.11	0.09	0.20	35.7	73.4	109
1395	0.09	0.06	0.16	38.0	76.6	115
1410	0.11	0.07	0.18	35.7	75.5	111

Table C.1-14: Kinetic data for the binary component adsorption of a 1-hexanol + 1-decanol mixture onto Activated Alumina F220 (T = 45°C; IC = 2.05 mass%)

Time (min)	***1-hexanol Concentra-tion (mass%)***	***1-octanol Concentra-tion (mass%)***	***Total Alcohol Concentra-tion (mass%)***	***1-hexanol Adsorbent Loading (mg/g)***	***1-octanol Adsorbent Loading (mg/g)***	***Total Alcohol Adsorbent Loading (mg/g)***
0	0.95	1.10	2.05	0.00	0.00	0.00
15	0.81	0.91	1.72	21.8	28.1	49.9
30	0.68	0.88	1.56	41.2	32.1	73.3
150	0.55	0.74	1.30	59.8	52.7	113
240	0.52	0.68	1.20	64.3	63.0	127
360	0.51	0.70	1.21	66.3	59.7	126
480	0.47	0.57	1.04	71.9	78.6	150
1380	0.47	0.65	1.12	72.3	66.5	139
1395	0.45	0.62	1.07	75.4	71.0	146
1410	0.44	0.56	0.99	76.8	80.9	158

Table C.1-15: Kinetic data for the binary component adsorption of a 1-hexanol + 1-decanol mixture onto Activated Alumina F220 (T = 45°C; IC = 3.02 mass%)

Time (min)	***1-hexanol Concentra-tion (mass%)***	***1-octanol Concentra-tion (mass%)***	***Total Alcohol Concentra-tion (mass%)***	***1-hexanol Adsorbent Loading (mg/g)***	***1-octanol Adsorbent Loading (mg/g)***	***Total Alcohol Adsorbent Loading (mg/g)***
0	1.47	1.55	3.02	0.00	0.00	0.00
15	1.27	1.42	2.69	30.5	19.3	49.8
30	1.19	1.36	2.55	42.7	27.6	70.4
150	1.00	1.19	2.19	71.0	53.9	125
240	0.97	1.20	2.16	76.2	52.0	128
360	0.98	1.21	2.19	73.9	50.1	124
1380	0.97	1.22	2.19	74.8	49.5	124
1395	0.97	1.22	2.18	75.7	49.7	125
1410	0.96	1.19	2.15	76.4	53.8	130

C.1.2.1.2 1-hexanol + 1-octanol

Table C.1-16: Kinetic data for the binary component adsorption of a 1-hexanol + 1-octanol mixture onto Activated Alumina F220 (T = 25°C; IC = 1.06 mass%)

Time (min)	***1-hexanol Concentra-tion (mass%)***	***1-octanol Concentra-tion (mass%)***	***Total Alcohol Concentra-tion (mass%)***	***1-hexanol Adsorbent Loading (mg/g)***	***1-octanol Adsorbent Loading (mg/g)***	***Total Alcohol Adsorbent Loading (mg/g)***
0	0.51	0.56	1.06	0.00	0.00	0.00
15	0.47	0.55	1.02	5.36	1.23	6.58
30	0.44	0.52	0.97	9.67	4.64	14.3
150	0.30	0.38	0.68	31.2	26.5	57.7
240	0.22	0.28	0.50	42.3	41.4	83.8
360	0.20	0.24	0.44	46.4	47.4	93.8
1380	0.19	0.22	0.41	46.8	50.7	97.5
1395	0.19	0.17	0.36	47.1	58.5	106
1410	0.17	0.20	0.37	50.3	53.5	104

Table C.1-17: Kinetic data for the binary component adsorption of a 1-hexanol + 1-octanol mixture onto Activated Alumina F220 (T = 25°C; IC = 1.92 mass%)

Time (min)	***1-hexanol Concentra-tion (mass%)***	***1-octanol Concentra-tion (mass%)***	***Total Alcohol Concentra-tion (mass%)***	***1-hexanol Adsorbent Loading (mg/g)***	***1-octanol Adsorbent Loading (mg/g)***	***Total Alcohol Adsorbent Loading (mg/g)***
0	0.93	0.98	1.92	0.00	0.00	0.00
15	0.78	0.87	1.66	22.4	16.8	39.2
30	0.71	0.83	1.53	33.4	23.9	57.2
150	0.58	0.67	1.25	53.3	46.8	100
230	0.56	0.63	1.19	55.6	52.9	108
350	0.49	0.59	1.08	66.5	58.8	125
450	0.52	0.57	1.09	62.3	61.8	124
1380	0.47	0.54	1.01	68.6	66.7	135
1395	0.48	0.55	1.03	67.7	65.5	133
1410	0.47	0.55	1.02	69.2	64.2	133

Table C.1-18: Kinetic data for the binary component adsorption of a 1-hexanol + 1-octanol mixture onto Activated Alumina F220 (T = 25°C; IC = 3.33 mass%)

Time (min)	***1-hexanol Concentra-tion (mass%)***	***1-octanol Concentra-tion (mass%)***	***Total Alcohol Concentra-tion (mass%)***	***1-hexanol Adsorbent Loading (mg/g)***	***1-octanol Adsorbent Loading (mg/g)***	***Total Alcohol Adsorbent Loading (mg/g)***
0	1.60	1.72	3.33	0.00	0.00	0.00
30	1.47	1.63	3.11	19.8	13.1	32.9
150	1.25	1.44	2.68	53.9	42.2	96.1
240	1.19	1.38	2.57	62.9	50.8	114
360	1.17	1.36	2.53	65.3	54.1	119
450	1.14	1.30	2.44	70.2	63.0	133
1380	1.10	1.29	2.39	75.4	65.0	140
1395	1.16	1.30	2.46	66.2	63.9	130
1410	1.16	1.29	2.46	66.3	64.3	131

Table C.1-19: Kinetic data for the binary component adsorption of a 1-hexanol + 1-octanol mixture onto Activated Alumina F220 (T = 45°C; IC = 0.83 mass%)

Time (min)	***1-hexanol Concentra-tion (mass%)***	***1-octanol Concentra-tion (mass%)***	***Total Alcohol Concentra-tion (mass%)***	***1-hexanol Adsorbent Loading (mg/g)***	***1-octanol Adsorbent Loading (mg/g)***	***Total Alcohol Adsorbent Loading (mg/g)***
0	0.40	0.43	0.83	0.00	0.00	0.00
15	0.32	0.36	0.67	13.2	10.5	23.7
30	0.25	0.30	0.56	22.5	19.1	41.6
150	0.15	0.17	0.32	38.6	38.2	76.8
240	0.13	0.15	0.27	41.7	42.1	83.9
360	0.12	0.14	0.27	42.1	42.9	84.9
480	0.14	0.16	0.30	40.3	40.2	80.5
1380	0.15	0.16	0.31	38.2	40.5	78.7
1395	0.15	0.15	0.30	38.5	41.2	79.7
1410	0.14	0.15	0.30	38.9	41.5	80.4

Table C.1-20: Kinetic data for the binary component adsorption of a 1-hexanol + 1-octanol mixture onto Activated Alumina F220 (T = 45°C; IC = 2.04 mass%)

Time (min)	***1-hexanol Concentra-tion (mass%)***	***1-octanol Concentra-tion (mass%)***	***Total Alcohol Concentra-tion (mass%)***	***1-hexanol Adsorbent Loading (mg/g)***	***1-octanol Adsorbent Loading (mg/g)***	***Total Alcohol Adsorbent Loading (mg/g)***
0	0.97	1.07	2.04	0.00	0.00	0.00
15	0.81	0.89	1.70	24.6	25.9	50.5
30	0.74	0.86	1.61	34.1	30.4	64.5
150	0.60	0.75	1.34	56.4	48.2	105
240	0.56	0.68	1.24	61.5	58.1	120
360	0.57	0.70	1.26	61.2	55.7	117
480	0.52	0.66	1.17	68.2	62.0	130
1380	0.56	0.65	1.21	62.5	62.1	125
1395	0.54	0.65	1.19	64.8	63.3	128
1410	0.52	0.66	1.18	67.6	61.1	129

Table C.1-21: Kinetic data for the binary component adsorption of a 1-hexanol + 1-octanol mixture onto Activated Alumina F220 (T = 45°C; IC = 2.39 mass%)

Time (min)	***1-hexanol Concentra-tion (mass%)***	***1-octanol Concentra-tion (mass%)***	***Total Alcohol Concentra-tion (mass%)***	***1-hexanol Adsorbent Loading (mg/g)***	***1-octanol Adsorbent Loading (mg/g)***	***Total Alcohol Adsorbent Loading (mg/g)***
0	0.96	1.43	2.39	0.00	0.00	0.00
15	0.85	1.31	2.16	16.6	17.9	34.5
30	0.75	1.23	1.98	32.0	30.1	62.1
150	0.64	1.01	1.65	48.6	63.9	113
240	0.62	1.02	1.64	51.4	61.6	113
360	0.64	1.00	1.64	48.3	64.8	113
480	0.63	1.00	1.64	49.2	64.6	114
1380	0.65	1.02	1.67	46.3	62.4	109
1395	0.60	1.00	1.60	55.1	64.7	120
1410	0.63	1.01	1.64	50.3	62.7	113

C.1.2.1.3 1-octanol + 1-decanol

Table C.1-22: Kinetic data for the binary component adsorption of a 1-octanol + 1-decanol mixture onto Activated Alumina F220 (T = 25°C; IC = 1.15 mass%)

Time (min)	***1-octanol Concentration (mass%)***	***1-decanol Concentration (mass%)***	***Total Alcohol Concentration (mass%)***	***1-octanol Adsorbent Loading (mg/g)***	***1-decanol Adsorbent Loading (mg/g)***	***Total Alcohol Adsorbent Loading (mg/g)***
0	0.66	0.49	1.15	0.00	0.00	0.00
15	0.66	0.46	1.12	0.54	3.53	4.06
30	0.60	0.42	1.02	9.25	9.88	19.1
150	0.41	0.27	0.67	37.9	33.0	70.9
240	0.36	0.25	0.61	44.8	35.6	80.4
360	0.29	0.19	0.48	54.8	44.3	99.1
450	0.27	0.17	0.44	57.8	47.4	105
1380	0.26	0.10	0.36	59.2	57.6	117
1395	0.27	0.10	0.37	58.7	57.4	116
1410	0.26	0.11	0.37	59.7	56.5	116

Table C.1-23: Kinetic data for the binary component adsorption of a 1-octanol + 1-decanol mixture onto Activated Alumina F220 (T = 25°C; IC = 1.96 mass%)

Time (min)	***1-octanol Concentration (mass%)***	***1-decanol Concentration (mass%)***	***Total Alcohol Concentration (mass%)***	***1-octanol Adsorbent Loading (mg/g)***	***1-decanol Adsorbent Loading (mg/g)***	***Total Alcohol Adsorbent Loading (mg/g)***
0	1.01	0.95	1.96	0.00	0.00	0.00
15	0.93	0.93	1.86	12.5	2.95	15.4
30	0.90	0.87	1.78	16.4	11.2	27.6
150	0.71	0.77	1.48	45.6	26.5	72.1
240	0.63	0.68	1.32	56.6	40.2	96.7
360	0.58	0.61	1.19	65.0	50.6	116
480	0.53	0.57	1.10	71.5	56.7	128
1380	0.50	0.52	1.03	75.9	64.1	140
1395	0.49	0.56	1.05	77.9	58.8	137
1410	0.49	0.55	1.04	77.6	59.9	138

Table C.1-24: Kinetic data for the binary component adsorption of a 1-octanol + 1-decanol mixture onto Activated Alumina F220 (T = 25°C; IC = 3.32 mass%)

Time (min)	1-octanol Concentration (mass%)	1-decanol Concentration (mass%)	Total Alcohol Concentration (mass%)	1-octanol Adsorbent Loading (mg/g)	1-decanol Adsorbent Loading (mg/g)	Total Alcohol Adsorbent Loading (mg/g)
0	1.67	1.64	3.32	0.00	0.00	0.00
15	1.49	1.53	3.02	18.4	11.7	30.1
30	1.47	1.51	2.98	20.8	13.3	34.1
150	1.30	1.36	2.66	37.7	28.0	65.7
240	1.21	1.28	2.49	46.1	36.6	82.8
360	1.01	1.07	2.08	66.2	57.4	124
450	0.95	1.04	1.98	72.6	60.5	133
1380	0.91	0.97	1.88	75.8	67.4	143
1395	0.91	0.98	1.89	75.9	66.4	142
1410	0.90	0.96	1.86	77.2	67.8	145

Table C.1-25: Kinetic data for the binary component adsorption of a 1-octanol + 1-decanol mixture onto Activated Alumina F220 (T = 45°C; IC = 1.01 mass%)

Time (min)	1-octanol Concentration (mass%)	1-decanol Concentration (mass%)	Total Alcohol Concentration (mass%)	1-octanol Adsorbent Loading (mg/g)	1-decanol Adsorbent Loading (mg/g)	Total Alcohol Adsorbent Loading (mg/g)
0	0.39	0.62	1.01	0.00	0.00	0.00
15	0.32	0.43	0.75	10.8	28.8	39.6
30	0.23	0.35	0.58	24.4	40.4	64.8
150	0.09	0.10	0.19	44.8	78.3	123
240	0.08	0.04	0.11	46.5	87.5	134
360	0.06	0.02	0.07	49.6	90.4	140
480	0.06	0.02	0.08	49.5	89.7	139
1380	0.08	0.01	0.08	47.1	91.9	139
1395	0.07	0.02	0.09	48.1	89.3	137
1410	0.08	0.01	0.09	46.7	90.7	137

Table C.1-26: Kinetic data for the binary component adsorption of a 1-octanol + 1-decanol mixture onto Activated Alumina F220 (T = 45°C; IC = 2.19 mass%)

Time (min)	***1-octanol Concentra-tion (mass%)***	***1-decanol Concentra-tion (mass%)***	***Total Alcohol Concentra-tion (mass%)***	***1-octanol Adsorbent Loading (mg/g)***	***1-decanol Adsorben t Loading (mg/g)***	***Total Alcohol Adsorbent Loading (mg/g)***
0	1.02	1.17	2.19	0.00	0.00	0.00
15	0.89	1.05	1.95	18.6	18.3	36.9
30	0.82	0.98	1.80	30.2	28.5	58.7
150	0.66	0.81	1.47	54.0	54.9	109
240	0.60	0.76	1.37	63.1	61.6	125
360	0.58	0.69	1.27	65.7	73.1	139
480	0.58	0.74	1.32	66.4	65.9	132
1380	0.58	0.74	1.32	66.0	65.8	132
1395	0.58	0.74	1.32	66.1	65.5	132
1410	0.56	0.68	1.24	70.0	74.2	144

Table C.1-27: Kinetic data for the binary component adsorption of a 1-octanol + 1-decanol mixture onto Activated Alumina F220 (T = 45°C; IC = 3.07 mass%)

Time (min)	***1-octanol Concentra-tion (mass%)***	***1-decanol Concentra-tion (mass%)***	***Total Alcohol Concentra-tion (mass%)***	***1-octanol Adsorbent Loading (mg/g)***	***1-decanol Adsorben t Loading (mg/g)***	***Total Alcohol Adsorbent Loading (mg/g)***
0	1.51	1.56	3.07	0.00	0.00	0.00
15	1.35	1.50	2.85	23.7	9.5	33.1
30	1.29	1.41	2.70	32.8	23.3	56.1
150	1.10	1.27	2.38	60.8	43.3	104
240	1.05	1.22	2.27	68.9	51.3	120
360	1.02	1.21	2.23	72.7	52.6	125
1380	1.02	1.22	2.24	72.8	51.5	124
1395	1.01	1.20	2.22	74.3	53.6	128
1410	1.01	1.18	2.19	74.3	57.7	132

C.1.2.2 ***Selexsorb CDx®***

C.1.2.2.1 1-hexanol + 1-decanol

Table C.1-28: Kinetic data for the binary component adsorption of a 1-hexanol + 1-decanol mixture onto Selexsorb CDx® (T = 25°C; IC = 1.20 mass%)

Time (min)	*1-hexanol Concentra-tion (mass%)*	*1-decanol Concentra-tion (mass%)*	*Total Alcohol Concentra-tion (mass%)*	*1-hexanol Adsorbent Loading (mg/g)*	*1-decanol Adsorbent Loading (mg/g)*	*Total Alcohol Adsorbent Loading (mg/g)*
0	0.59	0.61	1.20	0.00	0.00	0.00
15	0.54	0.52	1.06	7.76	13.2	21.0
30	0.45	0.53	0.98	21.1	12.0	33.1
150	0.34	0.45	0.79	37.0	23.7	60.7
240	0.26	0.33	0.60	49.1	40.8	89.9
360	0.23	0.27	0.50	54.4	50.1	104
480	0.30	0.26	0.56	44.0	51.6	96
1380	0.23	0.15	0.39	53.6	67.6	121
1395	0.26	0.21	0.47	49.6	59.3	109
1410	0.25	0.20	0.45	51.1	60.9	112

Table C.1-29: Kinetic data for the binary component adsorption of a 1-hexanol + 1-decanol mixture onto Selexsorb CDx® (T = 25°C; IC = 2.10 mass%)

Time (min)	*1-hexanol Concentra-tion (mass%)*	*1-decanol Concentra-tion (mass%)*	*Total Alcohol Concentra-tion (mass%)*	*1-hexanol Adsorbent Loading (mg/g)*	*1-decanol Adsorbent Loading (mg/g)*	*Total Alcohol Adsorbent Loading (mg/g)*
0	1.04	1.06	2.10	0.00	0.00	0.00
15	0.95	1.00	1.95	13.6	8.94	22.6
30	0.86	0.97	1.83	26.3	13.1	39.5
150	0.70	0.79	1.50	49.9	40.0	89.9
240	0.64	0.76	1.40	59.3	45.0	104
360	0.61	0.73	1.35	63.7	48.9	113
480	0.60	0.78	1.39	65.0	41.1	106
1380	0.56	0.72	1.28	71.2	51.2	122
1395	0.56	0.69	1.25	71.0	55.9	127
1410	0.57	0.73	1.30	70.5	49.5	120

Table C.1-30: Kinetic data for the binary component adsorption of a 1-hexanol + 1-decanol mixture onto Selexsorb CDx® (T = 25°C; IC = 3.38 mass%)

Time (min)	*1-hexanol Concentra-tion (mass%)*	*1-decanol Concentra-tion (mass%)*	*Total Alcohol Concentra-tion (mass%)*	*1-hexanol Adsorbent Loading (mg/g)*	*1-decanol Adsorbent Loading (mg/g)*	*Total Alcohol Adsorbent Loading (mg/g)*
0	1.44	1.94	3.38	0.00	0.00	0.00
15	1.31	1.88	3.20	12.7	5.6	18.4
30	1.28	1.81	3.10	15.9	13.2	29.1
150	1.14	1.63	2.77	30.9	31.5	62.4
240	1.08	1.59	2.67	37.5	36.1	73.6
360	1.12	1.52	2.64	33.1	43.2	76.3
480	1.03	1.32	2.35	42.1	63.8	106
1380	0.82	1.29	2.11	64.5	66.8	131
1395	0.85	1.28	2.12	61.1	68.6	130
1410	0.86	1.28	2.14	59.8	67.9	128

Table C.1-31: Kinetic data for the binary component adsorption of a 1-hexanol + 1-decanol mixture onto Selexsorb CDx® (T = 45°C; IC = 1.13 mass%)

Time (min)	*1-hexanol Concentra-tion (mass%)*	*1-octanol Concentra-tion (mass%)*	*Total Alcohol Concentra-tion (mass%)*	*1-hexanol Adsorbent Loading (mg/g)*	*1-octanol Adsorbent Loading (mg/g)*	*Total Alcohol Adsorbent Loading (mg/g)*
0	0.51	0.63	1.13	0.00	0.00	0.00
15	0.47	0.54	1.01	5.5	12.7	18.2
30	0.29	0.45	0.74	32.5	27.4	59.9
150	0.20	0.32	0.52	45.8	47.3	93.1
240	0.15	0.28	0.43	53.6	52.9	106
360	0.13	0.21	0.34	57.1	64.3	121
480	0.08	0.09	0.18	64.0	81.7	146
1380	0.08	0.11	0.19	64.1	79.1	143
1395	0.09	0.10	0.18	63.8	81.1	145
1410	0.09	0.11	0.19	64.0	79.1	143

Table C.1-32: Kinetic data for the binary component adsorption of a 1-hexanol + 1-decanol mixture onto Selexsorb CDx® (T = 45°C; IC = 2.07 mass%)

Time (min)	***1-hexanol Concentration (mass%)***	***1-octanol Concentration (mass%)***	***Total Alcohol Concentration (mass%)***	***1-hexanol Adsorbent Loading (mg/g)***	***1-octanol Adsorbent Loading (mg/g)***	***Total Alcohol Adsorbent Loading (mg/g)***
0	1.03	1.04	2.07	0.00	0.00	0.00
15	0.88	1.03	1.91	22.3	2.2	24.5
30	0.83	0.97	1.80	31.2	10.3	41.5
150	0.68	0.87	1.55	53.0	26.5	79.5
240	0.61	0.80	1.41	64.1	36.9	101
360	0.54	0.72	1.26	74.6	48.0	123
1380	0.52	0.74	1.26	77.8	45.5	123
1395	0.49	0.75	1.24	82.0	43.7	126
1410	0.49	0.76	1.24	82.8	42.8	126

Table C.1-33: Kinetic data for the binary component adsorption of a 1-hexanol + 1-decanol mixture onto Selexsorb CDx® (T = 45°C; IC = 2.94 mass%)

Time (min)	***1-hexanol Concentration (mass%)***	***1-octanol Concentration (mass%)***	***Total Alcohol Concentration (mass%)***	***1-hexanol Adsorbent Loading (mg/g)***	***1-octanol Adsorbent Loading (mg/g)***	***Total Alcohol Adsorbent Loading (mg/g)***
0	1.26	1.68	2.94	0.00	0.00	0.00
15	1.16	1.62	2.78	14.0	9.20	23.2
30	1.08	1.51	2.60	25.9	25.5	51.4
150	0.95	1.48	2.44	45.4	29.7	75.0
240	0.90	1.44	2.34	53.3	36.7	90.0
360	0.83	1.40	2.23	64.5	41.8	106
480	0.70	1.39	2.09	82.8	43.5	126
1380	0.73	1.39	2.12	78.6	43.8	122
1395	0.74	1.32	2.05	77.7	54.3	132
1410	0.74	1.34	2.08	77.1	51.1	128

C.1.2.2.2 1-hexanol + 1-octanol

Table C.1-34: Kinetic data for the binary component adsorption of a 1-hexanol + 1-octanol mixture onto Selexsorb CDx® (T = 25°C; IC = 1.30 mass%)

Time (min)	***1-hexanol Concentra-tion (mass%)***	***1-octanol Concentra-tion (mass%)***	***Total Alcohol Concentra-tion (mass%)***	***1-hexanol Adsorbent Loading (mg/g)***	***1-octanol Adsorbent Loading (mg/g)***	***Total Alcohol Adsorbent Loading (mg/g)***
0	0.66	0.63	1.30	0.00	0.00	0.00
15	0.62	0.57	1.19	6.56	8.79	15.3
30	0.54	0.54	1.08	18.8	13.9	32.7
240	0.46	0.50	0.97	30.0	19.4	49.4
360	0.40	0.44	0.84	39.7	28.7	68.4
480	0.33	0.39	0.72	49.8	36.6	86.4
1380	0.35	0.38	0.73	46.4	38.4	84.8
1395	0.36	0.38	0.74	44.9	37.6	82.6
1410	0.36	0.37	0.74	44.6	38.8	83.5

Table C.1-35: Kinetic data for the binary component adsorption of a 1-hexanol + 1-octanol mixture onto Selexsorb CDx® (T = 25°C; IC = 1.98 mass%)

Time (min)	***1-hexanol Concentra-tion (mass%)***	***1-octanol Concentra-tion (mass%)***	***Total Alcohol Concentra-tion (mass%)***	***1-hexanol Adsorbent Loading (mg/g)***	***1-octanol Adsorbent Loading (mg/g)***	***Total Alcohol Adsorbent Loading (mg/g)***
0	1.00	0.98	1.98	0.00	0.00	0.00
15	0.93	0.89	1.82	11.3	13.7	25.0
30	0.81	0.81	1.62	29.3	25.1	54.3
150	0.67	0.71	1.38	49.9	39.9	89.8
240	0.65	0.70	1.36	51.9	41.7	93.6
360	0.59	0.64	1.24	61.3	50.3	112
1380	0.51	0.57	1.08	73.7	61.8	136
1395	0.52	0.58	1.09	72.4	60.8	133
1410	0.51	0.58	1.09	73.0	60.2	133

Table C.1-36: Kinetic data for the binary component adsorption of a 1-hexanol + 1-octanol mixture onto Selexsorb CDx® (T = 25°C; IC = 3.16 mass%)

Time (min)	1-hexanol Concentration (mass%)	1-octanol Concentration (mass%)	Total Alcohol Concentration (mass%)	1-hexanol Adsorbent Loading (mg/g)	1-octanol Adsorbent Loading (mg/g)	Total Alcohol Adsorbent Loading (mg/g)
0	1.55	1.61	3.16	0.00	0.00	0.00
15	1.41	1.45	2.86	20.4	24.2	44.7
30	1.36	1.43	2.79	28.5	26.4	54.9
150	1.30	1.38	2.68	37.4	34.2	71.7
240	1.22	1.30	2.51	49.5	47.1	96.6
360	1.18	1.29	2.46	55.6	48.2	104
450	1.10	1.21	2.31	66.4	59.7	126
1380	1.08	1.20	2.28	70.7	61.3	132
1395	1.10	1.22	2.32	67.6	58.3	126
1410	1.08	1.18	2.26	70.3	64.0	134

Table C.1-37: Kinetic data for the binary component adsorption of a 1-hexanol + 1-octanol mixture onto Selexsorb CDx® (T = 45°C; IC = 1.21 mass%)

Time (min)	1-hexanol Concentration (mass%)	1-octanol Concentration (mass%)	Total Alcohol Concentration (mass%)	1-hexanol Adsorbent Loading (mg/g)	1-octanol Adsorbent Loading (mg/g)	Total Alcohol Adsorbent Loading (mg/g)
0	0.57	0.65	1.21	0.00	0.00	0.00
15	0.38	0.47	0.84	27.8	27.0	54.8
30	0.35	0.43	0.77	32.8	32.6	65.4
150	0.20	0.29	0.49	54.6	52.9	107
240	0.20	0.29	0.49	54.6	52.9	107
360	0.18	0.25	0.43	56.9	59.6	117
1380	0.15	0.21	0.35	62.2	65.9	128
1395	0.13	0.18	0.31	65.3	69.2	134
1410	0.13	0.17	0.29	65.5	71.6	137

Table C.1-38: Kinetic data for the binary component adsorption of a 1-hexanol + 1-octanol mixture onto Selexsorb CDx® (T = 45°C; IC = 1.31 mass%)

Time (min)	***1-hexanol Concentra-tion (mass%)***	***1-octanol Concentra-tion (mass%)***	***Total Alcohol Concentra-tion (mass%)***	***1-hexanol Adsorbent Loading (mg/g)***	***1-octanol Adsorbent Loading (mg/g)***	***Total Alcohol Adsorbent Loading (mg/g)***
0	0.72	0.59	1.31	0.00	0.00	0.00
15	0.61	0.54	1.16	16.1	6.6	22.7
30	0.55	0.50	1.05	25.6	13.6	39.2
150	0.42	0.36	0.78	44.5	34.7	79.2
240	0.31	0.33	0.64	61.6	38.5	100
360	0.30	0.29	0.59	62.9	44.3	107
480	0.27	0.26	0.53	67.0	49.2	116
1380	0.29	0.29	0.58	63.8	44.6	108
1395	0.29	0.28	0.57	64.5	46.2	111
1410	0.28	0.25	0.53	65.7	51.2	117

Table C.1-39: Kinetic data for the binary component adsorption of a 1-hexanol + 1-octanol mixture onto Selexsorb CDx® (T = 45°C; IC = 3.08 mass%)

Time (min)	***1-hexanol Concentra-tion (mass%)***	***1-octanol Concentra-tion (mass%)***	***Total Alcohol Concentra-tion (mass%)***	***1-hexanol Adsorbent Loading (mg/g)***	***1-octanol Adsorbent Loading (mg/g)***	***Total Alcohol Adsorbent Loading (mg/g)***
0	1.51	1.57	3.08	0.00	0.00	0.00
15	1.37	1.45	2.82	21.1	17.9	39.0
30	1.33	1.42	2.75	27.9	22.4	50.4
150	1.14	1.26	2.40	55.4	46.7	102
240	1.07	1.22	2.29	66.1	52.3	118
360	1.05	1.18	2.22	70.0	58.4	128
1380	0.98	1.14	2.12	79.6	63.6	143
1395	0.95	1.16	2.10	84.9	61.3	146
1410	0.93	1.13	2.07	86.5	65.1	152

C.1.2.2.3 1-octanol + 1-decanol

Table C.1-40: Kinetic data for the binary component adsorption of a 1-octanol + 1-decanol mixture onto Selexsorb CDx® (T = 25°C; IC = 1.26 mass%)

Time (min)	***1-octanol Concentration (mass%)***	***1-decanol Concentration (mass%)***	***Total Alcohol Concentration (mass%)***	***1-octanol Adsorbent Loading (mg/g)***	***1-decanol Adsorbent Loading (mg/g)***	***Total Alcohol Adsorbent Loading (mg/g)***
0	0.63	0.62	1.26	0.00	0.00	0.00
15	0.57	0.55	1.12	9.97	11.07	21.0
30	0.55	0.53	1.08	12.5	13.9	26.3
150	0.42	0.42	0.83	32.0	31.1	63.1
240	0.37	0.37	0.74	39.0	38.3	77.3
360	0.31	0.30	0.61	47.8	49.1	96.9
450	0.31	0.30	0.62	47.7	47.9	95.6
1380	0.29	0.20	0.49	50.8	63.0	114
1395	0.30	0.20	0.49	50.2	63.6	114
1410	0.29	0.20	0.50	50.5	62.6	113

Table C.1-41: Kinetic data for the binary component adsorption of a 1-octanol + 1-decanol mixture onto Selexsorb CDx® (T = 25°C; IC = 2.34 mass%)

Time (min)	***1-octanol Concentration (mass%)***	***1-decanol Concentration (mass%)***	***Total Alcohol Concentration (mass%)***	***1-octanol Adsorbent Loading (mg/g)***	***1-decanol Adsorbent Loading (mg/g)***	***Total Alcohol Adsorbent Loading (mg/g)***
0	1.16	1.18	2.34	0.00	0.00	0.00
15	1.08	1.15	2.24	10.8	3.00	13.8
30	1.01	1.05	2.05	19.4	16.3	35.7
150	0.72	0.77	1.49	51.4	46.3	97.6
240	0.63	0.71	1.34	56.9	49.4	106
360	0.57	0.63	1.20	58.7	54.5	113
1380	0.46	0.51	0.97	61.9	59.0	121
1395	0.44	0.48	0.93	59.7	57.7	117
1410	0.44	0.51	0.95	56.6	52.6	109

Table C.1-42: Kinetic data for the binary component adsorption of a 1-octanol + 1-decanol mixture onto Selexsorb CDx® (T = 25°C; IC = 3.31 mass%)

Time (min)	***1-octanol Concentration (mass%)***	***1-decanol Concentration (mass%)***	***Total Alcohol Concentration (mass%)***	***1-octanol Adsorbent Loading (mg/g)***	***1-decanol Adsorbent Loading (mg/g)***	***Total Alcohol Adsorbent Loading (mg/g)***
0	1.60	1.71	3.31	0.00	0.00	0.00
15	1.52	1.62	3.14	12.6	12.5	25.1
30	1.45	1.57	3.02	23.1	20.7	43.8
150	1.32	1.48	2.80	42.4	34.5	76.9
240	1.30	1.45	2.75	45.9	37.8	83.7
360	1.25	1.41	2.66	53.5	44.0	97.6
450	1.23	1.41	2.64	56.2	44.3	101
1380	1.12	1.32	2.43	73.1	58.5	132
1395	1.10	1.26	2.36	75.6	67.5	143
1410	1.10	1.28	2.38	75.3	64.5	140

Table C.1-43: Kinetic data for the binary component adsorption of a 1-octanol + 1-decanol mixture onto Selexsorb CDx® (T = 45°C; IC = 0.95 mass%)

Time (min)	***1-octanol Concentration (mass%)***	***1-decanol Concentration (mass%)***	***Total Alcohol Concentration (mass%)***	***1-octanol Adsorbent Loading (mg/g)***	***1-decanol Adsorbent Loading (mg/g)***	***Total Alcohol Adsorbent Loading (mg/g)***
0	0.55	0.40	0.95	0.00	0.00	0.00
15	0.43	0.31	0.74	17.4	13.7	31.2
30	0.39	0.29	0.68	23.7	16.9	40.5
150	0.27	0.18	0.45	42.3	32.4	74.7
240	0.21	0.13	0.34	50.4	39.9	90.3
360	0.18	0.09	0.27	55.6	45.8	101
480	0.10	0.02	0.12	66.6	56.3	123
1380	0.10	0.01	0.11	67.2	57.6	125
1395	0.10	0.01	0.11	67.1	58.0	125
1410	0.09	0.00	0.09	68.0	59.7	128

Table C.1-44: Kinetic data for the binary component adsorption of a 1-octanol + 1-decanol mixture onto Selexsorb CDx® (T = 45°C; IC = 1.67 mass%)

Time (min)	1-octanol Concentration (mass%)	1-decanol Concentration (mass%)	Total Alcohol Concentration (mass%)	1-octanol Adsorbent Loading (mg/g)	1-decanol Adsorbent Loading (mg/g)	Total Alcohol Adsorbent Loading (mg/g)
0	0.76	0.92	1.67	0.00	0.00	0.00
15	0.68	0.83	1.50	12.2	13.6	25.8
30	0.61	0.80	1.41	21.8	17.7	39.5
150	0.48	0.63	1.11	42.6	42.6	85.1
240	0.45	0.63	1.08	46.2	43.2	89.5
360	0.40	0.57	0.97	53.2	52.1	105
480	0.38	0.51	0.89	56.9	60.5	117
1380	0.36	0.50	0.85	60.3	62.8	123
1395	0.35	0.50	0.85	61.0	63.0	124
1410	0.35	0.49	0.85	60.7	63.6	124

Table C.1-45: Kinetic data for the binary component adsorption of a 1-octanol + 1-decanol mixture onto Selexsorb CDx® (T = 45°C; IC = 2.78 mass%)

Time (min)	1-octanol Concentration (mass%)	1-decanol Concentration (mass%)	Total Alcohol Concentration (mass%)	1-octanol Adsorbent Loading (mg/g)	1-decanol Adsorbent Loading (mg/g)	Total Alcohol Adsorbent Loading (mg/g)
0	1.29	1.49	2.78	0.00	0.00	0.00
15	1.15	1.36	2.51	21.4	19.5	40.9
30	1.10	1.36	2.45	29.1	19.6	48.7
150	0.97	1.20	2.17	48.9	42.8	91.7
240	0.90	1.12	2.02	59.0	54.7	114
360	0.82	1.11	1.93	70.7	56.9	128
480	0.82	1.11	1.93	71.2	56.5	128
1380	0.83	1.08	1.91	69.1	61.1	130
1395	0.84	1.10	1.94	67.2	58.6	126
1410	0.83	1.12	1.95	69.9	54.8	125

C.1.2.3 *Selexsorb CD®*

C.1.2.3.1 1-hexanol + 1-decanol

Table C.1-46: Kinetic data for the binary component adsorption of a 1-hexanol + 1-decanol mixture onto Selexsorb CD® (T = 25°C; IC = 1.01 mass%)

Time (min)	*1-hexanol Concentration (mass%)*	*1-decanol Concentration (mass%)*	*Total Alcohol Concentration (mass%)*	*1-hexanol Adsorbent Loading (mg/g)*	*1-decanol Adsorbent Loading (mg/g)*	*Total Alcohol Adsorbent Loading (mg/g)*
0	0.50	0.51	1.01	0.00	0.00	0.00
15	0.43	0.45	0.88	11.1	8.6	19.7
30	0.39	0.40	0.79	16.5	16.2	32.6
150	0.29	0.32	0.61	32.1	28.3	60.3
240	0.24	0.27	0.51	39.3	36.4	75.8
360	0.18	0.20	0.37	48.2	47.2	95.4
480	0.11	0.09	0.20	58.4	63.6	122
1380	0.11	0.07	0.18	58.3	66.2	124
1395	0.13	0.08	0.22	55.0	64.0	119
1410	0.13	0.07	0.20	55.2	65.9	121

Table C.1-47: Kinetic data for the binary component adsorption of a 1-hexanol + 1-decanol mixture onto Selexsorb CD® (T = 25°C; IC = 2.43 mass%)

Time (min)	*1-hexanol Concentration (mass%)*	*1-decanol Concentration (mass%)*	*Total Alcohol Concentration (mass%)*	*1-hexanol Adsorbent Loading (mg/g)*	*1-decanol Adsorbent Loading (mg/g)*	*Total Alcohol Adsorbent Loading (mg/g)*
0	1.22	1.21	2.43	0.00	0.00	0.00
15	1.09	1.12	2.21	18.5	14.0	32.5
30	1.06	1.10	2.16	24.2	15.7	39.9
150	0.88	1.01	1.89	50.0	30.0	79.9
240	0.83	0.96	1.78	57.7	37.9	95.7
360	0.78	0.92	1.70	65.4	42.4	108
480	0.77	0.92	1.69	66.1	43.9	110
1380	0.69	0.84	1.52	79.1	55.7	135
1395	0.68	0.82	1.50	79.8	57.9	138
1410	0.67	0.82	1.49	80.8	58.0	139

Table C.1-48: Kinetic data for the binary component adsorption of a 1-hexanol + 1-decanol mixture onto Selexsorb CD® (T = 25°C; IC = 3.05 mass%)

Time (min)	1-hexanol Concentration (mass%)	1-decanol Concentration (mass%)	Total Alcohol Concentration (mass%)	1-hexanol Adsorbent Loading (mg/g)	1-decanol Adsorbent Loading (mg/g)	Total Alcohol Adsorbent Loading (mg/g)
0	1.51	1.54	3.05	0.00	0.00	0.00
15	1.43	1.47	2.91	11.9	9.55	21.5
30	1.33	1.38	2.71	27.3	24.0	51.3
150	1.26	1.31	2.58	37.6	33.6	71.2
240	1.15	1.29	2.44	55.1	36.6	91.7
360	1.07	1.25	2.32	66.3	43.2	110
1380	0.94	1.10	2.04	86.7	65.3	152
1395	0.95	1.12	2.07	84.4	62.1	147
1410	0.94	1.11	2.05	86.5	63.2	150
1415	0.95	1.11	2.07	88.8	68.8	158

Table C.1-49: Kinetic data for the binary component adsorption of a 1-hexanol + 1-decanol mixture onto Selexsorb CD® (T = 45°C; IC = 0.55 mass%)

Time (min)	1-hexanol Concentration (mass%)	1-octanol Concentration (mass%)	Total Alcohol Concentration (mass%)	1-hexanol Adsorbent Loading (mg/g)	1-octanol Adsorbent Loading (mg/g)	Total Alcohol Adsorbent Loading (mg/g)
0	0.24	0.32	0.55	0.00	0.00	0.00
15	0.16	0.21	0.37	14.0	17.7	31.7
30	0.14	0.19	0.33	16.3	21.4	37.7
150	0.07	0.08	0.16	28.3	39.7	68.0
240	0.06	0.04	0.10	30.7	47.7	78.3
360	0.04	0.00	0.04	33.3	54.3	87.6
480	0.00	0.00	0.00	40.9	54.3	95.2
1380	0.03	0.00	0.03	36.2	54.3	90.5
1395	0.00	0.00	0.00	40.9	54.3	95.2
1410	0.00	0.00	0.00	40.9	54.3	95.2

Table C.1-50: Kinetic data for the binary component adsorption of a 1-hexanol + 1-decanol mixture onto Selexsorb CD® (T = 45°C; IC = 2.29 mass%)

Time (min)	1-hexanol Concentration (mass%)	1-octanol Concentration (mass%)	Total Alcohol Concentration (mass%)	1-hexanol Adsorbent Loading (mg/g)	1-octanol Adsorbent Loading (mg/g)	Total Alcohol Adsorbent Loading (mg/g)
0	1.11	1.18	2.29	0.00	0.00	0.00
15	0.97	1.10	2.06	21.7	12.5	34.1
30	0.82	1.02	1.83	43.9	24.8	68.7
150	0.75	1.00	1.75	53.7	27.1	80.8
240	0.67	0.93	1.59	66.7	37.6	104
360	0.57	0.88	1.45	81.3	44.7	126
1380	0.56	0.84	1.40	82.6	51.5	134
1395	0.50	0.85	1.35	91.6	50.1	142
1410	0.51	0.82	1.33	89.7	54.6	144

Table C.1-51: Kinetic data for the binary component adsorption of a 1-hexanol + 1-decanol mixture onto Selexsorb CD® (T = 45°C; IC = 3.03 mass%)

Time (min)	1-hexanol Concentration (mass%)	1-octanol Concentration (mass%)	Total Alcohol Concentration (mass%)	1-hexanol Adsorbent Loading (mg/g)	1-octanol Adsorbent Loading (mg/g)	Total Alcohol Adsorbent Loading (mg/g)
0	1.45	1.58	3.03	0.00	0.00	0.00
15	1.28	1.39	2.68	25.0	28.0	53.0
30	1.27	1.47	2.74	27.6	16.4	44.0
150	1.08	1.37	2.45	55.9	31.7	87.5
240	0.98	1.29	2.27	70.5	44.1	115
360	0.96	1.23	2.19	74.1	52.4	127
480	0.93	1.23	2.16	78.1	52.3	130
1380	0.95	1.17	2.12	75.7	61.8	138
1395	0.93	1.13	2.06	79.1	66.9	146
1410	0.98	1.17	2.15	70.3	62.0	132

C.1.2.3.2 1-hexanol + 1-octanol

Table C.1-52: Kinetic data for the binary component adsorption of a 1-hexanol + 1-octanol mixture onto Selexsorb CD® (T = 25°C; IC = 1.02 mass%)

Time (min)	***1-hexanol Concentra-tion (mass%)***	***1-octanol Concentra-tion (mass%)***	***Total Alcohol Concentra-tion (mass%)***	***1-hexanol Adsorbent Loading (mg/g)***	***1-octanol Adsorbent Loading (mg/g)***	***Total Alcohol Adsorbent Loading (mg/g)***
0	0.49	0.53	1.02	0.00	0.00	0.00
15	0.38	0.44	0.81	13.4	10.4	23.8
30	0.35	0.45	0.81	16.3	8.4	24.7
150	0.31	0.35	0.66	21.0	20.7	41.7
230	0.23	0.28	0.50	30.9	28.7	59.6
350	0.18	0.24	0.42	36.1	33.6	69.7
450	0.17	0.22	0.39	37.3	36.0	73.3
1380	0.09	0.10	0.19	47.0	49.5	96.5
1395	0.09	0.10	0.19	47.0	49.5	96.5
1410	0.10	0.10	0.20	46.0	49.3	95.3

Table C.1-53: Kinetic data for the binary component adsorption of a 1-hexanol + 1-octanol mixture onto Selexsorb CD® (T = 25°C; IC = 1.75 mass%)

Time (min)	***1-hexanol Concentra-tion (mass%)***	***1-octanol Concentra-tion (mass%)***	***Total Alcohol Concentra-tion (mass%)***	***1-hexanol Adsorbent Loading (mg/g)***	***1-octanol Adsorbent Loading (mg/g)***	***Total Alcohol Adsorbent Loading (mg/g)***
0	0.80	0.95	1.75	0.00	0.00	0.00
15	0.78	0.88	1.66	2.61	7.42	10.0
30	0.71	0.79	1.49	10.5	17.4	27.9
150	0.47	0.61	1.07	36.3	36.8	73.1
230	0.44	0.53	0.97	39.3	44.8	84.1
350	0.44	0.51	0.95	39.2	46.8	86.0
450	0.40	0.47	0.87	43.8	51.6	95.4
1380	0.31	0.44	0.75	53.7	54.6	108
1395	0.29	0.42	0.71	55.4	56.4	112
1410	0.32	0.45	0.77	52.2	53.8	106

Table C.1-54: Kinetic data for the binary component adsorption of a 1-hexanol + 1-octanol mixture onto Selexsorb CD® (T = 25°C; IC = 3.12 mass%)

Time (min)	1-hexanol Concentration (mass%)	1-octanol Concentration (mass%)	Total Alcohol Concentration (mass%)	1-hexanol Adsorbent Loading (mg/g)	1-octanol Adsorbent Loading (mg/g)	Total Alcohol Adsorbent Loading (mg/g)
0	1.53	1.60	3.12	0.00	0.00	0.00
15	1.44	1.56	3.00	12.8	4.8	17.6
30	1.42	1.54	2.96	15.8	8.3	24.0
150	1.25	1.37	2.63	41.0	33.3	74.3
240	1.19	1.33	2.52	50.4	39.3	89.7
360	1.12	1.27	2.39	60.3	49.2	109
450	1.11	1.26	2.37	62.8	50.0	113
1380	1.01	1.17	2.18	77.4	63.1	140
1395	1.01	1.17	2.18	76.7	64.0	141
1410	1.02	1.20	2.21	76.0	59.8	136

Table C.1-55: Kinetic data for the binary component adsorption of a 1-hexanol + 1-octanol mixture onto Selexsorb CD® (T = 45°C; IC = 1.03 mass%)

Time (min)	1-hexanol Concentration (mass%)	1-octanol Concentration (mass%)	Total Alcohol Concentration (mass%)	1-hexanol Adsorbent Loading (mg/g)	1-octanol Adsorbent Loading (mg/g)	Total Alcohol Adsorbent Loading (mg/g)
0	0.47	0.56	1.03	0.00	0.00	0.00
15	0.36	0.44	0.80	16.2	17.6	33.7
30	0.37	0.42	0.79	15.1	20.9	36.0
150	0.21	0.28	0.50	38.4	40.7	79.0
240	0.20	0.25	0.45	40.1	46.0	86.2
360	0.15	0.20	0.36	47.6	52.7	100
480	0.16	0.19	0.35	47.1	54.1	101
1380	0.15	0.16	0.31	48.4	59.2	108
1395	0.15	0.17	0.32	47.6	57.8	105
1410	0.14	0.17	0.31	48.6	57.7	106

Table C.1-56: Kinetic data for the binary component adsorption of a 1-hexanol + 1-octanol mixture onto Selexsorb CD® (T = 45°C; IC = 1.99 mass%)

Time (min)	1-hexanol Concentration (mass%)	1-octanol Concentration (mass%)	Total Alcohol Concentration (mass%)	1-hexanol Adsorbent Loading (mg/g)	1-octanol Adsorbent Loading (mg/g)	Total Alcohol Adsorbent Loading (mg/g)
0	0.91	1.08	1.99	0.00	0.00	0.00
15	0.77	1.01	1.78	21.0	10.8	31.8
30	0.73	0.93	1.66	27.4	23.3	50.7
150	0.61	0.79	1.40	44.8	44.1	89.0
240	0.52	0.71	1.22	59.2	56.9	116
360	0.48	0.65	1.13	64.5	65.8	130
480	0.33	0.55	0.88	86.9	79.9	167
1380	0.34	0.56	0.90	85.2	78.8	164
1395	0.36	0.53	0.90	81.8	82.9	165
1410	0.32	0.54	0.86	89.1	81.7	171

Table C.1-57: Kinetic data for the binary component adsorption of a 1-hexanol + 1-octanol mixture onto Selexsorb CD® (T = 45°C; IC = 3.38 mass%)

Time (min)	1-hexanol Concentration (mass%)	1-octanol Concentration (mass%)	Total Alcohol Concentration (mass%)	1-hexanol Adsorbent Loading (mg/g)	1-octanol Adsorbent Loading (mg/g)	Total Alcohol Adsorbent Loading (mg/g)
0	1.67	1.72	3.38	0.00	0.00	0.00
15	1.49	1.63	3.12	26.8	13.2	40.1
30	1.46	1.57	3.03	31.0	22.4	53.4
150	1.26	1.38	2.64	61.4	50.1	111
240	1.17	1.37	2.54	74.3	52.0	126
360	1.10	1.27	2.37	85.6	66.7	152
1380	1.07	1.28	2.35	89.9	65.6	155
1395	1.03	1.25	2.28	95.4	70.6	166
1410	1.03	1.26	2.29	96.0	69.1	165

C.1.2.3.3 1-octanol + 1-decanol

Table C.1-58: Kinetic data for the binary component adsorption of a 1-octanol + 1-decanol mixture onto Selexsorb CD® (T = 25°C; IC = 0.98 mass%)

Time (min)	*1-octanol Concentration (mass%)*	*1-decanol Concentration (mass%)*	*Total Alcohol Concentration (mass%)*	*1-octanol Adsorbent Loading (mg/g)*	*1-decanol Adsorbent Loading (mg/g)*	*Total Alcohol Adsorbent Loading (mg/g)*
0	0.53	0.46	0.98	0.00	0.00	0.00
15	0.45	0.40	0.85	8.23	6.27	14.5
30	0.45	0.39	0.84	8.38	7.20	15.6
150	0.32	0.28	0.60	21.7	19.2	40.9
230	0.32	0.36	0.67	22.3	10.7	33.0
350	0.26	0.21	0.46	28.6	26.6	55.2
450	0.23	0.18	0.40	31.7	29.8	61.5
1380	0.11	0.04	0.16	43.9	44.0	87.9
1395	0.12	0.05	0.17	42.9	43.5	86.4
1410	0.11	0.05	0.16	43.9	43.4	87.2

Table C.1-59: Kinetic data for the binary component adsorption of a 1-octanol + 1-decanol mixture onto Selexsorb CD® (T = 25°C; IC = 2.10 mass%)

Time (min)	*1-octanol Concentration (mass%)*	*1-decanol Concentration (mass%)*	*Total Alcohol Concentration (mass%)*	*1-octanol Adsorbent Loading (mg/g)*	*1-decanol Adsorbent Loading (mg/g)*	*Total Alcohol Adsorbent Loading (mg/g)*
0	1.09	1.01	2.10	0.00	0.00	0.00
15	1.00	0.96	1.96	12.5	7.89	20.4
30	0.99	0.92	1.91	14.7	13.0	27.7
150	0.84	0.83	1.68	36.7	26.4	63.1
240	0.79	0.80	1.59	43.9	32.0	75.8
360	0.75	0.74	1.49	50.5	39.9	90.5
1380	0.63	0.69	1.32	67.7	48.0	116
1395	0.67	0.69	1.36	61.9	48.5	110
1410	0.69	0.69	1.37	59.7	48.5	108

Table C.1-60: Kinetic data for the binary component adsorption of a 1-octanol + 1-decanol mixture onto Selexsorb CD® (T = 25°C; IC = 3.10 mass%)

Time (min)	***1-octanol Concentra-tion (mass%)***	***1-decanol Concentra-tion (mass%)***	***Total Alcohol Concentra-tion (mass%)***	***1-octanol Adsorbent Loading (mg/g)***	***1-decanol Adsorbent Loading (mg/g)***	***Total Alcohol Adsorbent Loading (mg/g)***
0	1.53	1.57	3.10	0.00	0.00	0.00
15	1.50	1.56	3.07	3.45	0.91	4.36
30	1.47	1.54	3.01	7.68	5.06	12.7
150	1.32	1.42	2.74	31.5	21.8	53.2
240	1.22	1.36	2.58	45.7	31.4	77.1
360	1.13	1.26	2.39	58.5	46.4	105
390	1.09	1.24	2.33	64.4	49.2	114
1380	0.96	1.10	2.06	84.2	70.3	154
1395	0.94	1.06	2.00	87.6	75.5	163
1410	0.95	1.06	2.01	86.1	76.4	163

Table C.1-61: Kinetic data for the binary component adsorption of a 1-octanol + 1-decanol mixture onto Selexsorb CD® (T = 45°C; IC = 1.18 mass%)

Time (min)	***1-octanol Concentra-tion (mass%)***	***1-decanol Concentra-tion (mass%)***	***Total Alcohol Concentra-tion (mass%)***	***1-octanol Adsorbent Loading (mg/g)***	***1-decanol Adsorbent Loading (mg/g)***	***Total Alcohol Adsorbent Loading (mg/g)***
0	0.60	0.58	1.18	0.00	0.00	0.00
15	0.59	0.57	1.16	1.33	1.22	2.54
30	0.52	0.50	1.03	12.0	10.0	22.0
150	0.45	0.46	0.91	22.2	16.5	38.7
240	0.31	0.33	0.64	41.4	35.0	76.4
360	0.28	0.28	0.55	46.8	42.6	89.4
480	0.24	0.25	0.49	51.3	46.8	98.1
1380	0.22	0.21	0.42	54.9	52.5	107
1395	0.15	0.14	0.29	64.1	62.1	126
1410	0.16	0.12	0.28	63.7	64.6	128

Table C.1-62: Kinetic data for the binary component adsorption of a 1-octanol + 1-decanol mixture onto Selexsorb CD® (T = 45°C; IC = 2.06 mass%)

Time (min)	1-octanol Concentration (mass%)	1-decanol Concentration (mass%)	Total Alcohol Concentration (mass%)	1-octanol Adsorbent Loading (mg/g)	1-decanol Adsorbent Loading (mg/g)	Total Alcohol Adsorbent Loading (mg/g)
0	1.00	1.07	2.06	0.00	0.00	0.00
15	0.89	0.97	1.86	16.5	14.2	30.6
30	0.86	0.96	1.82	21.1	15.3	36.4
150	0.70	0.78	1.48	45.1	43.7	88.9
240	0.64	0.74	1.38	54.8	49.0	104
360	0.60	0.70	1.30	60.4	55.7	116
480	0.52	0.64	1.16	72.6	64.7	137
1380	0.51	0.61	1.12	74.7	69.0	144
1395	0.52	0.63	1.15	72.6	66.1	139
1410	0.50	0.56	1.07	75.1	76.3	151

Table C.1-63: Kinetic data for the binary component adsorption of a 1-octanol + 1-decanol mixture onto Selexsorb CD® (T = 45°C; IC = 3.00 mass%)

Time (min)	1-octanol Concentration (mass%)	1-decanol Concentration (mass%)	Total Alcohol Concentration (mass%)	1-octanol Adsorbent Loading (mg/g)	1-decanol Adsorbent Loading (mg/g)	Total Alcohol Adsorbent Loading (mg/g)
0	1.52	1.48	3.00	0.00	0.00	0.00
15	1.44	1.45	2.89	11.8	3.9	15.7
30	1.37	1.41	2.78	22.4	10.0	32.3
150	1.18	1.23	2.40	51.6	37.5	89.1
240	1.14	1.25	2.39	56.4	34.6	90.9
360	1.11	1.17	2.28	61.5	46.3	108
480	1.07	1.11	2.18	67.8	54.7	123
1380	1.04	1.07	2.10	72.7	61.7	134
1395	1.02	1.12	2.14	74.4	54.0	128
1410	1.02	1.09	2.11	74.7	58.3	133

C.2 Equilibrium Data

C.2.1 Single Component Systems

For the single component adsorption, the equilibrium data at both temperatures is provided. Note that the data at 25°C was obtained from a study conducted by Groenewald and was not measured in this study [8]. It was, however, included here since additional data points measured in this study were added to the datasets of Groenewald.

Table C.2-1: Equilibrium data for the single component adsorption of 1-hexanol, 1-octanol and 1-decanol onto Activated Alumina F220

1-hexanol				1-octanol				1-decanol			
25°C		45°C		25°C		45°C		25°C		45°C	
C_e (mg/mL)	q_e (mg/g)	C_e (mg/mL)	q_e (mg/g)	C_e (mg/mL)	q_e (mg/g)	C_e (mg/mL)	q_e (mg/g)	C_e (mg/mL)	q_e (mg/g)	C_e (mg/mL)	q_e (mg/g)
0.00	0.00	0.00	0.00	0.00	0.00	0.00	0.00	0.00	0.00	0.00	0.00
0.40	53.6	0.25	60.0	0.93	63.4	0.43	72.8	0.97	81.6	0.58	62.0
2.19	97.2	0.70	87.1	2.82	91.7	1.11	91.2	3.27	94.8	0.96	98.1
3.13	104	2.51	98.5	6.35	106	2.05	113	4.43	109	1.78	111
4.11	112	4.38	96.5			4.22	110			4.69	119
5.47	110	5.47	110			6.37	113			5.76	116

Table C.2-2: Equilibrium data for the single component adsorption of 1-hexanol, 1-octanol and 1-decanol onto Selexsorb CDx®

1-hexanol				1-octanol				1-decanol			
25°C		45°C		25°C		45°C		25°C		45°C	
C_e (mg/mL)	q_e (mg/g)	C_e (mg/mL)	q_e (mg/g)	C_e (mg/mL)	q_e (mg/g)	C_e (mg/mL)	q_e (mg/g)	C_e (mg/mL)	q_e (mg/g)	C_e (mg/mL)	q_e (mg/g)
0.00	0.00	0.00	0.00	0.00	0.00	0.00	0.00	0.00	0.00	0.00	0.00
0.84	64.6	0.44	73.2	1.22	56.9	0.41	58.0	0.68	58.2	0.28	73.1
2.79	84.4	0.57	60.2	4.22	72.7	1.26	86.2	2.92	85.2	0.52	95.2
5.58	92.0	2.05	112	7.49	83.7	1.97	108	6.96	82.3	1.86	123
		2.40	116			4.41	114	7.11	78.7	3.74	134
		6.40	122			5.36	110			5.88	142

Table C.2-3: Equilibrium data for the single component adsorption of 1-hexanol, 1-octanol and 1-decanol onto Selexsorb CD®

1-hexanol				1-octanol				1-decanol			
25°C		45°C		25°C		45°C		25°C		45°C	
C_e (mg/mL)	q_e (mg/g)	C_e (mg/mL)	q_e (mg/g)	C_e (mg/mL)	q_e (mg/g)	C_e (mg/mL)	q_e (mg/g)	C_e (mg/mL)	q_e (mg/g)	C_e (mg/mL)	q_e (mg/g)
0.00	0.00	0.00	0.00	0.00	0.00	0.00	0.00	0.00	0.00	0.00	0.00
0.48	63.9	0.28	59.2	6.68	88.0	0.16	57.5	0.68	59.7	0.45	69.6
2.63	89.0	0.57	93.0	3.70	73.0	0.59	98.0	2.87	86.8	0.75	92.6
5.27	96.7	1.36	105	1.25	55.1	2.17	120	4.10	72.6	2.35	129
		1.57	107			2.75	124	5.56	82.8	2.74	128
		3.52	116			5.51	114	6.38	92.8	5.79	128
		5.91	120								

C.2.2 Binary Component Systems

C.2.2.1 *Activated Alumina F220*

Table C.2-4: Equilibrium data for the binary component adsorption of a 1-hexanol + 1-decanol mixture onto Activated Alumina F220

25°C				45°C			
1-hexanol C_e (mg/mL)	1-decanol C_e (mg/mL)	1-hexanol q_e (mg/g)	1-decanol q_e (mg/g)	1-hexanol C_e (mg/mL)	1-decanol C_e (mg/mL)	1-hexanol q_e (mg/g)	1-decanol q_e (mg/g)
0.00	0.00	0.00	0.00	0.00	0.00	0.00	0.00
1.94	3.01	57.4	55.1	2.09	3.15	70.2	64.1
4.41	12.0	55.8	91.9	1.95	2.79	54.4	43.4
9.17	3.32	95.4	26.2	3.82	5.47	84.2	68.7
1.62	0.09	121.66	50.1	4.87	6.33	89.8	52.1
3.82	1.36	134.28	49.0	7.00	8.92	85.0	60.2
2.47	11.6	34.4	87.8	2.28	13.74	39.2	104
0.90	2.47	44.7	87.8	1.29	5.36	31.5	92.7
1.19	4.68	39.5	108	3.86	0.77	89.7	23.1
5.94	7.10	80.6	48.0	3.60	1.18	99.5	34.0
				14.3	4.26	119	21.0
				0.77	0.58	36.8	74.7
				3.39	4.57	74.8	72.8
				7.26	9.05	75.9	51.0

Table C.2-5: Equilibrium data for the binary component adsorption of a 1-hexanol + 1-octanol mixture onto Activated Alumina F220

25°C				45°C			
1-hexanol C_e (mg/mL)	1-octanol C_e (mg/mL)	1-hexanol q_e (mg/g)	1-octanol q_e (mg/g)	1-hexanol C_e (mg/mL)	1-octanol C_e (mg/mL)	1-hexanol q_e (mg/g)	1-octanol q_e (mg/g)
0.00	0.00	0.00	0.00	0.00	0.00	0.00	0.00
1.39	1.49	48.0	53.6	0.52	0.17	65.2	45.4
3.56	4.09	68.5	65.5	0.92	0.89	59.2	59.1
8.64	9.80	68.4	62.8	0.99	1.31	46.1	54.9
9.76	3.54	105	32.9	2.08	0.74	86.2	28.6
2.03	0.71	103	35.7	2.51	1.07	86.9	29.8
4.22	1.60	101	30.8	1.65	2.25	64.5	58.1
2.85	9.44	36.1	93.3	0.32	3.18	10.5	136
1.28	6.52	32.0	100	1.63	2.70	65.3	72.1
8.97	3.24	85.8	26.2	2.33	2.96	62.2	60.4
2.99	3.11	86.5	69.7	1.17	4.62	31.4	106
				4.47	5.66	68.3	60.4
				5.33	6.70	73.9	62.3
				2.71	9.66	39.0	98.5
				8.86	3.87	101	30.9
				2.35	13.7	37.4	116

Table C.2-6: Equilibrium data for the binary component adsorption of a 1-octanol + 1-decanol mixture onto Activated Alumina F220

25°C				45°C			
1-octanol C_e (mg/mL)	1-decanol C_e (mg/mL)	1-octanol q_e (mg/g)	1-decanol q_e (mg/g)	1-octanol C_e (mg/mL)	1-decanol C_e (mg/mL)	1-octanol q_e (mg/g)	1-decanol q_e (mg/g)
0.00	0.00	0.00	0.00	0.00	0.00	0.00	0.00
1.94	0.75	59.5	57.6	0.75	0.46	56.5	57.9
3.73	4.06	77.1	60.9	2.46	2.98	63.0	67.7
6.79	7.30	76.7	67.0	1.52	1.68	63.8	61.5
9.03	3.63	109	37.0	4.33	5.58	73.2	55.4
5.96	2.26	98.3	46.3	9.98	3.24	104	25.8
2.88	10.2	40.6	102	7.38	8.66	75.6	53.7
0.90	3.36	35.8	111	3.17	16.1	33.3	97.4
7.71	4.76	94.2	45.2	2.44	9.02	33.8	73.5
2.60	2.53	71.6	68.7	1.11	2.67	46.1	115
				6.72	2.05	111	27.5
				3.66	0.44	101	28.3
				0.55	0.10	47.2	90.7
				4.33	5.44	67.4	68.5
				7.59	8.97	74.7	54.9

C.2.2.2 *Selexsorb CDx®*

Table C.2-7: Equilibrium data for the binary component adsorption of a 1-hexanol + 1-decanol mixture onto Selexsorb CDx®

25°C				45°C			
1-hexanol C_e (mg/mL)	1-decanol C_e (mg/mL)	1-hexanol q_e (mg/g)	1-decanol q_e (mg/g)	1-hexanol C_e (mg/mL)	1-decanol C_e (mg/mL)	1-hexanol q_e (mg/g)	1-decanol q_e (mg/g)
0.00	0.00	0.00	0.00	0.00	0.00	0.00	0.00
1.78	1.41	53.1	62.6	1.78	1.41	53.1	62.6
4.24	5.33	70.9	52.2	4.24	5.33	70.9	52.2
6.68	9.71	57.2	67.5	6.68	9.71	57.2	67.5
3.75	1.43	103.48	36.3	3.75	1.43	103	36.3
8.53	3.78	105.75	24.4	8.53	3.78	106	24.4
2.10	6.76	48.6	87.8	2.10	6.76	48.6	87.8
6.70	7.07	75.5	40.5	1.10	9.63	24.2	117
1.10	9.63	24.2	117	1.81	4.95	37.1	88.6
1.81	4.95	37.1	88.6	2.18	3.29	65.8	60.8
2.18	3.29	65.8	60.8	6.70	7.07	75.5	40.5

Table C.2-8: Equilibrium data for the binary component adsorption of a 1-hexanol + 1-octanol mixture onto Selexsorb CDx®

25°C				45°C			
1-hexanol C_e (mg/mL)	1-octanol C_e (mg/mL)	1-hexanol q_e (mg/g)	1-octanol q_e (mg/g)	1-hexanol C_e (mg/mL)	1-octanol C_e (mg/mL)	1-hexanol q_e (mg/g)	1-octanol q_e (mg/g)
0.00	0.00	0.00	0.00	0.00	0.00	0.00	0.00
2.73	2.87	44.4	37.3	0.27	0.12	34.6	35.8
3.86	4.31	73.0	60.9	0.98	1.46	46.5	54.3
8.09	8.93	70.8	63.3	2.32	2.86	66.8	53.5
8.44	3.29	97.8	27.7	1.22	1.23	44.5	43.5
1.46	0.44	83.2	27.5	1.46	2.04	67.1	65.6
6.38	2.30	116	43.9	3.96	5.35	80.2	60.9
3.34	11.0	30.4	70.2	6.27	8.34	72.6	43.5
1.47	5.86	41.5	107	7.08	9.16	84.9	52.9
6.30	7.11	67.0	53.0	2.27	13.5	36.7	100
0.50	1.32	37.1	123	0.02	3.92	50.0	74.8
1.02	3.85	55.0	141	0.00	0.46	29.3	83.5
3.69	1.48	88.9	26.6	4.64	1.75	112	27.2
1.76	5.28	35.8	80.6	2.32	1.00	76.3	23.7
				6.67	2.33	97.3	20.6

Table C.2-9: Equilibrium data for the binary component adsorption of a 1-octanol + 1-decanol mixture onto Selexsorb CDx®

25°C				45°C			
1-octanol C_e (mg/mL)	1-decanol C_e (mg/mL)	1-octanol q_e (mg/g)	1-decanol q_e (mg/g)	1-octanol C_e (mg/mL)	1-decanol C_e (mg/mL)	1-octanol q_e (mg/g)	1-decanol q_e (mg/g)
0.00	0.00	0.00	0.00	0.00	0.00	0.00	0.00
2.20	1.53	50.7	62.8	0.70	0.05	67.7	58.7
3.39	3.77	59.4	56.4	2.66	3.71	60.7	63.1
8.43	9.73	72.1	61.5	6.17	8.31	70.4	57.5
8.04	3.06	103	33.2	0.80	0.87	61.1	63.4
9.75	3.16	107	33.6	2.51	3.15	63.4	66.4
3.93	1.15	78.2	38.4	0.80	0.23	44.5	53.2
2.49	9.73	34.5	90.2	2.21	2.53	57.6	50.2
1.12	3.50	45.0	92.2	4.04	5.36	74.4	71.6
0.65	1.76	27.6	82.0	5.36	5.95	80.7	64.4
5.93	6.91	79.2	75.1	1.99	7.71	33.6	79.4
2.42	2.17	67.5	52.4	2.19	8.35	34.2	77.1
				2.48	9.01	55.6	125
				10.79	6.11	95.7	35.3
				3.83	1.06	107	30.1

C.2.2.3 *Selexsorb CD®*

Table C.2-10: Equilibrium data for the binary component adsorption of a 1-hexanol + 1-decanol mixture onto Selexsorb CD®

25°C				45°C			
1-hexanol C_e (mg/mL)	1-decanol C_e (mg/mL)	1-hexanol q_e (mg/g)	1-decanol q_e (mg/g)	1-hexanol C_e (mg/mL)	1-decanol C_e (mg/mL)	1-hexanol q_e (mg/g)	1-decanol q_e (mg/g)
0.00	0.00	0.00	0.00	0.00	0.00	0.00	0.00
2.07	3.20	68.8	64.0	0.94	0.55	56.1	65.6
1.16	1.85	71.5	67.1	5.11	6.19	79.9	57.2
3.77	5.71	90.9	58.2	7.04	8.30	86.6	64.9
5.37	7.39	84.3	40.8	3.89	1.34	101	33.1
7.33	11.2	83.3	40.0	10.7	3.38	74.1	35.9
1.94	9.33	45.6	84.3	1.68	0.38	103	48.1
0.36	0.20	33.1	121	1.18	5.34	50.0	87.9
8.59	3.67	105	18.2	2.19	10.0	50.6	104
3.63	1.28	97.4	26.2	0.59	1.67	35.1	104
				2.18	3.51	61.8	66.3
				4.88	6.99	90.4	59.8

Table C.2-11: Equilibrium data for the binary component adsorption of a 1-hexanol + 1-octanol mixture onto Selexsorb CD®

25°C				45°C			
1-hexanol C_e (mg/mL)	1-octanol C_e (mg/mL)	1-hexanol q_e (mg/g)	1-octanol q_e (mg/g)	1-hexanol C_e (mg/mL)	1-octanol C_e (mg/mL)	1-hexanol q_e (mg/g)	1-octanol q_e (mg/g)
0.00	0.00	0.00	0.00	0.00	0.00	0.00	0.00
0.69	0.76	46.4	49.3	0.38	0.27	62.7	62.4
2.32	3.32	53.8	54.9	1.46	2.00	68.7	63.7
7.53	8.77	78.3	63.8	1.88	2.63	71.0	68.5
8.26	3.43	114	31.2	3.58	5.01	77.2	66.7
0.44	0.04	101	33.0	4.82	6.13	87.1	67.1
3.49	1.15	162	42.4	1.63	2.70	65.3	72.1
3.10	10.8	34.2	79.8	2.35	13.7	37.4	116
3.38	11.4	45.4	91.9	1.35	5.63	37.3	95.3
8.14	3.13	108	28.2	4.99	1.83	97.7	27.0
5.63	6.69	81.7	66.7	7.77	2.87	108	25.8
2.38	2.85	64.6	59.3	7.52	3.71	120	28.3

Table C.2-12: Equilibrium data for the binary component adsorption of a 1-octanol + 1-decanol mixture onto Selexsorb CD®

25°C				45°C			
1-octanol C_e (mg/mL)	1-decanol C_e (mg/mL)	1-octanol q_e (mg/g)	1-decanol q_e (mg/g)	1-octanol C_e (mg/mL)	1-decanol C_e (mg/mL)	1-octanol q_e (mg/g)	1-decanol q_e (mg/g)
0.00	0.00	0.00	0.00	0.00	0.00	0.00	0.00
0.87	0.36	43.5	43.5	0.38	0.27	62.7	62.4
4.99	5.15	63.1	48.3	1.46	2.00	68.7	63.7
7.91	8.64	70.6	62.5	1.88	2.63	71.0	68.5
5.76	1.75	109	45.3	3.58	5.01	77.2	66.7
9.26	2.92	111	44.8	4.82	6.13	87.1	67.1
2.30	8.51	45.0	105	1.63	2.70	65.3	72.1
0.71	3.19	32.9	120	2.35	13.7	37.4	116
0.69	3.03	26.2	95.4	1.35	5.63	37.3	95.3
3.86	1.00	92.6	25.2	4.99	1.83	97.7	27.0
2.35	2.34	70.1	62.1	7.77	2.87	108	25.8
5.81	7.26	65.8	61.3	7.52	3.71	120	28.3

Appendix D: Processed Data

Appendix Contents

D.1 Single Component Adsorption

D.1.1 Activated Alumina F220

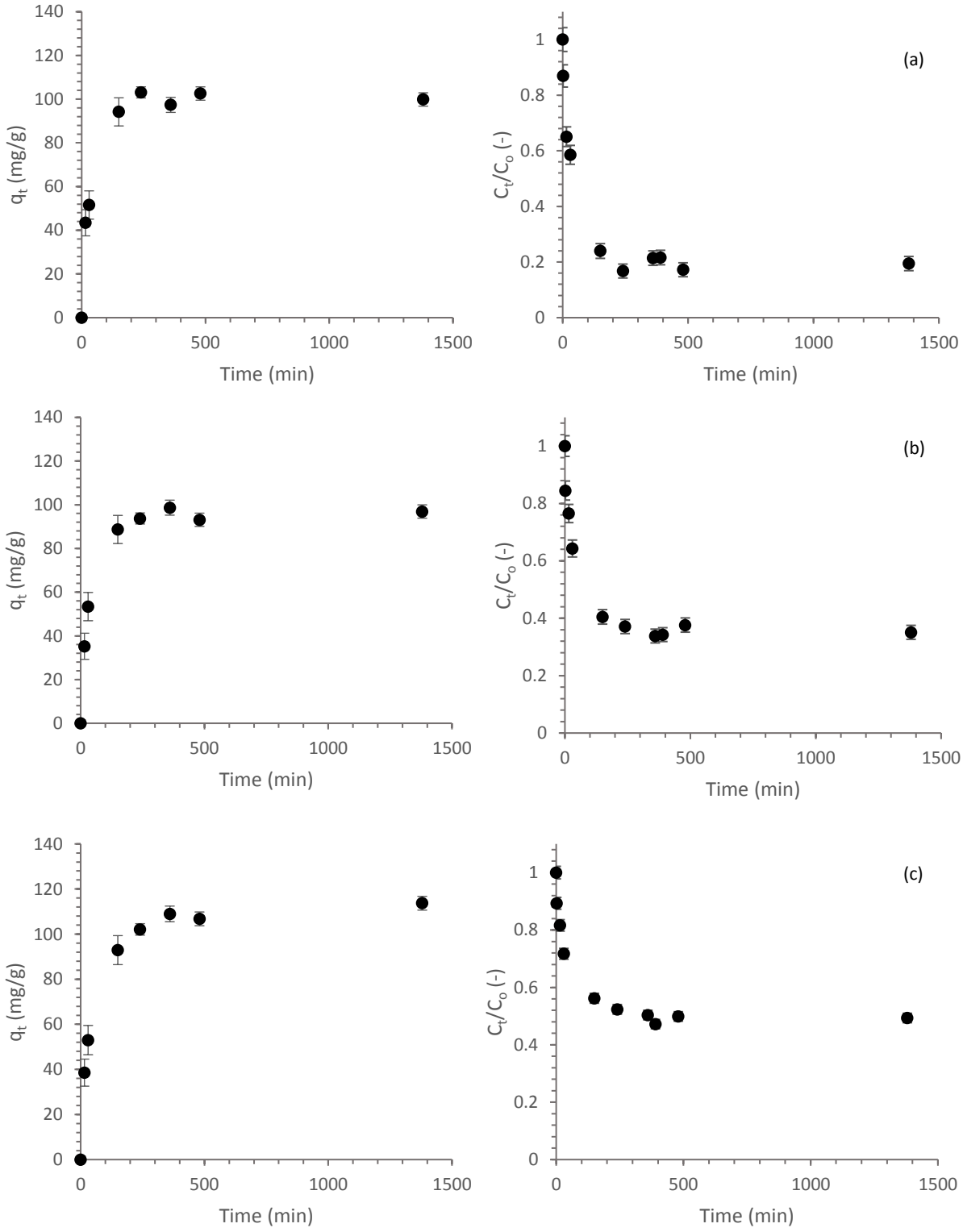

Figure D.1-1: Time profiles (left) and corresponding concentration decay plots (right) for the single component adsorption of 1-hexanol onto AA-F220, at 45°C, and initial adsorbate concentrations of (a) 0.85 mass%; (b) 1.01 mass%; and, (c) 1.51 mass%

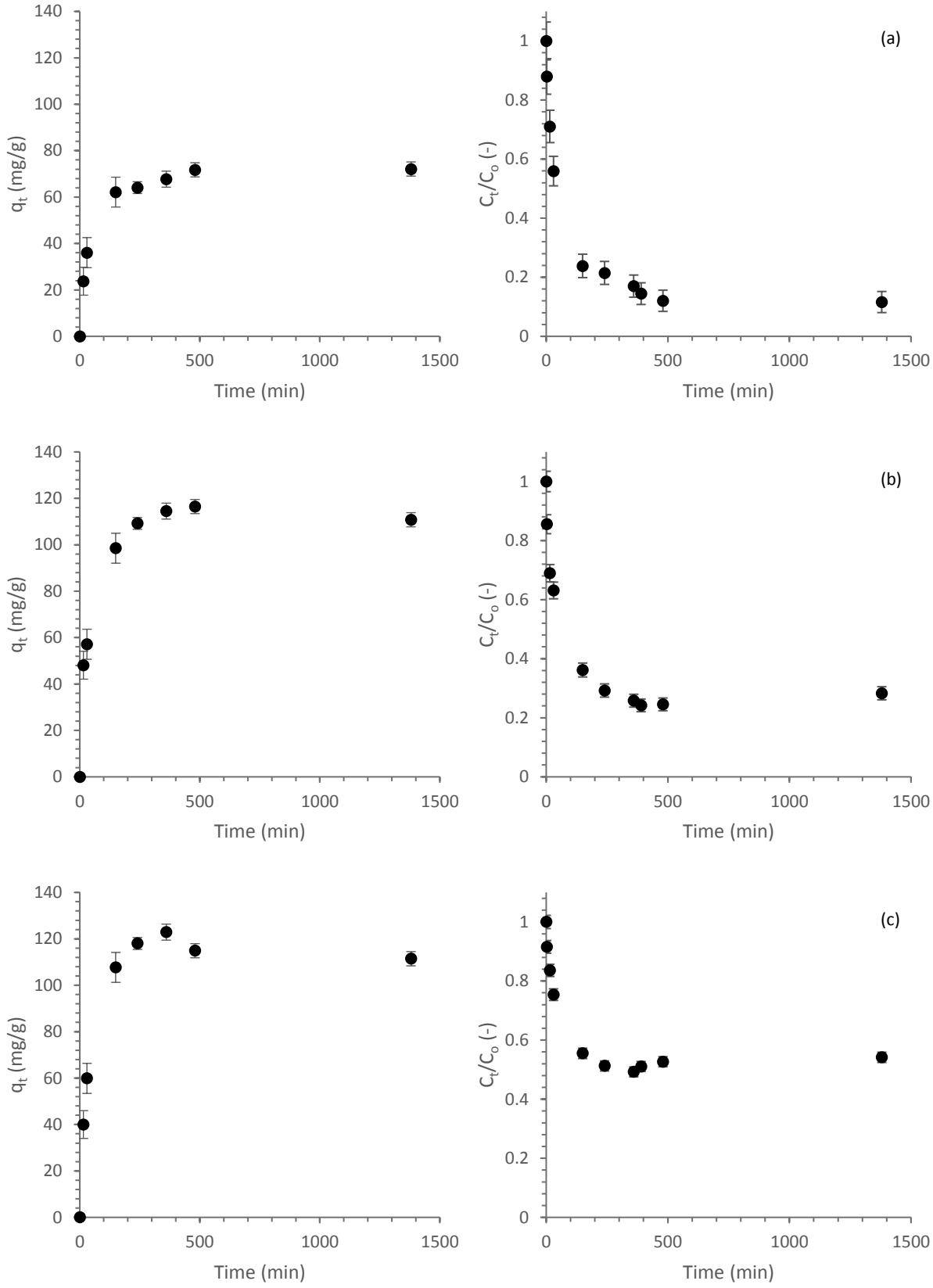

Figure D.1-2: Time profiles (left) and corresponding concentration decay plots (right) for the single component adsorption of 1-octanol onto AA-F220, at 45°C, and initial adsorbate concentrations of (a) 0.56 mass%; (b) 1.05 mass%; and, (c) 1.61 mass%

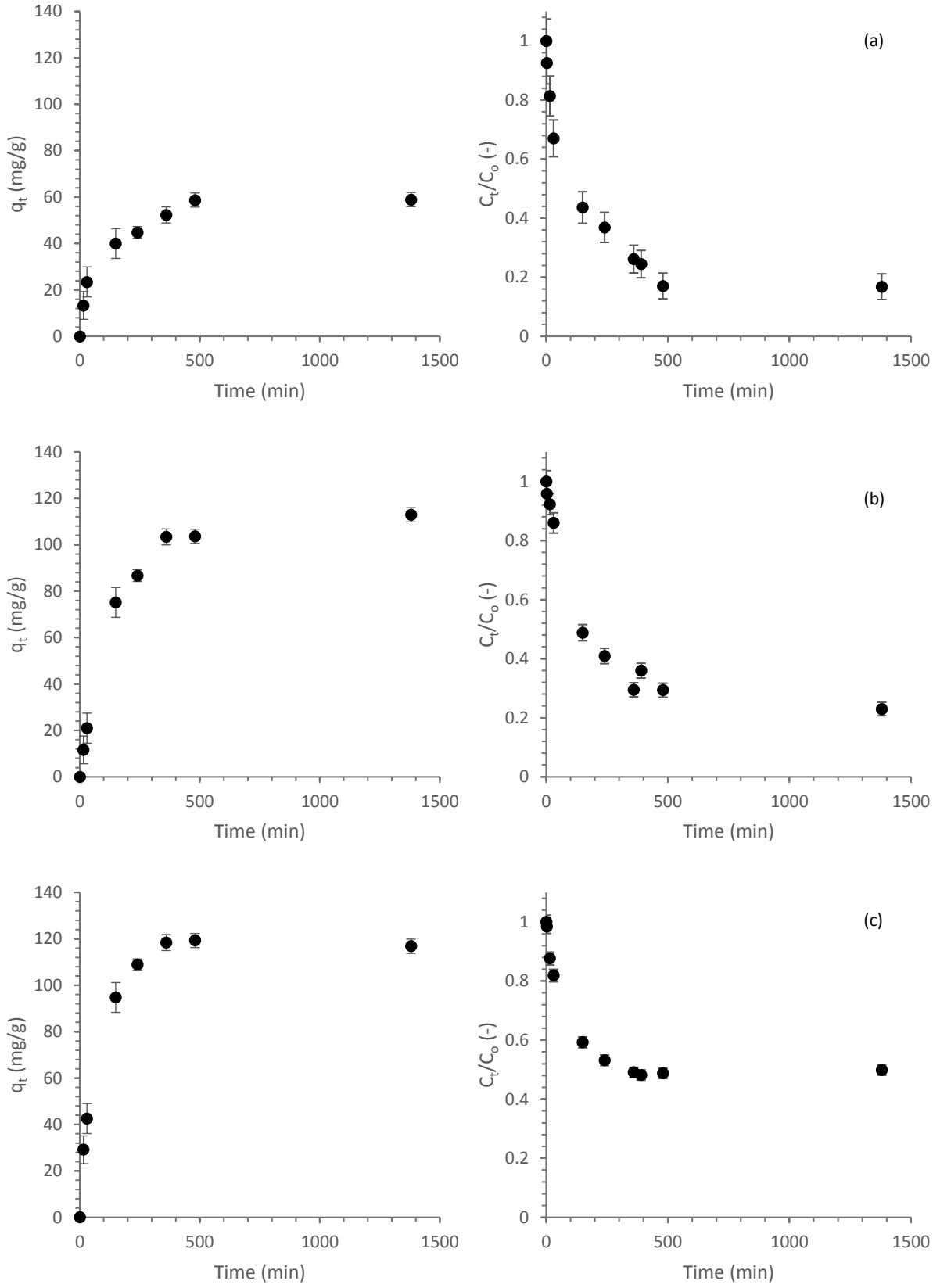

Figure D.1-3: Time profiles (left) and corresponding concentration decay plots (right) for the single component adsorption of 1-decanol onto AA-F220, at 45°C, and initial adsorbate concentrations of (a) 0.49 mass%; (b) 0.98 mass%; and, (c) 1.56 mass%

D.1.2 Selexsorb CDx®

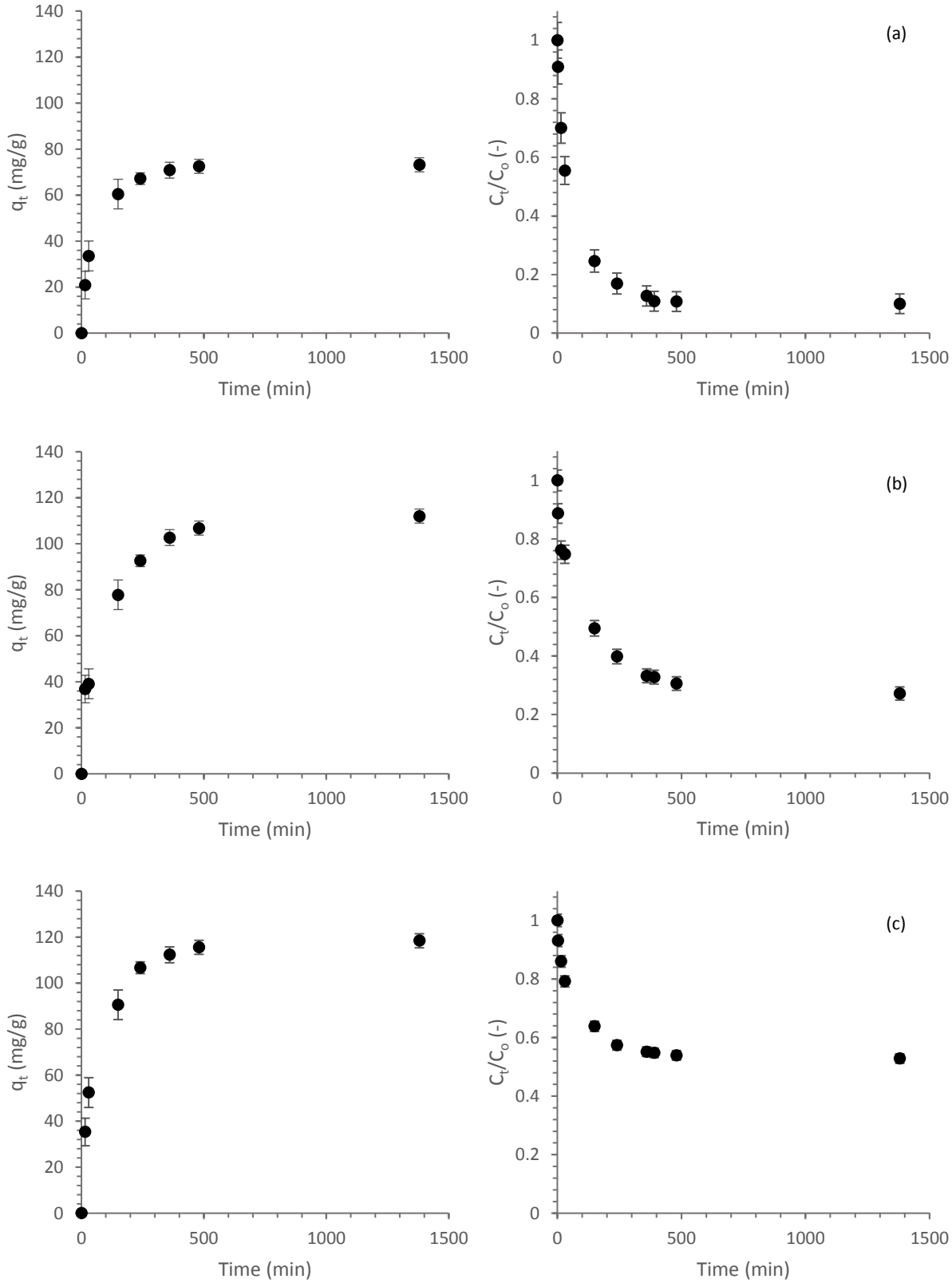

Figure D.1-4: Time profiles (left) and corresponding concentration decay plots (right) for the single component adsorption of 1-hexanol onto SCDX, at 45°C, and initial adsorbate concentrations of (a) 0.59 mass%; (b) 1.02 mass%; and, (c) 1.71 mass%

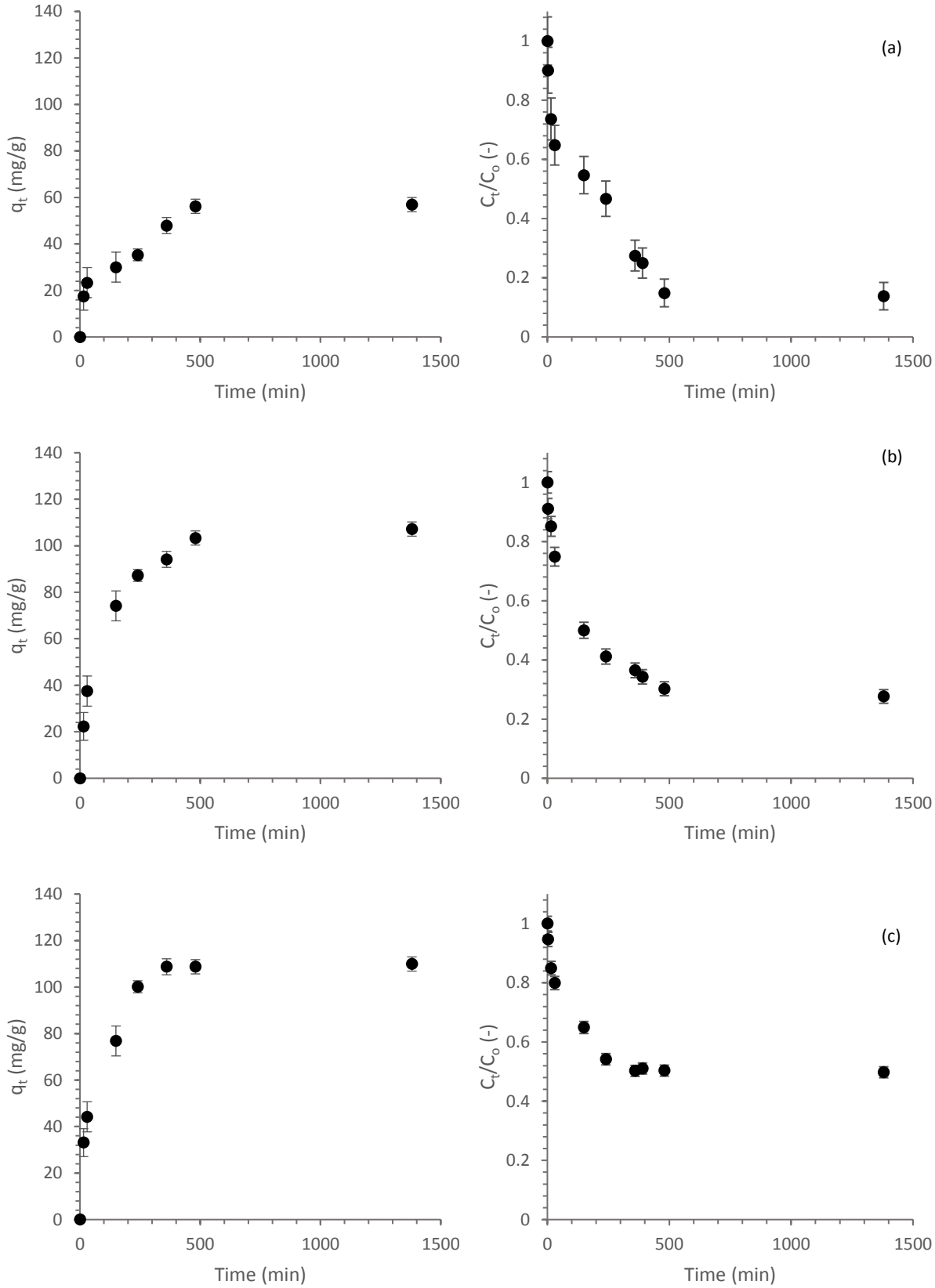

Figure D.1-5: Time profiles (left) and corresponding concentration decay plots (right) for the single component adsorption of 1-octanol onto SCDX, at 45°C, and initial adsorbate concentrations of (a) 0.44 mass%; (b) 1.00 mass%; and, (c) 1.46 mass%

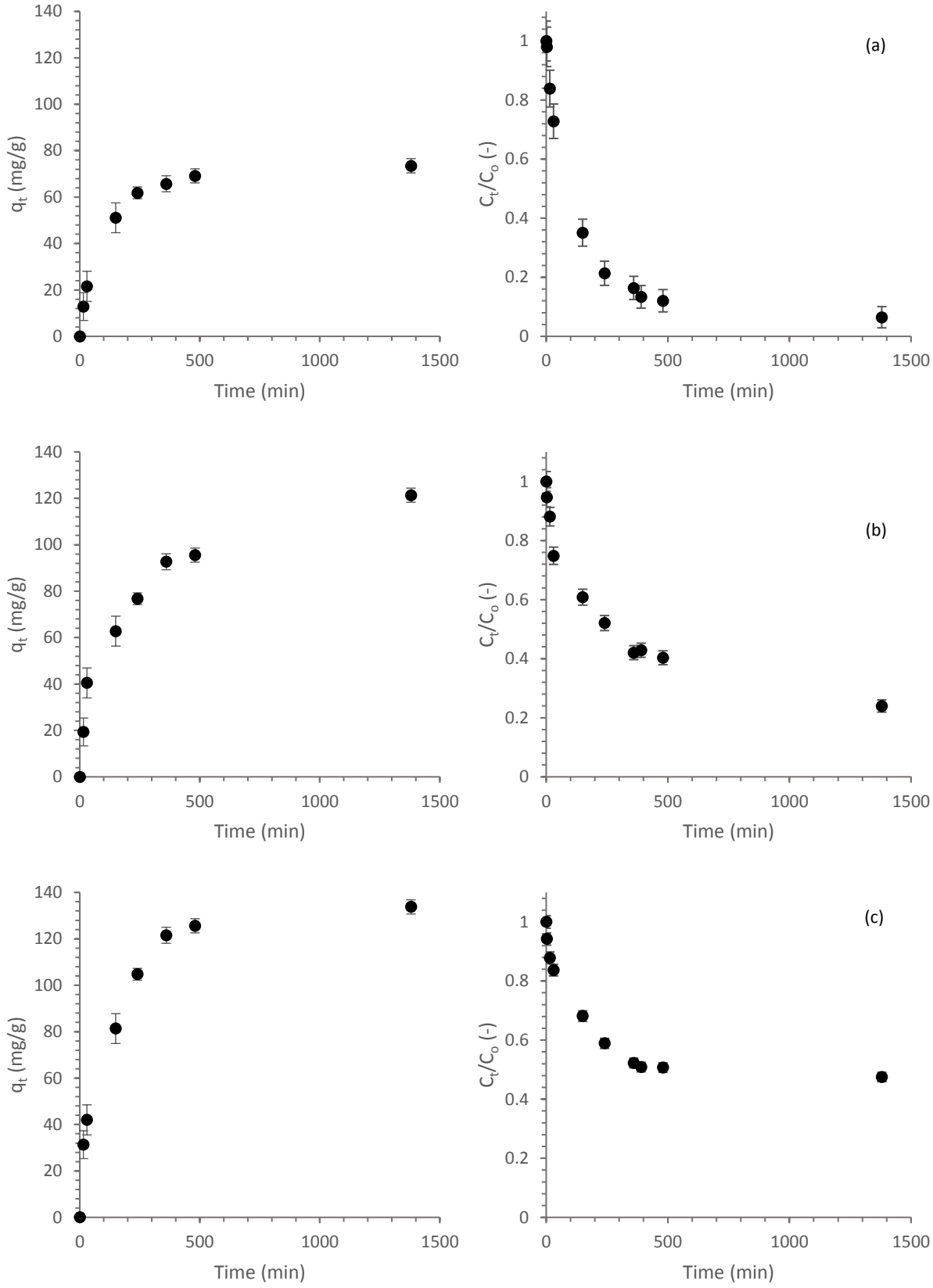

Figure D.1-6: Time profiles (left) and corresponding concentration decay plots (right) for the single component adsorption of 1-decanol onto SCDX, at 45°C, and initial adsorbate concentrations of (a) 0.54 mass%; (b) 1.08 mass%; and, (c) 1.69 mass%

D.1.3 Selexsorb CD®

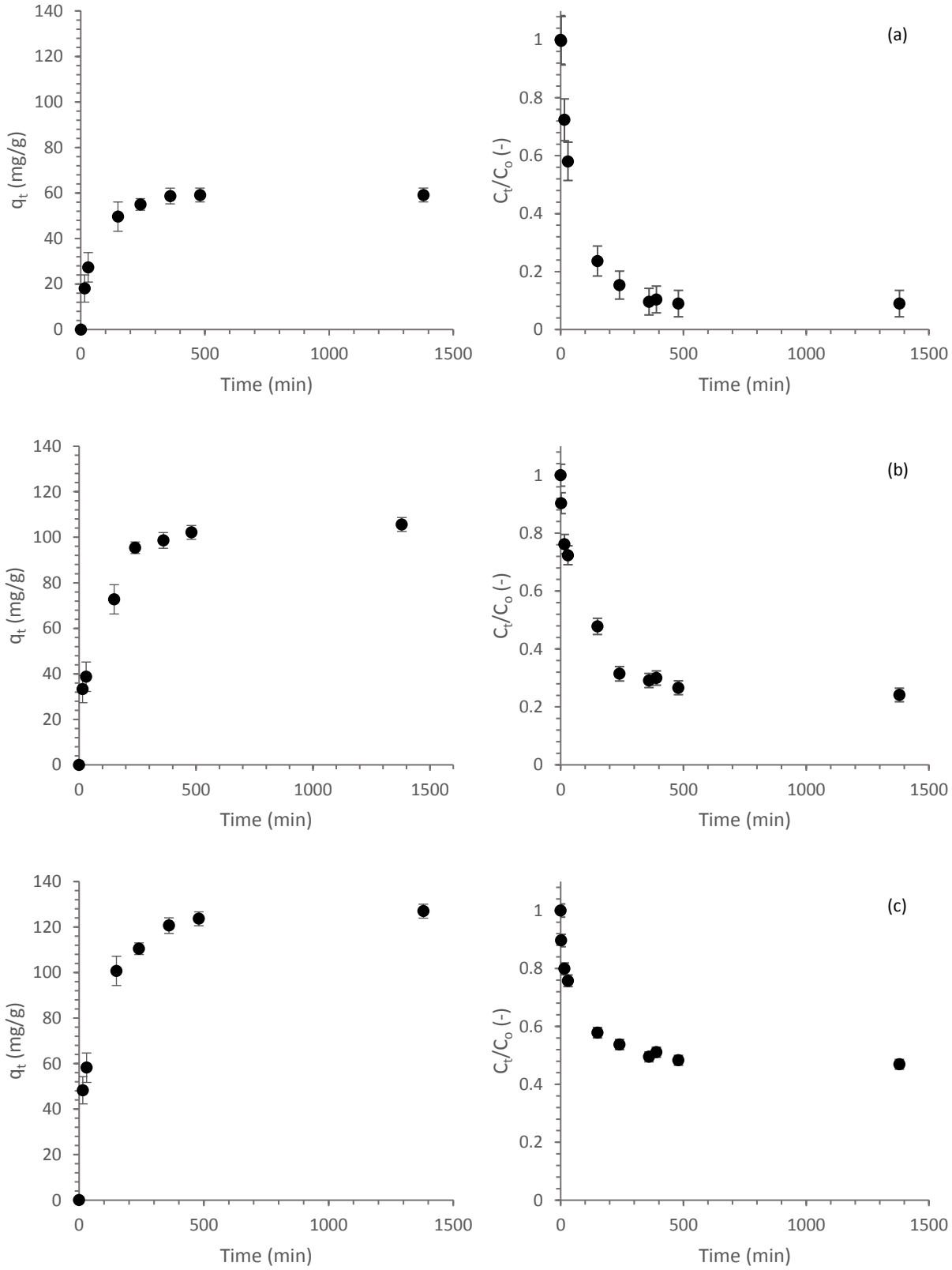

Figure D.1-7: Time profiles (left) and corresponding concentration decay plots (right) for the single component adsorption of 1-hexanol onto SCD, at 45°C, and initial adsorbate concentrations of (a) 0.55 mass%; (b) 1.01 mass%; and, (c) 1.51 mass%

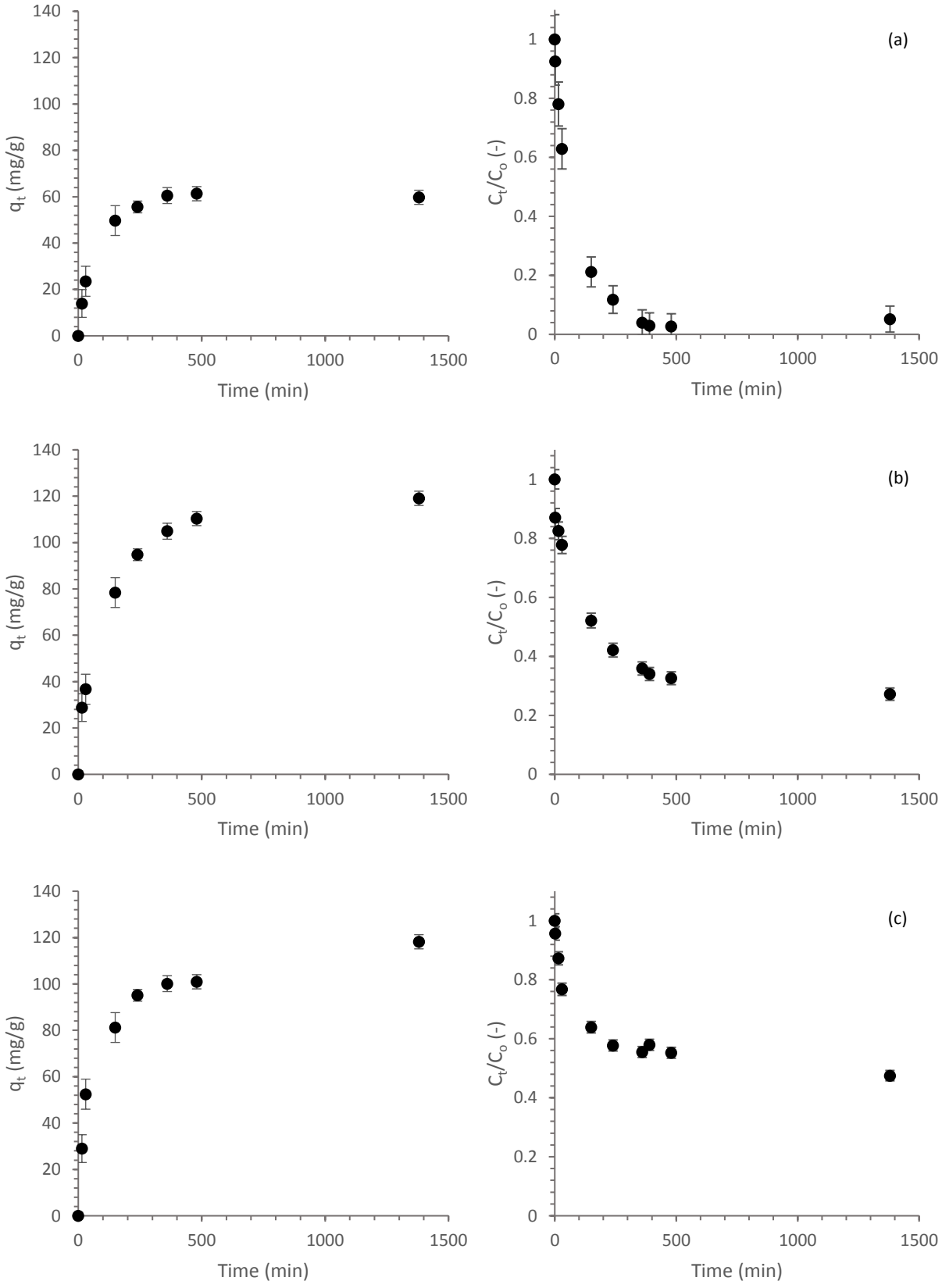

Figure D.1-8: Time profiles (left) and corresponding concentration decay plots (right) for the single component adsorption of 1-octanol onto SCD, at 45°C, and initial adsorbate concentrations of (a) 0.43 mass%; (b) 1.10 mass%; and, (c) 1.53 mass%

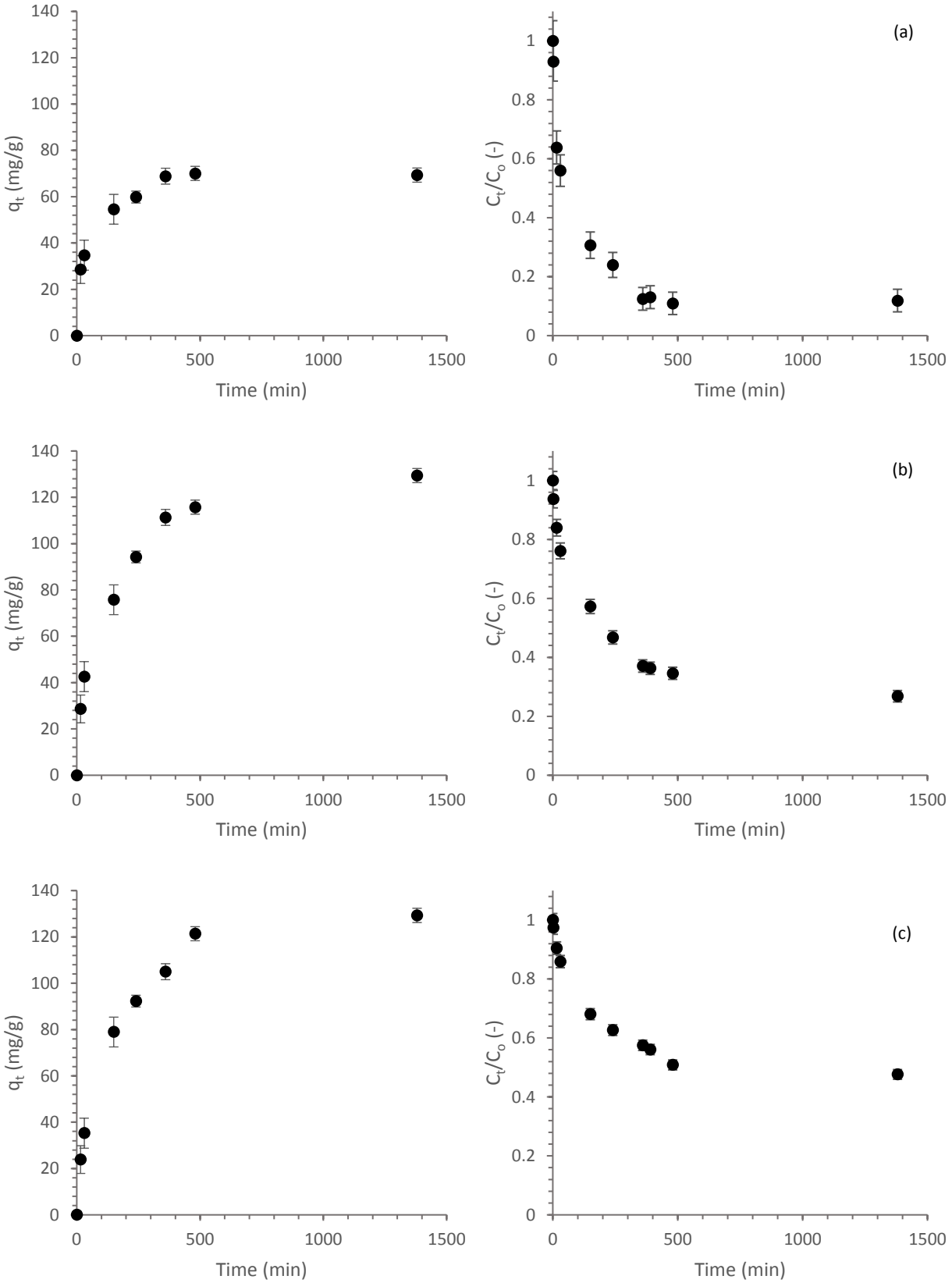

Figure D.1-9: Time profiles (left) and corresponding concentration decay plots (right) for the single component adsorption of 1-decanol onto SCD, at 45°C, and initial adsorbate concentrations of (a) 0.53 mass%; (b) 1.18 mass%; and, (c) 1.63 mass%

D.2 Binary Component Adsorption

D.2.1 Activated Alumina F220

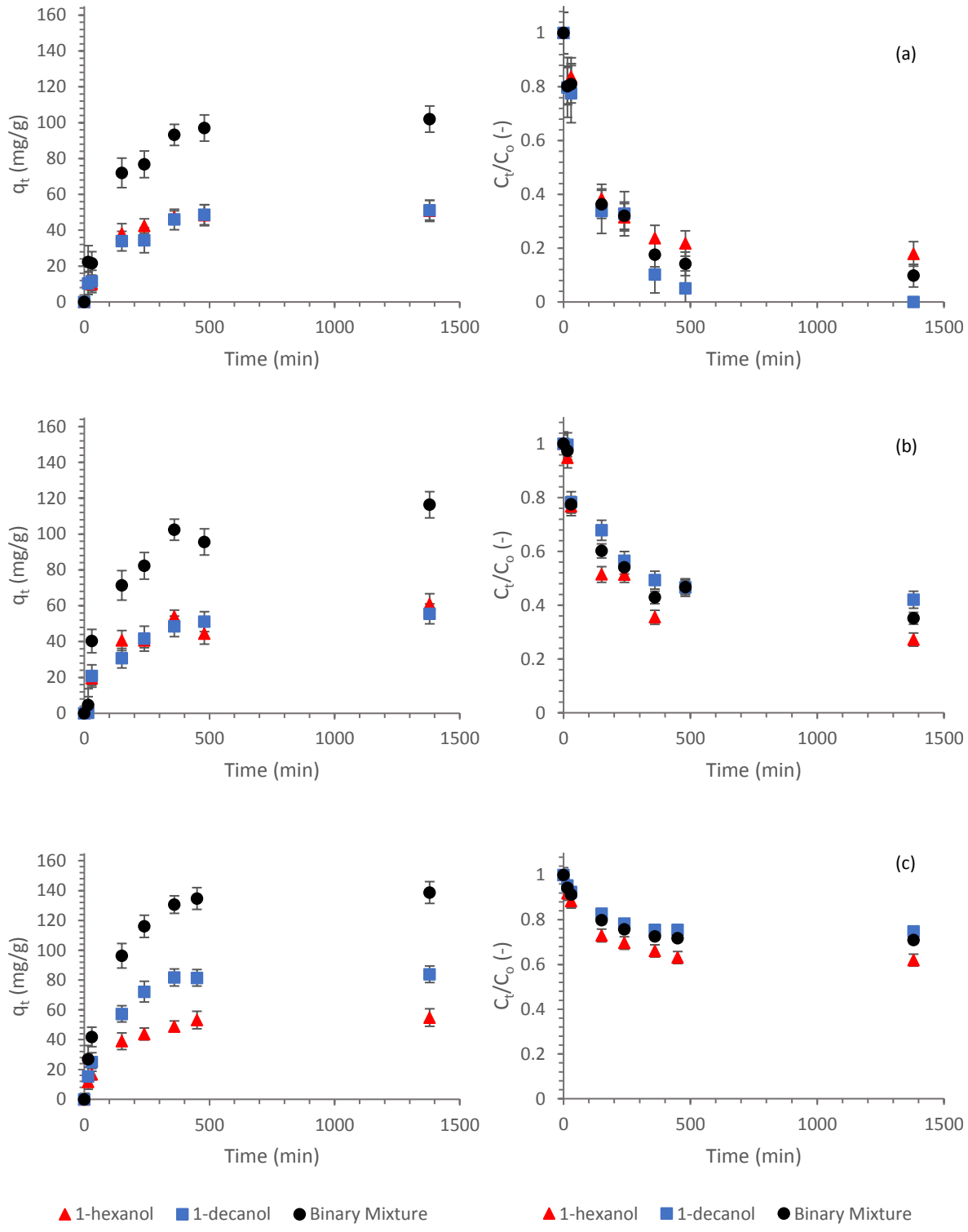

Figure D.2-1: Time profiles (left) and corresponding concentration decay plots (right) for the binary component adsorption of 1-hexanol and 1-decanol onto AA-F220, at 25°C, and initial adsorbate concentrations of (a) 0.41 mass% 1-hexanol, 0.34 mass% 1-decanol and 0.75 mass% binary mixture; (b) 0.82 mass% 1-hexanol, 0.94 mass% 1-decanol and 1.76 mass% binary mixture; and, (c) 0.96 mass% 1-hexanol, 2.22 mass% 1-decanol and 3.18 mass% binary mixture

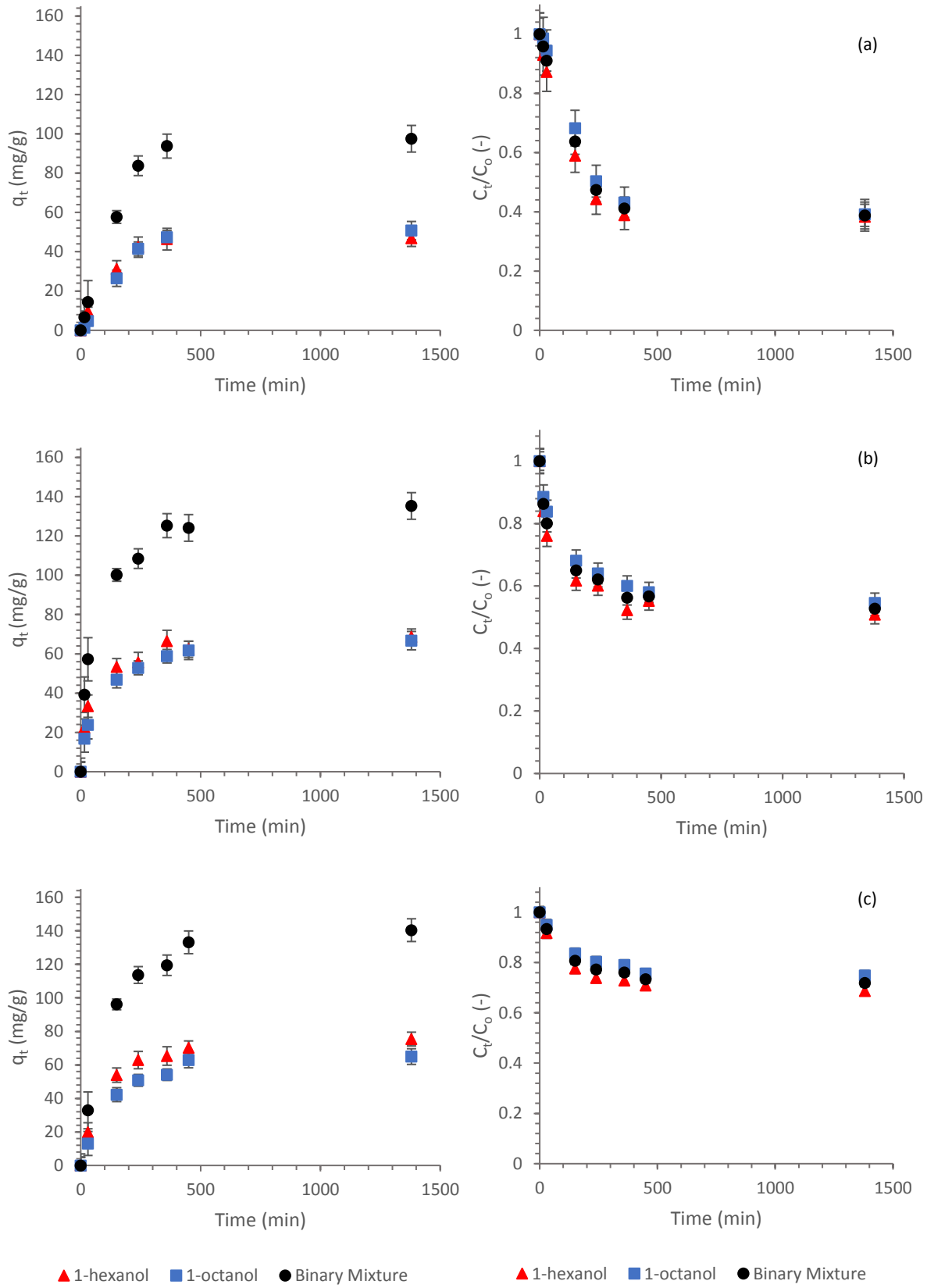

Figure D.2-2: Time profiles (left) and corresponding concentration decay plots (right) for the binary component adsorption of 1-hexanol and 1-octanol onto AA-F220, at 25°C, and initial adsorbate concentrations of (a) 0.51 mass% 1-hexanol, 0.56 mass% 1-octanol and 1.06 mass% binary mixture; (b) 0.93 mass% 1-hexanol, 0.99 mass% 1-octanol and 1.92 mass% binary mixture; and, (c) 1.60 mass% 1-hexanol, 1.72 mass% 1-octanol and 3.33 mass% binary mixture

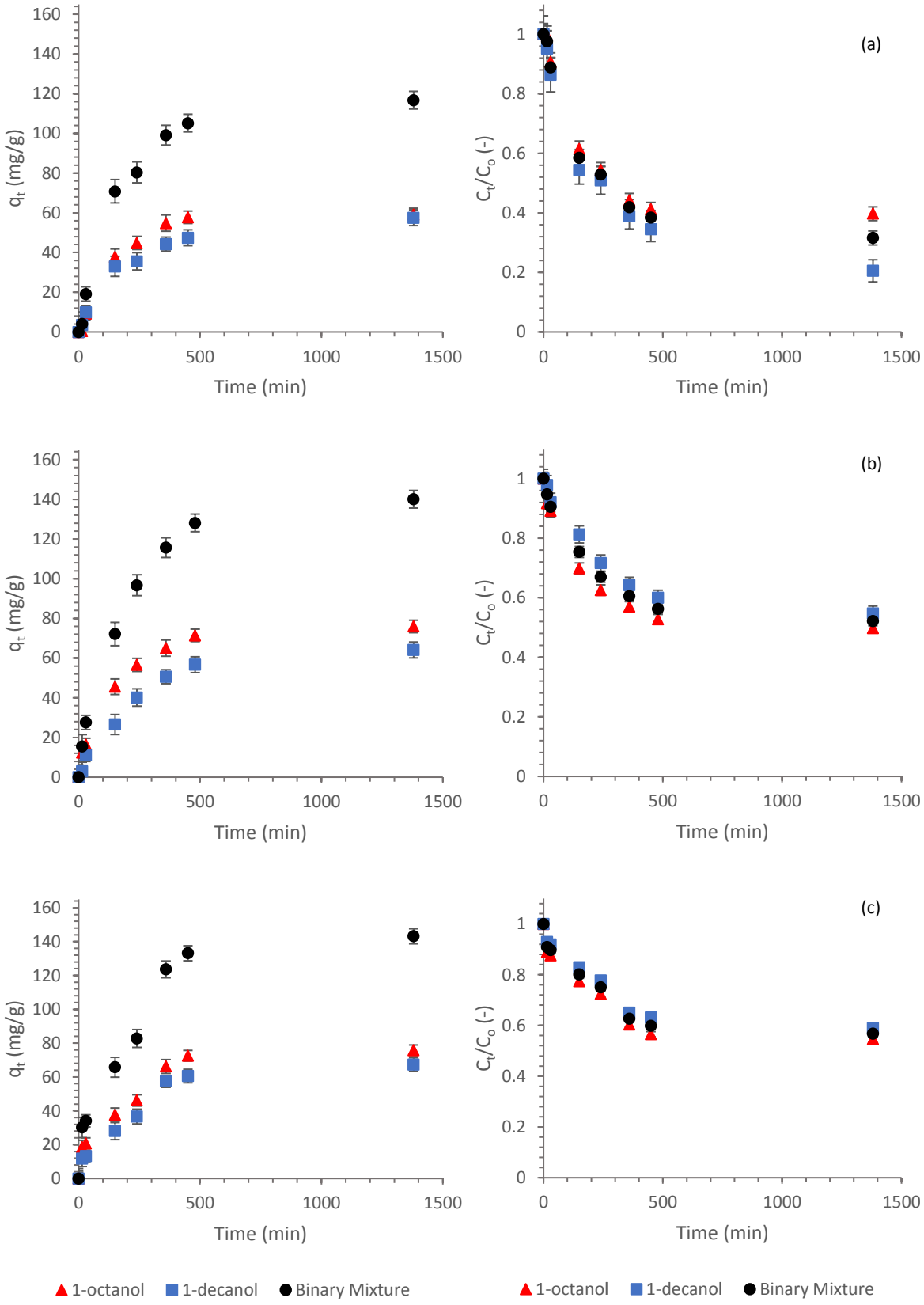

Figure D.2-3: Time profiles (left) and corresponding concentration decay plots (right) for the binary component adsorption of 1-octanol and 1-decanol onto AA-F220, at 25°C, and initial adsorbate concentrations of (a) 0.66 mass% 1-octanol, 0.49 mass% 1-decanol and 1.15 mass% binary mixture; (b) 1.01 mass% 1-octanol, 0.95 mass% 1-decanol and 1.96 mass% binary mixture; and, (c) 1.67 mass% 1-octanol, 1.64 mass% 1-decanol and 3.32 mass% binary mixture

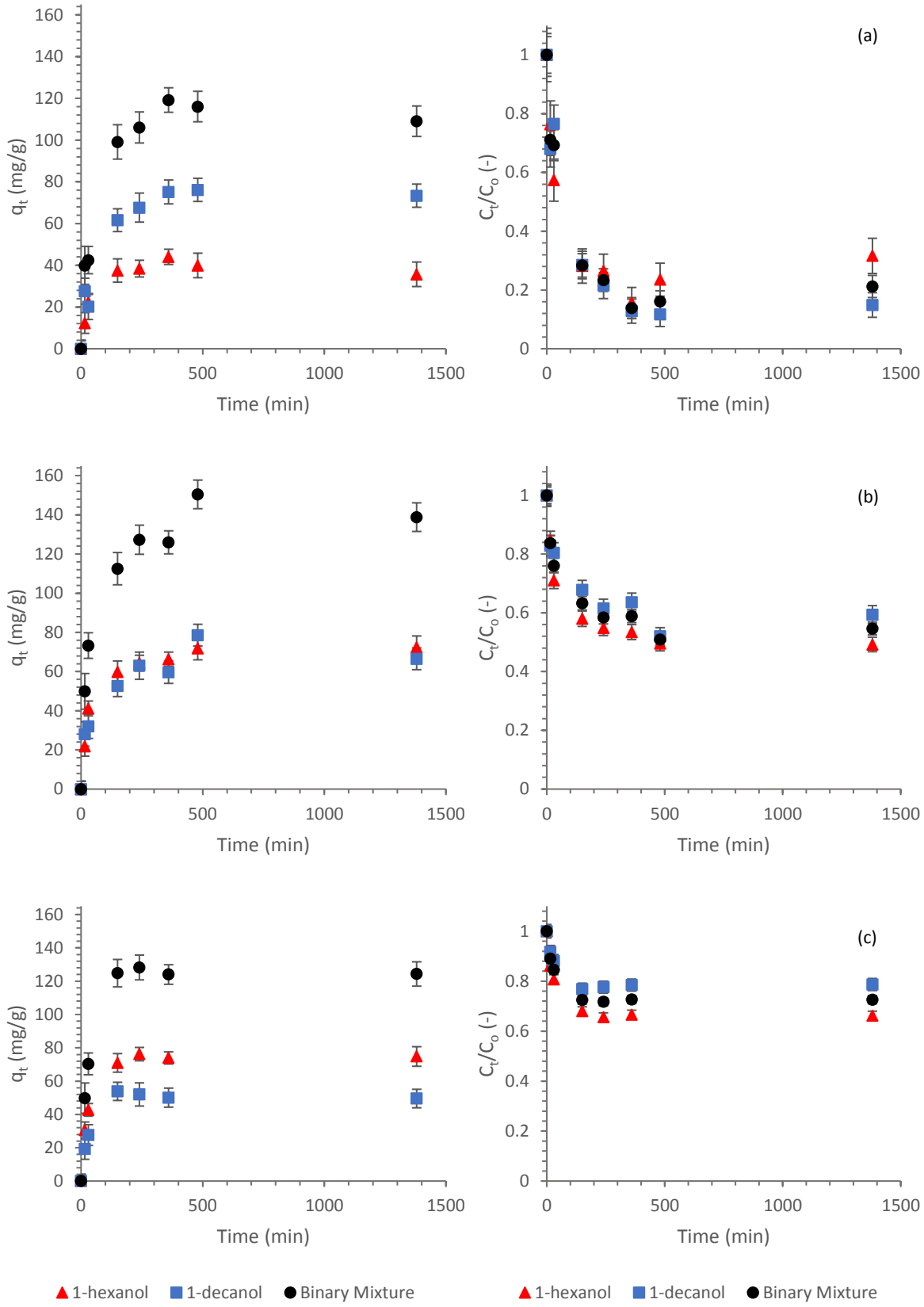

Figure D.2-4: Time profiles (left) and corresponding concentration decay plots (right) for the binary component adsorption of 1-hexanol and 1-decanol onto AA-F220, at 45°C, and initial adsorbate concentrations of (a) 0.35 mass% 1-hexanol, 0.57 mass% 1-decanol and 0.92 mass% binary mixture; (b) 0.95 mass% 1-hexanol, 1.10 mass% 1-decanol and 2.05 mass% binary mixture; and, (c) 1.47 mass% 1-hexanol, 1.55 mass% 1-decanol and 3.02 mass% binary mixture

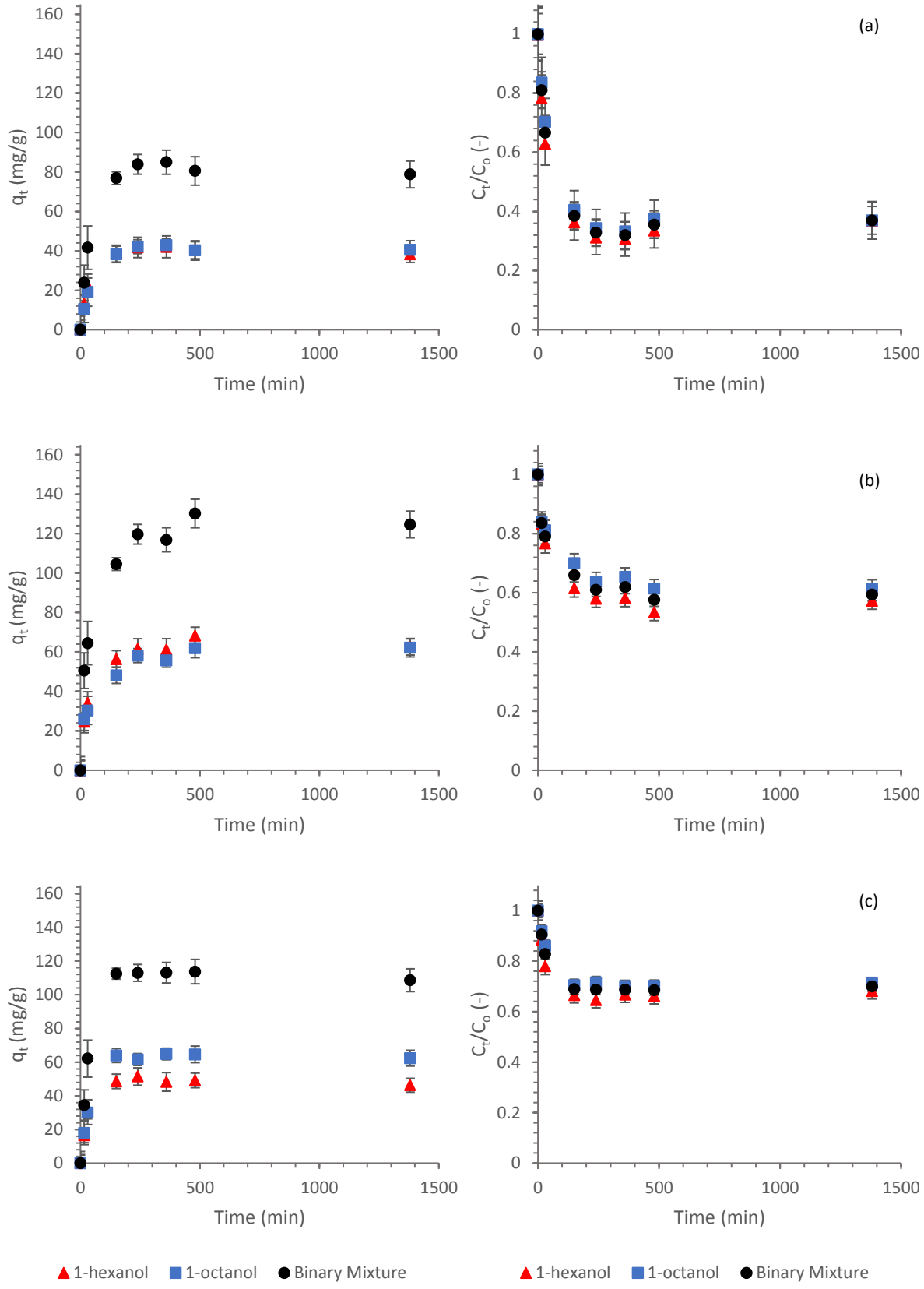

Figure D.2-5: Time profiles (left) and corresponding concentration decay plots (right) for the binary component adsorption of 1-hexanol and 1-octanol onto AA-F220, at 45°C, and initial adsorbate concentrations of (a) 0.40 mass% 1-hexanol, 0.43 mass% 1-octanol and 0.83 mass% binary mixture; (b) 0.97 mass% 1-hexanol, 1.07 mass% 1-octanol and 2.04 mass% binary mixture; and, (c) 0.96 mass% 1-hexanol, 1.43 mass% 1-octanol and 2.39 mass% binary mixture

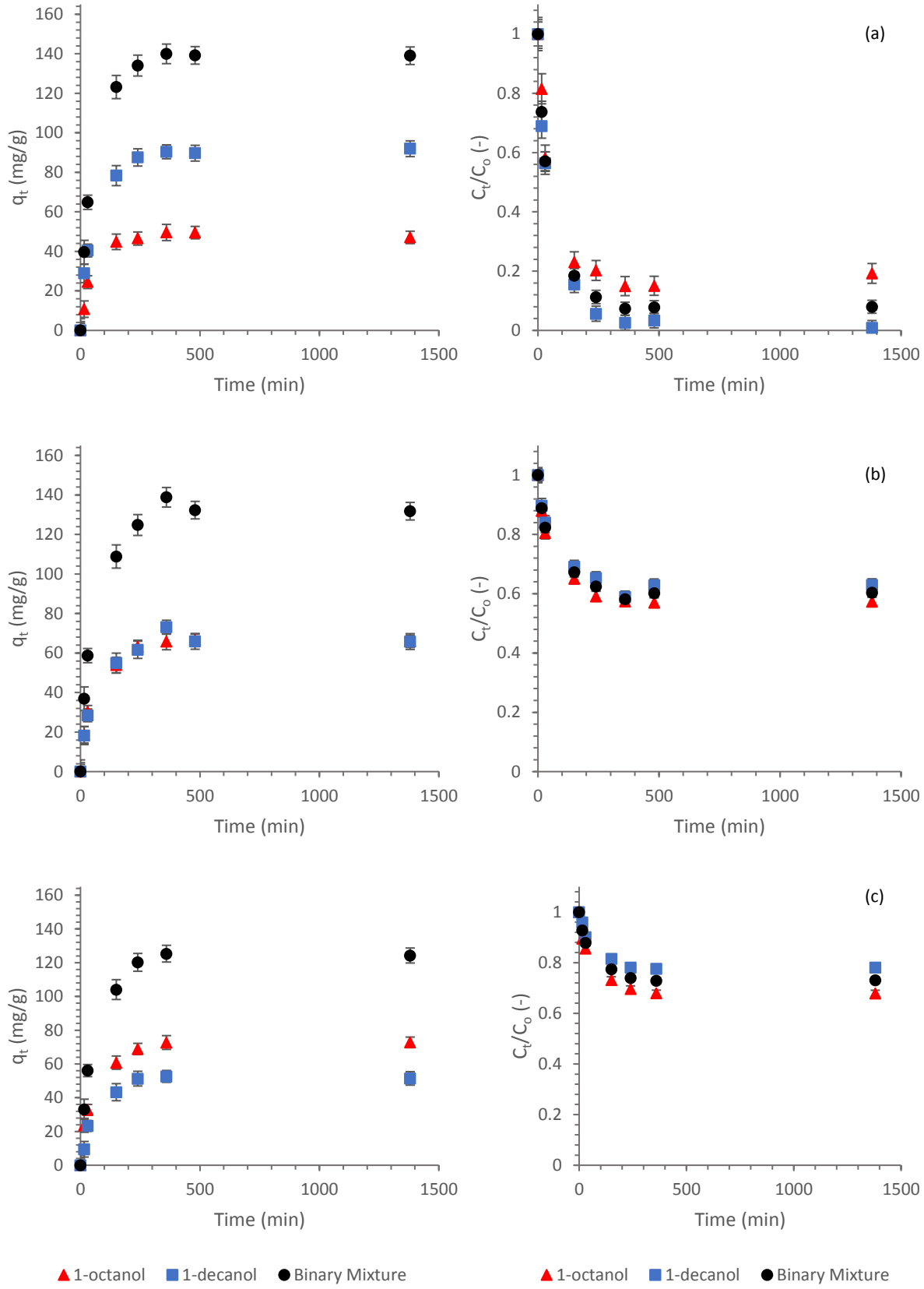

Figure D.2-6: Time profiles (left) and corresponding concentration decay plots (right) for the binary component adsorption of 1-octanol and 1-decanol onto AA-F220, at 45°C, and initial adsorbate concentrations of (a) 0.39 mass% 1-octanol, 0.62 mass% 1-decanol and 1.01 mass% binary mixture; (b) 1.02 mass% 1-octanol, 1.17 mass% 1-decanol and 2.19 mass% binary mixture; and, (c) 1.51 mass% 1-octanol, 1.56 mass% 1-decanol and 3.07 mass% binary mixture

D.2.2 Selexsorb CDx®

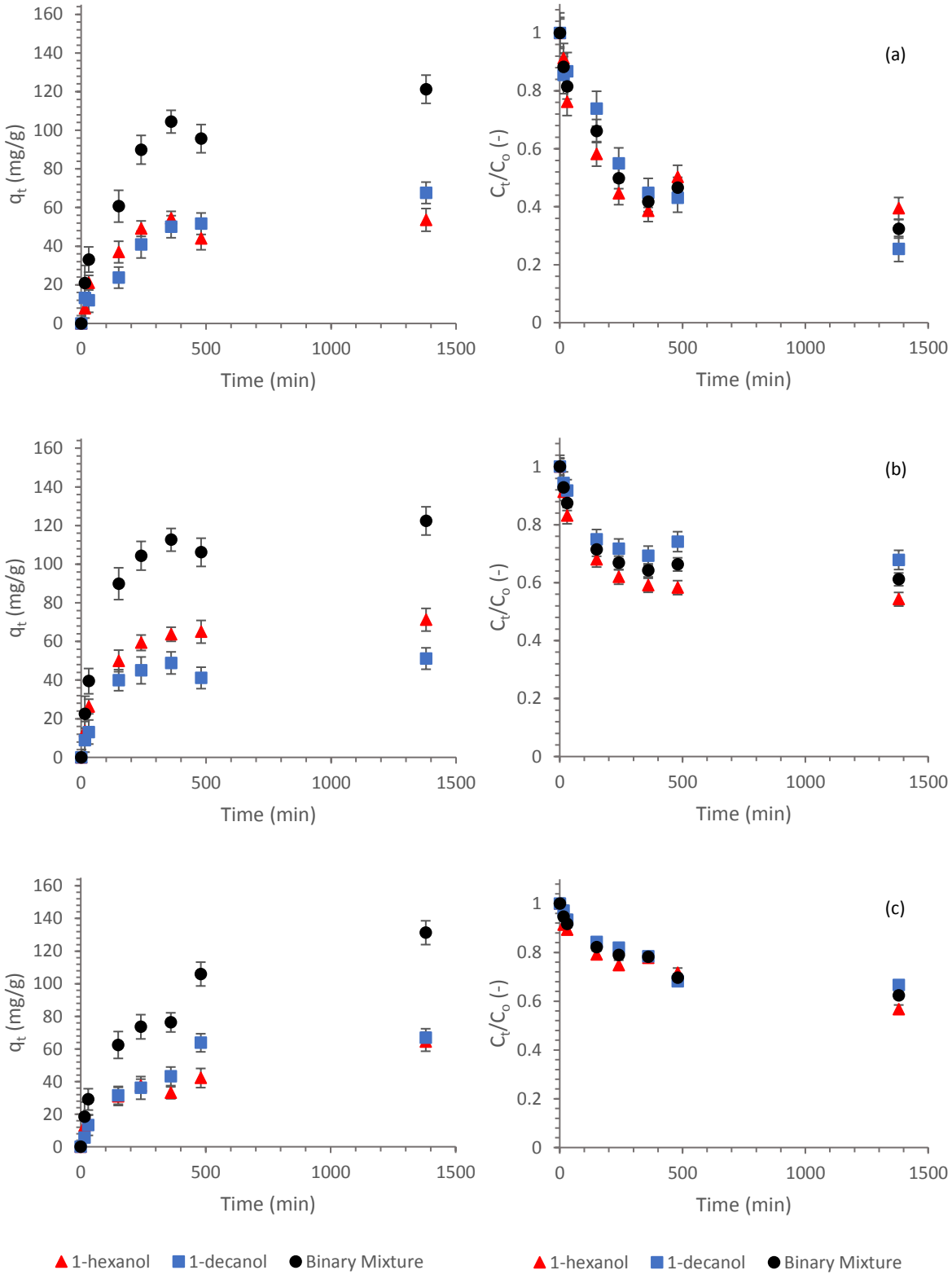

Figure D.2-7: Time profiles (left) and corresponding concentration decay plots (right) for the binary component adsorption of 1-hexanol and 1-decanol onto SCDX, at 25°C, and initial adsorbate concentrations of (a) 0.59 mass% 1-hexanol, 0.61 mass% 1-decanol and 1.20 mass% binary mixture; (b) 1.04 mass% 1-hexanol, 1.06 mass% 1-decanol and 2.10 mass% binary mixture; and, (c) 1.44 mass% 1-hexanol, 1.94 mass% 1-decanol and 3.38 mass% binary mixture

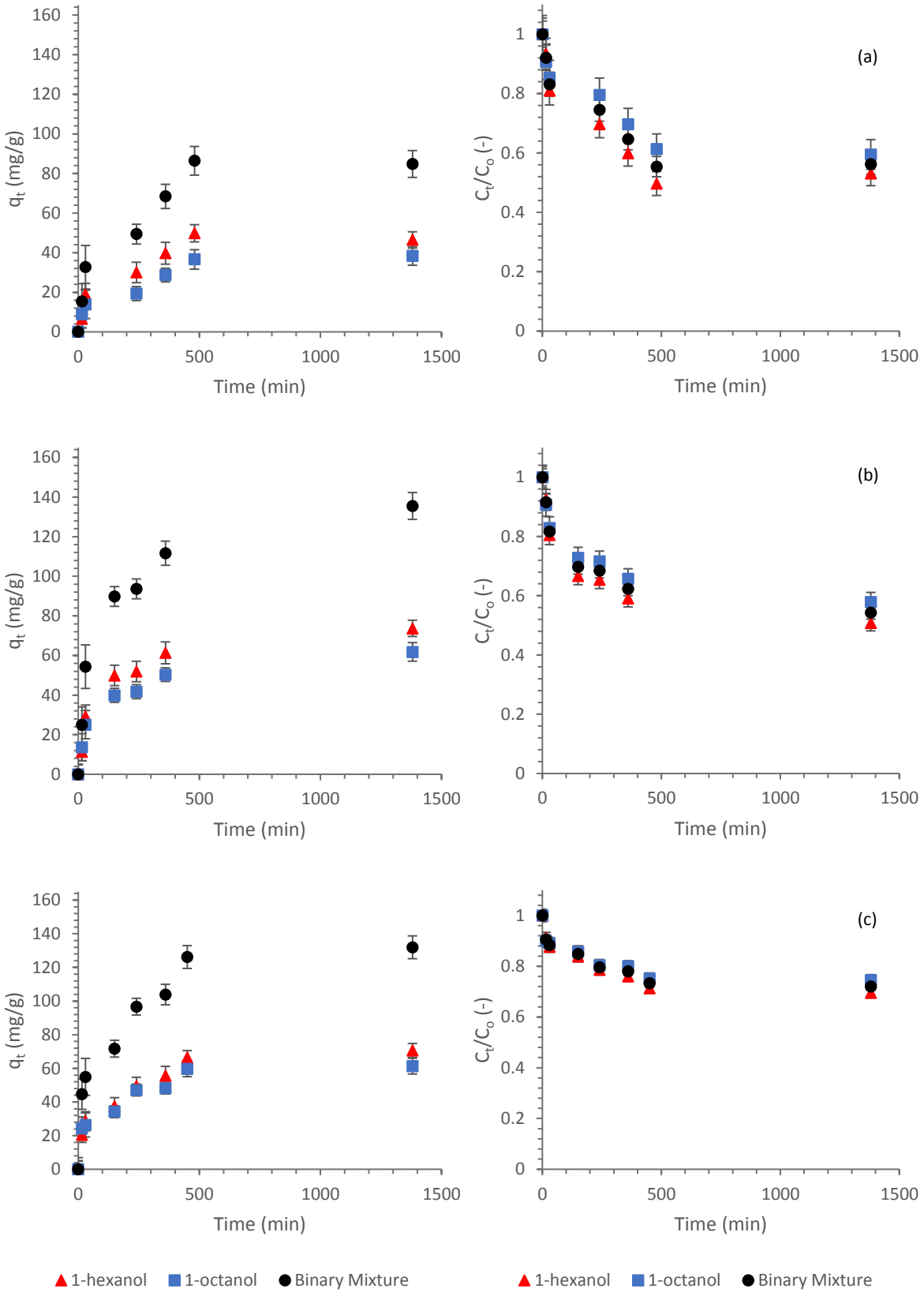

Figure D.2-8: Time profiles (left) and corresponding concentration decay plots (right) for the binary component adsorption of 1-hexanol and 1-octanol onto SCDX, at 25°C, and initial adsorbate concentrations of (a) 0.66 mass% 1-hexanol, 0.63 mass% 1-octanol and 1.30 mass% binary mixture; (b) 1.00 mass% 1-hexanol, 0.98 mass% 1-octanol and 1.98 mass% binary mixture; and, (c) 1.55 mass% 1-hexanol, 1.61 mass% 1-octanol and 3.16 mass% binary mixture

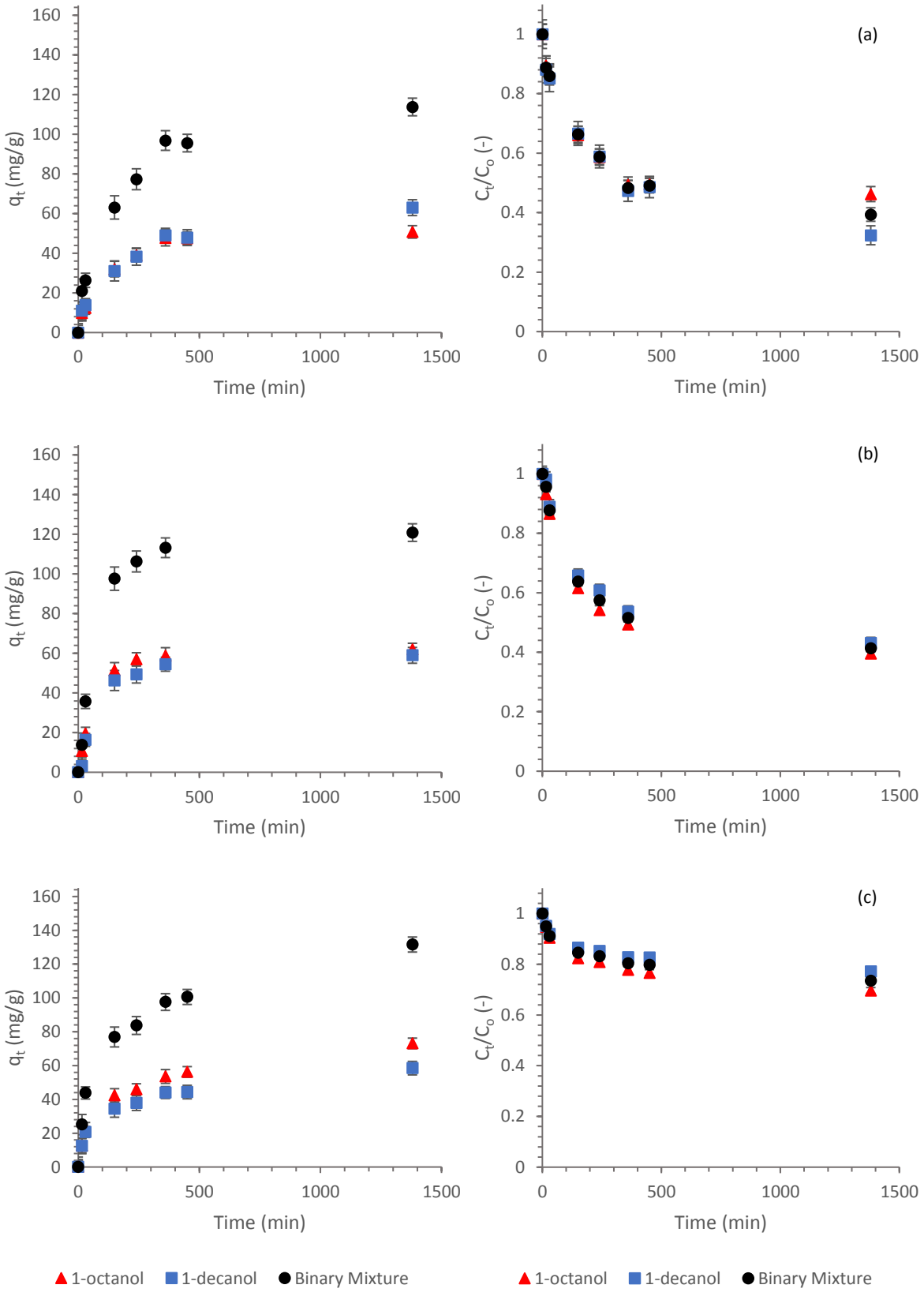

Figure D.2-9: Time profiles (left) and corresponding concentration decay plots (right) for the binary component adsorption of 1-octanol and 1-decanol onto SCDX, at 25°C, and initial adsorbate concentrations of (a) 0.63 mass% 1-octanol, 0.62 mass% 1-decanol and 1.26 mass% binary mixture; (b) 1.16 mass% 1-octanol, 1.18 mass% 1-decanol and 2.34 mass% binary mixture; and, (c) 1.60 mass% 1-octanol, 1.71 mass% 1-decanol and 3.31 mass% binary mixture

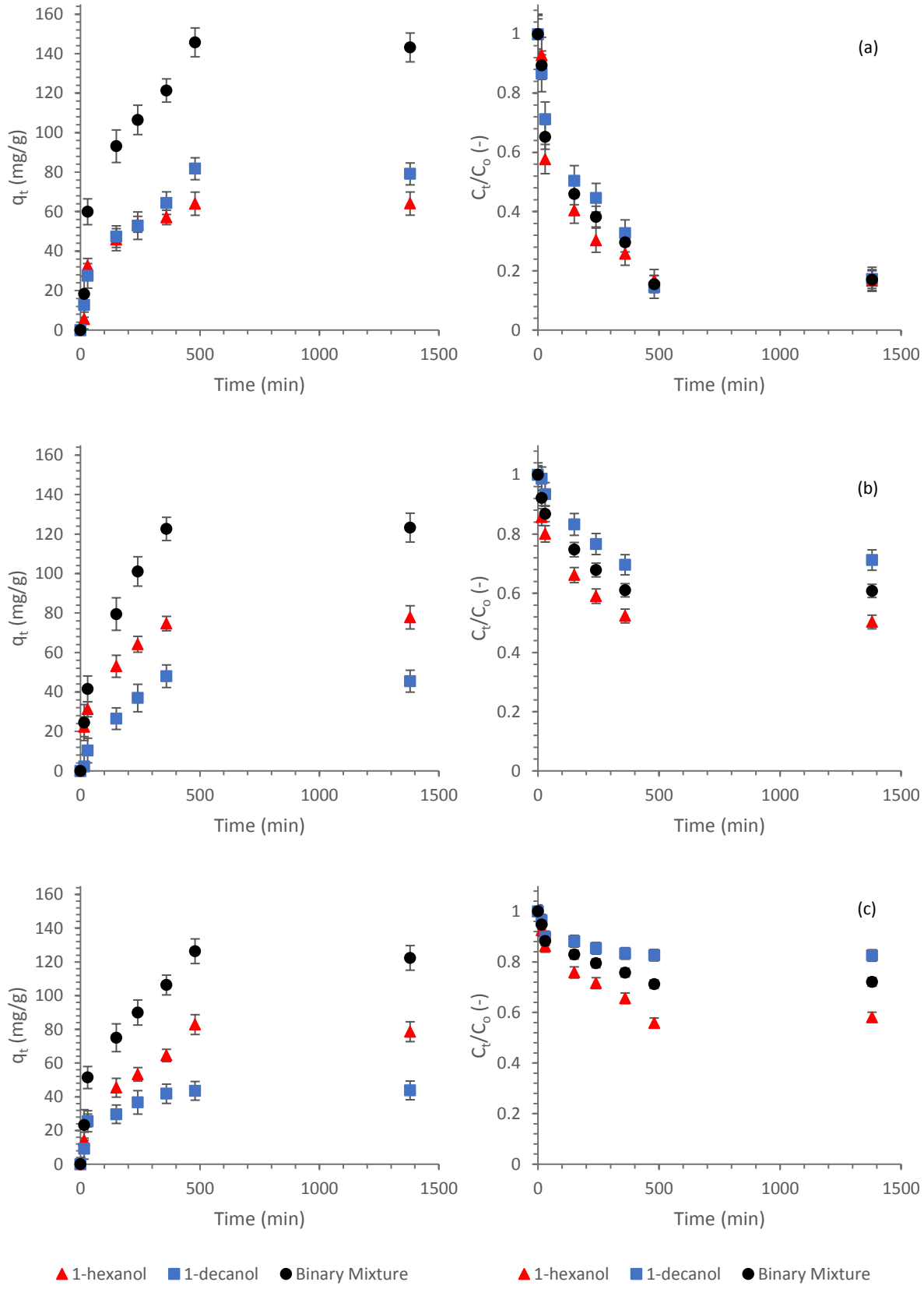

Figure D.2-10: Time profiles (left) and corresponding concentration decay plots (right) for the binary component adsorption of 1-hexanol and 1-decanol onto SCDX, at 45°C, and initial adsorbate concentrations of (a) 0.51 mass% 1-hexanol, 0.63 mass% 1-decanol and 1.13 mass% binary mixture; (b) 1.03 mass% 1-hexanol, 1.04 mass% 1-decanol and 2.07 mass% binary mixture; and, (c) 1.26 mass% 1-hexanol, 1.68 mass% 1-decanol and 2.94 mass% binary mixture

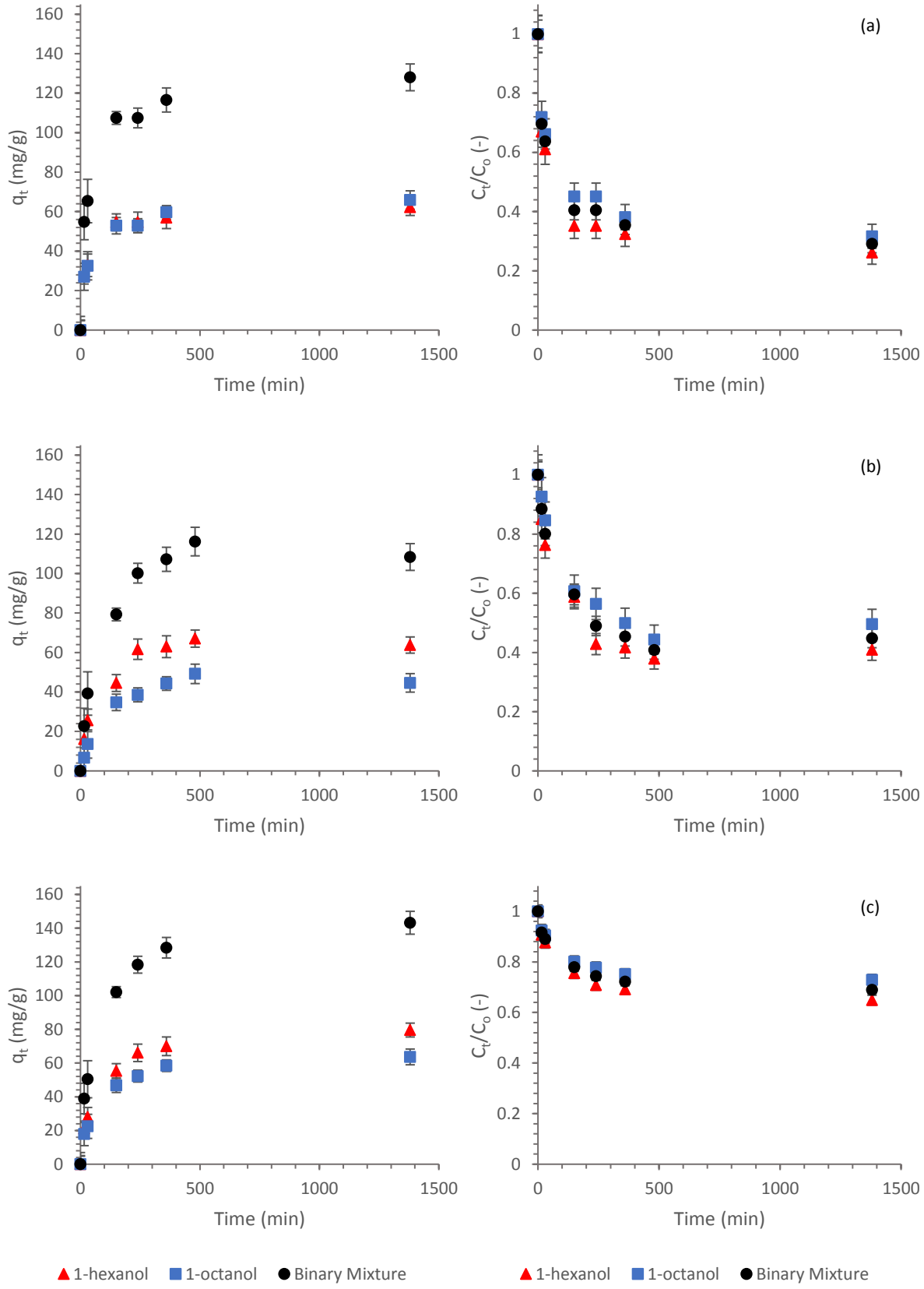

Figure D.2-11: Time profiles (left) and corresponding concentration decay plots (right) for the binary component adsorption of 1-hexanol and 1-octanol onto SCDX, at 45°C, and initial adsorbate concentrations of (a) 0.57 mass% 1-hexanol, 0.65 mass% 1-octanol and 1.21 mass% binary mixture; (b) 0.72 mass% 1-hexanol, 0.59 mass% 1-octanol and 1.31 mass% binary mixture; and, (c) 1.51 mass% 1-hexanol, 1.57 mass% 1-octanol and 3.08 mass% binary mixture

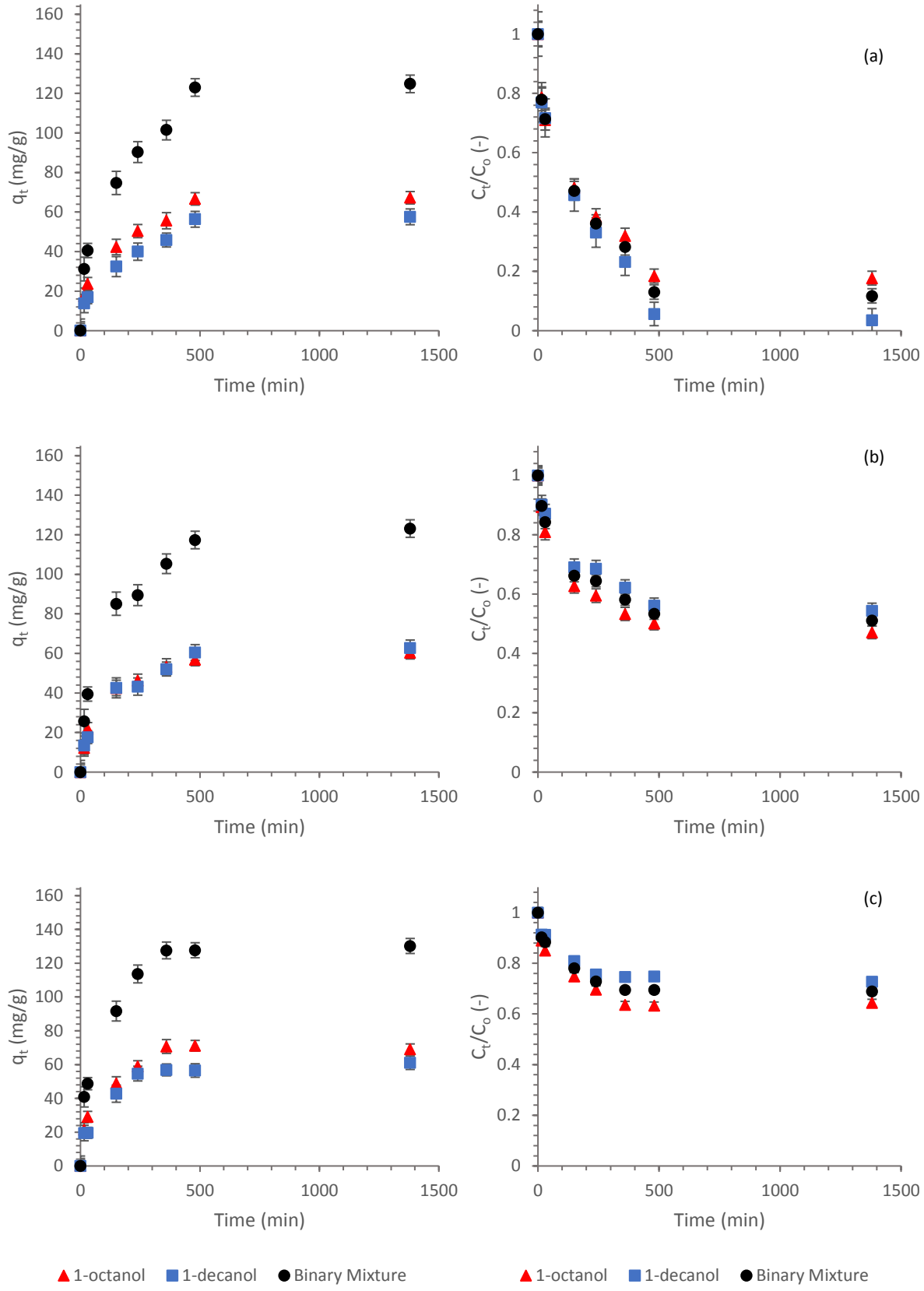

Figure D.2-12: Time profiles (left) and corresponding concentration decay plots (right) for the binary component adsorption of 1-octanol and 1-decanol onto SCDX, at 45°C, and initial adsorbate concentrations of (a) 0.55 mass% 1-octanol, 0.40 mass% 1-decanol and 0.95 mass% binary mixture; (b) 0.76 mass% 1-octanol, 0.92 mass% 1-decanol and 1.67 mass% binary mixture; and, (c) 1.29 mass% 1-octanol, 1.49 mass% 1-decanol and 2.78 mass% binary mixture

D.2.3 Selexsorb CD®

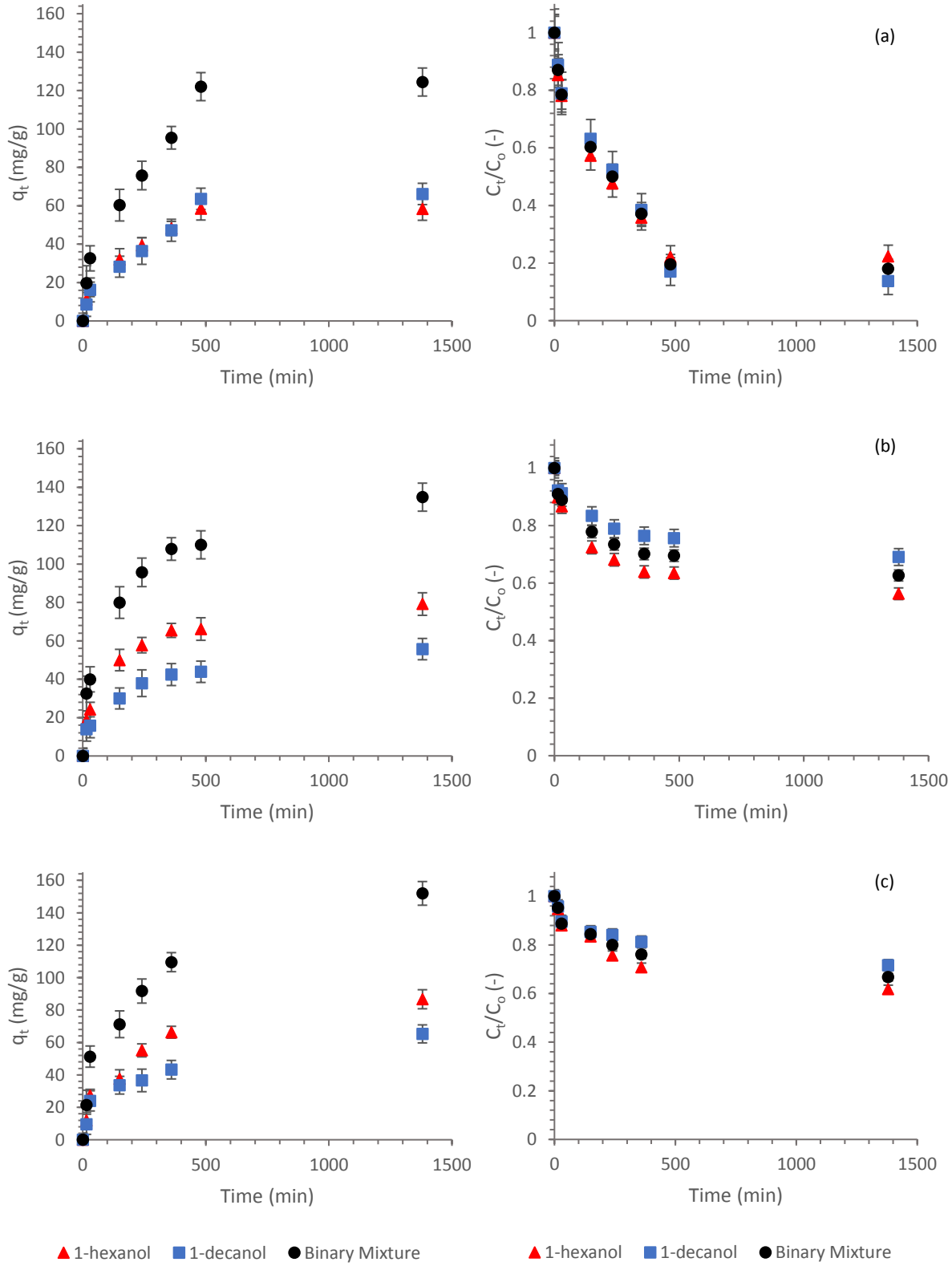

Figure D.2-13: Time profiles (left) and corresponding concentration decay plots (right) for the binary component adsorption of 1-hexanol and 1-decanol onto SCD, at 25°C, and initial adsorbate concentrations of (a) 0.50 mass% 1-hexanol, 0.51 mass% 1-decanol and 1.01 mass% binary mixture; (b) 1.22 mass% 1-hexanol, 1.21 mass% 1-decanol and 2.43 mass% binary mixture; and, (c) 1.51 mass% 1-hexanol, 1.54 mass% 1-decanol and 3.05 mass% binary mixture

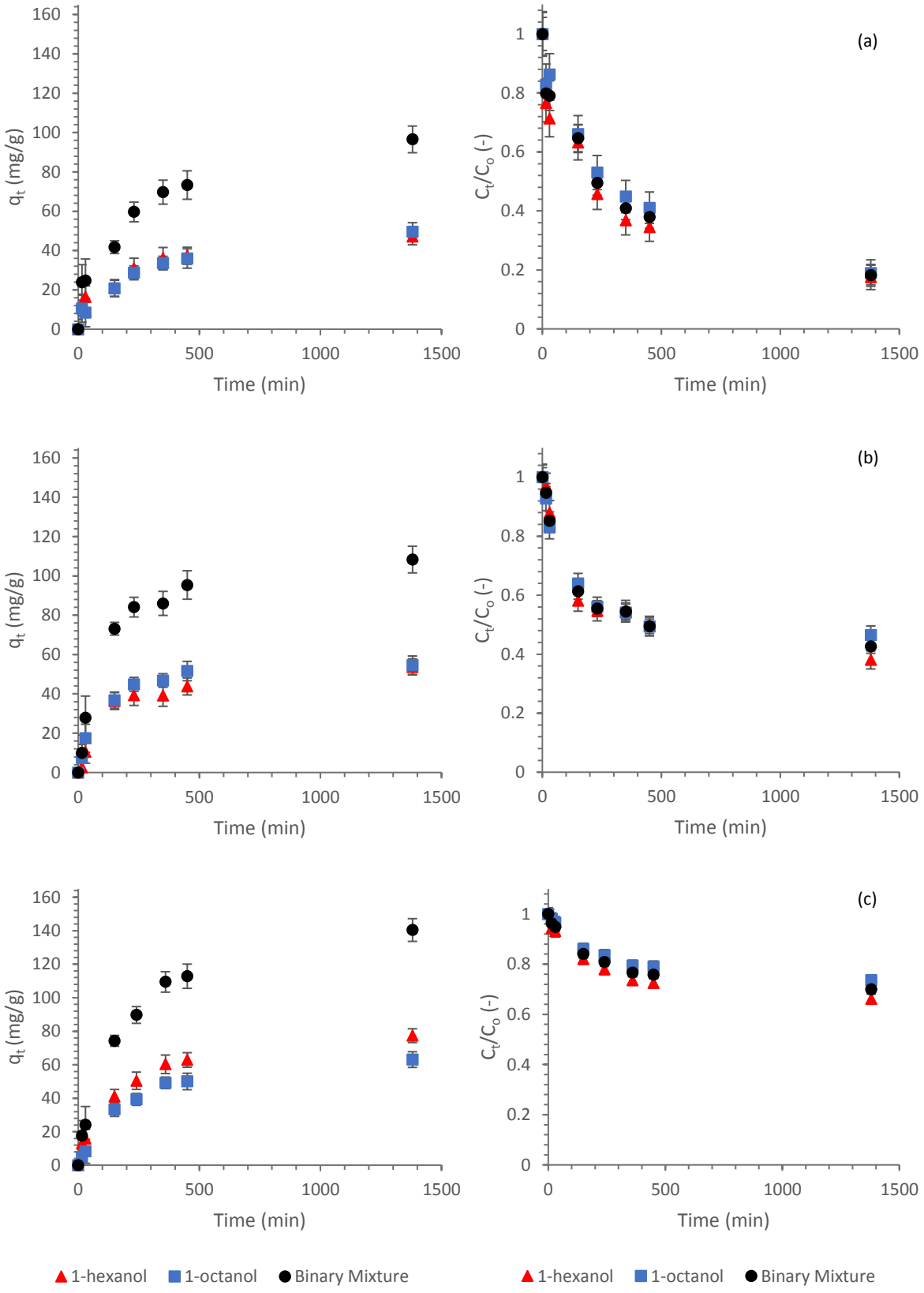

Figure D.2-14: Time profiles (left) and corresponding concentration decay plots (right) for the binary component adsorption of 1-hexanol and 1-octanol onto SCD, at 25°C, and initial adsorbate concentrations of (a) 0.49 mass% 1-hexanol, 0.53 mass% 1-octanol and 1.02 mass% binary mixture; (b) 0.81 mass% 1-hexanol, 0.95 mass% 1-octanol and 1.75 mass% binary mixture; and, (c) 1.53 mass% 1-hexanol, 1.60 mass% 1-octanol and 3.12 mass% binary mixture

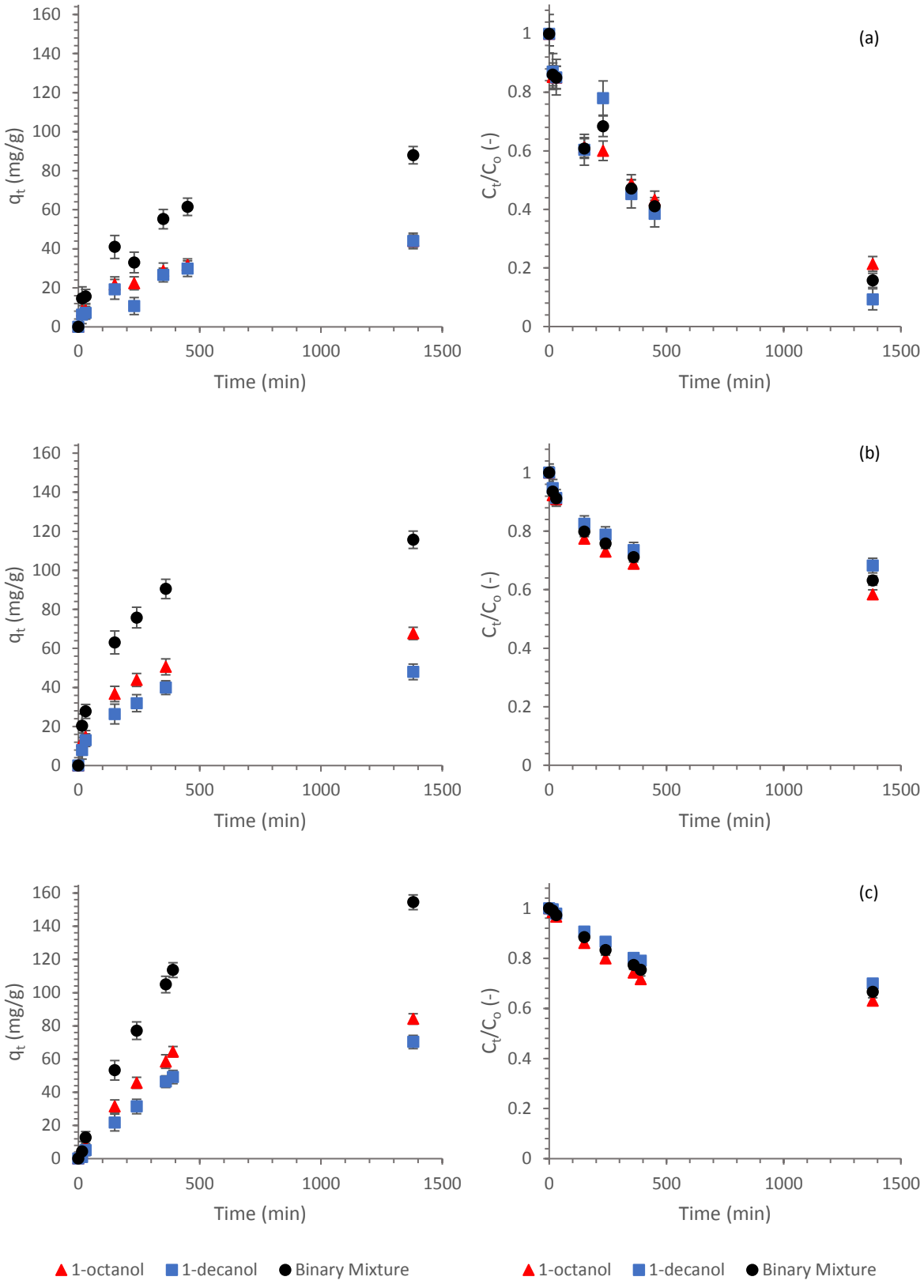

Figure D.2-15: Time profiles (left) and corresponding concentration decay plots (right) for the binary component adsorption of 1-octanol and 1-decanol onto SCD, at 25°C, and initial adsorbate concentrations of (a) 0.53 mass% 1-octanol, 0.46 mass% 1-decanol and 0.98 mass% binary mixture; (b) 1.09 mass% 1-octanol, 1.01 mass% 1-decanol and 2.10 mass% binary mixture; and, (c) 1.53 mass% 1-octanol, 1.57 mass% 1-decanol and 3.10 mass% binary mixture

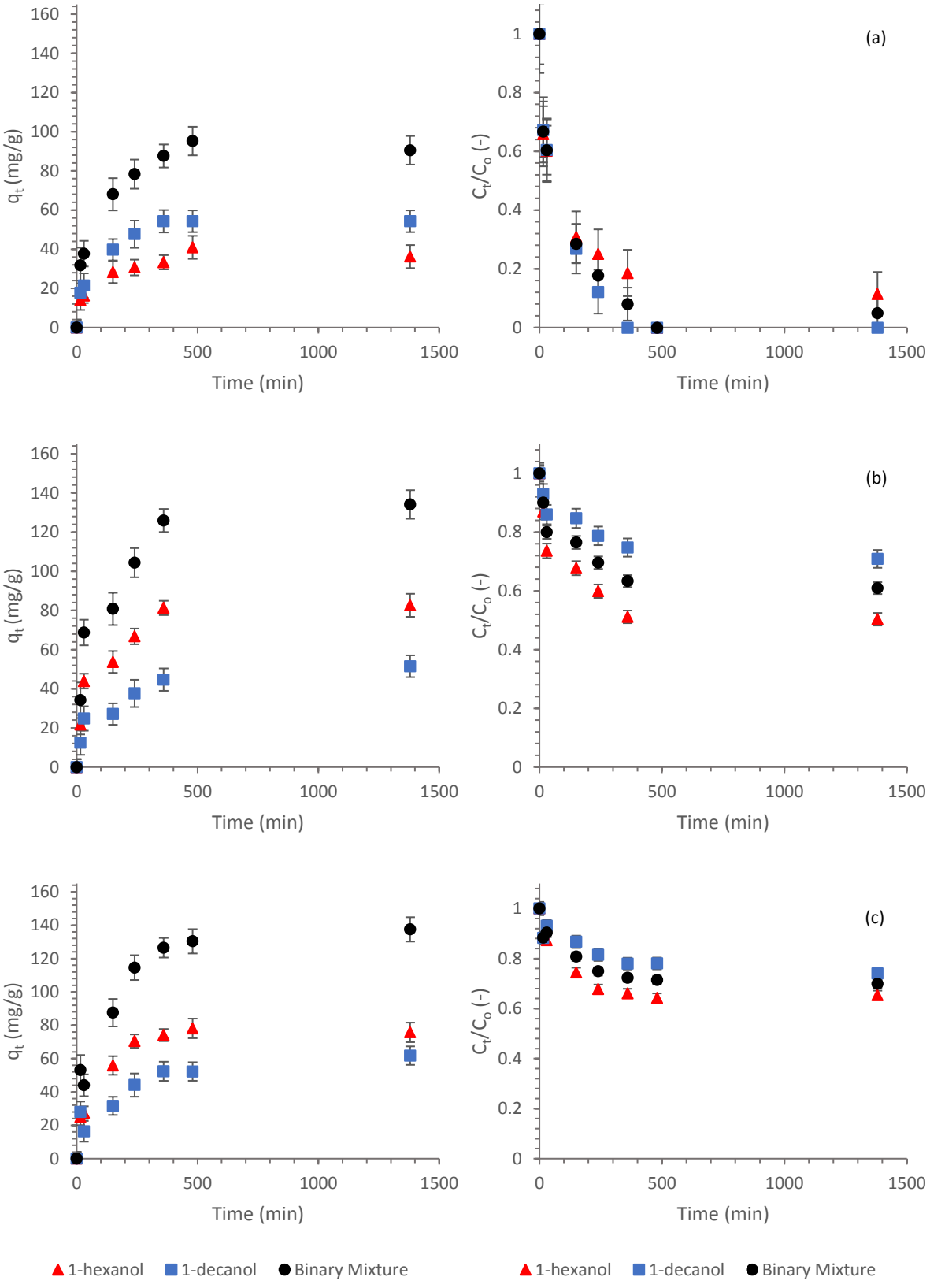

Figure D.2-16: Time profiles (left) and corresponding concentration decay plots (right) for the binary component adsorption of 1-hexanol and 1-decanol onto SCD, at 45°C, and initial adsorbate concentrations of (a) 0.24 mass% 1-hexanol, 0.32 mass% 1-decanol and 0.55 mass% binary mixture; (b) 1.11 mass% 1-hexanol, 1.18 mass% 1-decanol and 2.29 mass% binary mixture; and, (c) 1.45 mass% 1-hexanol, 1.58 mass% 1-decanol and 3.03 mass% binary mixture

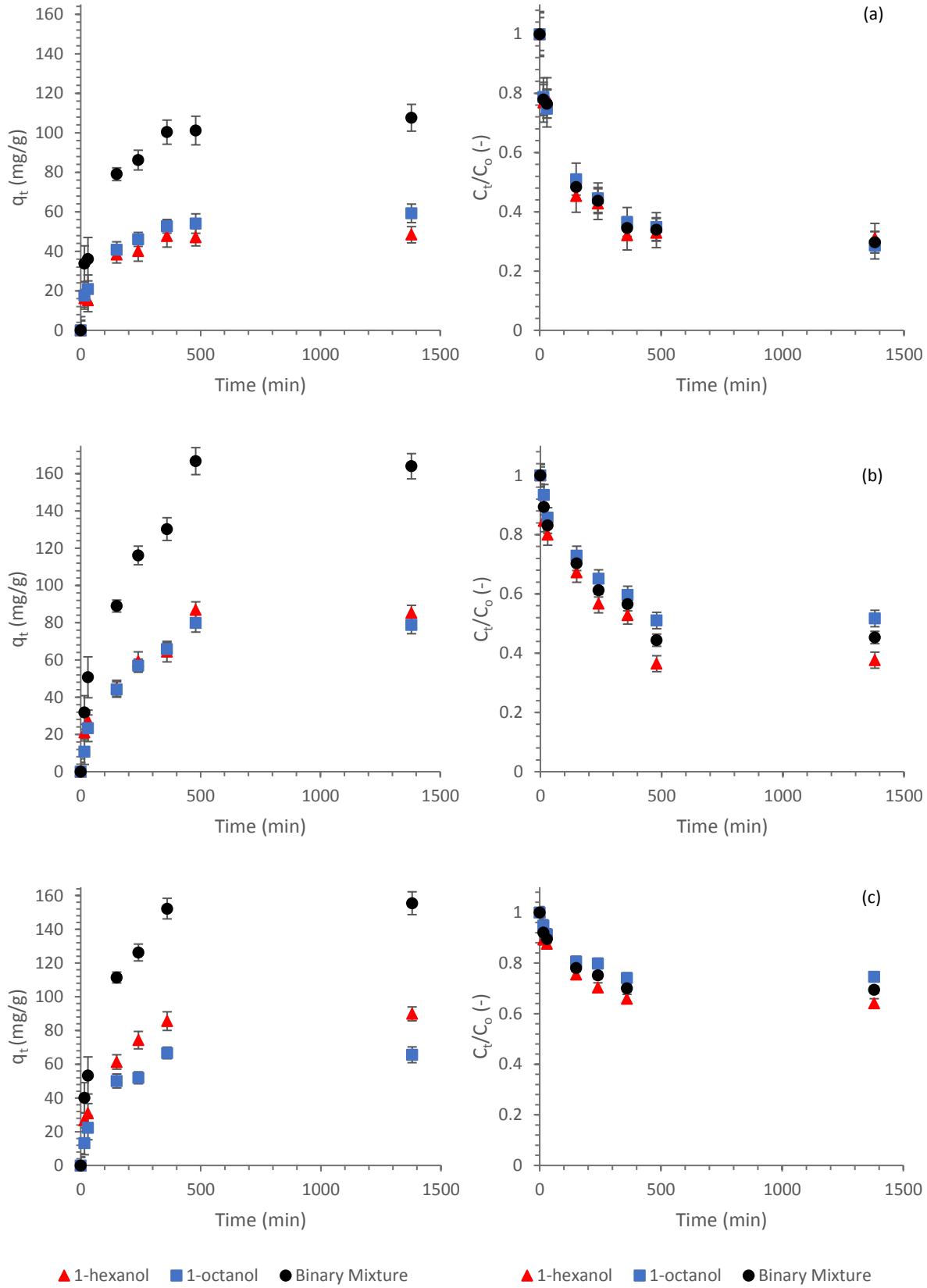

Figure D.2-17: Time profiles (left) and corresponding concentration decay plots (right) for the binary component adsorption of 1-hexanol and 1-octanol onto SCD, at 45°C, and initial adsorbate concentrations of (a) 0.47 mass% 1-hexanol, 0.56 mass% 1-octanol and 1.03 mass% binary mixture; (b) 0.91 mass% 1-hexanol, 1.09 mass% 1-octanol and 1.99 mass% binary mixture; and, (c) 1.67 mass% 1-hexanol, 1.72 mass% 1-octanol and 3.38 mass% binary mixture

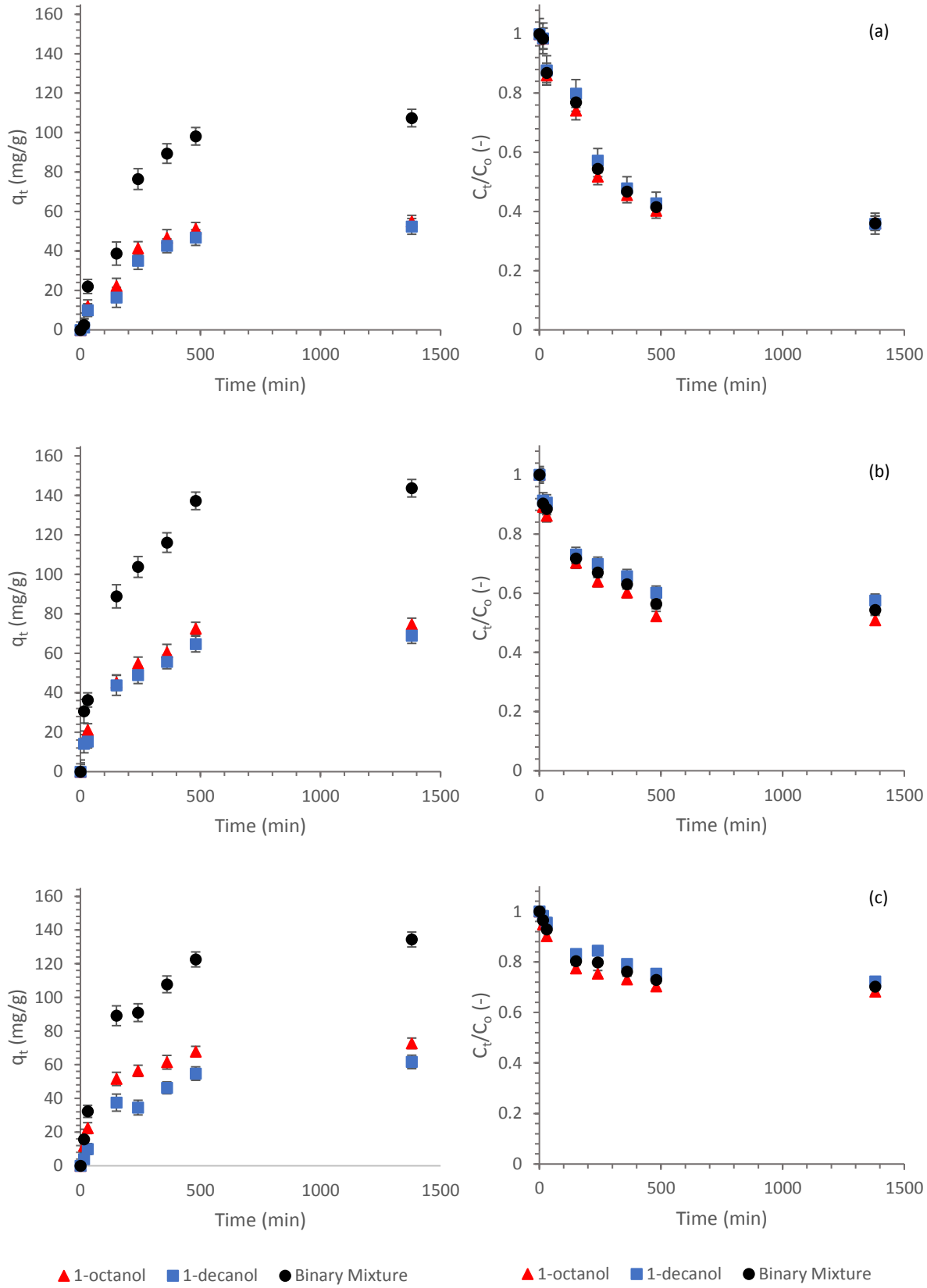

Figure D.2-18: Time profiles (left) and corresponding concentration decay plots (right) for the binary component adsorption of 1-octanol and 1-decanol onto SCD, at 45°C, and initial adsorbate concentrations of (a) 0.60 mass% 1-octanol, 0.58 mass% 1-decanol and 1.18 mass% binary mixture; (b) 1.00 mass% 1-octanol, 1.07 mass% 1-decanol and 2.06 mass% binary mixture; and, (c) 1.52 mass% 1-octanol, 1.48 mass% 1-decanol and 3.00 mass% binary mixture

Appendix E: Adsorbent Characterisation

Appendix Contents

E.1 Additional Theory on Adsorbents

Adsorbents are engineered such that it is fit for specific applications. These materials need to have certain characteristics such as [20]:

(i) Large specific surface area;

(ii) High porosity; and,

(iii) Large pore network.

E.1.1 Specific Surface Area

Both the external as well as the internal surface area of adsorbents influence the adsorption process. External surface area is more related to the rate of adsorption whereas internal surface area is more related to adsorbent loading [10].

The internal surface area of adsorbents is one of its most pivotal properties. A large number of adsorption sites are situated on the internal surface area of adsorbents; therefore, a larger internal surface area allows for a greater adsorbent loading. Internal surface area is also closely related to the number of micropores present in an adsorbent.

E.1.2 Adsorbent Density and Porosity

Adsorbent porosity and density are closely related. Density refers to the mass per volume. Particle porosity refers to the void fraction of the total particle volume [10]. The relationship between porosity and density is denoted by Equation E.1-1, with V the volume and ρ_p and ρ_m the particle and material densities respectively.

$$\varepsilon_p = \frac{V_{pore}}{V_{total}} = 1 - \frac{\rho_p}{\rho_m} \qquad [\text{ E.1-1 }]$$

For effective adsorption, it is desirable for adsorbents to have a large porosity. A large porosity indicates a large pore network and a considerable number of pores inside the adsorbent particle.

E.1.3 Pore Size Distribution

Pores can be classified based on their structure and size. Generally, the IUPAC pore size classification system is used, however, several other classification systems exist [25]. The three main pore sizes are micropores, mesopores and macropores. Typically macro- and mesopores are used as passage from the outer surface of the adsorbent to the micropores, *i.e.* transport pores, where most of the adsorption occurs [10].

Table E.1-1 provides a summary of but a few pore size classification systems.

Table E.1-1: Pore size classification

Pore Classification	***Pore Width, W (nm)***		
	[25]	[114]	[115]
Submicropore	$W < 0.4$		
Ultramicropore		$W < 0.7$	$0.001 < W < 0.05$
Supermicropore		$0.7 < W < 2$	
Micropore	$0.4 < W < 2$	$W < 2$	$0.05 < W < 0.3$
Mesopore	$2 < W < 50$	$2 < W < 50$	$0.3 < W < 0.75$
Mesopore	$W > 50$	$W > 50$	$W > 50$

As mentioned, pores can also be classified based on structure. According to IUPAC, these classes are [116]:

(i) Closed pores;

(ii) Blind pores (one-ended open pores);

(iii) Through pores (two-ended open pores);

(iv) Open pores.

Closed pores refer to pores that are enclosed and inaccessible to adsorbate molecules [117]. These pores arise as a result of insufficient heating during the activation process [117]. Blind pores are open at one end only, through pores are open on both sides and open pores are entirely open to the surroundings, as depicted in Figure E.1-1.

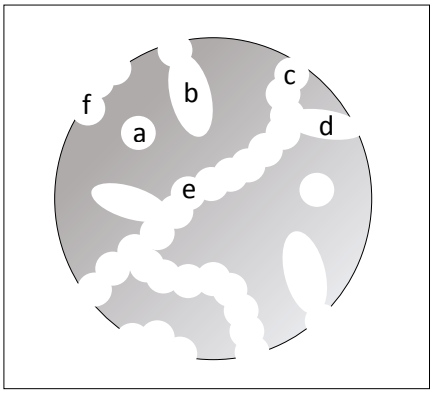

Figure E.1-1: Schematic diagram of different pore classes. (a) Closed pore; (b) Blind pore; (c) Open pore; (d) Open pore; (e) Through pore; and, (f) Open pore (Redrawn from [116]).

E.2 Pore Structure

E.2.1 Activated Alumina F220

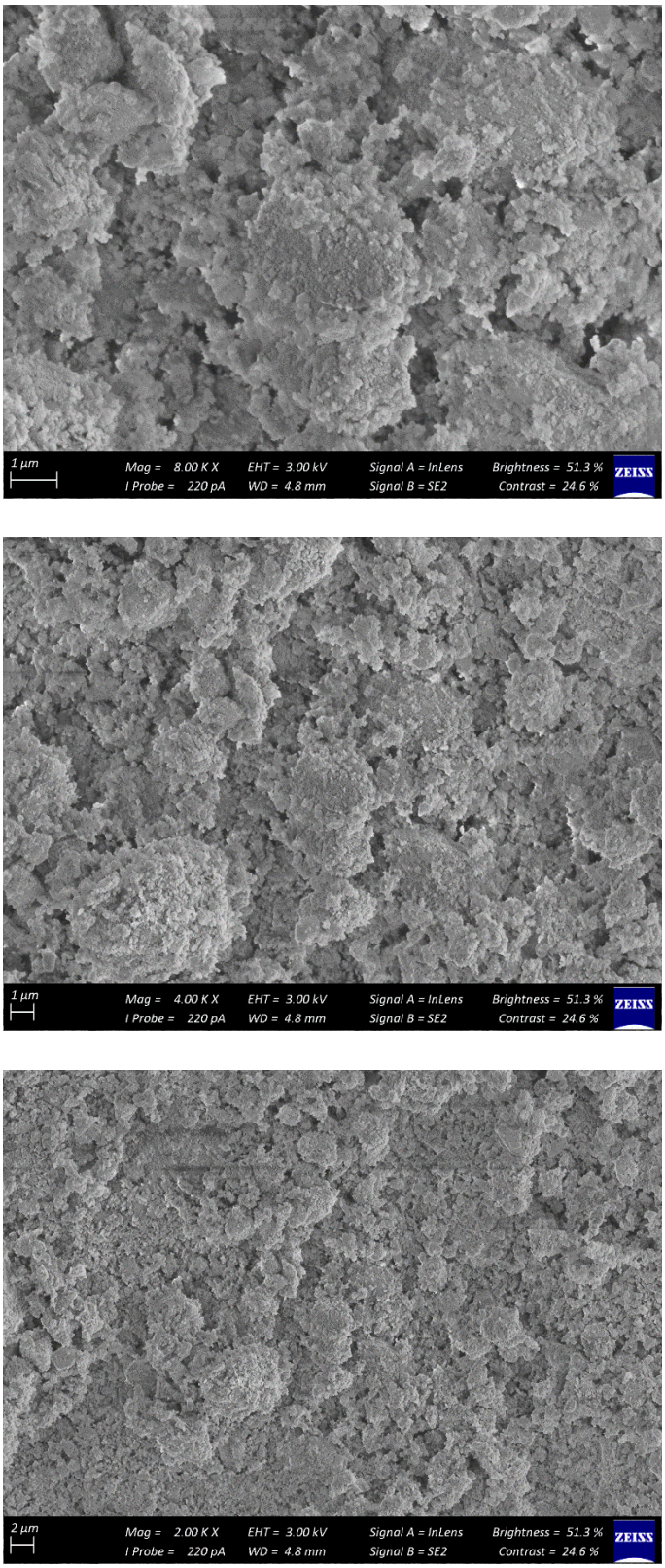

Figure E.2-1: SEM images of blank Activated Alumina F220 pore structure at the centre area of the adsorbent bead

E.2.2 Selexsorb CDx®

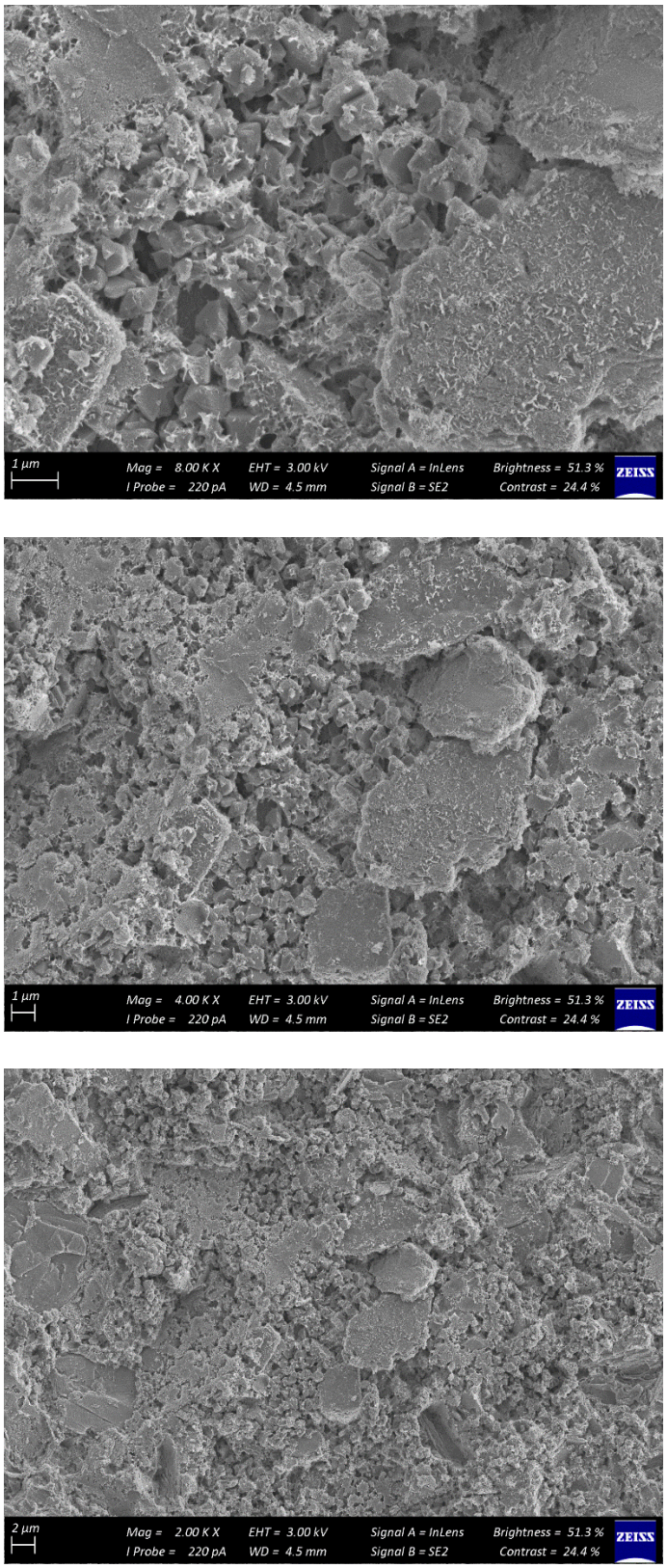

Figure E.2-2: SEM images of blank Selexsorb CDx® pore structure at the centre area of the adsorbent bead

E.2.3 Selexsorb CD®

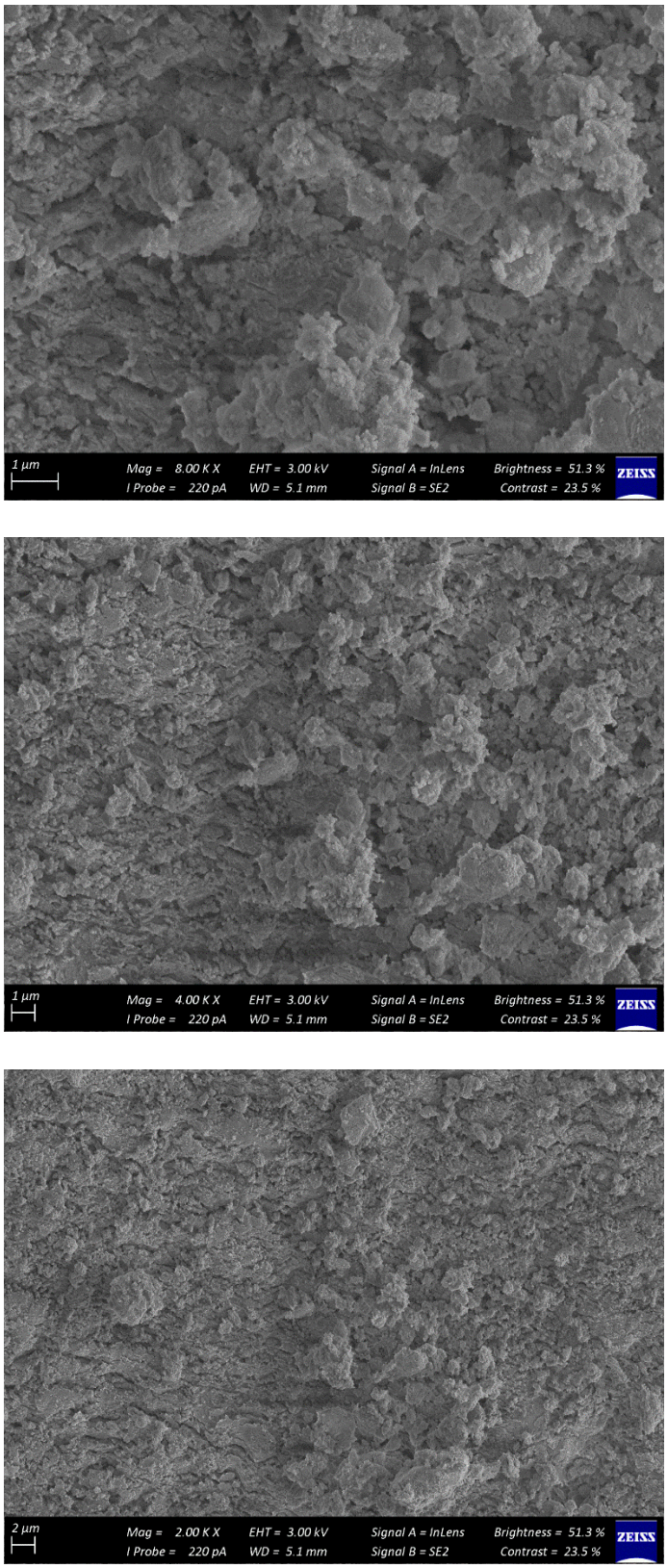

Figure E.2-3: SEM images of blank Selexsorb CD® pore structure at the centre area of the adsorbent bead

E.3 Adsorbent Composition

E.3.1 Methodology

EDX analysis determines the elemental composition of a sample at a specific position on the sample. EDX analysis was conducted for each of the three adsorbents investigated in this study. For each adsorbent sample, EDX was done in two straight lines in parallel, determining the composition at 50 different positions on each line (Figure E.3-1). An additional line, called the sum line, was investigated in the middle of the two straight lines (line 1 and line 2). The composition was also determined at 50 equally spaced positions along the sum line. Therefore, 150 different compositions were obtained for each adsorbent, since 50 different compositions were obtained along each of the three different lines. An average of the 150 different compositions was assumed to be an accurate representation of the composition of the adsorbents.

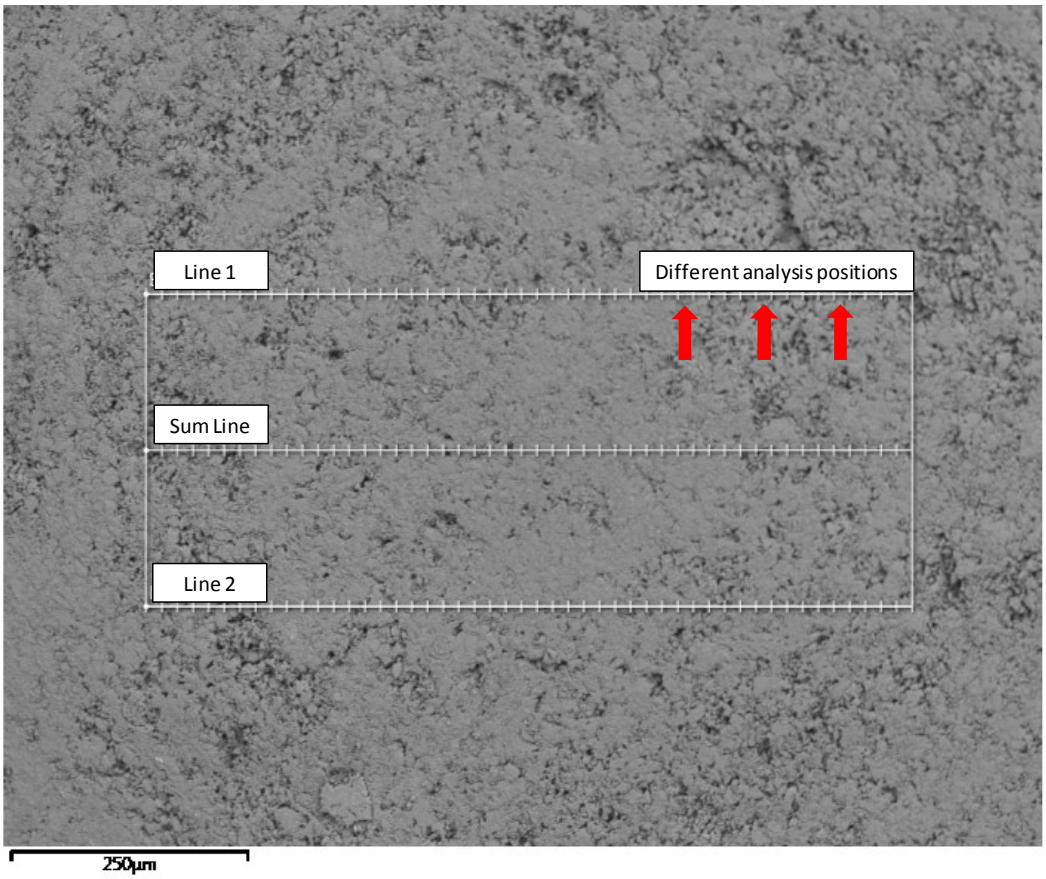

Figure E.3-1: Representation of two horizontal lines (with 50 different positions on each) on a sectioned AA-F220 adsorbent sample where EDX analysis was conducted

Since adsorbent particles are very porous, EDX analysis sometimes provides inaccurate results (very high or low compositions of a specific element at a specific position) due to pores/roughness in the area of analysis. An example of such an occurrence is depicted in Figure E.3-2 where oxygen and aluminium both exhibit outlier compositions due to a rough area in the surface of the adsorbent at that position of analysis. It can be seen that the composition obtained at this position is not in accordance with the compositions obtained

at the other positions along the line of investigation. However, by taking the average composition of 150 different positions on the adsorbent, this inaccuracy is addressed.

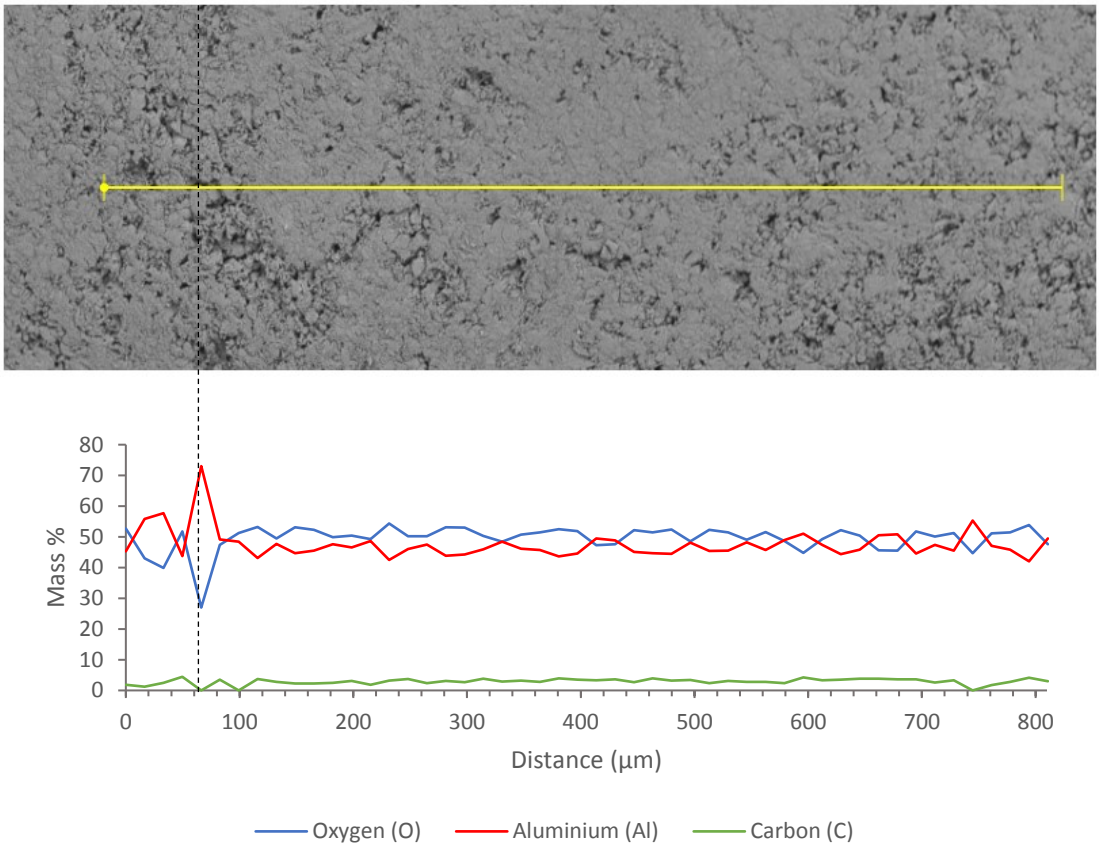

Figure E.3-2: EDX analysis composition of an AA-F220 adsorbent sample at different positions on a straight line

E.3.2 Energy-dispersive X-ray (EDX) Analysis Results

The EDX analysis results obtained for AA-F220, SCDX and SCD are provided below. For each adsorbent the following is provided:

(i) An image of each line of investigation (lines 1, 2 and the sum line) on a sectioned sample of the adsorbent;

(ii) The composition graph associated with the specific line; and,

(iii) The average composition of each line.

E.3.2.1 ***Activated Alumina F220***

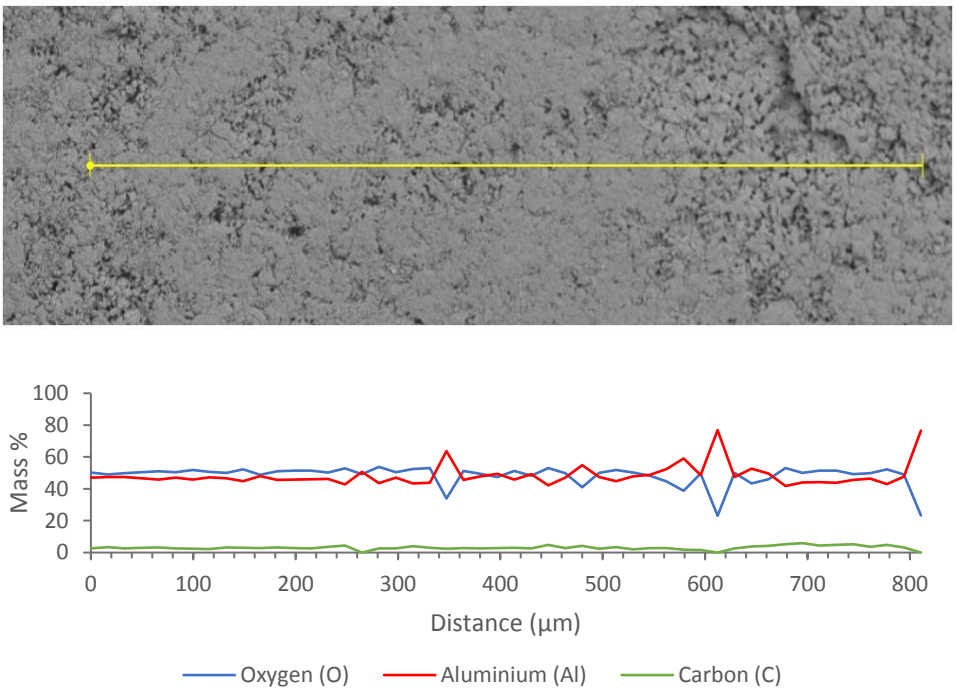

Figure E.3-3: Electron image of line 1 on Activated Alumina F220 and its associated EDX composition graph

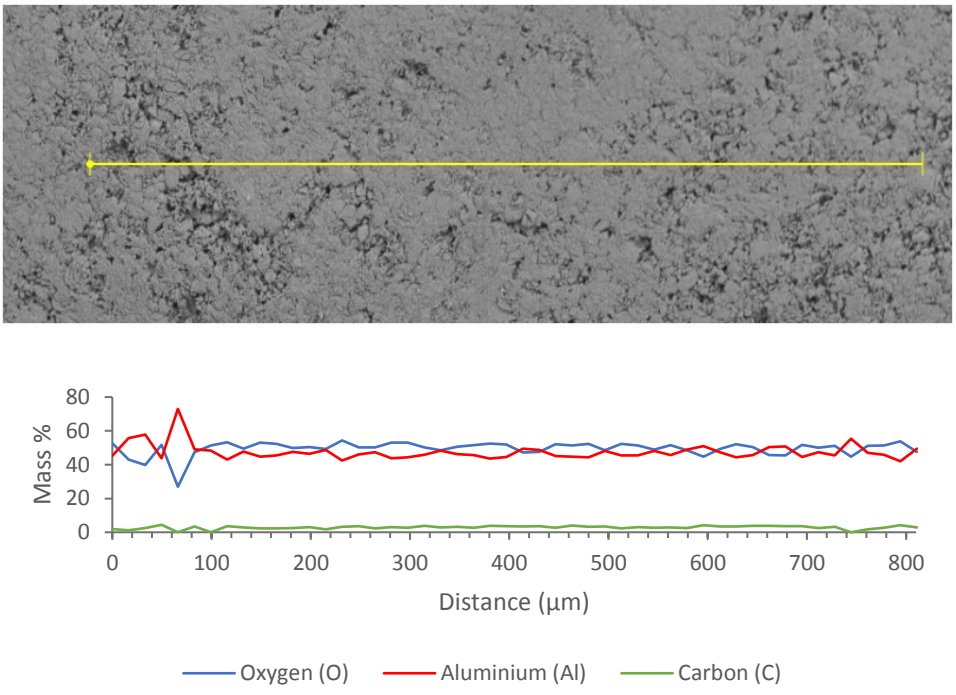

Figure E.3-4: Electron image of line 2 on Activated Alumina F220 and its associated EDX composition graph

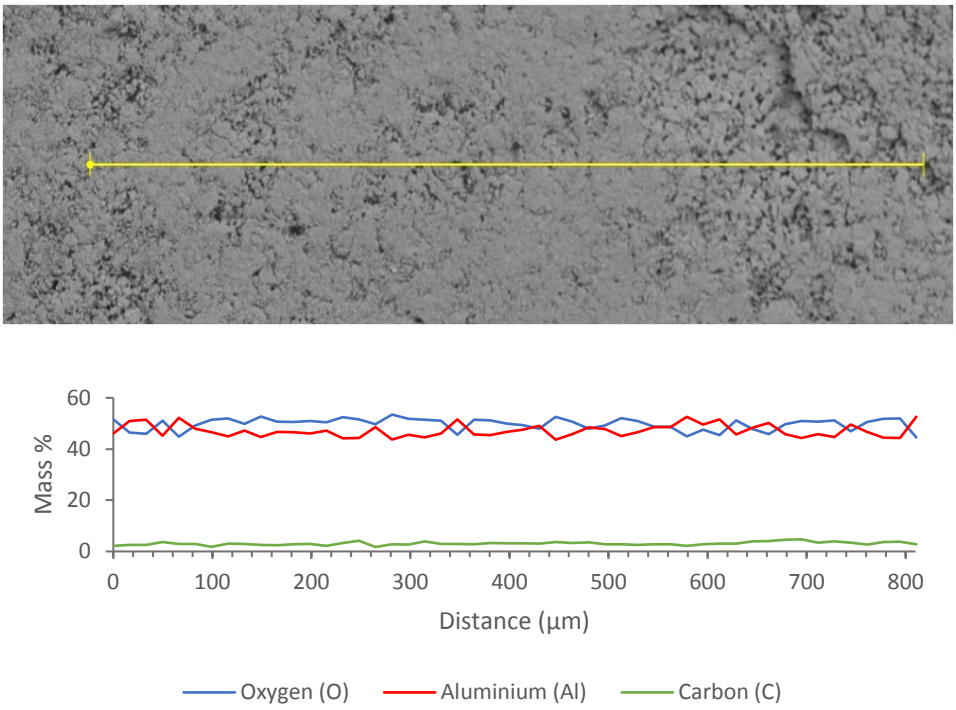

Figure E.3-5: Electron image of the sum line on Activated Alumina F220 and its associated EDX composition graph

Table E.3-1: Average EDX composition of Activated Alumina F220

Element (mass%)	***Line 1***	***Line 2***	***Sum line***	***Average***
Aluminium (Al)	47.9	47.5	47.0	47.5
Oxygen (O)	49.0	49.6	49.8	49.5
Sodium (Na)	0.0	0.0	0.0	0.0
Carbon (C	3.1	2.9	3.1	3.0
Silica (Si)	0.0	0.0	0.0	0.0

E.3.2.2 ***Selexsorb CDx®***

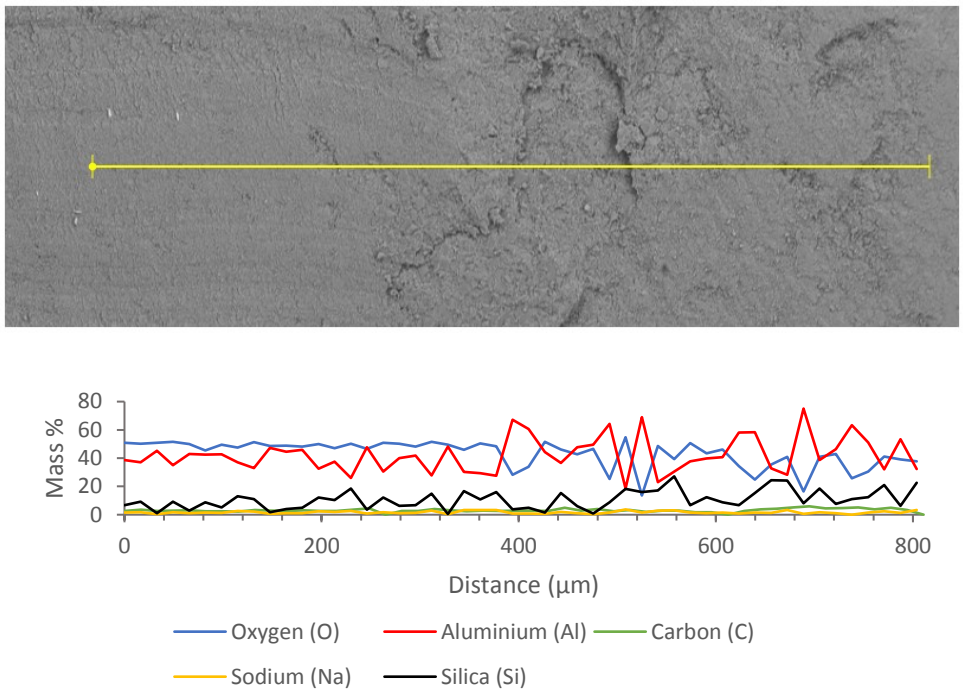

Figure E.3-6: Electron image of the line 1 on Selexsorb CDx® and its associated EDX composition graph

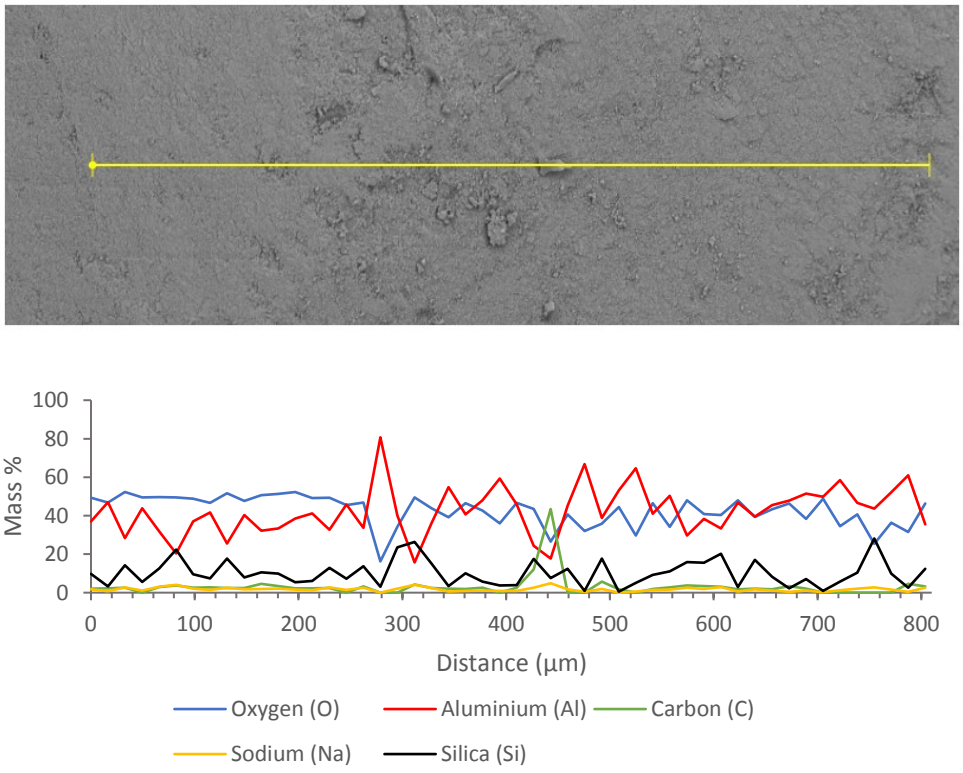

Figure E.3-7: Electron image of the line 2 on Selexsorb CDx® and its associated EDX composition graph

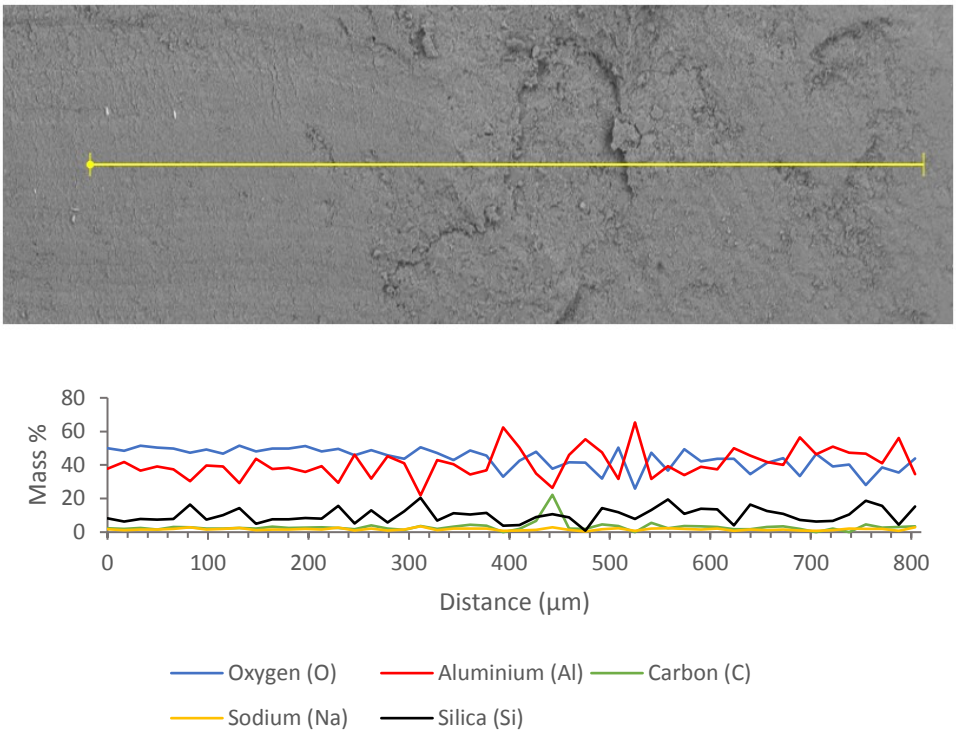

Figure E.3-8: Electron image of the sum line on Selexsorb CDx® and its associated EDX composition graph

Table E.3-2: Average EDX composition of Selexsorb CDx®

Element (mass%)	***Line 1***	***Line 2***	***Sum line***	***Average***
Aluminium (Al)	42.2	42.3	41.1	41.9
Oxygen (O)	43.2	42.7	44.0	43.3
Sodium (Na)	1.7	1.7	1.7	1.7
Carbon (C	2.3	3.1	3.1	2.8
Silica (Si)	10.6	10.2	10.1	10.3

E.3.2.3 ***Selexsorb CD®***

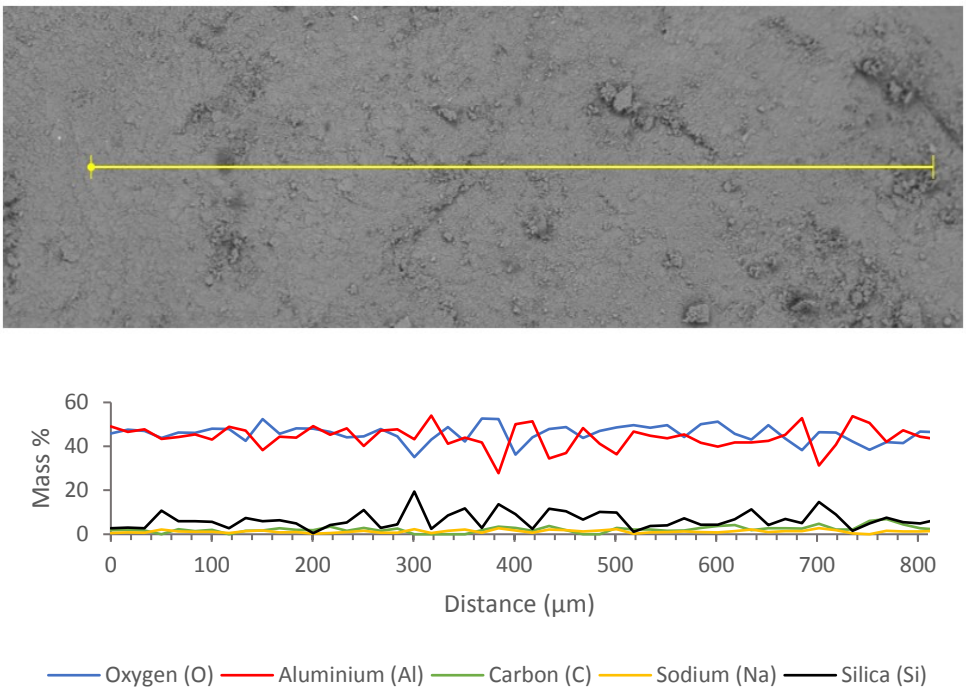

Figure E.3-9: Electron image of the line 1 on Selexsorb CD® and its associated EDX composition graph

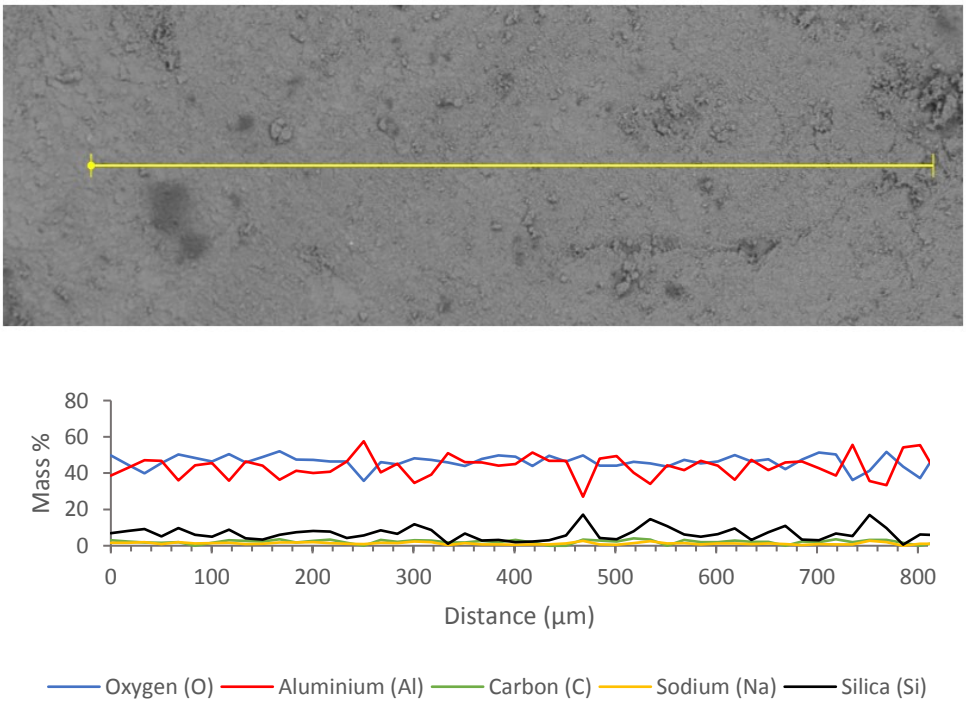

Figure E.3-10: Electron image of the line 2 on Selexsorb CD® and its associated EDX composition graph

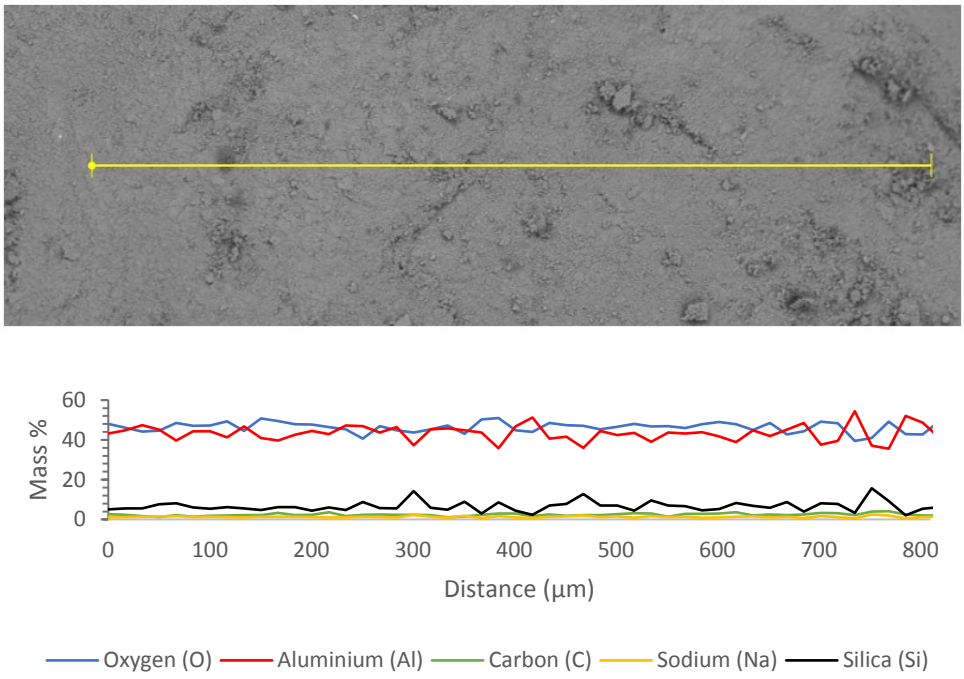

Figure E.3-11: Electron image of the sum line on Selexsorb CD® and its associated EDX composition graph

Table E.3-3: Average EDX composition of Selexsorb CD®

Element (mass%)	***Line 1***	***Line 2***	***Sum line***	***Average***
Aluminium (Al)	44.2	43.6	43.4	43.7
Oxygen (O)	45.8	46.3	46.3	46.1
Sodium (Na)	1.3	1.3	1.3	1.3
Carbon (C	2.2	2.2	2.4	2.3
Silica (Si)	6.5	6.7	6.6	6.6

Appendix F: Experimental Adsorption Results

Appendix Contents

F.1 Calculation Methodology

In Chapter 5, two parameters are used to investigate the experimental adsorption data. These parameters are:

(i) Normalised adsorbate concentration (in the bulk solution); and,

(ii) Adsorbent loading.

F.1.1 Normalised Adsorbate Concentration

In this section, a methodology will be outlined for the determination of the normalised liquid concentration, C_t/C_o.

The system that will be used as an example is the single component system comprising 1-hexanol onto AA-F220, at 45°C.

The GC provided the mass of each component in every sample in the following form:

Table F.1-1: GC raw data of the single component adsorption of 1-hexanol onto AA-F220 (T = 45°C)

	Mass (mg)	
	1-hexanol	*n-decane*
Time = 0 min	1.24	122
Time = 1380 min	0.38	106

Using the data provided by the GC, the mass fraction of each alcohol in the system was calculated by use of Equation F.1-1.

$$X_i = \frac{m_i}{m_{total}} \qquad [\text{ F.1-1 }]$$

Therefore, the mass fraction of 1-hexanol in this system at time 0 min and time 1380 min were as follows:

$$X_{1-hexanol,o} = \frac{1.244}{1.244+122.4} = 1.005\ mass\%$$

$$X_{1-hexanol,1380min} = \frac{0.3750}{0.3750+105.9} = 0.3528\ mass\%$$

The normalised liquid concentration was determined with Equation F.1-2.

$$\frac{C_t}{C_o} = \frac{X_{i,t}}{X_{i,o}} \qquad [\text{ F.1-2 }]$$

Therefore, C_t/C_o of 1-hexanol at 1380 min was:

$$\left(\frac{C_t}{C_o}\right)_{1-hexanol,1380min} = \frac{0.3528}{1.005} = 0.35$$

F.1.2 Adsorbent Loading

The system that will be used as an example is the binary component mixture comprising 1-hexanol and 1-octanol onto SCDx, at 45°C.

The GC provided the mass of each component in every sample in the following form:

Table F.1-2: GC raw data of the binary mixture of 1-hexanol and 1-octanol onto SCDx (T = 45°C)

	Mass (mg)		
	1-hexanol	*1-octanol*	*n-decane*
Time = 0 min	0.78	0.64	107
Time = 1380 min	0.32	0.32	108

Using the data provided by the GC, the mass fraction of each alcohol in the binary mixture was calculated by use of Equation F.1-1.

$$X_i = \frac{m_i}{m_{total}} \qquad [\text{ F.1-1 }]$$

Therefore, the mass fractions of 1-hexanol and 1-octanol in this system at time 0 min and time 1380 min were as follows:

$$X_{1-hexanol,o} = \frac{0.7801}{0.7801+0.6395+107.2} = 0.7180\ mass\%$$

$$X_{1-hexanol,1380min} = \frac{0.3177}{0.3177+0.3157+107.7} = 0.2933\ mass\%$$

$$X_{1-octanol,o} = \frac{0.6395}{0.7801+0.6395+107.2} = 0.5885\ mass\%$$

$$X_{1-octanol,1380min} = \frac{0.3157}{0.3177+0.3157+107.7} = 0.2915\ mass\%$$

As mentioned in the experimental methodology, the mass of the adsorbent and mass of the solution were measured before the adsorption experiments (Table F.1-3).

Table F.1-3: Experimental measurements

Adsorbent Mass (g)	***Solution Mass (g)***
10.04	150.8

Using all above given data and experimental measurements, the adsorbent loading of each of the alcohols in the mixture was determined using Equation F.1-2.

$$q_i = \frac{(X_{i,o}m_{solution} - X_{i,t}m_{solution})}{m_{adsorbent}} \qquad [\text{ F.1-2 }]$$

Therefore, the adsorbent loading of 1-hexanol and 1-octanol at 1380 min were as follows:

$$q_{1-hexanol,1380} = \frac{(0.007180(150.8) - 0.002933(150.8))}{10.04} = 63.79\ mg/g$$

$$q_{1-octanol} = \frac{(0.005885(150.8) - 0.002915(150.8))}{10.04} = 44.60\ mg/g$$

Lastly, the total adsorbent loading of the binary mixture was the sum of the components, *i.e.* 108.4 mg/g.

F.2 Interaction Effect in Binary Component Systems

F.2.1 Interaction Effect Calculation Methodology

The interaction parameter is the ratio of the equilibrium adsorbent loading of a component in a binary mixture and a single component system (Equation 2.5-1), as discussed in Chapter 2 (Section 2.5).

$$R_{q,i} = \frac{q_{i,binary}}{q_{i,single}}$$

The system that will be used as an example is the binary component mixture of 1-hexanol and 1-octanol onto SCDx, at 45°C. The adsorbent loadings of this system are provided in Table F.2-1.

Table F.2-1: Adsorbent loadings onto SCDx (T = 45°C; IC = 1 mass%)

	Adsorbent loading (mg/g)	
	1-hexanol	*1-decanol*
Binary Component System	80.9	44.0
Single Component System	112	123

Therefore, the interaction parameters are as follows:

$$R_{q,1-hexanol} = \frac{80.85}{112.4} = 0.7193$$

$$R_{q,1-octanol} = \frac{44.01}{122.5} = 0.3592$$

F.2.2 Interaction Effect Graphs

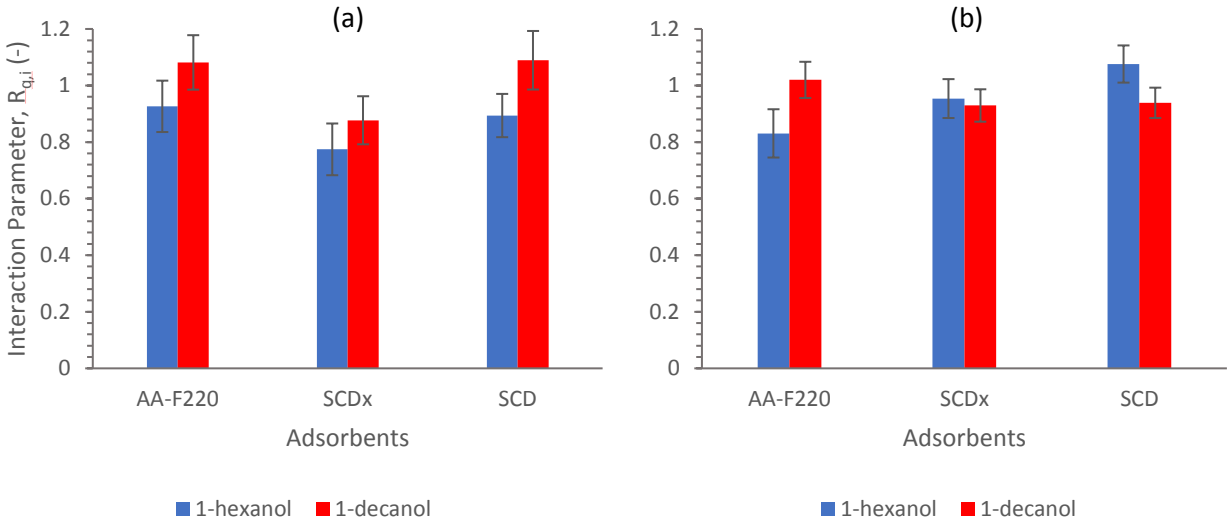

Figure F.2-1: Comparison of the interaction parameters corresponding to 1-hexanol and 1-decanol in a binary component system at (a) 25°C; and, (b) 45°C (component IC = 0.5 mass%)

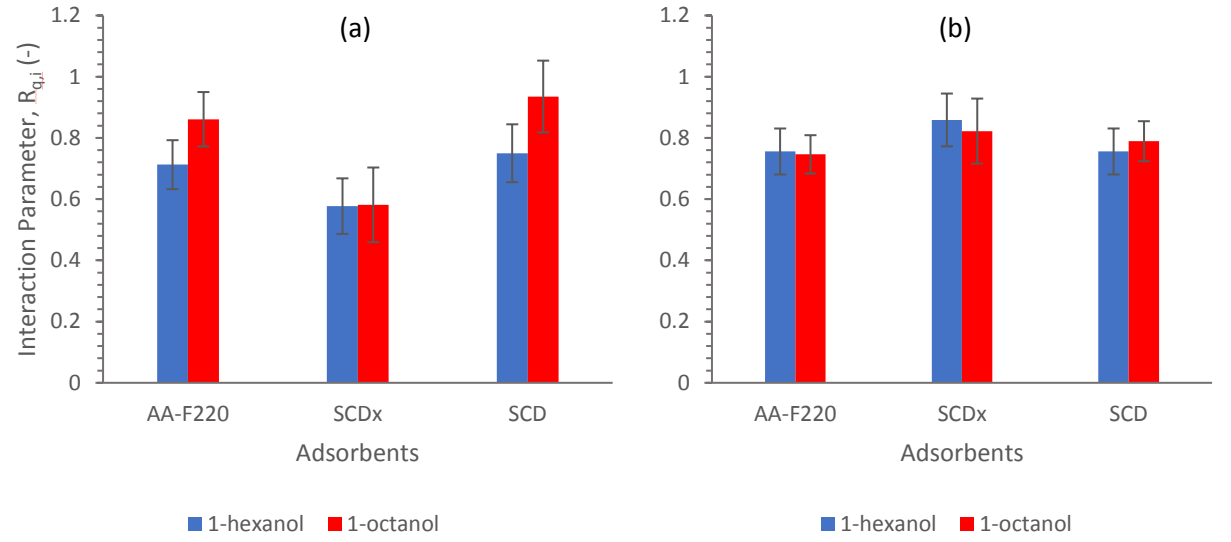

Figure F.2-2: Comparison of the interaction parameters corresponding to 1-hexanol and 1-octanol in a binary component system at (a) 25°C; and, (b) 45°C (component IC = 0.5 mass%)

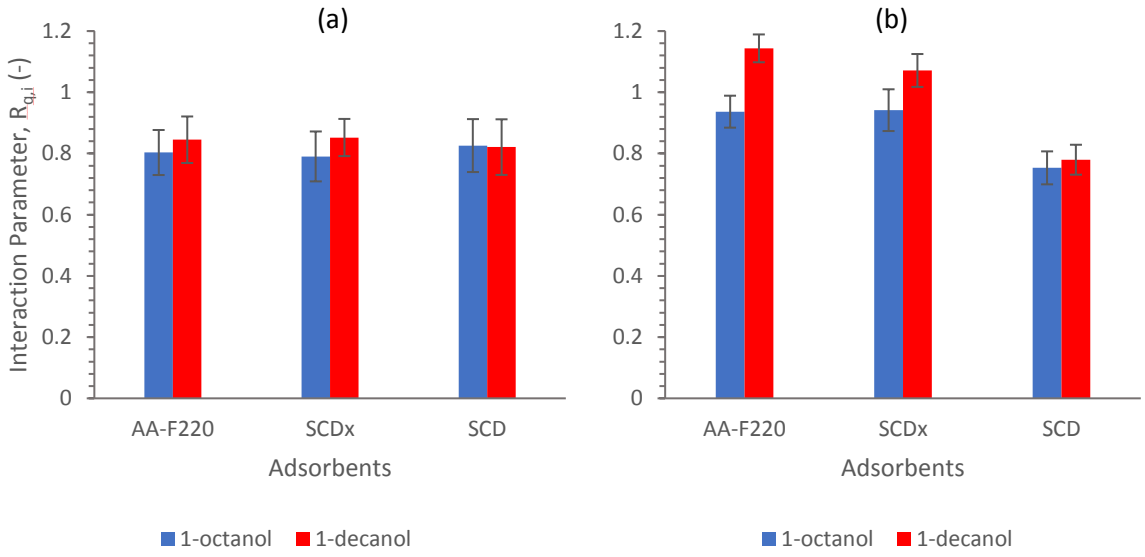

Figure F.2-3: Comparison of the interaction parameters corresponding to 1-octanol and 1-decanol in a binary component system at (a) 25°C; and, (b) 45°C (component IC = 0.5 mass%)

Appendix G: Adsorption Equilibrium Modelling

Appendix Contents

G.1 Isotherm Modelling

Typically, adsorption isotherm modelling is done by the minimisation method using an error function specific to the application.

G.1.1 Error Functions

Several error functions exist for the determination of non-linear model parameters. Some of these error functions are, however, bias toward certain experimental conditions which results in inaccurate model parameters when used incorrectly [65]. The most widely used error functions in the modelling of adsorption data are the following [51], [65], [110]:

(i) Sum of absolute errors (SAE);

(ii) Sum of squares of errors (SSE);

(iii) Hybrid fractional error (HYBRID);

(iv) Marquardt's percentage standard deviation (MPSD); and,

(v) Average relative error (ARE).

In recent studies, however, the SSE, HYBRID and MPSD functions seem to be the most commonly used.

G.1.1.1 *Sum of the Squares of Errors (SSE)*

The SSE function seem to be the most widely used error function in adsorption studies [51], [65]. This function is represented by Equation G.1-1.

$$SSE = \sum_{i=1}^{n}\left(q_{e,pred} - q_{e,exp}\right)_i^2 \qquad [\text{G.1-1}]$$

Where, $q_{e,exp}$ Experimentally determined equilibrium adsorbent loading (*mg/g*); and,

$q_{e,pred}$ Equilibrium adsorbent loading as predicted with specific model (*mg/g*).

Although the SSE function is very widely used for non-linear regression, this function tends to exhibit smaller errors at higher liquid-phase concentrations than at lower concentrations [51], [65]. This results in the model providing more accurate correlations and model parameters for higher end liquid-phase concentrations which is not always accurate.

G.1.1.2 *Hybrid Fractional Error Function*

The HYBRID function is also widely used. The SSE function was further developed to be used for lower end concentrations which resulted in the HYBRID, denoted by Equation G.1-2 [51], [65].

$$HYBRID = \frac{100}{n-p}\sum_{i=1}^{n}\left(\frac{\left(q_{e,exp} - q_{e,pred}\right)_i^2}{q_{e,exp}}\right)_i \qquad [\text{G.1-2}]$$

Where, n Number of data points; and,

p Number of regression parameters in the model.

This error function incorporates an experimentally measured equilibrium adsorbent loading which ensures that the error remains relative to that measured value instead of increasing as concentration increases [51], [65]. The HYBRID function also accounts for the degrees of freedom in the system by subtracting the number of model parameters from the number of data points measured [110].

G.1.1.3 *Marquardt's Percent Standard Deviation*

The MPSD function is represented by Equation G.1-3.

$$MPSD = 100\left(\sqrt{\frac{1}{n-p}\sum_{i=1}^{n}\left(\frac{(q_{e,exp}-q_{e,pred})}{q_{e,exp}}\right)_i^2}\right) \qquad [\text{G.1-3}]$$

The MPSD follows a "geometric mean error distribution" and incorporates the degrees of freedom of the system [51], [65], [110]. This error function also incorporates an experimentally measured equilibrium adsorbent loading which allows for the error to remain relative to this measured adsorbent loading value.

G.1.2 Modelling Methodology

For the purposes of this study, the modelling of both the single component as well as the binary component systems were done by the error function minimisation method. The HYBRID function (Equation G.1-2) was employed and the minimisation was done with the Solver Add-in package in Microsoft Excel®. The HYBRID function was minimised to obtain the smallest possible error between the model predicted adsorbent loadings and the experimentally determined adsorbent loadings.

The concentration range investigated in this study was rather low, therefore the most suitable error function for the modelling of the systems in question were chosen to be the HYBRID function. This error function is known to be more accurate at lower end concentrations than the SSE function. In addition, a term for the degrees of freedom is incorporated to make the error function more model specific.

G.2 Binary Component Adsorption

G.2.1 Parity Plots of Various Equilibrium Isotherm Models

The discussions accompanying the parity plots entail a comparison of the different forms of the LM and different forms of the RPM for each binary component system investigated.

G.2.1.1 *Activated Alumina*

For the system of 1-hexanol and 1-decanol, the non-modified isotherms, *i.e.* non-modified LM and non-modified RPM, seemed to be less adequate in describing the equilibrium behaviour, with the non-modified LM having a slightly higher correlation coefficient than the non-modified RPM isotherm for both temperatures. With regards to the different forms of the LM, the Extended LM proved to be the most suitable at 25°C, whereas the Modified LM proved to be the best at 45°C.

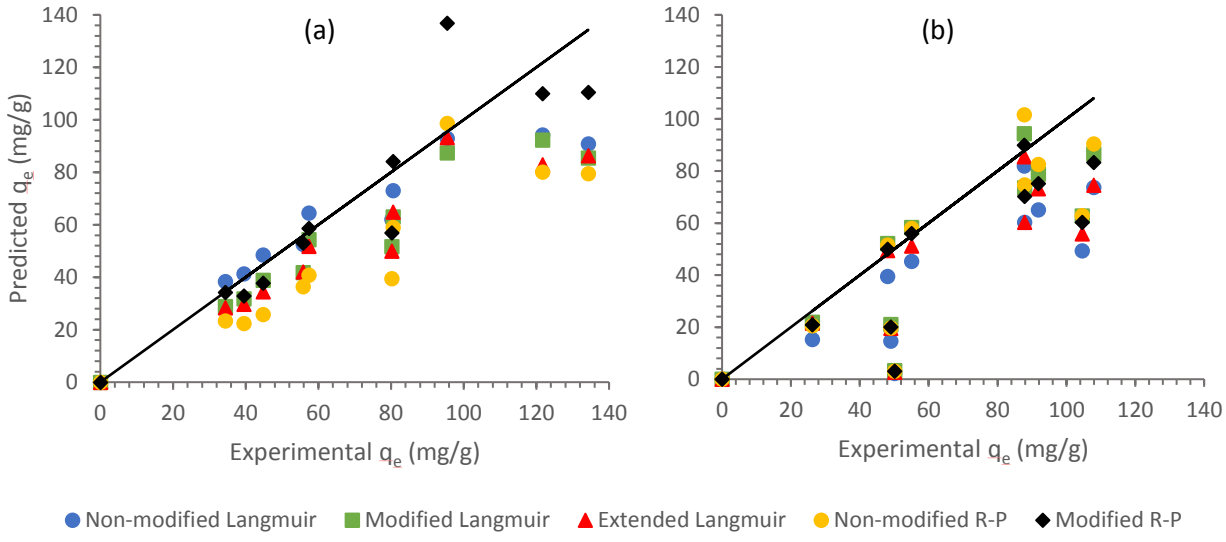

Figure G.2-1: Predicted vs. experimental equilibrium adsorbent loadings for the comparison of different forms of the binary Langmuir and Redlich-Peterson isotherm models for the adsorption of a) 1-hexanol; and, b) 1-decanol in the system of 1-hexanol + 1-decanol (50:50 by mass) onto Activated Alumina F220 (T = 25°C)

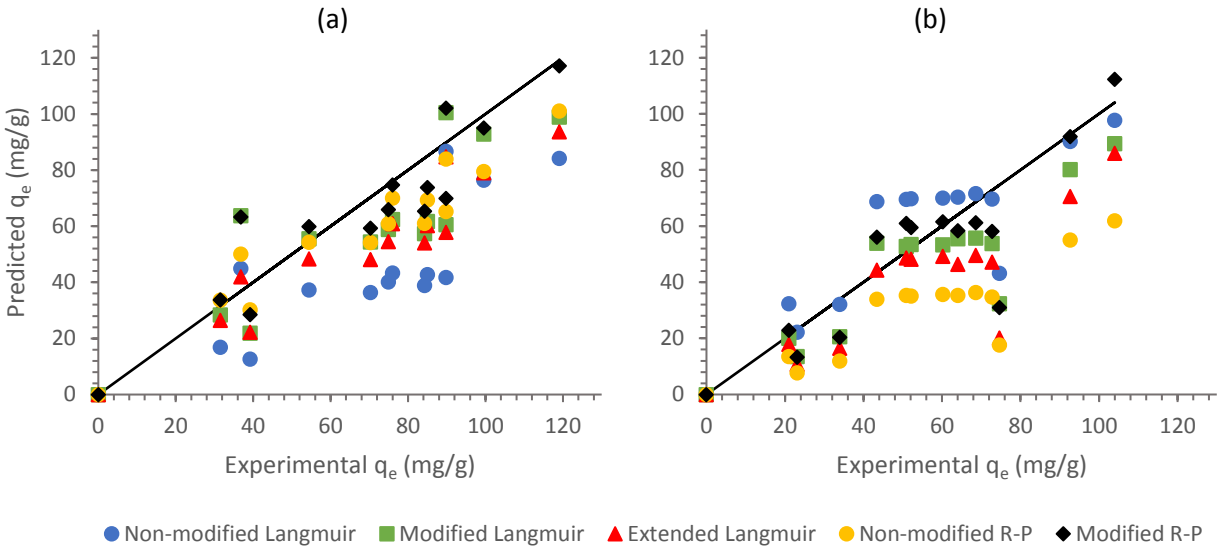

Figure G.2-2: Predicted vs. experimental equilibrium adsorbent loadings for the comparison of different forms of the binary Langmuir and Redlich-Peterson isotherm models for the adsorption of a) 1-hexanol; and, b) 1-decanol in the system of 1-hexanol + 1-decanol (50:50 by mass) onto Activated Alumina F220 (T = 45°C)

When comparing the non-modified isotherms for the system of 1-hexanol and 1-octanol, the non-modified Langmuir isotherm proved to be the better of the two at the lower temperature of 25°C whereas the non-modified Redlich-Peterson isotherm seemed better at 45°C. The Modified Langmuir isotherm had the highest correlation coefficient of the different Langmuir isotherms at both temperatures.

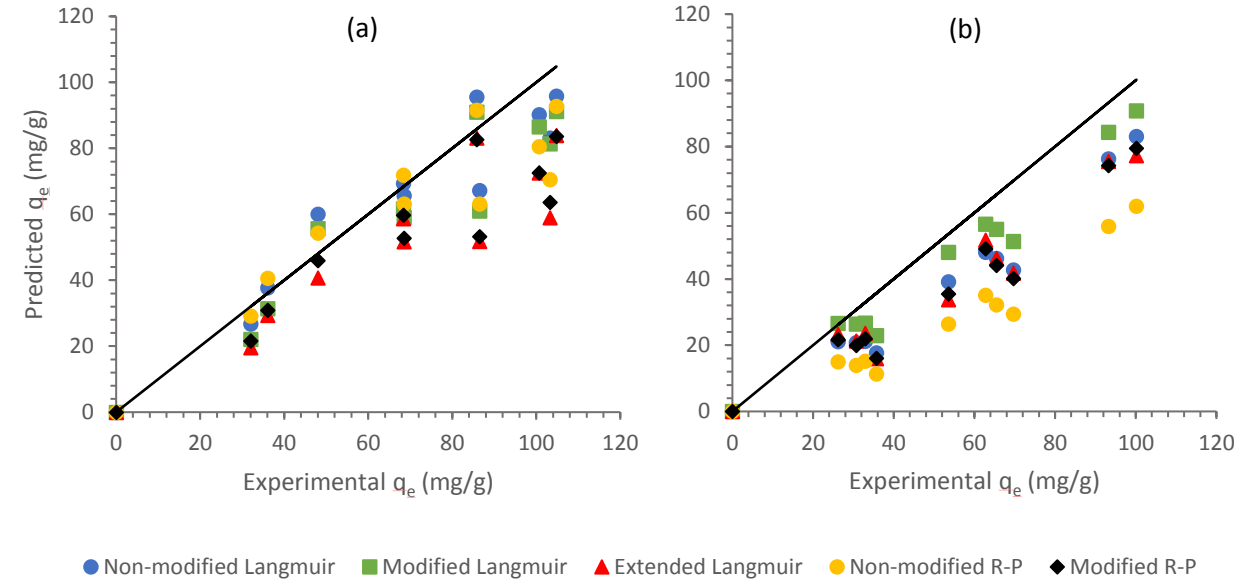

Figure G.2-3: Predicted vs. experimental equilibrium adsorbent loadings for the comparison of different forms of the binary Langmuir and Redlich-Peterson isotherm models for the adsorption of a) 1-hexanol; and, b) 1-octanol in the system of 1-hexanol + 1-octanol (50:50 by mass) onto Activated Alumina F220 (T = 25°C)

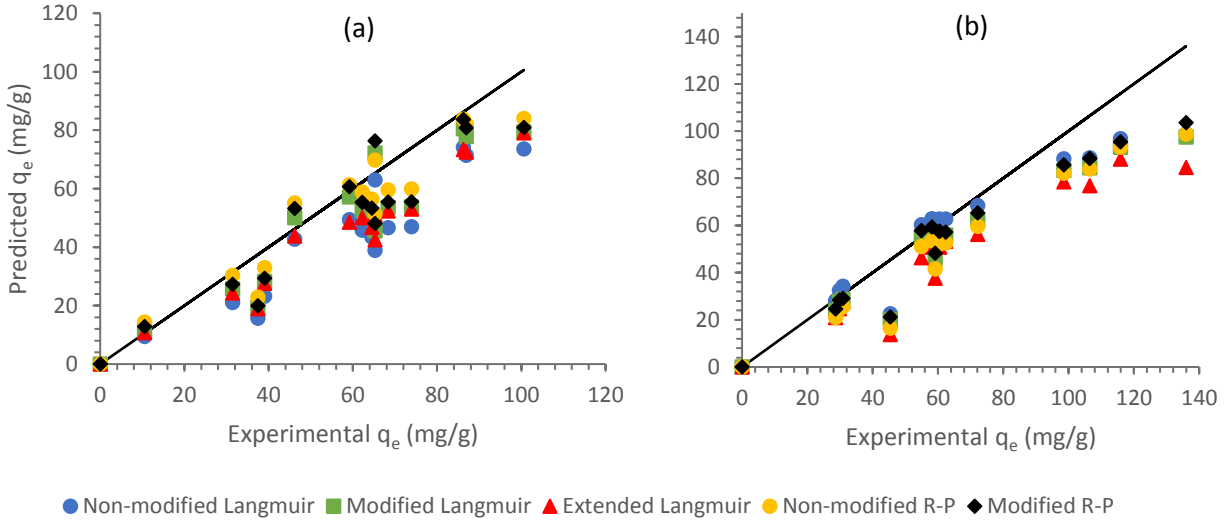

Figure G.2-4: Predicted vs. experimental equilibrium adsorbent loadings for the comparison of different forms of the binary Langmuir and Redlich-Peterson isotherm models for the adsorption of a) 1-hexanol; and, b) 1-octanol in the system of 1-hexanol + 1-octanol (50:50 by mass) onto Activated Alumina F220 (T = 45°C)

For the system of 1-octanol and 1-decanol, the non-modified Langmuir isotherm seemed to be better at 25°C whereas the non-modified Redlich-Peterson isotherm was the better fit at 45°C. The non-modified Langmuir and Extended Langmuir isotherms had the highest correlation coefficients of the Langmuir isotherms at 25°C and 45°C, respectively.

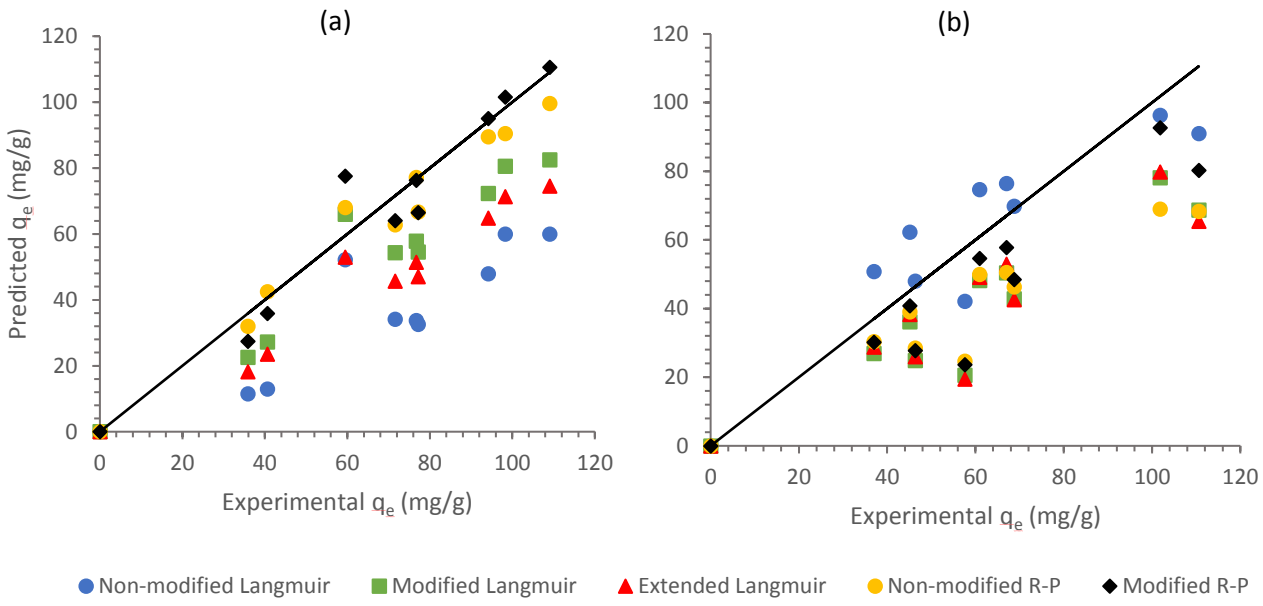

Figure G.2-5: Predicted vs. experimental equilibrium adsorbent loadings for the comparison of different forms of the binary Langmuir and Redlich-Peterson isotherm models for the adsorption of a) 1-octanol; and, b) 1-decanol in the system of 1-octanol + 1-decanol (50:50 by mass) onto Activated Alumina F220 (T = 25°C)

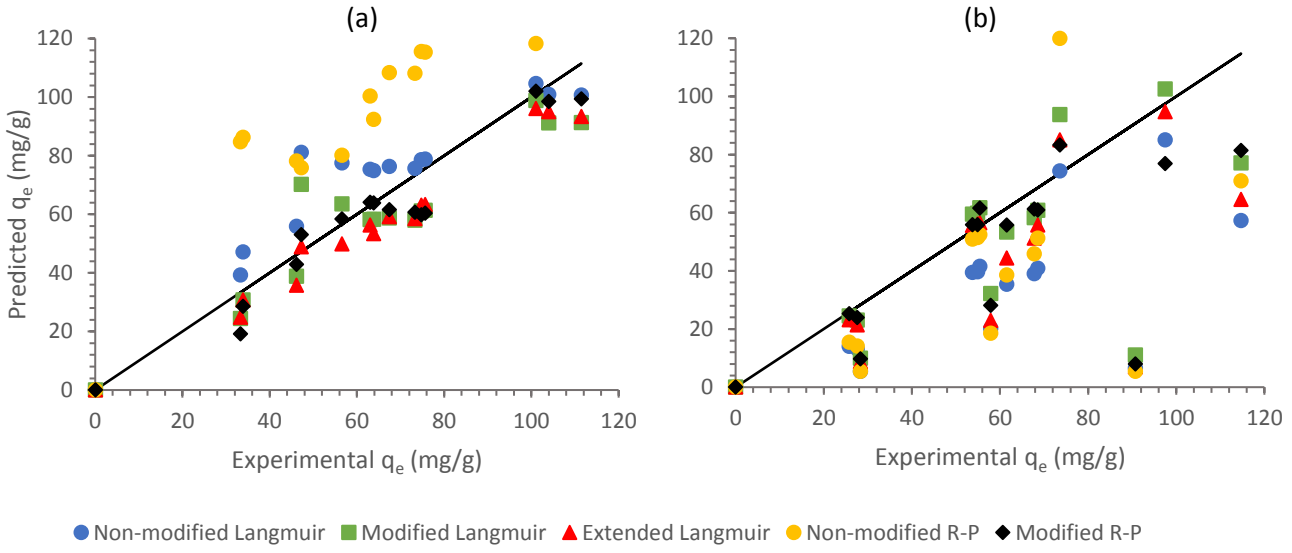

Figure G.2-6: Predicted vs. experimental equilibrium adsorbent loadings for the comparison of different forms of the binary Langmuir and Redlich-Peterson isotherm models for the adsorption of a) 1-octanol; and, b) 1-decanol in the system of 1-octanol + 1-decanol (50:50 by mass) onto Activated Alumina F220 (T = 45°C)

G.2.1.2 ***Selexsorb CDx®***

For the system of 1-hexanol and 1-decanol, the non-modified isotherm with the highest correlation coefficient was the non-modified Langmuir isotherm at both temperatures. The best form of the Langmuir isotherm was the Extended Langmuir isotherm at 25°C and the non-modified Langmuir isotherm at 45°C.

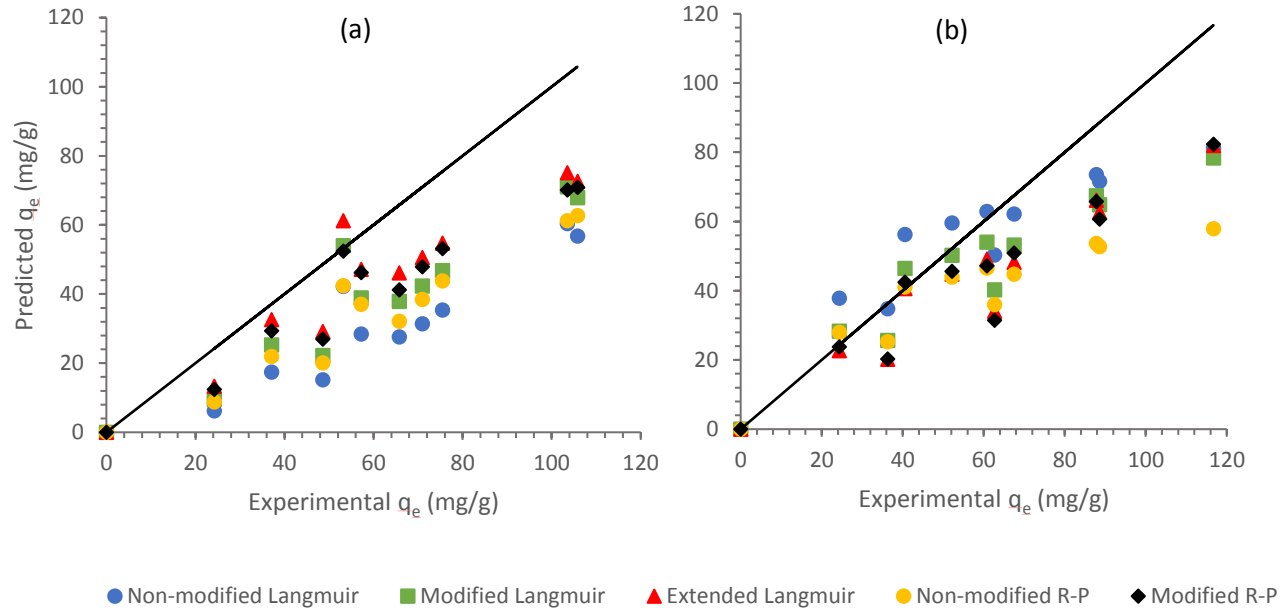

Figure G.2-7: Predicted vs. experimental equilibrium adsorbent loadings for the comparison of different forms of the binary Langmuir and Redlich-Peterson isotherm models for the adsorption of a) 1-hexanol; and, b) 1-decanol in the system of 1-hexanol + 1-decanol (50:50 by mass) onto Selexsorb CDx® (T = 25°C)

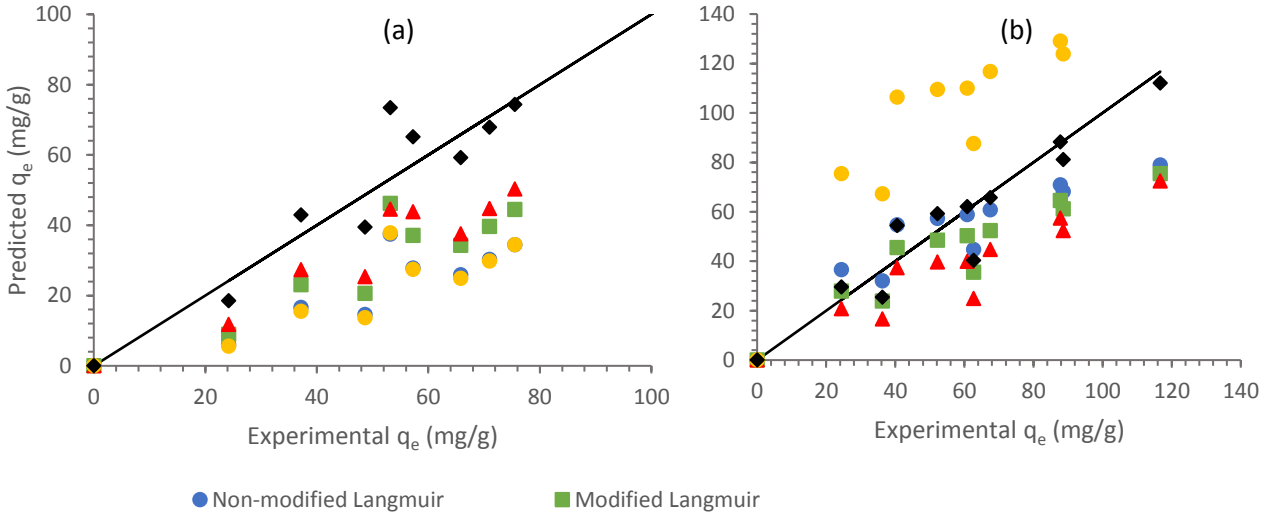

Figure G.2-8: Predicted vs. experimental equilibrium adsorbent loadings for the comparison of different forms of the binary Langmuir and Redlich-Peterson isotherm models for the adsorption of a) 1-hexanol; and, b) 1-decanol in the system of 1-hexanol + 1-decanol (50:50 by mass) onto Selexsorb CDx® (T = 45°C)

When comparing the non-modified isotherms for the system of 1-hexanol and 1-octanol, the non-modified Redlich-Peterson isotherm proved to be better at 25°C whereas the non-modified Langmuir isotherm proved to be better at 45°C. The best Langmuir isotherms were the non-modified Langmuir and the Modified Langmuir isotherms at 25°C and 45°C, respectively.

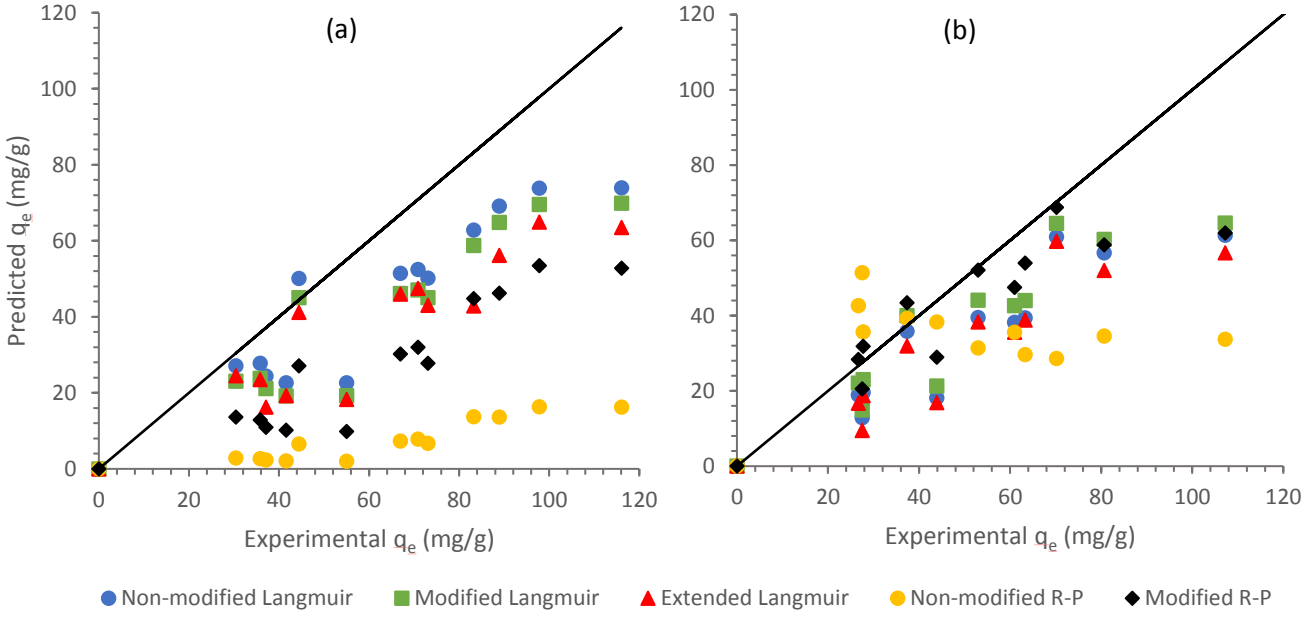

Figure G.2-9: Predicted vs. experimental equilibrium adsorbent loadings for the comparison of different forms of the binary Langmuir and Redlich-Peterson isotherm models for the adsorption of a) 1-hexanol; and, b) 1-octanol in the system of 1-hexanol + 1-octanol (50:50 by mass) onto Selexsorb CDx® (T = 25°C)

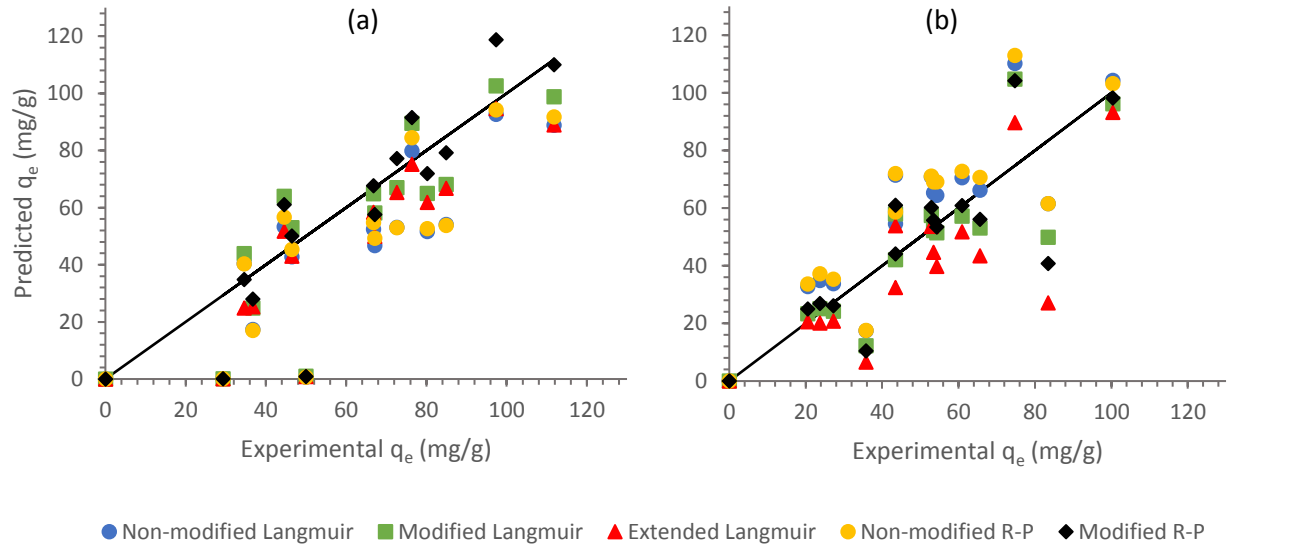

Figure G.2-10: Predicted vs. experimental equilibrium adsorbent loadings for the comparison of different forms of the binary Langmuir and Redlich-Peterson isotherm models for the adsorption of a) 1-hexanol; and, b) 1-octanol in the system of 1-hexanol + 1-octanol (50:50 by mass) onto Selexsorb CDx® (T = 45°C)

For the system of 1-octanol and 1-decanol, the non-modified Langmuir isotherm had the highest correlation coefficient when comparing the non-modified isotherms. The Extended Langmuir seemed to be the best fit among the different forms of the Langmuir isotherm.

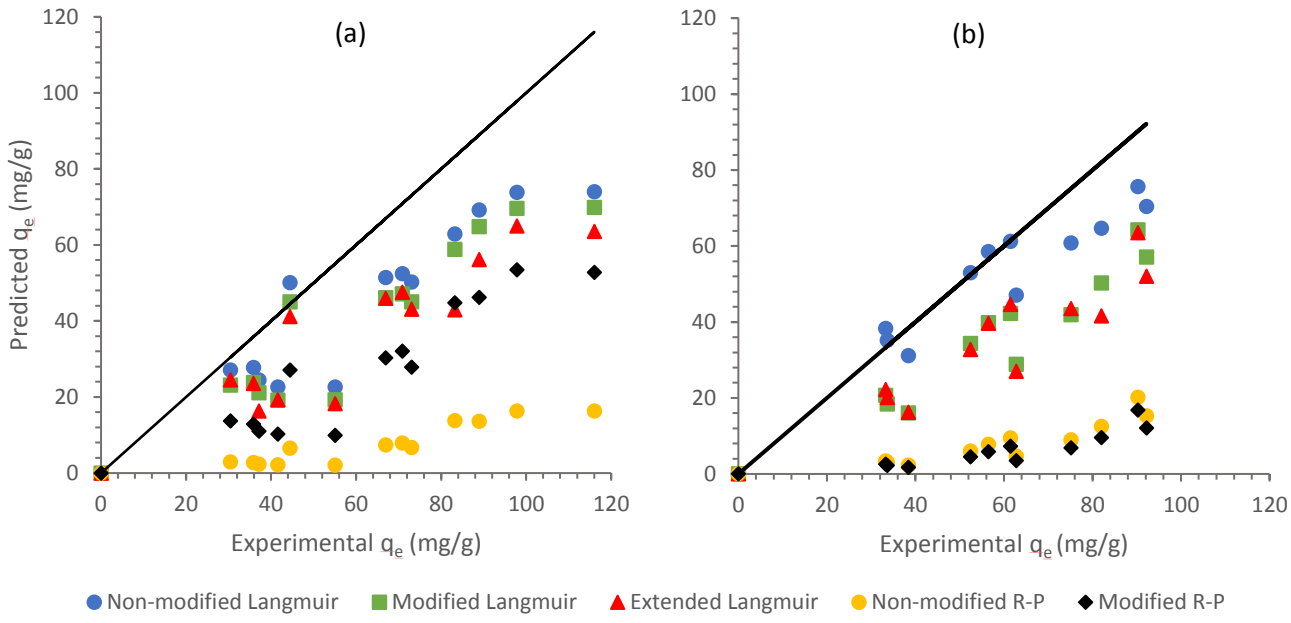

Figure G.2-11: Predicted vs. experimental equilibrium adsorbent loadings for the comparison of different forms of the binary Langmuir and Redlich-Peterson isotherm models for the adsorption of a) 1-octanol; and, b) 1-decanol in the system of 1-octanol + 1-decanol (50:50 by mass) onto Selexsorb CDx® (T = 25°C)

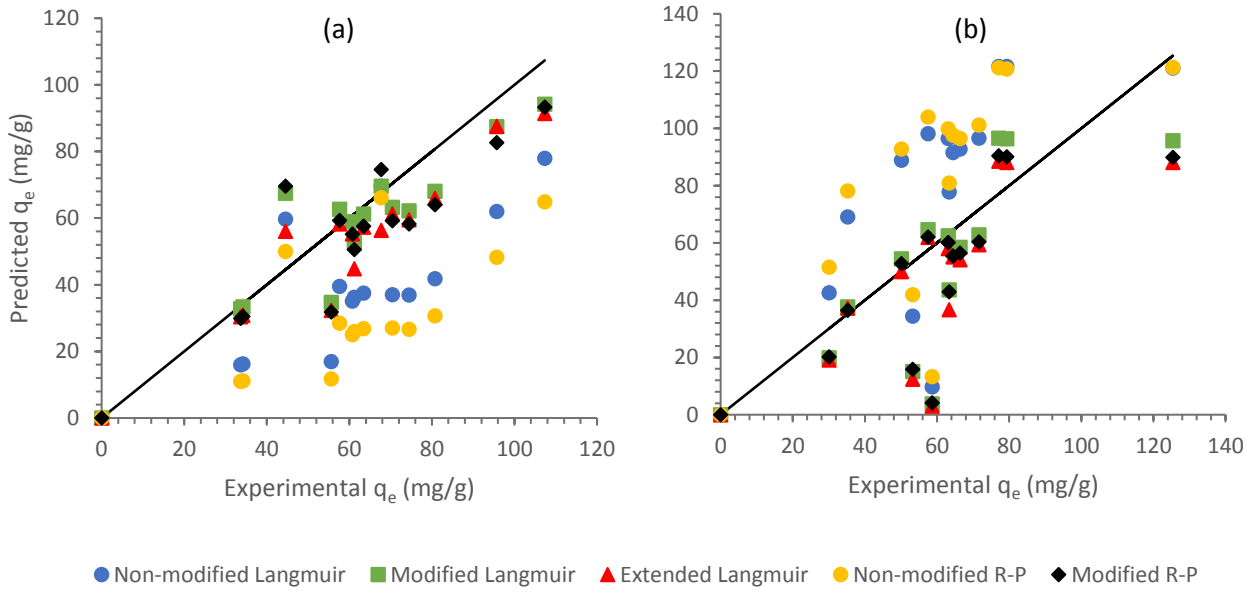

Figure G.2-12: Predicted vs. experimental equilibrium adsorbent loadings for the comparison of different forms of the binary Langmuir and Redlich-Peterson isotherm models for the adsorption of a) 1-octanol; and, b) 1-decanol in the system of 1-octanol + 1-decanol (50:50 by mass) onto Selexsorb CDx® (T = 45°C)

G.2.1.3 ***Selexsorb CD®***

For the system of 1-hexanol and 1-decanol onto SCD, the non-modified Langmuir isotherm seemed to be the best isotherm of the two non-modified isotherms. The Extended and non-modified isotherms were the best Langmuir isotherms at 25°C and 45°C respectively.

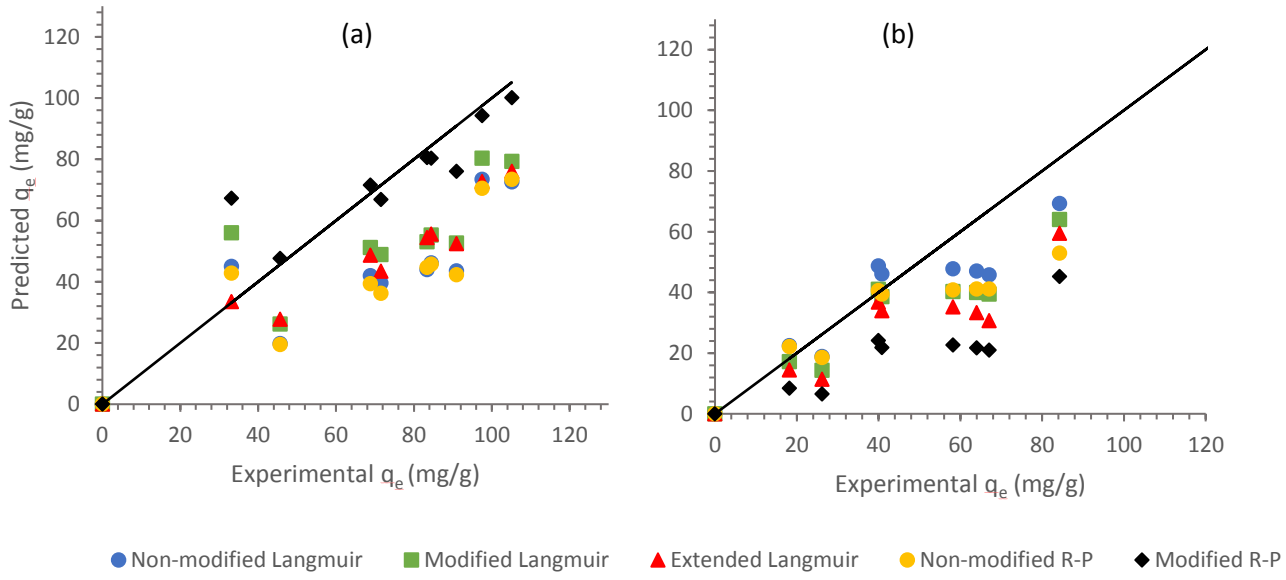

Figure G.2-13: Predicted vs. experimental equilibrium adsorbent loadings for the comparison of different forms of the binary Langmuir and Redlich-Peterson isotherm models for the adsorption of a) 1-hexanol; and, b) 1-decanol in the system of 1-hexanol + 1-decanol (50:50 by mass) onto Selexsorb CD® (T = 25°C)

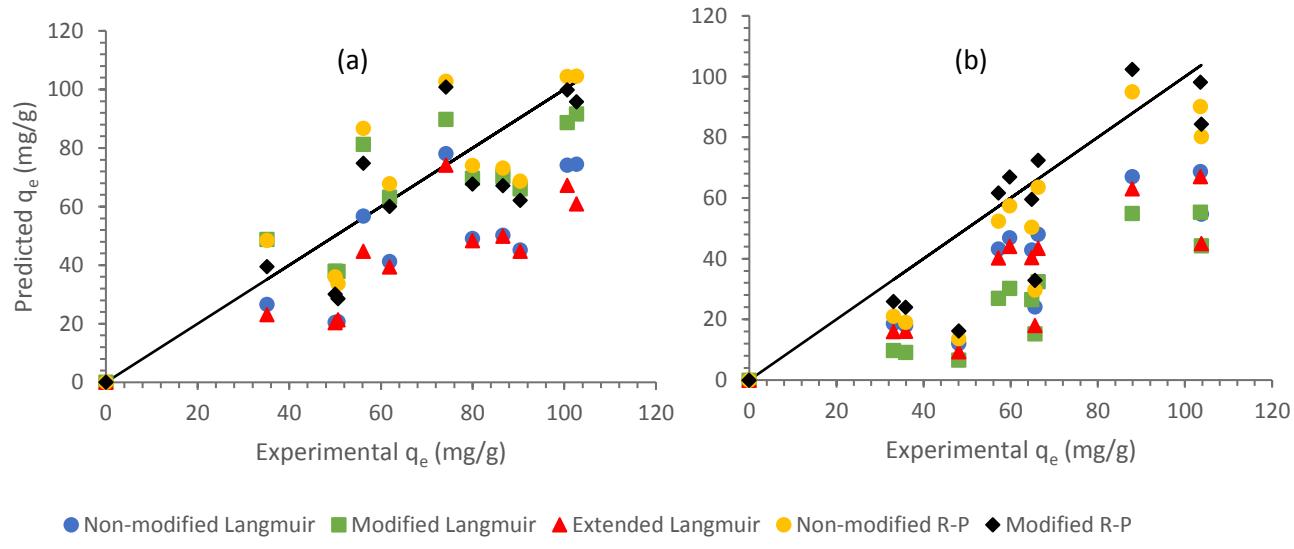

Figure G.2-14: Predicted vs. experimental equilibrium adsorbent loadings for the comparison of different forms of the binary Langmuir and Redlich-Peterson isotherm models for the adsorption of a) 1-hexanol; and, b) 1-decanol in the system of 1-hexanol + 1-decanol (50:50 by mass) onto Selexsorb CD® (T = 45°C)

At 25°C the non-modified Langmuir proved to be the best whereas at 45°C the non-modified Redlich-Peterson isotherm was the best for the system of 1-hexanol and 1-octanol. At both temperatures, the Modified Langmuir proved to be the best form of the Langmuir isotherm.

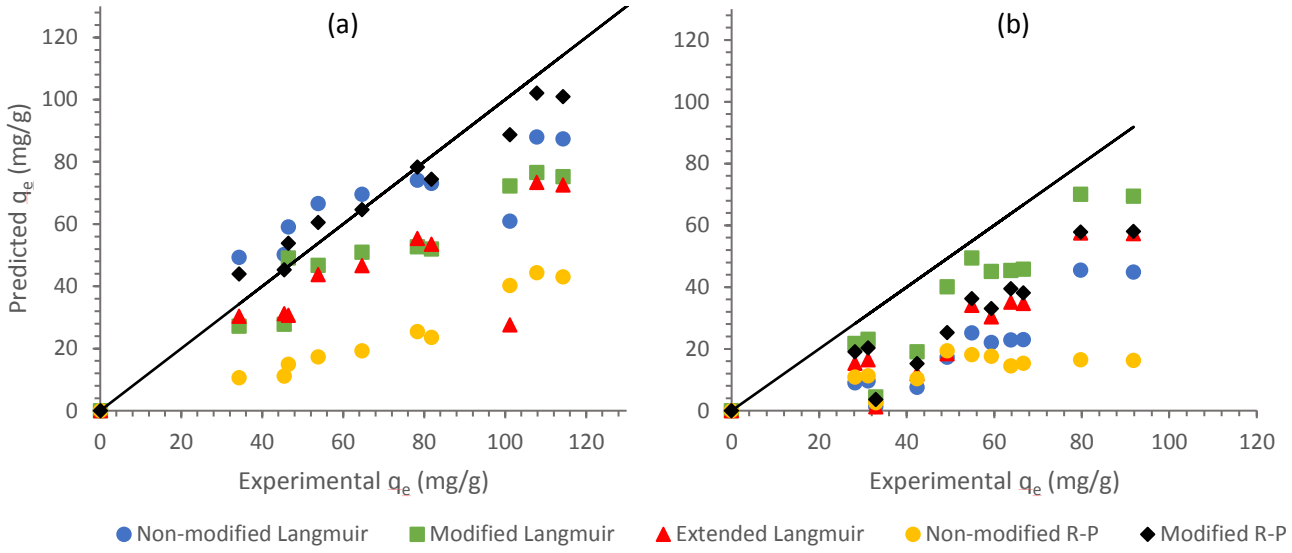

Figure G.2-15: Predicted vs. experimental equilibrium adsorbent loadings for the comparison of different forms of the binary Langmuir and Redlich-Peterson isotherm models for the adsorption of a) 1-hexanol; and, b) 1-octanol in the system of 1-hexanol + 1-octanol (50:50 by mass) onto Selexsorb CD® (T = 25°C)

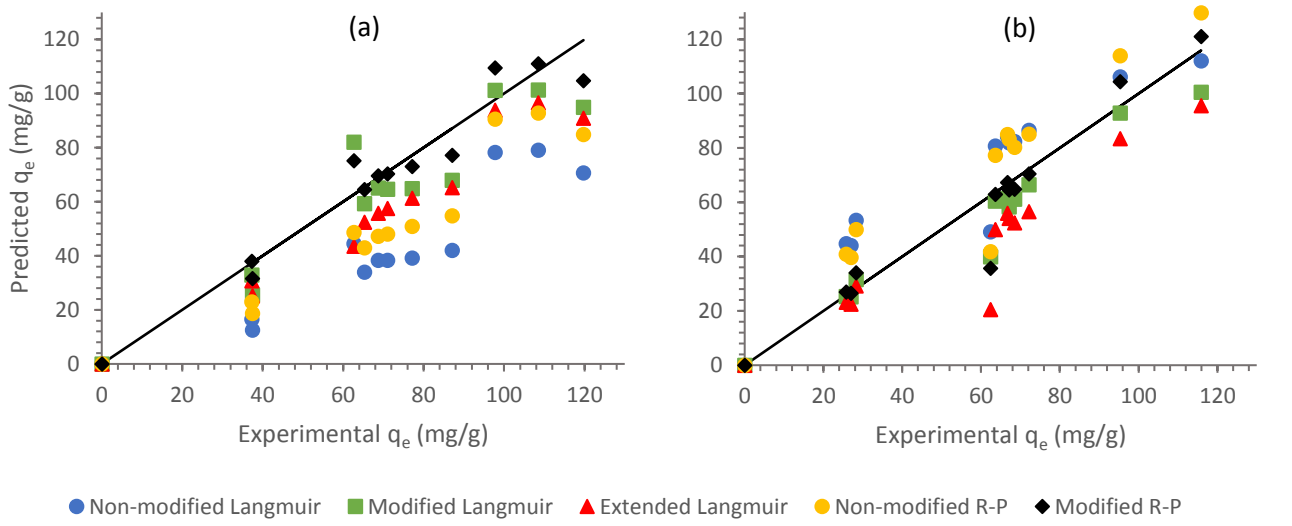

Figure G.2-16: Predicted vs. experimental equilibrium adsorbent loadings for the comparison of different forms of the binary Langmuir and Redlich-Peterson isotherm models for the adsorption of a) 1-hexanol; and, b) 1-octanol in the system of 1-hexanol + 1-octanol (50:50 by mass) onto Selexsorb CD® (T = 45°C)

For the system of 1-octanol and 1-decanol, the non-modified Langmuir isotherm had a higher correlation coefficient than the non-modified Redlich-Peterson isotherm. Similar to the system of 1-hexanol and 1-octanol, the Modified Langmuir seemed to be the most suitable form of the Langmuir isotherms.

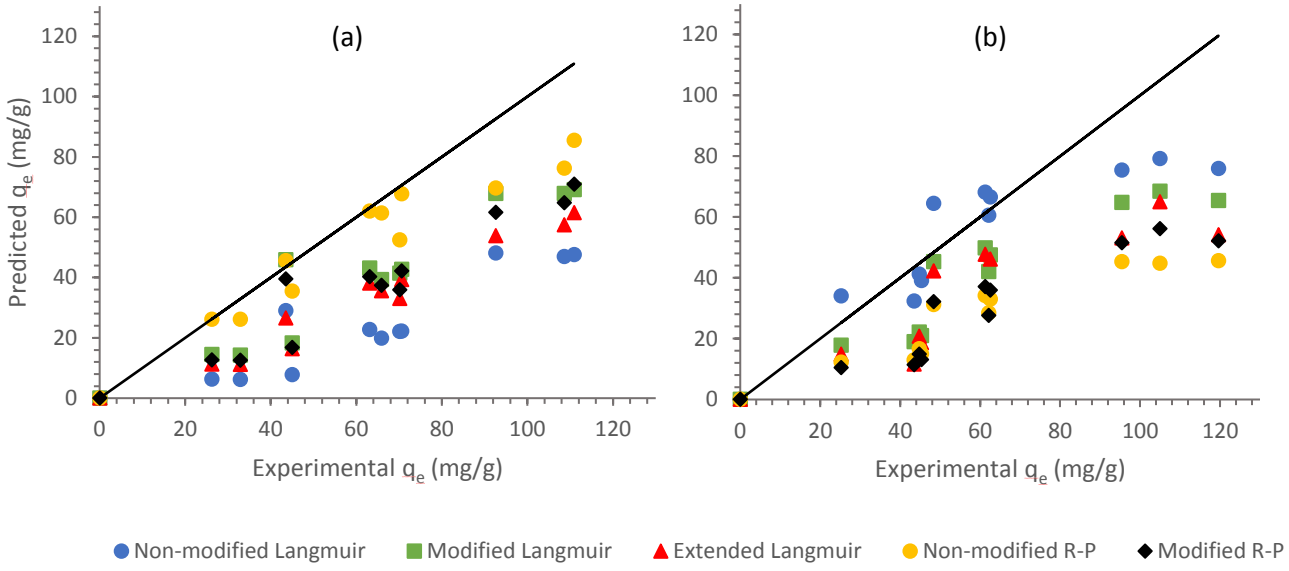

Figure G.2-17: Predicted vs. experimental equilibrium adsorbent loadings for the comparison of different forms of the binary Langmuir and Redlich-Peterson isotherm models for the adsorption of a) 1-octanol; and, b) 1-decanol in the system of 1-octanol + 1-decanol (50:50 by mass) onto Selexsorb CD® (T = 25°C)

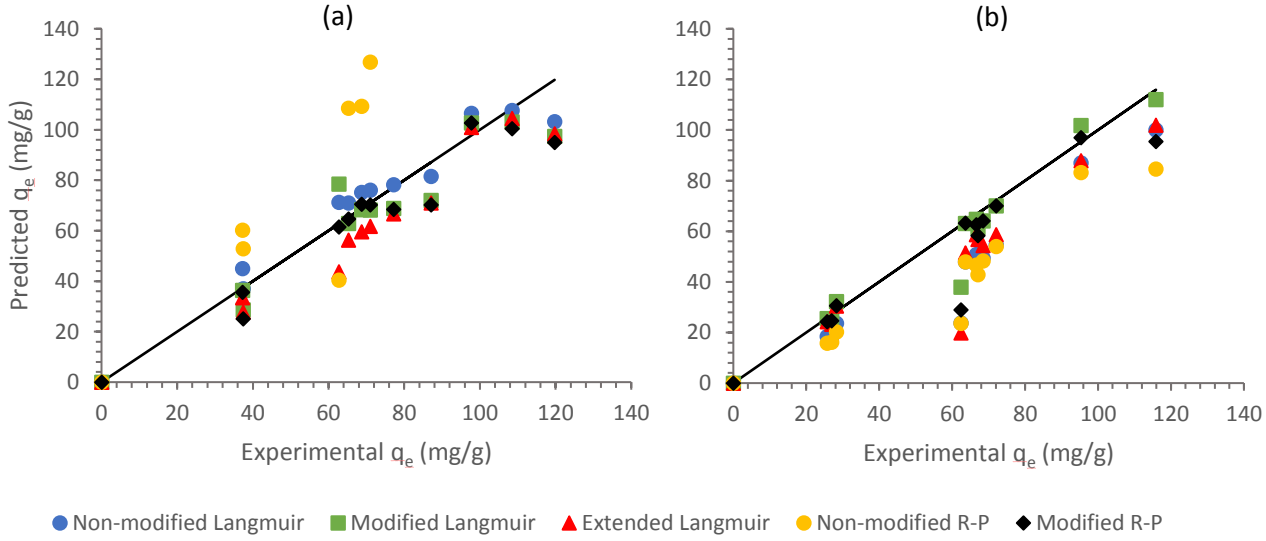

Figure G.2-18: Predicted vs. experimental equilibrium adsorbent loadings for the comparison of different forms of the binary Langmuir and Redlich-Peterson isotherm models for the adsorption of a) 1-octanol; and, b) 1-decanol in the system of 1-octanol + 1-decanol (50:50 by mass) onto Selexsorb CD® (T = 45°C)

G.2.2 Isotherm Models

The Extended Freundlich isotherm model is the most suitable for the prediction and correlation of the binary systems investigated in this study. Since the Extended Freundlich isotherm comprises six regression parameters, models with the second highest correlation coefficients were also identified. These models were the Extended Sips model and the Modified Redlich-Peterson model. In this section, examples of the best models fitted on the data of various systems investigated in this study are provided to serve as examples and to allow for comparison. Consequently, the isotherms provided here correspond to those discussed in Section 6.3.1.

G.2.2.1 ***Activated Alumina***

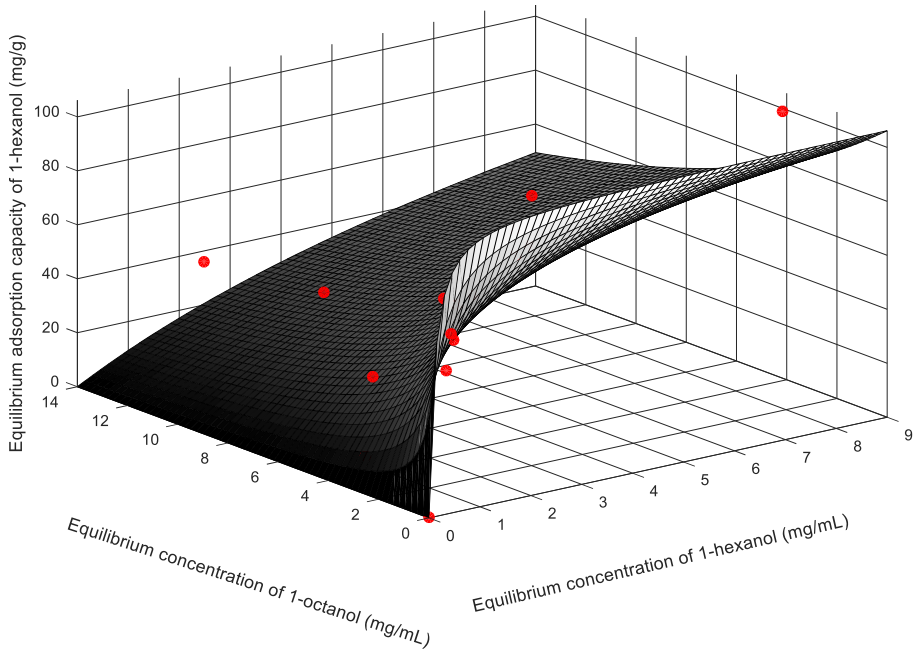

c) Modified Redlich-Peterson isotherm for 1-hexanol in a binary adsorption system of 1-hexanol + 1-octanol

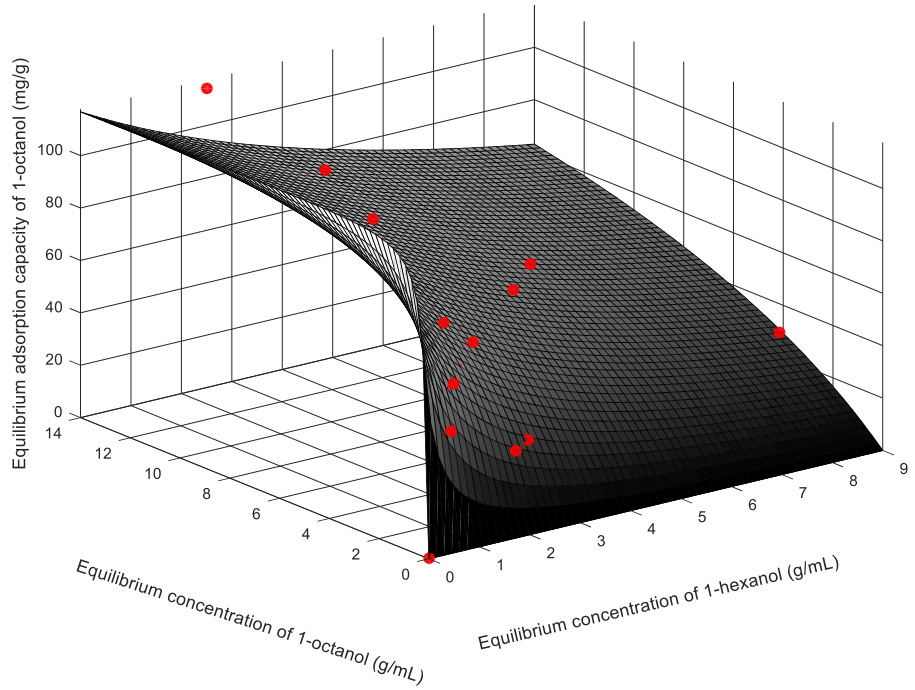

d) Modified Redlich-Peterson isotherm for 1-octanol in a binary adsorption system of 1-hexanol + 1-octanol

Figure G.2-19: Modified Redlich-Peterson isotherms for the binary component adsorption of a) 1-hexanol; and, b) 1-octanol onto AA-F220 (T = 45°C)

G.2.2.2 ***Selexsorb CDx®***

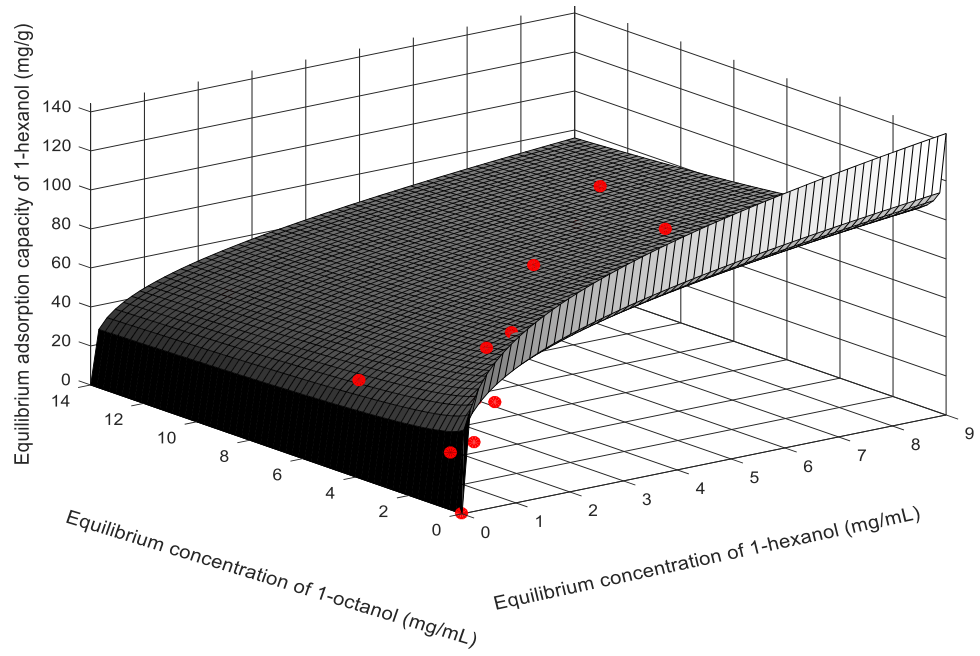

a) Extended Freundlich isotherm for 1-hexanol in a binary adsorption system of 1-hexanol + 1-octanol

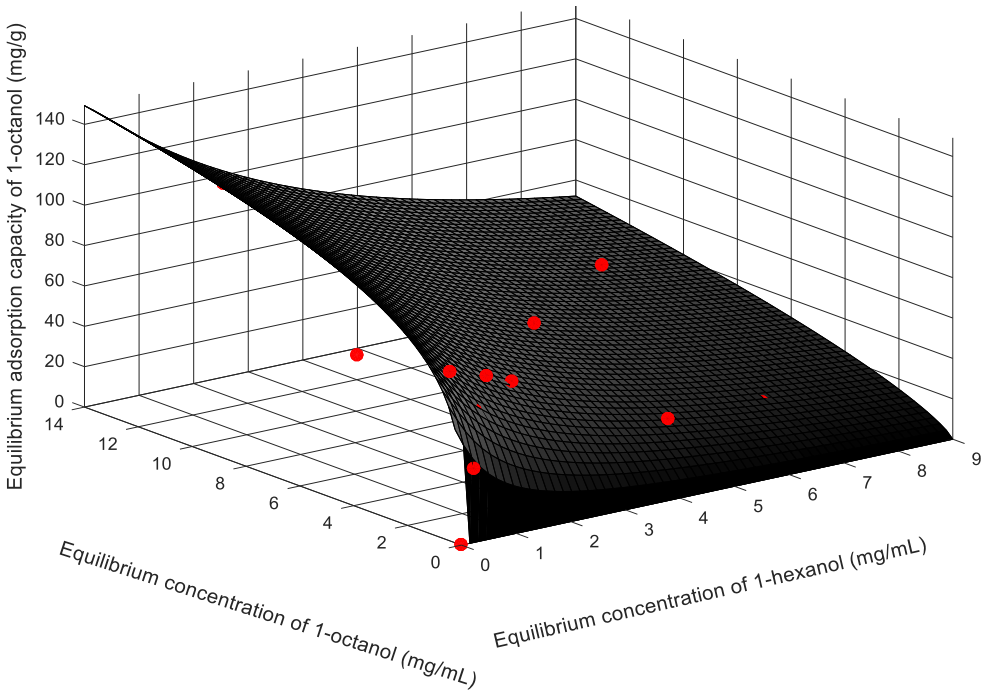

b) Extended Freundlich isotherm for 1-octanol in a binary adsorption system of 1-hexanol + 1-octanol

Figure G.2-20: Extended Freundlich isotherms for the binary component adsorption of 1-hexanol + 1-octanol onto SCDx (T = 45°C)

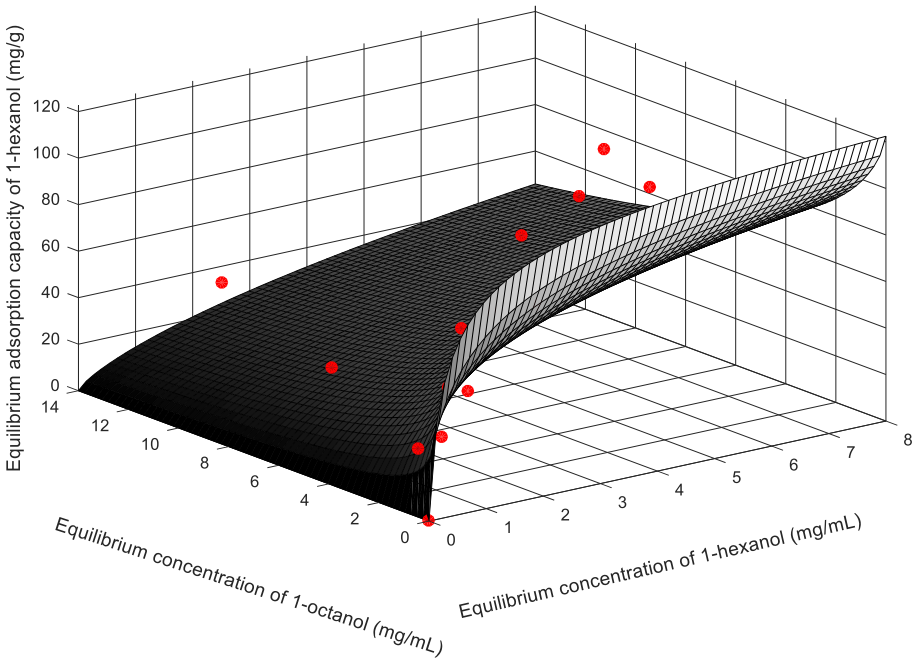

c) Extended Sips isotherm for 1-hexanol in a binary adsorption system of 1-hexanol + 1-octanol

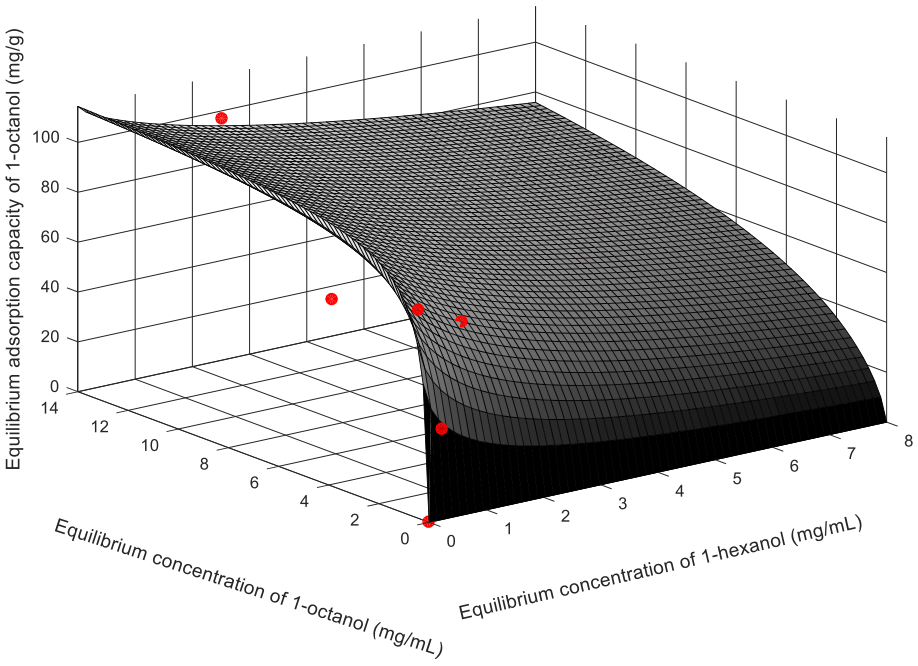

d) Extended Sips isotherm for 1-octanol in a binary adsorption system of 1-hexanol + 1-octanol

Figure G.2-21: Extended Sips isotherms for the binary component adsorption of 1-hexanol + 1-octanol onto SCDx (T = 45°C)

G.2.2.3 ***Selexsorb CD®***

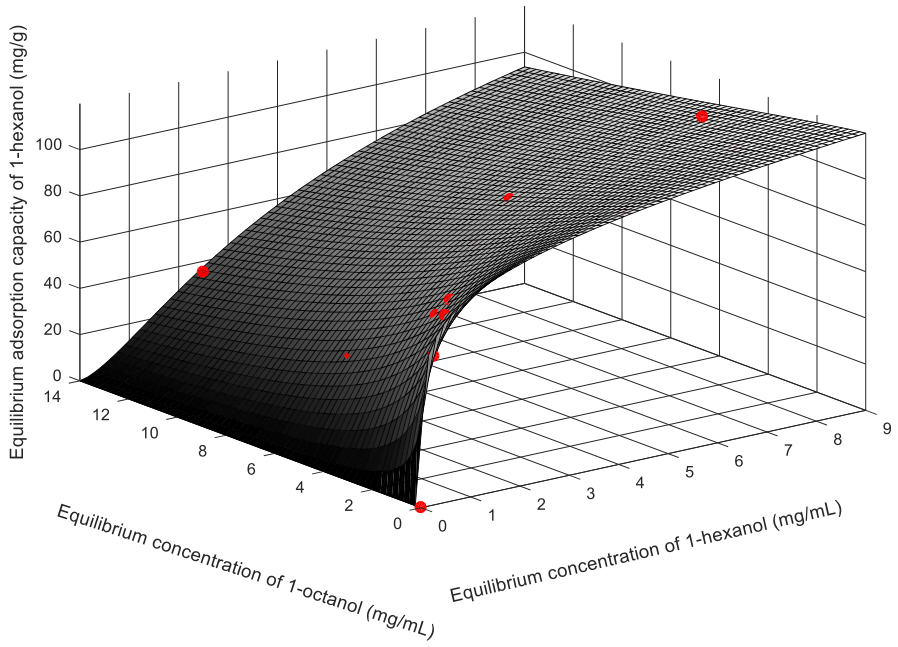

a) Extended Freundlich isotherm for 1-hexanol in a binary adsorption system of 1-hexanol + 1-octanol

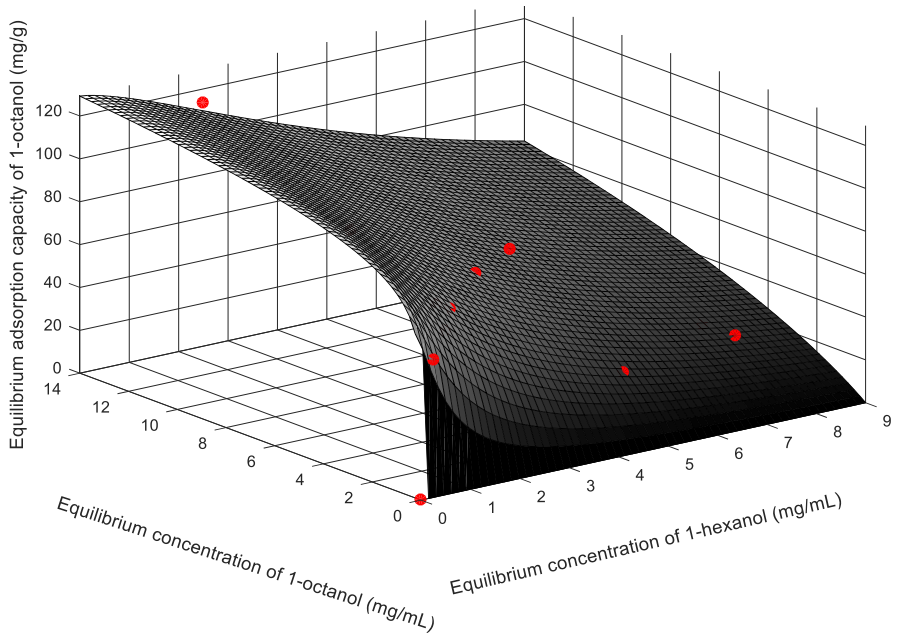

b) Extended Freundlich isotherm for 1-octanol in a binary adsorption system of 1-hexanol + 1-octanol

Figure G.2-22: Extended Freundlich isotherms for the binary component adsorption of 1-hexanol + 1-octanol onto SCD (T = 45°C)

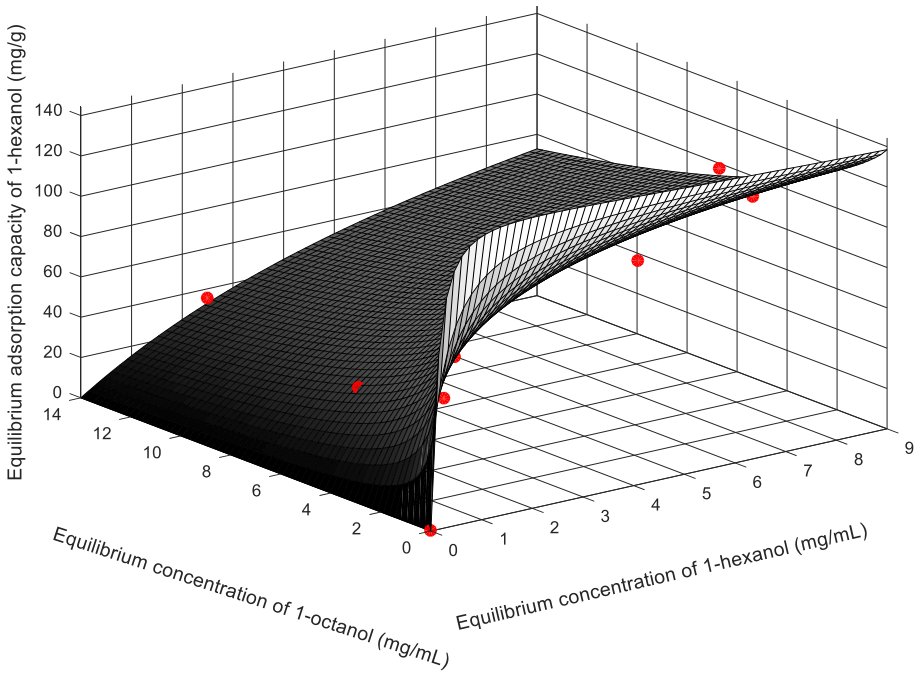

c) Modified Redlich-Peterson isotherm for 1-hexanol in a binary adsorption system of 1-hexanol + 1-octanol

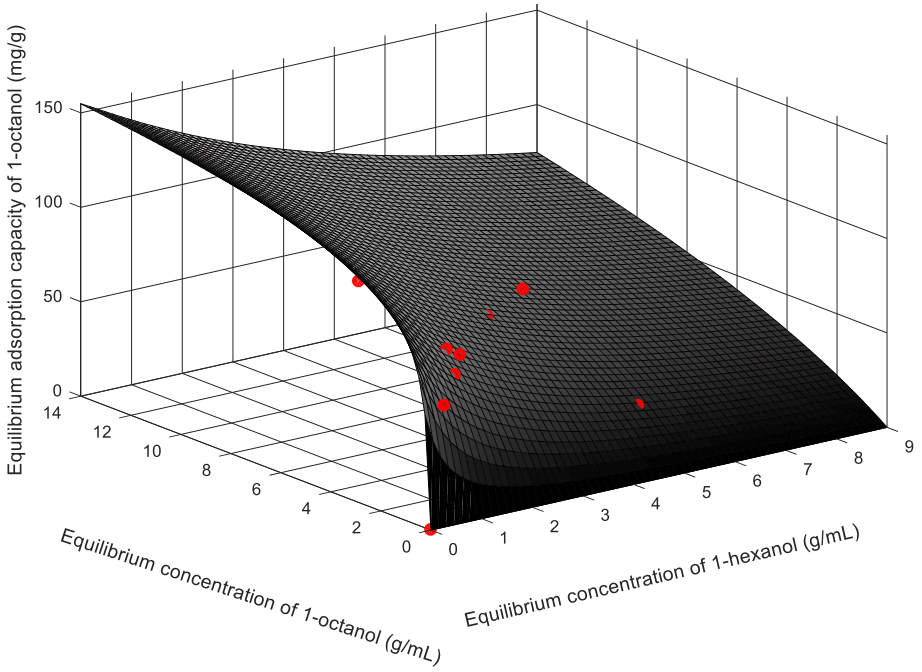

d) Modified Redlich-Peterson isotherm for 1-octanol in a binary adsorption system of 1-hexanol + 1-octanol

Figure G.2-23: Modified Redlich-Peterson isotherms for the binary component adsorption of 1-hexanol + 1-octanol onto SCD (T = 45°C)

Appendix H: Adsorption Kinetic Modelling

Appendix Contents

H.1 Modelling Methodology

The Solver Add-in package in Microsoft Excel® was used for the minimisation of the HYBRID error function [51], [65] (Equation H.1-1).

$$HYBRID = \frac{100}{n-p}\sum_{i=1}^{n}\left(\frac{\left(q_{t,exp}-q_{t,pred}\right)_i^2}{q_{t,exp}}\right)_i \qquad [\text{H.1-1}]$$

Where, n Number of data points;

p Number of regression parameters in specific model;

$q_{t,exp}$ Experimentally determined adsorbent loading at time t (mg/g); and,

$q_{t,pred}$ Model predicted adsorbent loading at time t (mg/g).

In order to identify the most suitable model, the correlation coefficient (R^2) [109] and MPSD [51], [65] were determined and compared for each model. The correlation coefficient is denoted by Equation H.1-2 and the MPSD by Equation H.1-3.

$$R^2 = \frac{\sum\left(q_{t,pred}-\overline{q_{t,exp}}\right)^2}{\sum\left(q_{t,pred}-\overline{q_{t,exp}}\right)^2+\sum\left(q_{t,pred}-q_{t,exp}\right)^2} \qquad [\text{H.1-2}]$$

$$MPSD = 100\left(\sqrt{\frac{1}{n-p}\sum_{i=1}^{n}\left(\frac{\left(q_{t,exp}-q_{t,pred}\right)_i^2}{q_{t,exp}}\right)_i}\right) \qquad [\text{H.1-3}]$$

H.2 Single Component Adsorption

In this section of the appendix, the single component adsorption kinetic model parameters are provided for the systems of 1-hexanol, 1-octanol and 1-decanol, at various initial adsorbate concentrations and both temperatures (25°C and 45°C). Thereafter, the IPD model parameters are provided. As mentioned, the single component parameters provided at 25°C were modelled using data obtained from a study conducted by Groenewald [8].

H.2.1 Activated Alumina F220

Table H.2-1: Kinetic model parameters for the single component adsorption onto Activated Alumina F220 (T = 25°C)

Model Parameters	***1-hexanol***			***1-octanol***			***1-decanol***		
Initial Concentration (mass%)	***0.50***	***0.99***	***1.32***	***0.57***	***1.03***	***1.59***	***0.35***	***1.13***	***1.36***
$q_{e,exp}$ $(mg.g^{-1})$	66.3	97.2	112	63.4	91.7	106	48.3	94.8	109
Pseudo-first-order Model									
$q_{e,cal}$ $(mg.g^{-1})$	65.0	97.7	107	61.2	87.9	103	46.9	92.9	103
k_1 (min^{-1})	0.02	0.02	0.01	0.02	0.02	0.01	0.02	0.01	0.02
R^2	0.98	0.96	0.98	0.98	0.98	0.98	0.99	0.96	0.97
MPSD (%)	7.20	10.5	7.88	7.81	9.51	9.64	4.70	18.9	9.54
Pseudo-second-order Model									
$q_{e,cal}$ $(mg.g^{-1})$	73.7	115	134	69.5	104	124	53.0	112	122
k_2 $(x10^{-3}\ g.(mg.min)^{-1})$	0.34	0.15	0.08	0.35	0.16	0.11	0.49	0.10	0.14
R^2	1.00	0.98	0.99	1.00	0.99	0.99	1.00	0.97	0.99
MPSD (%)	4.05	6.98	5.13	4.57	5.23	5.32	1.02	14.3	5.36
Pseudo-nth-order Model									
n (-)	2.49	2.24	2.72	3.70	3.30	2.97	2.49	2.14	3.00
$q_{e,cal}$ $(mg.g^{-1})$	79.8	121	159	91.8	132	152	57.4	115	147
k_n $(x10^{-5}\ g^{n-1}.mg^{1-n}.min^{-1})$	3.58	4.23	0.15	0.01	0.02	0.06	6.17	5.13	0.07
R^2	1.00	0.98	0.99	1.00	1.00	1.00	1.00	0.97	0.99
MPSD (%)	3.46	6.72	4.74	3.60	4.00	4.48	0.45	14.0	4.03
Elovich Model									
β $(g.mg^{-1})$	0.07	0.04	0.04	0.07	0.05	0.04	0.10	0.05	0.04
α $(mg.(g.min)^{-1})$	4.23	4.44	3.42	3.89	3.96	3.90	3.08	3.46	4.76
R^2	0.99	0.98	0.99	1.00	1.00	1.00	1.00	0.96	1.00
MPSD (%)	2.95	6.16	7.99	3.64	4.42	6.06	2.26	13.6	3.32

Table H.2-2: Kinetic model parameters for the single component adsorption onto Activated Alumina F220 (T = 45°C)

Model Parameters	***1-hexanol***			***1-octanol***			***1-decanol***		
Initial Concentration (mass%)	***0.84***	***1.01***	***1.51***	***0.56***	***1.04***	***1.61***	***0.49***	***0.98***	***1.56***
$q_{e,exp}$ $(mg.g^{-1})$	96.5	98.5	110.4	72.8	112.7	113.4	62.0	111	116
Pseudo-first-order Model									
$q_{e,cal}$ $(mg.g^{-1})$	97.5	95.5	106	68.9	111	115	53.6	109	115
k_1 (min^{-1})	0.03	0.03	0.03	0.03	0.03	0.03	0.02	0.01	0.02
R^2	0.98	0.97	0.98	0.98	0.97	0.98	0.95	0.99	0.99
MPSD (%)	21.0	24.1	19.9	20.5	23.6	22.4	23.8	24.1	7.23
Pseudo-second-order Model									
$q_{e,cal}$ $(mg.g^{-1})$	101	100	113	73.6	117	121	58.8	126	126
k_2 $(x10^{-3}\ g.(mg.min)^{-1})$	0.50	0.45	0.32	0.48	0.40	0.32	0.35	0.07	0.15
R^2	0.98	0.98	0.99	0.99	0.98	0.98	0.98	0.99	0.98
MPSD (%)	15.5	21.2	15.0	15.6	18.0	18.4	18.9	23.5	8.11
Pseudo-nth-order Model									
n (-)	2.46	4.29	2.41	2.68	2.45	1.62	2.52	1.27	1.31
$q_{e,cal}$ $(mg.g^{-1})$	105	123	118	78.9	121	118	63.1	112	117
k_n $(x10^{-5}\ g^{n-1}.mg^{1-n}.min^{-1})$	6.62	0.00	4.67	2.58	5.26	180	3.88	219	397
R^2	0.97	0.97	0.99	0.99	0.98	0.98	0.99	1.00	0.99
MPSD (%)	13.6	17.0	13.6	14.4	17.0	20.3	17.6	23.4	5.08
Elovich Model									
β $(g.mg^{-1})$	0.07	0.08	0.06	0.10	0.06	0.06	0.12	0.06	0.05
α $(mg.(g.min)^{-1})$	24.5	31.0	18.1	12.3	31.7	25.9	6.29	6.74	11.0
R^2	0.87	0.94	0.96	0.96	0.95	0.91	0.96	0.88	0.92
MPSD (%)	12.2	13.9	10.8	11.7	10.4	15.4	22.0	74.2	20.6

Table H.2-3: Intra-particle diffusion model parameters for the adsorption of a single alcohol onto Activated Alumina F220 (T = 25°C)

Alcohol	***Initial Concentration (mass%)***	***Intra-particle Diffusion Model Parameters***		
		θ ($mg.g^{-1}$)	k_{ip} $(mg/g.min^{0.5})$	R^2
1-hexanol	0.50	38.3	1.52	0.99
	0.99	4.73	5.66	1.00
	1.32	55.2	2.24	0.99
1-octanol	0.57	36.6	1.38	1.00
	1.03	28.6	3.30	0.92
	1.59	26.6	4.12	1.00
1-decanol	0.35	29.1	1.03	0.98
	1.13	15.5	4.07	1.00
	1.36	30.7	4.00	1.00

Table H.2-4: Intra-particle diffusion model parameters for the adsorption of a single alcohol onto Activated Alumina F220 (T = 45°C)

Alcohol	***Initial Concentration (mass%)***	***Intra-particle Diffusion Model Parameters***		
		θ ($mg.g^{-1}$)	k_{ip} $(mg/g.min^{0.5})$	R^2
1-hexanol	0.84	60.6	2.74	1.00
	1.01	72.9	1.32	0.97
	1.51	66.8	2.19	0.98
1-octanol	0.56	49.7	0.98	0.95
	1.04	70.9	2.34	0.97
	1.61	89.6	1.64	0.77
1-decanol	0.49	16.9	1.85	0.99
	0.98	37.4	3.15	0.83
	1.56	54.5	3.38	0.99

H.2.2 Selexsorb CDx®

Table H.2-5: Kinetic model parameters for the single component adsorption onto Selexsorb CDx® (T = 25°C)

Model Parameters	***1-hexanol***			***1-octanol***			***1-decanol***		
Initial Concentration (mass%)	***0.56***	***0.97***	***1.40***	***0.56***	***1.05***	***1.57***	***0.49***	***0.99***	***1.52***
$q_{e,exp}$ $(mg.g^{-1})$	64.6	84.4	92.0	56.9	72.7	83.7	58.2	85.2	78.7
Pseudo-first-order Model									
$q_{e,cal}$ $(mg.g^{-1})$	60.4	81.2	89.8	53.7	70.3	81.0	57.3	80.2	75.1
k_1 (min^{-1})	0.02	0.02	0.02	0.02	0.01	0.01	0.01	0.02	0.01
R^2	0.97	0.97	0.97	0.97	0.98	0.96	0.99	0.97	0.97
MPSD (%)	8.47	9.95	9.72	10.3	11.5	13.0	8.26	9.21	11.5
Pseudo-second-order Model									
$q_{e,cal}$ $(mg.g^{-1})$	69.4	96.5	106	63.9	84.4	97.9	70.1	95.1	90.4
k_2 $(x10^{-3}\ g.(mg.min)^{-1})$	0.31	0.16	0.16	0.25	0.17	0.13	0.18	0.18	0.16
R^2	0.98	0.99	0.99	0.99	0.99	0.98	1.00	0.99	0.99
MPSD (%)	5.76	5.87	5.91	6.93	7.68	7.86	5.36	5.41	7.07
Pseudo-nth-order Model									
n (-)	2.54	3.84	3.45	2.97	3.59	3.57	2.18	3.16	2.23
$q_{e,cal}$ $(mg.g^{-1})$	76.4	136	140	82.6	115	134	72.7	119	94.5
k_n $(x10^{-5}\ g^{n-1}.mg^{1-n}.min^{-1})$	2.67	0.00	0.01	0.19	0.01	0.00	7.88	0.05	5.16
R^2	0.99	1.00	0.99	0.99	0.99	0.99	1.00	0.99	0.99
MPSD (%)	5.36	4.10	4.69	8.70	6.77	6.50	5.18	4.15	6.62
Elovich Model									
β $(g.mg^{-1})$	0.07	0.05	0.05	0.08	0.06	0.05	0.07	0.05	0.05
α $(mg.(g.min)^{-1})$	3.39	3.53	4.02	2.33	2.87	3.12	2.07	3.59	3.02
R^2	0.98	1.00	0.99	0.99	0.99	0.99	1.00	0.99	0.99
MPSD (%)	5.21	4.98	5.03	7.37	8.33	7.12	7.69	4.17	6.14

Table H.2-6: Kinetic model parameters for the single component adsorption onto Selexsorb CDx® (T = 45°C)

Model Parameters	***1-hexanol***			***1-octanol***			***1-decanol***		
Initial Concentration (mass%)	***0.59***	***1.02***	***1.71***	***0.44***	***1.00***	***1.46***	***0.54***	***1.08***	***1.69***
$q_{e,exp}$ $(mg.g^{-1})$	73.2	112	122	58.0	108	110	73.1	123	142
Pseudo-first-order Model									
$q_{e,cal}$ $(mg.g^{-1})$	70.8	103	113	47.0	99.2	104	69.6	108	126
k_1 (min^{-1})	0.02	0.02	0.02	0.02	0.01	0.02	0.01	0.01	0.01
R^2	0.99	0.95	0.97	0.82	0.97	0.96	0.99	0.94	0.96
MPSD (%)	6.45	28.5	24.1	31.3	26.5	23.7	8.01	35.0	30.2
Pseudo-second-order Model									
$q_{e,cal}$ $(mg.g^{-1})$	77.3	113	123	53.6	111	113	78.5	118	139
k_2 $(x10^{-3}\ g.(mg.min)^{-1})$	0.31	0.21	0.23	0.43	0.16	0.22	0.17	0.10	0.11
R^2	0.96	0.98	0.99	0.91	0.99	0.98	1.00	0.97	0.98
MPSD (%)	20.9	24.5	20.3	25.9	22.0	17.8	6.27	25.2	24.4
Pseudo-nth-order Model									
n (-)	1.60	2.45	2.31	3.47	2.31	2.29	1.31	2.39	2.91
$q_{e,cal}$ $(mg.g^{-1})$	74.0	118	127	63.9	116	117	86.4	125	157
k_n $(x10^{-5}\ g^{n-1}.mg^{1-n}.min^{-1})$	178.6	2.56	5.36	0.09	3.57	5.63	440	1.37	0.11
R^2	1.00	0.98	0.99	0.94	0.99	0.98	0.86	0.97	0.99
MPSD (%)	8.63	23.4	19.3	21.7	22.6	17.5	41.4	24.1	22.2
Elovich Model									
β $(g.mg^{-1})$	0.08	0.06	0.06	0.13	0.06	0.06	0.07	0.06	0.05
α $(mg.(g.min)^{-1})$	7.27	17.3	18.5	7.30	11.5	14.4	7.97	9.56	14.0
R^2	0.96	0.96	0.97	0.94	0.95	0.95	0.86	0.94	0.95
MPSD (%)	12.4	17.3	15.7	15.8	29.4	15.3	53.4	35.1	26.7

Table H.2-7: Intra-particle diffusion model parameters for the adsorption of a single alcohol onto Selexsorb CDx® (T = 25°C)

Alcohol	***Initial Concentration (mass%)***	***Intra-particle Diffusion Model Parameters***		
		θ ($mg.g^{-1}$)	k_{ip} ($mg/g.min^{0.5}$)	R^2
1-hexanol	0.56	24.28	2.16	1.00
	0.97	22.35	3.28	0.98
	1.40	31.08	3.28	0.73
1-octanol	0.56	28.29	1.25	0.99
	1.05	18.76	2.84	0.96
	1.57	9.05	3.87	0.99
1-decanol	0.49	21.85	1.90	1.00
	0.99	21.23	3.34	0.93
	1.52	8.78	3.70	1.00

Table H.2-8: Intra-particle diffusion model parameters for the adsorption of a single alcohol onto Selexsorb CDx® (T = 45°C)

Alcohol	***Initial Concentration (mass%)***	***Intra-particle Diffusion Model Parameters***		
		θ ($mg.g^{-1}$)	k_{ip} ($mg/g.min^{0.5}$)	R^2
1-hexanol	0.59	47.8	1.53	0.98
	1.02	75.2	1.44	0.99
	1.71	85.2	1.41	0.99
1-octanol	0.44	9.19	2.00	0.95
	1.00	39.8	2.91	0.98
	1.46	80.1	1.37	0.80
1-decanol	0.54	43.7	1.18	0.95
	1.08	21.0	3.55	0.90
	1.69	12.6	5.75	0.99

H.2.3 Selexsorb CD®

Table H.2-9: Kinetic model parameters for the single component adsorption onto Selexsorb CD® (T = 25°C)

Model Parameters	***1-hexanol***			***1-octanol***			***1-decanol***		
Initial Concentration (mass%)	***0.51***	***0.98***	***1.39***	***0.55***	***1.02***	***1.53***	***0.51***	***1.08***	***1.34***
$q_{e,exp}$ $(mg.g^{-1})$	63.9	89.0	96.7	55.1	73.0	88.0	59.7	72.6	82.8
Pseudo-first-order Model									
$q_{e,cal}$ $(mg.g^{-1})$	60.7	81.8	94.1	52.7	70.1	83.1	57.4	67.9	80.3
k_1 (min^{-1})	0.02	0.02	0.01	0.02	0.01	0.01	0.01	0.01	0.01
R^2	0.97	0.95	0.97	0.98	0.97	0.96	0.98	0.96	0.97
MPSD (%)	7.97	11.4	10.9	6.97	12.7	11.8	9.02	13.1	11.5
Pseudo-second-order Model									
$q_{e,cal}$ $(mg.g^{-1})$	69.3	95.6	113	61.4	84.1	99.4	68.8	81.3	98.7
k_2 $(x10^{-3}\ g.(mg.min)^{-1})$	0.34	0.20	0.13	0.31	0.17	0.15	0.21	0.18	0.12
R^2	0.99	0.98	0.98	1.00	0.99	0.99	1.00	0.98	0.99
MPSD (%)	4.11	7.28	6.51	2.77	8.57	7.28	5.70	9.00	6.76
Pseudo-nth-order Model									
n (-)	3.10	3.08	3.42	3.34	3.65	3.78	2.92	2.26	2.17
$q_{e,cal}$ $(mg.g^{-1})$	83.6	117	149	78.4	116	139	85.6	85.6	102.2
k_n $(x10^{-5}\ g^{n-1}.mg^{1-n}.min^{-1})$	0.20	0.08	0.01	0.06	0.00	0.00	0.22	5.28	5.21
R^2	1.00	0.98	0.99	1.00	0.99	0.99	1.00	0.98	0.99
MPSD (%)	2.68	7.19	4.91	1.37	7.56	5.88	5.88	8.49	6.35
Elovich Model									
β $(g.mg^{-1})$	0.07	0.05	0.04	0.08	0.06	0.05	0.07	0.06	0.05
α $(mg.(g.min)^{-1})$	3.77	4.25	3.77	2.59	2.92	3.50	2.34	2.89	2.82
R^2	1.00	0.99	0.99	1.00	0.99	0.99	1.00	0.98	0.99
MPSD (%)	1.10	4.53	5.41	0.86	8.72	6.58	6.39	7.94	6.55

Table H.2-10: Kinetic model parameters for the single component adsorption onto Selexsorb CD® (T = 45°C)

Model Parameters	***1-hexanol***			***1-octanol***			***1-decanol***		
Initial Concentration (mass%)	***0.43***	***0.96***	***1.59***	***0.43***	***1.10***	***1.53***	***0.53***	***1.18***	***1.63***
$q_{e,exp}$ $(mg.g^{-1})$	59.2	107	120	57.5	120	114	69.6	129	128
Pseudo-first-order Model									
$q_{e,cal}$ $(mg.g^{-1})$	58.7	98.7	118	59.2	110	102	66.1	116	118
k_1 (min^{-1})	0.01	0.02	0.03	0.02	0.01	0.02	0.03	0.01	0.01
R^2	0.98	0.96	0.96	0.99	0.95	0.95	0.96	0.95	0.97
MPSD (%)	1.39	26.6	25.1	18.9	30.3	19.9	14.3	29.0	26.0
Pseudo-second-order Model									
$q_{e,cal}$ $(mg.g^{-1})$	66.2	108	126	69.2	122	113	78.7	129	132
k_2 $(x10^{-3}\ g.(mg.min)^{-1})$	0.22	0.22	0.31	0.47	0.14	0.22	0.40	0.12	0.09
R^2	0.97	0.98	0.98	0.94	0.98	0.98	0.96	0.98	0.99
MPSD (%)	1.62	22.1	20.9	25.1	25.5	14.9	12.5	22.3	18.1
Pseudo-nth-order Model									
n (-)	0.97	3.08	2.42	2.18	2.38	2.33	2.88	2.71	2.79
$q_{e,cal}$ $(mg.g^{-1})$	58.6	117	132	70.6	129	117	87.1	143	156
k_n $(x10^{-5}\ g^{n-1}.mg^{1-n}.min^{-1})$	1616	0.16	4.09	21.7	2.11	4.88	0.75	0.34	0.11
R^2	0.98	0.98	0.98	0.94	0.98	0.99	0.96	0.99	0.99
MPSD (%)	1.38	18.5	19.7	26.3	26.2	14.1	10.3	20.3	20.6
Elovich Model									
β $(g.mg^{-1})$	0.10	0.07	0.06	0.10	0.06	0.06	0.08	0.06	0.05
α $(mg.(g.min)^{-1})$	5.16	14.6	30.7	8.71	14.8	13.0	9.56	12.6	10.4
R^2	0.95	0.96	0.97	0.91	0.95	0.99	0.95	0.96	0.95
MPSD (%)	10.6	16.4	9.92	33.5	28.3	15.8	11.0	24.4	33.4

Table H.2-11: Intra-particle diffusion model parameters for the adsorption of a single alcohol onto Selexsorb CD® (T = 25°C)

Alcohol	***Initial Concentration (mass%)***	***Intra-particle Diffusion Model Parameters***		
		θ ($mg.g^{-1}$)	k_{ip} ($mg/g.min^{0.5}$)	R^2
1-hexanol	0.51	24.6	2.07	0.99
	0.98	19.8	3.44	1.00
	1.39	4.68	5.14	0.99
1-octanol	0.55	23.0	1.65	0.99
	1.02	13.5	3.12	1.00
	1.53	19.7	3.40	1.00
1-decanol	0.51	21.7	1.94	0.99
	1.08	7.45	3.37	0.99
	1.34	7.42	3.92	0.99

Table H.2-12: Intra-particle diffusion model parameters for the adsorption of a single alcohol onto Selexsorb CD® (T = 45°C)

Alcohol	***Initial Concentration (mass%)***	***Intra-particle Diffusion Model Parameters***		
		θ ($mg.g^{-1}$)	k_{ip} ($mg/g.min^{0.5}$)	R^2
1-hexanol	0.43	33.5	1.35	0.98
	0.96	79.9	0.97	0.84
	1.59	71.8	2.44	0.93
1-octanol	0.43	31.3	1.53	0.99
	1.10	47.5	3.05	1.00
	1.53	59.4	2.01	0.73
1-decanol	0.53	29.9	1.99	0.98
	1.18	11.6	5.28	1.00
	1.63	31.5	3.90	1.00

H.3 Binary Component Adsorption

The binary component kinetic parameters as well as the intra-particle diffusion model parameters are provided here. The kinetic parameters are provided in such a way that the different initial adsorbate concentrations are grouped together in each table.

H.3.1 Activated Alumina F220

Table H.3-1: Kinetic model parameters for the adsorption of a binary alcohol mixture (1-hexanol + 1-decanol) onto Activated Alumina F220 (T = 25°C)

Model Parameters	***1-hexanol (1-H) + 1-decanol (1-D) mixture***					
	1-H	***1-D***	***1-H***	***1-D***	***1-H***	***1-D***
Initial Concentration (mass%)	***0.41***	***0.34***	***0.82***	***0.94***	***0.96***	***2.22***
$q_{e.exp}$ $(mg.g^{-1})$	50.5	51.2	57.4	55.1	55.8	91.9
Pseudo-first-order Model						
$q_{e.cal}$ $(mg.g^{-1})$	49.4	49.2	53.7	59.0	52.1	85.6
k_1 (min^{-1})	0.01	0.01	0.01	0.00	0.01	0.01
R^2	0.99	0.97	0.95	0.90	0.97	0.98
MPSD (%)	16.0	16.6	21.1	236	10.9	11.2
Pseudo-second-order Model						
$q_{e.cal}$ $(mg.g^{-1})$	55.4	54.9	61.9	78.5	58.2	95.7
k_2 $(x10^{-3}\ g.(mg.min)^{-1})$	0.20	0.19	0.15	0.03	0.25	0.12
R^2	0.98	0.99	0.96	0.86	1.00	0.99
MPSD (%)	16.8	11.3	25.9	236	4.49	4.34
Pseudo-n^{th}-order Model						
n (-)	1.25	2.22	1.57	1.35	1.95	1.93
$q_{e.cal}$ $(mg.g^{-1})$	50.5	56.7	57.7	60.7	57.6	94.6
k_n $(x10^{-5}\ g^{n-1}.mg^{1-n}.min^{-1})$	382	7.52	88.6	74.6	30.5	17.5
R^2	0.99	0.99	0.96	0.88	1.00	0.99
MPSD (%)	15.9	11.0	23.9	245	4.68	4.44
Elovich Model						
β $(g.mg^{-1})$	0.10	0.10	0.08	0.08	0.10	0.06
α $(mg.(g.min)^{-1})$	1.59	1.53	1.31	0.92	2.15	2.83
R^2	0.94	0.97	0.95	0.95	0.97	0.97
MPSD (%)	21.9	13.9	16.9	25.6	7.91	8.15

Table H.3-2: Kinetic model parameters for the adsorption of a binary alcohol mixture (1-hexanol + 1-octanol) onto Activated Alumina F220 (T = 25°C)

Model Parameters	***1-hexanol (1-H) + 1-octanol (1-O) mixture***					
	1-H	***1-O***	***1-H***	***1-O***	***1-H***	***1-O***
Initial Concentration (mass%)	***0.51***	***0.56***	***0.93***	***0.99***	***1.60***	***1.72***
$q_{e.exp}$ $(mg.g^{-1})$	48.0	53.6	68.5	65.5	68.4	62.8
Pseudo-first-order Model						
$q_{e.cal}$ $(mg.g^{-1})$	48.5	56.0	63.1	60.4	68.7	63.6
k_1 (min^{-1})	0.01	0.00	0.03	0.02	0.01	0.01
R^2	1.00	0.97	0.95	0.96	0.99	0.99
MPSD (%)	3.15	52.0	8.54	10.7	3.85	3.83
Pseudo-second-order Model						
$q_{e.cal}$ $(mg.g^{-1})$	54.5	69.2	68.4	67.1	75.8	71.7
k_2 $(x10^{-3}\ g.(mg.min)^{-1})$	0.16	0.05	0.45	0.29	0.19	0.12
R^2	0.98	0.94	0.99	1.00	0.97	0.99
MPSD (%)	9.66	57.4	4.15	4.53	7.00	5.89
Pseudo-n^{th}-order Model						
n (-)	0.98	1.03	2.92	2.36	1.13	1.23
$q_{e.cal}$ $(mg.g^{-1})$	39.8	41.3	75.9	70.3	69.3	64.8
k_n $(x10^{-5}\ g^{n-1}.mg^{1-n}.min^{-1})$	2893	1835	0.84	5.96	644	294
R^2	0.77	0.68	0.99	1.00	0.99	1.00
MPSD (%)	64.1	265	3.01	3.62	3.54	2.50
Elovich Model						
β $(g.mg^{-1})$	0.10	0.08	0.10	0.09	0.07	0.07
α $(mg.(g.min)^{-1})$	1.13	0.83	7.71	3.54	2.76	1.40
R^2	0.94	0.96	0.97	0.98	0.91	0.95
MPSD (%)	13.3	36.4	6.98	6.43	13.420	10.0

Table H.3-3: Kinetic model parameters for the adsorption of a binary alcohol mixture (1-octanol + 1-decanol) onto Activated Alumina F220 (T = 25°C)

Model Parameters	***1-octanol (1-O) + 1-decanol (1-D) mixture***					
	1-O	***1-D***	***1-O***	***1-D***	***1-O***	***1-D***
Initial Concentration (mass%)	***0.66***	***0.49***	***1.01***	***0.95***	***1.67***	***1.64***
$q_{e.exp}$ *(mg.g^{-1})*	59.5	57.6	77.1	60.9	76.7	67.0
Pseudo-first-order Model						
$q_{e.cal}$ *(mg.g^{-1})*	63.3	55.9	74.6	61.6	74.5	67.1
k_1 *(min^{-1})*	0.00	0.01	0.01	0.00	0.01	0.00
R^2	0.94	0.99	0.99	0.99	0.96	0.98
MPSD (%)	167	9.71	14.0	15.3	26.4	24.9
Pseudo-second-order Model						
$q_{e.cal}$ *(mg.g^{-1})*	81.1	65.3	83.8	72.9	79.7	75.8
k_2 *(x10^{-3} g.(mg.min)$^{-1}$)*	0.04	0.08	0.11	0.06	0.12	0.07
R^2	0.89	1.00	1.00	0.98	0.96	0.97
MPSD (%)	171	13.7	7.42	21.4	18.5	19.8
Pseudo-nth-order Model						
n (-)	1.03	1.03	2.04	1.10	2.32	2.49
$q_{e.cal}$ *(mg.g^{-1})*	63.6	56.0	84.3	62.2	82.7	81.7
k_n *(x10^{-5} g^{n-1}.mg^{1-n}.min^{-1})*	322	450	8.860	298	2.95	0.81
R^2	0.94	0.99	1.00	0.99	0.96	0.97
MPSD (%)	168	9.65	7.34	16.0	17.3	18.5
Elovich Model						
β (g.mg^{-1})	0.07	0.08	0.07	0.08	0.07	0.08
α (mg.(g.min)$^{-1}$)	0.99	1.05	2.01	1.08	2.64	1.55
R^2	0.95	0.99	0.98	0.97	0.95	0.94
MPSD (%)	11.3	7.34	11.8	10.7	13.1	19.0

Table H.3-4: Kinetic model parameters for the adsorption of a binary alcohol mixture (1-hexanol + 1-decanol) onto Activated Alumina F220 (T = 45°C)

Model Parameters	***1-hexanol (1-H) + 1-decanol (1-D) mixture***					
	1-H	***1-D***	***1-H***	***1-D***	***1-H***	***1-D***
Initial Concentration (mass%)	***0.348***	***0.574***	***0.953***	***1.097***	***1.472***	***1.546***
$q_{e.exp}$ *(mg.g^{-1})*	36.8	74.7	74.8	72.8	75.9	51.0
Pseudo-first-order Model						
$q_{e.cal}$ *(mg.g^{-1})*	38.4	74.2	69.5	66.6	74.7	51.4
k_1 *(min^{-1})*	0.03	0.01	0.03	0.03	0.03	0.03
R^2	0.97	0.97	0.96	0.89	1.00	0.99
MPSD (%)	5.72	17.7	7.33	14.2	3.76	4.37
Pseudo-second-order Model						
$q_{e.cal}$ *(mg.g^{-1})*	40.5	81.1	75.2	72.2	78.8	54.1
k_2 *(x10^{-3} g.(mg.min)$^{-1}$)*	0.90	0.22	0.41	0.43	0.54	0.71
R^2	0.94	0.97	0.99	0.94	0.99	0.97
MPSD (%)	9.37	17.6	5.53	10.4	2.85	6.17
Pseudo-nth-order Model						
n (-)	1.49	1.47	2.29	3.61	1.31	1.36
$q_{e.cal}$ *(mg.g^{-1})*	38.3	76.7	77.6	86.2	82.0	52.8
k_n *(x10^{-5} g^{n-1}.mg^{1-n}.min^{-1})*	536	208	11.8	0.03	397	674
R^2	0.96	0.97	0.99	0.95	0.94	0.98
MPSD (%)	7.28	17.4	5.67	8.64	18.5	5.47
Elovich Model						
β (g.mg^{-1})	0.18	0.07	0.09	0.09	0.10	0.14
α (mg.(g.min)$^{-1}$)	6.98	4.36	7.80	9.64	22.7	11.9
R^2	0.83	0.92	0.96	0.94	0.93	0.88
MPSD (%)	17.9	20.4	10.7	8.85	10.5	13.3

Table H.3-5: Kinetic model parameters for the adsorption of a binary alcohol mixture (1-hexanol + 1-octanol) onto Activated Alumina F220 (T = 45°C)

Model Parameters	***1-hexanol (1-H) + 1-octanol (1-O) mixture***					
	1-H	***1-O***	***1-H***	***1-O***	***1-H***	***1-O***
Initial Concentration (mass%)	***0.40***	***0.43***	***0.97***	***1.07***	***0.96***	***1.43***
$q_{e.exp}$ $(mg.g^{-1})$	38.9	41.2	65.0	62.2	49.7	62.9
Pseudo-first-order Model						
$q_{e.cal}$ $(mg.g^{-1})$	39.8	41.3	63.1	58.3	49.9	63.8
k_1 (min^{-1})	0.03	0.02	0.03	0.03	0.03	0.02
R^2	0.99	1.00	0.98	0.95	0.98	1.00
MPSD (%)	3.02	2.20	6.22	10.52	5.59	2.07
Pseudo-second-order Model						
$q_{e.cal}$ $(mg.g^{-1})$	42.1	44.5	67.2	62.4	52.8	68.4
k_2 $(x10^{-3}\ g.(mg.min)^{-1})$	0.86	0.56	0.55	0.60	0.74	0.40
R^2	0.97	0.98	0.99	0.98	0.97	0.97
MPSD (%)	7.16	7.07	3.37	6.46	8.47	6.70
Pseudo-n^{th}-order Model						
n (-)	0.98	1.03	1.91	3.61	2.13	1.31
$q_{e.cal}$ $(mg.g^{-1})$	39.8	41.3	66.7	86.2	48.9	68.3
k_n $(x10^{-5}\ g^{n-1}.mg^{1-n}.min^{-1})$	2893	1836	79.3	0.03	63.0	397
R^2	0.99	1.00	0.99	0.92	0.93	0.97
MPSD (%)	3.02	2.22	3.39	13.2	11.4	12.7
Elovich Model						
β $(g.mg^{-1})$	0.17	0.14	0.11	0.12	0.14	0.09
α $(mg.(g.min)^{-1})$	7.19	3.06	12.5	12.7	9.72	5.73
R^2	0.87	0.89	0.94	0.97	0.89	0.88
MPSD (%)	16.0	15.3	9.50	6.63	15.8	15.0

Table H.3-6: Kinetic model parameters for the adsorption of a binary alcohol mixture (1-octanol + 1-decanol) onto Activated Alumina F220 (T = 45°C)

Model Parameters	***1-octanol (1-O) + 1-decanol (1-D) mixture***					
	1-O	***1-D***	***1-O***	***1-D***	***1-O***	***1-D***
Initial Concentration (mass%)	***0.39***	***0.62***	***1.02***	***1.17***	***1.51***	***1.56***
$q_{e.exp}$ *(mg.g^{-1})*	47.2	90.7	67.4	68.5	74.7	54.9
Pseudo-first-order Model						
$q_{e.cal}$ *(mg.g^{-1})*	47.9	88.8	65.0	66.5	71.0	53.0
k_1 *(min^{-1})*	0.02	0.02	0.02	0.02	0.02	0.02
R^2	0.99	0.99	0.98	0.97	0.98	0.98
MPSD (%)	6.39	5.70	5.90	7.49	6.83	8.08
Pseudo-second-order Model						
$q_{e.cal}$ *(mg.g^{-1})*	51.8	95.6	70.6	72.4	76.8	58.4
k_2 *(x10^{-3} g.(mg.min)$^{-1}$)*	0.46	0.29	0.35	0.31	0.36	0.30
R^2	0.97	0.99	0.99	0.98	1.00	0.98
MPSD (%)	10.8	3.63	2.89	5.22	3.18	11.0
Pseudo-nth-order Model						
n (-)	0.98	1.04	1.91	3.61	1.50	1.31
$q_{e.cal}$ *(mg.g^{-1})*	39.8	89.0	66.7	86.2	73.4	55.0
k_n *(x10^{-5} g^{n-1}.mg^{1-n}.min^{-1})*	2893	1836	79.3	0.03	290	397
R^2	0.83	0.99	0.98	0.95	1.00	0.99
MPSD (%)	15.9	5.55	10.8	15.1	4.16	8.37
Elovich Model						
β (g.mg^{-1})	0.12	0.07	0.09	0.08	0.09	0.10
α (mg.(g.min)$^{-1}$)	3.18	9.00	5.15	4.62	7.37	2.30
R^2	0.88	0.93	0.94	0.92	0.95	0.92
MPSD (%)	18.2	10.8	10.6	11.5	9.24	15.7

Table H.3-7: Intra-particle diffusion model parameters for the adsorption of a binary alcohol mixture onto Activated Alumina (T = 25°C)

Alcohol	***Initial Concentration (mass%)***	***Intra-particle Diffusion Model Parameters***		
		θ ($mg.g^{-1}$)	k_{ip} ($mg/g.min^{0.5}$)	R^2
1-hexanol + 1-decanol	0.75	36.2	2.83	0.95
	1.76	38.0	2.91	0.78
	3.17	65.1	3.34	0.96
1-hexanol + 1-octanol	1.06	39.3	2.87	0.93
	1.92	51.1	3.91	0.98
	3.33	51.0	3.81	0.95
1-octanol + 1-decanol	1.15	20.5	4.03	0.98
	1.96	4.15	5.77	0.98
	3.32	42.9	4.25	0.95

Table H.3-8: Intra-particle diffusion model parameters for the adsorption of a binary alcohol mixture onto Activated Alumina F220 (T = 45°C)

Alcohol	***Initial Concentration (mass%)***	***Intra-particle Diffusion Model Parameters***		
		θ ($mg.g^{-1}$)	k_{ip} ($mg/g.min^{0.5}$)	R^2
1-hexanol + 1-decanol	0.92	61.5	2.99	0.98
	2.05	70.5	3.41	0.83
	3.02	26.3	8.04	1.00
1-hexanol + 1-octanol	0.83	63.3	1.19	0.83
	2.04	79.1	2.26	0.81
	2.39	21.3	7.45	1.00
1-octanol + 1-decanol	1.01	93.7	2.49	0.96
	2.19	54.8	4.45	1.00
	3.07	67.6	3.14	0.91

H.3.2 Selexsorb CDx®

Table H.3-9: Kinetic model parameters for the adsorption of a binary alcohol mixture (1-hexanol + 1-decanol) onto Selexsorb CDx® (T = 25°C)

Model Parameters	***1-hexanol (1-H) + 1-decanol (1-D) mixture***					
	1-H	***1-D***	***1-H***	***1-D***	***1-H***	***1-D***
Initial Concentration (mass%)	***0.59***	***0.61***	***1.04***	***1.06***	***1.44***	***1.94***
$q_{e.exp}$ $(mg.g^{-1})$	53.1	62.6	70.9	52.2	57.2	67.5
Pseudo-first-order Model						
$q_{e.cal}$ $(mg.g^{-1})$	49.7	61.6	66.1	49.2	56.8	67.2
k_1 (min^{-1})	0.01	0.00	0.01	0.01	0.00	0.00
R^2	0.96	0.97	0.97	0.97	0.91	0.97
MPSD (%)	11.5	26.5	8.50	8.78	32.2	18.8
Pseudo-second-order Model						
$q_{e.cal}$ $(mg.g^{-1})$	55.2	69.6	73.8	55.6	58.9	77.5
k_2 $(x10^{-3}\ g.(mg.min)^{-1})$	0.28	0.08	0.22	0.22	0.15	0.06
R^2	0.96	0.97	1.00	0.98	0.91	0.97
MPSD (%)	13.9	22.5	3.64	7.48	21.7	12.0
Pseudo-n^{th}-order Model						
n (-)	1.34	3.07	2.13	1.60	3.04	3.04
$q_{e.cal}$ $(mg.g^{-1})$	51.1	81.5	75.0	52.5	66.6	71.3
k_n $(x10^{-5}\ g^{n-1}.mg^{1-n}.min^{-1})$	370	0.07	12.5	110	0.16	0.14
R^2	0.97	0.96	1.00	0.98	0.91	0.87
MPSD (%)	11.9	20.4	3.75	7.12	19.4	16.4
Elovich Model						
β $(g.mg^{-1})$	0.10	0.10	0.08	0.10	0.10	0.07
α $(mg.(g.min)^{-1})$	1.86	1.58	2.91	1.62	1.84	1.27
R^2	0.91	0.89	0.97	0.95	0.94	0.96
MPSD (%)	16.5	21.3	8.50	11.9	12.8	11.2

Table H.3-10: Kinetic model parameters for the adsorption of a binary alcohol mixture (1-hexanol + 1-octanol) onto onto Selexsorb CDx® (T = 25°C)

Model Parameters	***1-hexanol (1-H) + 1-octanol (1-O) mixture***					
	1-H	***1-O***	***1-H***	***1-O***	***1-H***	***1-O***
Initial Concentration (mass%)	***0.57***	***0.63***	***1.00***	***0.98***	***1.55***	***1.61***
$q_{e.exp}$ $(mg.g^{-1})$	44.4	37.3	73.0	60.9	70.8	63.3
Pseudo-first-order Model						
$q_{e.cal}$ $(mg.g^{-1})$	42.5	31.5	65.9	52.4	58.5	51.5
k_1 (min^{-1})	0.01	0.02	0.01	0.02	0.02	0.03
R^2	0.92	0.81	0.94	0.89	0.84	0.81
MPSD (%)	16.0	22.6	13.1	13.8	20.7	20.6
Pseudo-second-order Model						
$q_{e.cal}$ $(mg.g^{-1})$	47.9	36.5	74.5	59.5	66.6	57.3
k_2 $(x10^{-3}\ g.(mg.min)^{-1})$	0.28	0.43	0.19	0.32	0.31	0.51
R^2	0.95	0.91	0.98	0.97	0.93	0.90
MPSD (%)	14.2	18.8	9.97	8.54	15.1	16.1
Pseudo-n^{th}-order Model						
n (-)	2.13	3.97	2.92	3.80	4.19	5.04
$q_{e.cal}$ $(mg.g^{-1})$	49.0	47.7	85.3	75.3	87.9	81.3
k_n $(x10^{-5}\ g^{n-1}.mg^{1-n}.min^{-1})$	16.8	0.02	0.28	0.01	0.00	0.00
R^2	0.95	0.93	0.99	0.99	0.96	0.95
MPSD (%)	14.2	15.0	10.6	5.77	10.5	11.5
Elovich Model						
β $(g.mg^{-1})$	0.11	0.16	0.07	0.10	0.09	0.12
α $(mg.(g.min)^{-1})$	1.48	1.61	2.53	2.98	4.41	6.99
R^2	0.94	0.95	0.98	0.99	0.97	0.96
MPSD (%)	13.9	12.6	10.5	5.50	8.11	9.31

Table H.3-11: Kinetic model parameters for the adsorption of a binary alcohol mixture (1-octanol + 1-decanol) onto onto Selexsorb CDx® (T = 25°C)

Model Parameters	***1-octanol (1-O) + 1-decanol (1-D) mixture***					
	1-O	***1-D***	***1-O***	***1-D***	***1-O***	***1-D***
Initial Concentration (mass%)	***0.55***	***0.62***	***1.16***	***1.18***	***1.60***	***1.71***
$q_{e.exp}$ *(mg.g^{-1})*	50.7	62.8	59.4	56.4	72.1	61.5
Pseudo-first-order Model						
$q_{e.cal}$ *(mg.g^{-1})*	49.0	60.0	59.3	57.5	66.4	55.1
k_1 *(min^{-1})*	0.01	0.01	0.01	0.01	0.01	0.01
R^2	0.98	0.97	1.00	0.98	0.92	0.89
MPSD (%)	13.9	23.2	2.02	35.8	22.6	26.4
Pseudo-second-order Model						
$q_{e.cal}$ *(mg.g^{-1})*	54.5	66.3	65.2	65.6	73.2	59.5
k_2 *(x10^{-3} g.(mg.min)$^{-1}$)*	0.21	0.11	0.24	0.12	0.15	0.21
R^2	0.99	0.98	0.98	0.94	0.96	0.92
MPSD (%)	8.34	14.6	8.08	43.7	11.9	15.3
Pseudo-nth-order Model						
n (-)	1.84	3.05	0.99	1.03	3.76	4.35
$q_{e.cal}$ *(mg.g^{-1})*	53.3	77.4	59.3	57.7	95.3	83.6
k_n *(x10^{-5} g^{n-1}.mg^{1-n}.min^{-1})*	39.3	0.11	1362	685	0.00	0.00
R^2	0.99	0.99	1.00	0.98	0.98	0.96
MPSD (%)	8.62	10.99	2.02	36.26	7.18	9.79
Elovich Model						
β (g.mg^{-1})	0.10	0.09	0.09	0.08	0.08	0.09
α (mg.(g.min)$^{-1}$)	1.61	1.61	2.30	1.20	2.29	2.19
R^2	0.96	0.99	0.91	0.92	0.99	0.97
MPSD (%)	11.6	11.1	13.9	19.5	3.58	6.56

Table H.3-12: Kinetic model parameters for the adsorption of a binary alcohol mixture (1-hexanol + 1-decanol) onto Selexsorb CDx® (T = 45°C)

Model Parameters	***1-hexanol (1-H) + 1-decanol (1-D) mixture***					
	1-H	***1-D***	***1-H***	***1-D***	***1-H***	***1-D***
Initial Concentration (mass%)	***0.51***	***0.63***	***1.03***	***1.04***	***1.26***	***1.68***
$q_{e.exp}$ *(mg.g^{-1})*	64.0	79.6	80.9	44.0	80.9	52.8
Pseudo-first-order Model						
$q_{e.cal}$ *(mg.g^{-1})*	62.3	75.8	73.0	45.6	74.7	42.9
k_1 *(min^{-1})*	0.01	0.01	0.02	0.01	0.01	0.02
R^2	0.95	0.95	0.93	0.97	0.95	0.86
MPSD (%)	24.5	19.3	13.5	29.3	19.9	17.8
Pseudo-second-order Model						
$q_{e.cal}$ *(mg.g^{-1})*	70.6	83.1	81.2	52.2	81.4	48.6
k_2 *(x10^{-3} g.(mg.min)$^{-1}$)*	0.16	0.14	0.25	0.12	0.15	0.38
R^2	0.95	0.97	0.98	0.94	0.96	0.93
MPSD (%)	30.6	10.4	7.41	38.1	10.4	14.3
Pseudo-nth-order Model						
n (-)	1.24	3.04	3.72	1.65	2.89	2.48
$q_{e.cal}$ *(mg.g^{-1})*	60.0	96.9	101	47.6	92.8	52.2
k_n *(x10^{-5} g^{n-1}.mg^{1-n}.min^{-1})*	440	0.11	0.01	56.8	0.23	5.38
R^2	0.94	0.97	0.99	0.94	0.96	0.97
MPSD (%)	28.2	8.95	4.35	37.5	8.53	14.0
Elovich Model						
β (g.mg^{-1})	0.07	0.07	0.07	0.10	0.07	0.12
α (mg.(g.min)$^{-1}$)	1.70	2.54	4.93	0.88	2.66	2.21
R^2	0.92	0.97	0.98	0.92	0.96	0.95
MPSD (%)	23.9	8.14	5.18	13.7	7.88	14.3

Table H.3-13: Kinetic model parameters for the adsorption of a binary alcohol mixture (1-hexanol + 1-octanol) onto Selexsorb CDx® (T = 45°C)

Model Parameters	***1-hexanol (1-H) + 1-octanol (1-O) mixture***					
	1-H	***1-O***	***1-H***	***1-O***	***1-H***	***1-O***
Initial Concentration (mass%)	***0.57***	***0.65***	***0.76***	***0.75***	***1.51***	***1.57***
$q_{e.exp}$ *(mg.g^{-1})*	64.4	69.6	66.8	53.5	84.0	63.6
Pseudo-first-order Model						
$q_{e.cal}$ *(mg.g^{-1})*	59.4	61.2	63.2	51.6	75.5	58.8
k_1 *(min^{-1})*	0.03	0.03	0.01	0.01	0.01	0.02
R^2	0.96	0.92	0.98	0.99	0.94	0.96
MPSD (%)	9.01	11.5	11.2	7.51	13.5	11.2
Pseudo-second-order Model						
$q_{e.cal}$ *(mg.g^{-1})*	63.2	66.2	70.3	58.3	84.2	64.9
k_2 *(x10^{-3} g.(mg.min)$^{-1}$)*	0.68	0.54	0.23	0.20	0.20	0.31
R^2	0.99	0.97	1.00	0.98	0.99	0.99
MPSD (%)	5.35	7.40	6.46	8.12	7.19	6.20
Pseudo-nth-order Model						
n (-)	3.28	3.57	2.10	1.23	1.73	2.23
$q_{e.cal}$ *(mg.g^{-1})*	71.4	78.1	71.2	52.7	83.5	66.7
k_n *(x10^{-5} g^{n-1}.mg^{1-n}.min^{-1})*	0.31	0.06	15.4	421	58.3	11.7
R^2	0.99	0.99	0.99	0.99	0.98	0.99
MPSD (%)	3.56	4.39	6.37	6.43	10.0	5.74
Elovich Model						
β (g.mg^{-1})	0.12	0.11	0.08	0.09	0.07	0.09
α (mg.(g.min)$^{-1}$)	18.0	11.4	3.10	1.59	4.03	3.79
R^2	0.98	0.99	0.96	0.93	0.99	0.97
MPSD (%)	5.29	3.61	9.84	14.3	5.11	7.36

Table H.3-14: Kinetic model parameters for the adsorption of a binary alcohol mixture (1-octanol + 1-decanol) onto Selexsorb CDx® (T = 45°C)

Model Parameters	***1-octanol (1-O) + 1-decanol (1-D) mixture***					
	1-O	***1-D***	***1-O***	***1-D***	***1-O***	***1-D***
Initial Concentration (mass%)	***0.55***	***0.40***	***0.76***	***0.92***	***1.29***	***1.49***
$q_{e.exp}$ *(mg.g^{-1})*	67.7	58.7	60.7	63.1	70.4	57.5
Pseudo-first-order Model						
$q_{e.cal}$ *(mg.g^{-1})*	60.9	55.1	55.8	58.4	65.4	55.9
k_1 *(min^{-1})*	0.01	0.01	0.01	0.01	0.02	0.02
R^2	0.92	0.95	0.96	0.95	0.94	0.96
MPSD (%)	16.4	22.6	10.3	16.0	12.2	14.2
Pseudo-second-order Model						
$q_{e.cal}$ *(mg.g^{-1})*	67.5	59.0	62.5	65.3	71.5	61.0
k_2 *(x10^{-3} g.(mg.min)$^{-1}$)*	0.26	0.21	0.26	0.20	0.34	0.34
R^2	0.97	0.96	1.00	0.99	0.98	0.98
MPSD (%)	9.78	13.7	3.59	8.69	7.19	11.2
Pseudo-nth-order Model						
n (-)	3.28	3.57	2.10	1.23	2.51	2.23
$q_{e.cal}$ *(mg.g^{-1})*	71.4	78.1	71.2	52.7	75.8	66.7
k_n *(x10^{-5} g^{n-1}.mg^{1-n}.min^{-1})*	0.31	0.06	15	421	3.74	11.7
R^2	0.91	0.79	0.94	0.89	0.98	0.96
MPSD (%)	23.9	48.7	12.8	19.4	6.46	12.4
Elovich Model						
β (g.mg^{-1})	0.09	0.10	0.09	0.09	0.09	0.10
α (mg.(g.min)$^{-1}$)	3.35	2.18	2.50	2.27	5.58	4.09
R^2	0.98	0.98	0.98	0.98	0.94	0.94
MPSD (%)	5.46	8.40	6.55	7.91	8.82	12.6

Table H.3-15: Intra-particle diffusion model parameters for the adsorption of a binary alcohol mixture onto Selexsorb CDx® (T = 25°C)

Alcohol	***Initial Concentration (mass%)***	***Intra-particle Diffusion Model Parameters***		
		θ ($mg.g^{-1}$)	k_{ip} ($mg/g.min^{0.5}$)	R^2
1-hexanol + 1-decanol	1.20	23.6	3.74	0.68
	2.10	49.9	3.37	0.97
	3.38	10.2	4.04	0.83
1-hexanol + 1-octanol	1.30	11.6	3.08	0.89
	1.98	47.4	3.27	0.89
	3.16	5.56	5.54	0.94
1-octanol + 1-decanol	1.26	16.2	3.94	0.93
	2.34	69.7	2.31	0.99
	3.31	41.8	2.82	0.97

Table H.3-16: Intra-particle diffusion model parameters for the adsorption of a binary alcohol mixture onto Selexsorb CDx® (T = 45°C)

Alcohol	***Initial Concentration (mass%)***	***Intra-particle Diffusion Model Parameters***		
		θ ($mg.g^{-1}$)	k_{ip} ($mg/g.min^{0.5}$)	R^2
1-hexanol + 1-decanol	1.13	25.9	5.29	0.97
	2.07	29.7	4.31	0.97
	2.94	9.66	5.23	0.99
1-hexanol + 1-octanol	1.31	38.4	3.63	0.94
	1.51	55.9	2.85	0.98
	3.08	55.5	3.90	0.98
1-octanol + 1-decanol	0.95	10.3	5.03	0.95
	1.67	22.2	4.35	1.00
	2.78	28.1	5.32	0.98

H.3.3 Selexsorb CD®

Table H.3-17: Kinetic model parameters for the adsorption of a binary alcohol mixture (1-hexanol + 1-decanol) onto Selexsorb CD® (T = 25°C)

Model Parameters	***1-hexanol (1-H) + 1-decanol (1-D) mixture***					
	1-H	***1-D***	***1-H***	***1-D***	***1-H***	***1-D***
Initial Concentration (mass%)	***0.50***	***0.51***	***1.22***	***1.21***	***1.51***	***1.54***
$q_{e.exp}$ $(mg.g^{-1})$	56.1	65.6	79.9	57.2	86.6	64.9
Pseudo-first-order Model						
$q_{e.cal}$ $(mg.g^{-1})$	54.4	64.9	70.9	51.5	83.5	59.5
k_1 (min^{-1})	0.01	0.00	0.01	0.01	0.01	0.01
R^2	0.96	0.97	0.93	0.93	0.96	0.92
MPSD (%)	19.8	24.2	16.1	24.9	24.5	26.8
Pseudo-second-order Model						
$q_{e.cal}$ $(mg.g^{-1})$	59.4	72.6	79.7	56.0	90.3	62.1
k_2 $(x10^{-3}\ g.(mg.min)^{-1})$	0.19	0.08	0.18	0.21	0.09	0.17
R^2	0.97	0.96	0.98	0.96	0.97	0.94
MPSD (%)	10.7	17.5	8.89	15.6	16.8	16.2
Pseudo-n^{th}-order Model						
n (-)	3.21	2.91	2.95	2.67	2.99	3.16
$q_{e.cal}$ $(mg.g^{-1})$	70.9	86.3	92.7	60.7	89.1	69.4
k_n $(x10^{-5}\ g^{n-1}.mg^{1-n}.min^{-1})$	0.09	0.11	0.18	1.32	0.13	0.10
R^2	0.97	0.97	0.99	0.97	0.90	0.92
MPSD (%)	8.09	15.6	8.95	13.1	15.5	16.4
Elovich Model						
β $(g.mg^{-1})$	0.09	0.08	0.07	0.10	0.06	0.09
α $(mg.(g.min)^{-1})$	1.90	1.50	3.20	2.07	2.25	1.91
R^2	0.96	0.95	1.00	0.99	0.98	0.98
MPSD (%)	8.36	12.8	4.76	8.78	10.7	10.0

Table H.3-18: Kinetic model parameters for the adsorption of a binary alcohol mixture (1-hexanol + 1-octanol) onto onto Selexsorb CD® (T = 25°C)

Model Parameters	***1-hexanol (1-H) + 1-octanol (1-O) mixture***					
	1-H	***1-O***	***1-H***	***1-O***	***1-H***	***1-O***
Initial Concentration (mass%)	***0.49***	***0.53***	***0.80***	***0.95***	***1.53***	***1.60***
$q_{e.exp}$ $(mg.g^{-1})$	46.4	49.3	53.8	54.9	78.3	63.8
Pseudo-first-order Model						
$q_{e.cal}$ $(mg.g^{-1})$	46.2	53.1	81.0	78.7	0.01	0.01
k_1 (min^{-1})	0.02	0.02	0.01	0.01	0.01	0.00
R^2	0.92	0.97	0.97	0.98	0.98	0.99
MPSD (%)	30.2	26.1	22.8	8.91	19.1	6.07
Pseudo-second-order Model						
$q_{e.cal}$ $(mg.g^{-1})$	50.6	58.7	86.1	87.2	0.00	0.00
k_2 $(x10^{-3}\ g.(mg.min)^{-1})$	0.39	0.35	0.15	0.11	0.10	0.07
R^2	0.92	0.98	0.98	1.00	0.99	1.00
MPSD (%)	21.2	20.9	30.4	7.52	10.9	6.24
Pseudo-n^{th}-order Model						
n (-)	3.30	3.23	2.86	2.83	110	85.4
$q_{e.cal}$ $(mg.g^{-1})$	65.4	70.2	106	106	0.00	0.00
k_n $(x10^{-5}\ g^{n-1}.mg^{1-n}.min^{-1})$	0.10	0.11	0.14	0.15	0.22	66.2
R^2	0.95	0.98	0.97	0.99	1.00	1.00
MPSD (%)	15.8	18.2	33.3	8.30	8.81	4.02
Elovich Model						
β $(g.mg^{-1})$	0.12	0.10	0.07	0.06	5.08	2.63
α $(mg.(g.min)^{-1})$	3.09	3.71	3.51	2.16	1.91	1.10
R^2	0.97	0.96	0.98	0.97	0.99	0.99
MPSD (%)	12.3	21.5	7.83	9.34	11.8	19.2

Table H.3-19: Kinetic model parameters for the adsorption of a binary alcohol mixture (1-octanol + 1-decanol) onto onto Selexsorb CD® (T = 25°C)

Model Parameters	***1-octanol (1-O) + 1-decanol (1-D) mixture***					
	1-O	***1-D***	***1-O***	***1-D***	***1-O***	***1-D***
Initial Concentration (mass%)	***0.53***	***0.46***	***1.09***	***1.01***	***1.53***	***1.57***
$q_{e.exp}$ $(mg.g^{-1})$	43.5	43.5	63.1	48.3	70.6	62.5
Pseudo-first-order Model						
$q_{e.cal}$ $(mg.g^{-1})$	61.9	46.1	59.8	46.3	87.5	78.9
k_1 (min^{-1})	0.00	0.00	0.01	0.01	0.00	0.00
R^2	0.96	0.95	0.97	0.97	1.00	0.99
MPSD (%)	27.5	39.8	18.6	19.3	5.06	55.5
Pseudo-second-order Model						
$q_{e.cal}$ $(mg.g^{-1})$	46.0	58.7	65.7	73.7	109	66.4
k_2 $(x10^{-3}\ g.(mg.min)^{-1})$	0.13	0.35	0.15	0.14	0.03	0.09
R^2	0.97	0.63	0.98	0.77	0.99	0.84
MPSD (%)	20.0	149	10.9	41.4	11.6	161
Pseudo-n^{th}-order Model						
n (-)	3.77	1.77	3.24	3.41	1.10	1.10
$q_{e.cal}$ $(mg.g^{-1})$	60.1	56.7	79.3	62.6	88.9	81.2
k_n $(x10^{-5}\ g^{n-1}.mg^{1-n}.min^{-1})$	0.01	8.31	0.05	0.04	199	136
R^2	0.98	0.95	0.99	0.99	1.00	0.99
MPSD (%)	15.6	39.1	8.71	5.08	6.06	56.5
Elovich Model						
β $(g.mg^{-1})$	0.13	0.14	0.09	0.11	0.06	0.07
α $(mg.(g.min)^{-1})$	1.03	0.73	1.86	1.37	1.23	0.93
R^2	0.97	0.80	0.99	0.99	0.97	0.91
MPSD (%)	16.1	40.3	10.4	4.51	33.8	47.7

Table H.3-20: Kinetic model parameters for the adsorption of a binary alcohol mixture (1-hexanol + 1-decanol) onto Selexsorb CD® (T = 45°C)

Model Parameters	***1-hexanol (1-H) + 1-decanol (1-D) mixture***					
	1-H	***1-D***	***1-H***	***1-D***	***1-H***	***1-D***
Initial Concentration (mass%)	***0.47***	***0.50***	***1.11***	***1.18***	***1.45***	***1.58***
$q_{e.exp}$ *(mg.g^{-1})*	69.9	62.5	88.0	52.1	75.6	62.8
Pseudo-first-order Model						
$q_{e.cal}$ *(mg.g^{-1})*	69.8	62.7	76.6	43.2	72.8	59.1
k_1 *(min^{-1})*	0.00	0.00	0.02	0.02	0.02	0.01
R^2	0.99	0.97	0.88	0.82	0.96	0.89
MPSD (%)	15.7	19.3	15.5	20.6	13.1	28.3
Pseudo-second-order Model						
$q_{e.cal}$ *(mg.g^{-1})*	84.4	75.5	86.2	49.7	79.2	62.7
k_2 *(x10^{-3} g.(mg.min)$^{-1}$)*	0.04	0.04	0.27	0.40	0.28	0.21
R^2	1.00	0.97	0.95	0.92	0.97	0.90
MPSD (%)	13.6	15.1	11.1	15.5	9.67	22.9
Pseudo-nth-order Model						
n (-)	0.82	2.37	3.00	3.23	1.27	1.13
$q_{e.cal}$ *(mg.g^{-1})*	71.0	81.5	92.0	55.7	73.8	56.7
k_n *(x10^{-5} g^{n-1}.mg^{1-n}.min^{-1})*	594	0.75	0.35	0.34	588	548
R^2	0.99	0.97	0.95	0.94	0.97	0.87
MPSD (%)	18.7	14.3	10.5	13.1	11.5	26.8
Elovich Model						
β (g.mg^{-1})	0.07	0.08	0.07	0.12	0.08	0.10
α (mg.(g.min)$^{-1}$)	1.03	0.98	5.60	2.87	5.85	3.34
R^2	0.97	0.94	0.97	0.97	0.93	0.93
MPSD (%)	34.2	22.5	10.0	10.8	11.6	20.4

Table H.3-21: Kinetic model parameters for the adsorption of a binary alcohol mixture (1-hexanol + 1-octanol) onto Selexsorb CD® (T = 45°C)

Model Parameters	***1-hexanol (1-H) + 1-octanol (1-O) mixture***					
	1-H	***1-O***	***1-H***	***1-O***	***1-H***	***1-O***
Initial Concentration (mass%)	***0.47***	***0.56***	***0.91***	***1.08***	***1.67***	***1.72***
$q_{e.exp}$ *(mg.g^{-1})*	48.8	58.5	85.4	81.1	88.2	61.4
Pseudo-first-order Model						
$q_{e.cal}$ *(mg.g^{-1})*	46.2	53.1	81.0	78.7	86.0	64.9
k_1 *(min^{-1})*	0.02	0.02	0.01	0.01	0.01	0.01
R^2	0.97	0.94	0.93	0.98	0.94	0.97
MPSD (%)	14.6	13.4	25.4	16.9	15.4	9.72
Pseudo-second-order Model						
$q_{e.cal}$ *(mg.g^{-1})*	50.6	58.7	86.1	87.2	95.2	72.1
k_2 *(x10^{-3} g.(mg.min)$^{-1}$)*	0.39	0.35	0.15	0.11	0.19	0.21
R^2	0.98	0.99	0.94	0.98	0.98	0.99
MPSD (%)	12.2	8.06	15.8	8.64	9.57	4.25
Pseudo-nth-order Model						
n (-)	3.30	3.23	2.86	2.83	3.10	3.20
$q_{e.cal}$ *(mg.g^{-1})*	65.4	70.2	106	106	110	85.4
k_n *(x10^{-5} g^{n-1}.mg^{1-n}.min^{-1})*	0.10	0.11	0.14	0.15	0.10	0.08
R^2	0.96	0.98	0.96	0.98	0.99	0.98
MPSD (%)	13.1	11.6	18.9	9.17	7.57	5.52
Elovich Model						
β (g.mg^{-1})	0.12	0.10	0.07	0.06	0.06	0.08
α (mg.(g.min)$^{-1}$)	3.09	3.71	3.51	2.16	5.08	2.63
R^2	0.94	0.98	0.96	0.97	0.98	0.96
MPSD (%)	13.7	6.52	9.45	6.86	7.50	8.35

Table H.3-22: Kinetic model parameters for the adsorption of a binary alcohol mixture (1-octanol + 1-decanol) onto Selexsorb CD® (T = 45°C)

Model Parameters	***1-octanol (1-O) + 1-decanol (1-D) mixture***					
	1-O	***1-D***	***1-O***	***1-D***	***1-O***	***1-D***
Initial Concentration (mass%)	***0.60***	***0.58***	***1.00***	***1.07***	***1.52***	***1.48***
$q_{e.exp}$ *(mg.g^{-1})*	60.6	59.2	74.1	70.5	74.6	58.6
Pseudo-first-order Model						
$q_{e.cal}$ *(mg.g^{-1})*	61.9	61.2	69.6	66.4	68.8	57.2
k_1 *(min^{-1})*	0.00	0.00	0.01	0.01	0.01	0.01
R^2	0.98	0.97	0.96	0.96	0.97	0.97
MPSD (%)	48.1	39.7	17.7	17.6	9.27	10.6
Pseudo-second-order Model						
$q_{e.cal}$ *(mg.g^{-1})*	76.9	78.7	76.9	74.4	77.6	66.4
k_2 *(x10^{-3} g.(mg.min)$^{-1}$)*	0.04	0.03	0.17	0.13	0.16	0.09
R^2	0.96	0.96	0.98	0.98	1.00	0.97
MPSD (%)	56.9	46.0	9.55	11.7	2.81	14.5
Pseudo-nth-order Model						
n (-)	1.95	1.81	2.86	2.83	3.10	3.20
$q_{e.cal}$ *(mg.g^{-1})*	76.3	74.4	106	106	110	85.4
k_n *(x10^{-5} g^{n-1}.mg^{1-n}.min^{-1})*	5.34	8.00	0.14	0.15	0.10	0.08
R^2	0.96	0.96	0.95	0.91	0.83	0.83
MPSD (%)	56.1	44.8	15.1	18.8	40.1	95.5
Elovich Model						
β (g.mg^{-1})	0.08	0.08	0.07	0.07	0.07	0.08
α (mg.(g.min)$^{-1}$)	0.96	0.86	2.72	2.03	2.34	1.10
R^2	0.96	0.93	0.98	0.98	0.98	0.97
MPSD (%)	15.1	25.4	7.86	13.7	6.46	11.5

Table H.3-23: Intra-particle diffusion model parameters for the adsorption of a binary alcohol mixture onto Selexsorb CD® (T = 25°C)

Alcohol	***Initial Concentration (mass%)***	***Intra-particle Diffusion Model Parameters***		
		θ ($mg.g^{-1}$)	k_{ip} $(mg/g.min^{0.5})$	R^2
1-hexanol + 1-decanol	1.01	6.01	4.60	0.99
	2.43	43.9	3.17	0.93
	3.05	2.26	5.69	1.00
1-hexanol + 1-octanol	1.02	25.3	2.30	0.97
	1.75	55.9	1.77	0.80
	3.12	19.8	4.52	0.98
1-octanol + 1-decanol	0.98	0.58	2.80	0.72
	2.10	13.0	4.08	1.00
	3.10	-13.3	6.06	0.97

Table H.3-24: Intra-particle diffusion model parameters for the adsorption of a binary alcohol mixture onto Selexsorb CD® (T = 45°C)

Alcohol	***Initial Concentration (mass%)***	***Intra-particle Diffusion Model Parameters***		
		θ ($mg.g^{-1}$)	k_{ip} $(mg/g.min^{0.5})$	R^2
1-hexanol + 1-decanol	0.98	3.12	4.28	0.81
	2.29	-0.77	6.71	1.00
	3.03	77.1	2.49	0.94
1-hexanol + 1-octanol	1.03	39.1	3.17	0.97
	1.99	-4.47	7.58	0.96
	3.38	35.2	6.09	0.98
1-octanol + 1-decanol	1.18	24.2	3.39	1.00
	1.52	21.9	5.17	0.96
	3.38	40.9	3.60	0.92